INVESTIGATION OF SIGNIFICANT PARAMETERS IN GEAR HOBBING

A Thesis submitted to

THE UNIVERSITY OF ASTON IN BIRMINGHAM

for the Degree of

DOCTOR OF PHILOSOPHY

by

HANI M. N. RAAFAT, M.Sc., P.G.Dip.(Stats.), B.Sc.

Faculty of Engineering

March, 1977

Dedicated, with affection and gratitude to my parents.

CONTENTS

Page

ACKNOWLEDGMENTS

The author wishes to thank:-

Dr. D.A. Milner, Ph.D., B.Sc.(Eng.),C.Eng.,
M.I.Mech.E., M.I.Prod.E.
for his continued help, guidance and encouragement as Supervisor throughout the whole project.

Professor R.H. Thornley, Ph.D., D.Sc.,M.Sc.Tech.,
A.M.C.T., C.Eng., F.I.Mech.E.,
F.I.Prod.E., Mem. J.S.M.E.
for permitting this work to be carried out within the Department of Production Engineering.

Mr. G. Jones for his assistance with the strain gauges and instrumentation.

Mr. S. Twamley, Mr. J. Newman and Mr. T. Constable for their assistance and enthusiasm in the building of the rigs and manufacture of the test specimens.

Mr. T. Hopkins for his assistance in the Metrology Laboratory. Also the many other technicians who are too numerous to list but to whom one is, nevertheless, very much indebted.

Finally, Mrs. M. Bellamy for typing the script and without whose help this project could not have been submitted in its present form.

DECLARATION

No part of the work described in this Thesis has been submitted in support of an application for another degree or qualification of this or any other University or other institution of learning.

Hani Raafat

The author, after attending a five-year full-time course at Ain-shams University, Cairo, obtained his B.Sc. degree in Production Engineering, then was appointed to teach at the Technical College in Kuwait between 1968-1973. During this period he attended part-time evening courses at Kuwait University and gained a Post Graduate Diploma in Applied Statistics.

He came to this country in October 1973 and attended a one-year course at the University of Aston in Birmingham after which he obtained an M.Sc. degree in Production Technology and Management.

SUMMARY

This study was carried out in order to investigate the effect of cutting parameters on the conventional hobbing process in which the response is analysed and practically tested.

The investigation is in six sections:

(i) Assessment of cutting torques and power consumed during hobbing.
(ii) The study of the variation of gear teeth surface roughness
(iii) Investigation of generated vibrations during hobbing
(iv) Analysis of the mechanics of uncut-chip
(v) The study of tool wear and tool life
(vi) A general viewpoint of the economic problem in hobbing.

In section (i) tests were conducted in order to assess readily a method of determining cutting torque encountered by hob shaft. Power consumed during hobbing was also measured by changing various cutting parameters. Observations were taken when hobbing spur and helical gears. Unlike others, the effect of cutting speed was shown to have a significant effect both upon cutting torques and power consumed.

In section (ii) the nature of gear teeth surface was discussed. Axial feed, hob speed and hob D.P. were seen to have a highly significant influence on surface roughness.

In section (iii) investigation was carried out into the effect of cutting parameters upon the machine tool vibration. Stability was shown to depend strongly upon speed, feed and hob D.P.

In section (iv) a practical method to calculate volume of metal removed during hobbing is presented and a theoretical analysis of uncut-chip thickness and width is attempted.

In section (v) the wear mechanism in hobbing is discussed, "rake face" wear proved to be a suitable tool-life criterion when cutting materials less than (270 HB) under normal cutting consitions. Cutting speed was seen to have the highest significant influence on tool life, while axial feed was not significant.

Section (vi) combines all the previous effects of cutting parameters to give a general viewpoint of the economic problem in hobbing, where power, surface roughness and tangential cutting force were the only constraints restricting the operability region for the given machining conditions.

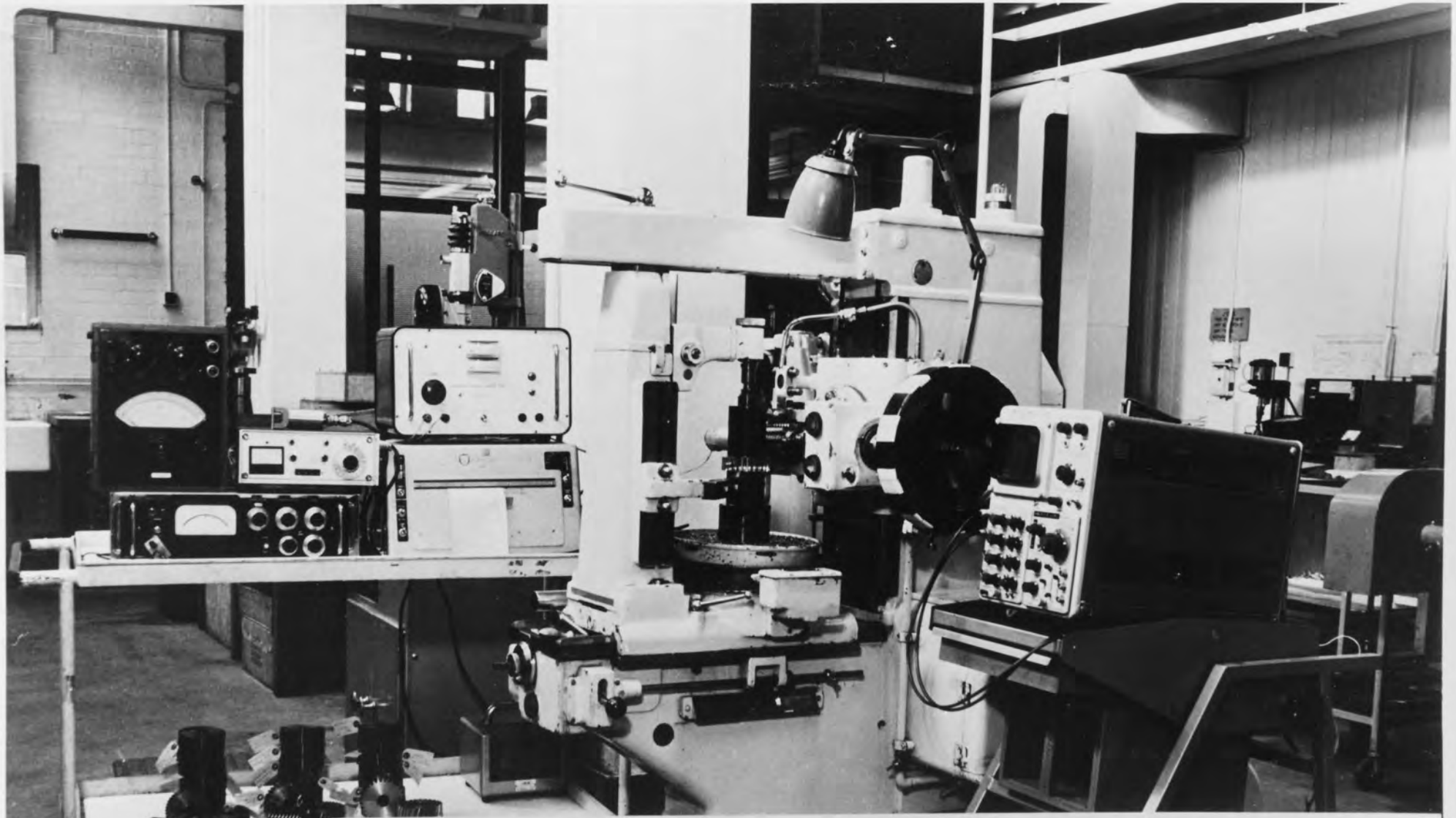

Fig.1 GENERAL VIEW OF SYKES HV 14 HOBBING MACHINE AND INSTRUMENTS

LIST OF FIGURES

Fig. No.

Fig.
No.

Fig.
No.

Fig.
No.

NOMENCLATURE

Symbol	Notation	Units
$\alpha_1, \alpha_2, \alpha_3, \ldots$	Coefficientes to be estimated	
a_{ij}	Technological coefficients	
$\bar{a}_{ij}$	Mean values of a_{ij}	
a_L, a_R, a_T	Chip surface area	mm^2
A_L, A_R, A_T	Chip cross-sectional area	mm^2
add	addendum	mm
b_i	constraint coefficient	
$\bar{b}_i$	mean value of b_i	
$\beta_0, \beta_1, \beta_2, \ldots$	parameters from the postulated models	
$b_0, b_1, b_2, \ldots$	least-squares estimates of $\beta_0, \beta_1, \beta_2, \ldots$	
C	Centre distance between gear and hob	mm
C.D.	Cutting depth	mm
c_o	Cost of operating time	£/edge
c_p	Total cost/piece	£/piece
c_t	Total cost	£
C.L.A.	Centre line average	μ
D_h	Outside diameter of hob	mm
D_{peak}	Maximum displacement of vibration	μm
d_s	Diameter of shaft	mm
d	Full depth of cut	mm
d.f.	Degrees of freedom	

Symbol	Notation	Units
ded	dedendum	mm
D.P.	Normal diametral pitch	
E	Young's modulus	N/m^2
En?	Type of steel	
f	Axial feed rate	mm/rev
f_s	Helical feed rate	mm/rev
F_a	Maximum loading of the feeding mechanism	N
F-ratio	Variance ratio	
F.S.	Factor of safety	
G	Modulus of rigidity	N/m^2
H	Objective function	
H_{max}	Maximum C.L.A. reading	μ
HB	Brinell hardness	
HRC	Rockwell 'C' scale hardness	
H.P.	Horse power	h.p.
Hz	Hertz	c.p.m.
J	polar moment of inertia	$(m)^4$
K	stiffness	Kg/m
K_o	generating portion of the hob	mm
L	uncut-chip length	mm
m	gear module	mm
M	bending moment	Nm
MSS	mean sum of squares	

Symbol	Notation	Units
MTRL	material	
N_h	hob speed	r.p.m.
P_{av}	average force	N
P_m	maximum force	N
$\bar{P}_m$	average of maximum force	N
P_R	radial component of cutting force	N
P_T	tangential component of force	N
P_v	vertical component of force	N
p_i	predetermined probability level to satisfy the ith constraint	
q	number of parameters to be estimated	
$r(a_{ij}a_{ik})$	correlation coefficient between a_{ij} and a_{ik}	
r_h	outside radius of the hob	mm
S	uncut-chip thickness	mm
s_h	number of starts in the hob	
S_s	shear stress	N/m^2
S^2	variance of estimated error	
S.S	sum of squares	
S_{YP}	yield stress	N/m^2
STD	standard deviation	
S_R	surface roughness	μ
T	tool life	(min/edge)
t	time to machine a gear blank	min/piece

Symbol	Notation	Units
t_h	handling time	min/piece
$t_{\nu,\gamma/2}$	students t-statistic with ν degree of freedom and γ level of significance	
T_m	maximum torque	Nm
$\bar{T}_m$	average of maximum torque	Nm
T_{av}	average torque	Nm
U	specific energy	J/Kg
U.T.S.	ultimate tensile strength	N/m^2
V	cutting speed	m/min
V_s'	volume of metal removed	mm^3/rev
V_s	volume of metal removed per unit time	mm^3/min
V_T	total volume of metal removed	mm^3
W	work done in hobbing per revolution of the blank	mJ
W_p	electrical power	Watts
x_o	unity at all levals	
X	matrix of indenpendent variables	
X'	transpose of X	
$(X'X)^{-1}$	inverse if $(X'X)$	
$\hat{y}$	the predicted value of tool-life on a log-scale	
E(y)	expected value of the average tool-life on a log-scale	
y	observed response in a log-scale	
Z_g	number of teeth in the gear blank	
Z_n	number of teeth in actual contact	

Symbol	Notation	Units
σ_{max}	maximum shear stress	N/m^2
$\sigma_{\alpha_1}, \sigma_{\alpha_2}$, ..	standard deviation of α_1, α_2 , ..	
α	normal pressure angle	
β	helix angle of the gear	
γ	lead angle of the hob	
Γ	setting angle of the hob	
ψ	angle of engagement or mean contact angle	
η	mechanical efficiency	
††	significant at the level of 0.01	
†	significant at the level of 0.05	
n.s.	not significant	

CHAPTER I

INTRODUCTION

1.1 Hobbing (Principle of Process)

Hobbing is regarded as the most accurate method of gear production and more thought and mechanical skill have been expended on hobbing machines and their correct functioning than on any other type of gear cutting machine.

The process lends itself to the production of most types of gears, and it is unlikely to be superceded in the foreseeable future, especially when large externally toothed cylindrical gears of high accuracy are required.

1.2 The Conventional Hobbing Process

In principle, hobbing is a continuous generating process in which the hob is carried on a spindle, the axis of which is oriented at such an angle to the work axis that its thread meshes with the teeth of the gear being cut. The work and hob are then caused to rotate with uniform motion and with relative rotational speed. Cutting is effected by feeding the hob radially into the work, where the hob teeth trace out involute curves across the face of the workpiece in a direction parallel to the axis of rotation of the workpiece as shown in Fig.2.

The hob's thread profile will make contact with the teeth on the work in a series of points as cutting proceeds. The point becomes shallow elliptical slices in the metal being cut as each hob tooth makes contact with the work.

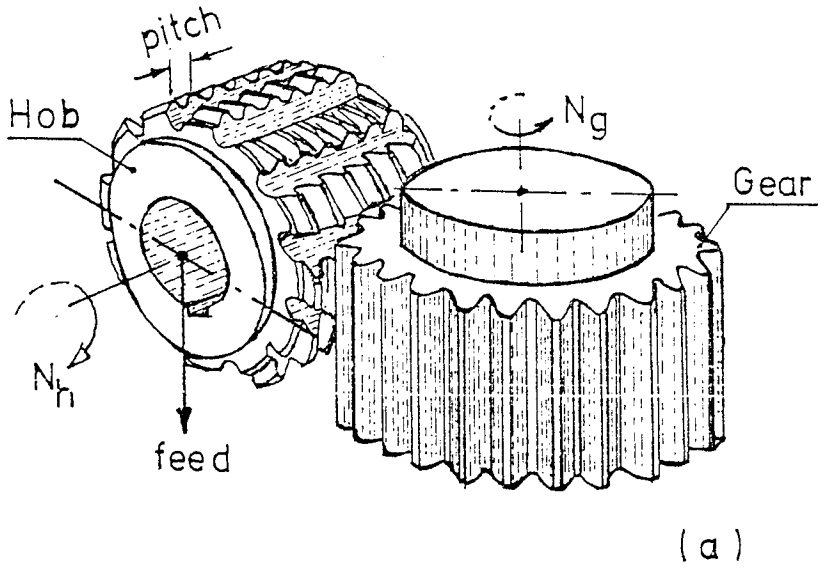

(a)

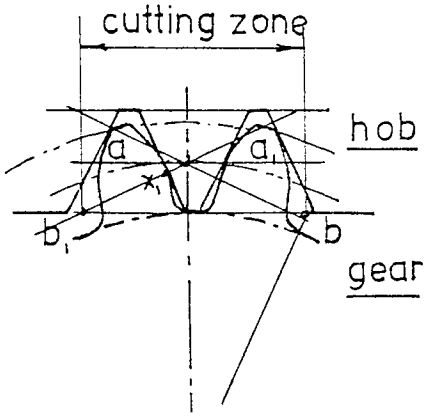

contact point
x_1 does not change

(b)

Fig. 2 CONVENTIONAL GEAR HOBBING

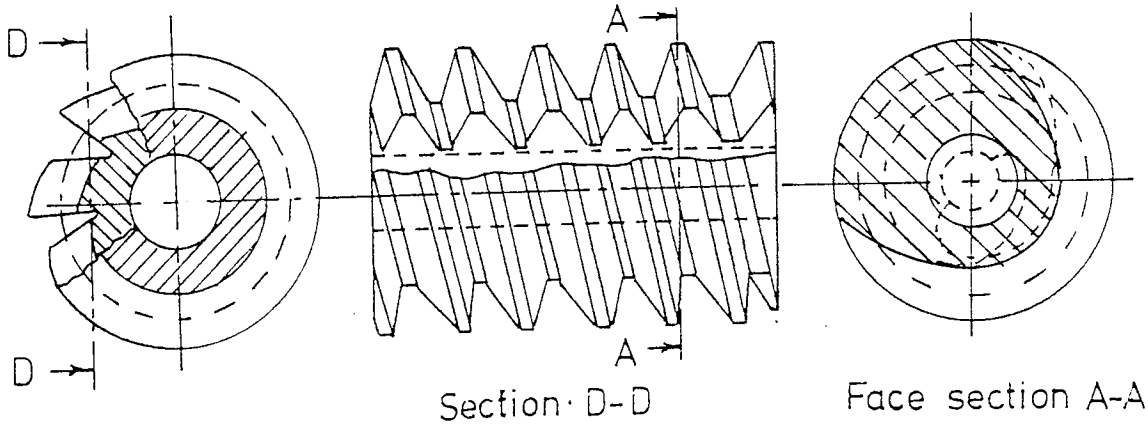

Section D-D

Face section A-A
of involute worm

Fig. 3 Involute worm as basic form of the hob

1.3 Hob Description

The conventional hob is made in high speed steel, hardened but not necessarily ground on the form. It can be likened to an involute worm provided with flutes or gashes usually at right angles to the helix and with the tooth profile suitably relieved behind the cutting edges thus formed. A number of threads may be provided but the single start is the most usual. This is preferred for the more accurate work while hobs of two or three starts are used for very high production where the gear is to be finished by some other medium.

1.4 Gear Hobs

As the worm-shaped hob is to produce an involute gear, its basic form must be that of an involute gear as shown in Fig.3. The basic hob body, the cutting edges lie on the flank faces, which represent an involute helical gear, more aptly termed an involute worm owing to the pronounced tooth helix.

As the cutting edges are formed by this involute helicoid intersecting with the radial helical rake, it assumes a curved shape due to the intersection of two helical planes.

The cutting edges must be suitably relieved to ensure the cutting action. For maintaining accuracy during sharpening, it is essential that the new cutting faces thus created lie in the same helicoid as when new.

The imaginary path of the cutting faces is termed the hob spiral, of which the profile represents that of an involute helical gear. Distinct from this, the basic profile of the hob

- as the basic profile of the standardized tooth system - represents a straight flank.

The difference between the profile of the hob spiral and the coresponding basic profile is in proportion to the lead angle of the hob spiral. With multi-start hobs, this difference is quite considerable, though frequently of little importance, particularly where the diameter of the single-start hob is adequate in relation to the module and an additional lead-in flank clearance is present.

In simplified form, hob frequently have axially parallel gashes which is in many cases fully adequate. The ideal form of the rake is a spiral perpendicular to that of the hob teeth. Hobs used on the highest precision work require a helical gash. This problem is not merely one of profile accuracy, but also of cutting efficiency.

A hob can operate in two ways: with feed in direction of the axis of the gear to be produced as shown in Fig. 4. for hobbing spur or helical gears when the individual cutting faces do not alter position. The progressive motion of the rack is not due to a physical displacement of the individual cutting faces but to the rotation of the teeth. Fig. 5 shows the feed to the cutter at a tangent to the workpiece for hobbing worm wheels. The individual cutting faces travel physically in the direction of the hob feed.

A third method offered is diagonal hobbing of spur and helical gears. This difference is more important than is generally realized, as it has to be taken into account when, for

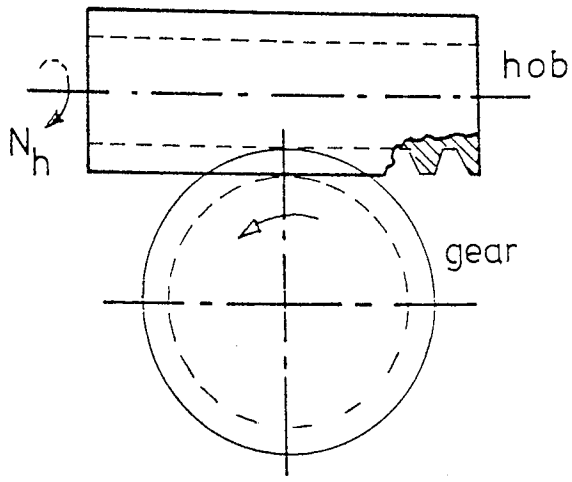

Fig. 4 FEED IN THE GEAR AXIS DIRECTION

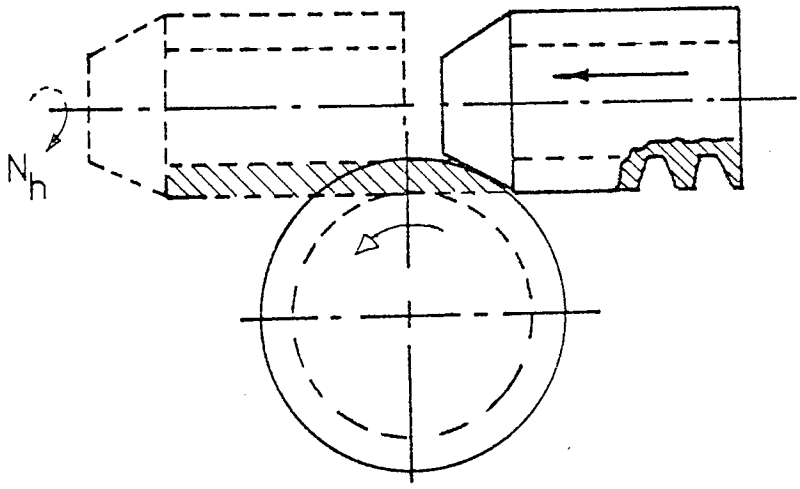

Fig. 5 FEED IN A TANGENT TO THE GEAR

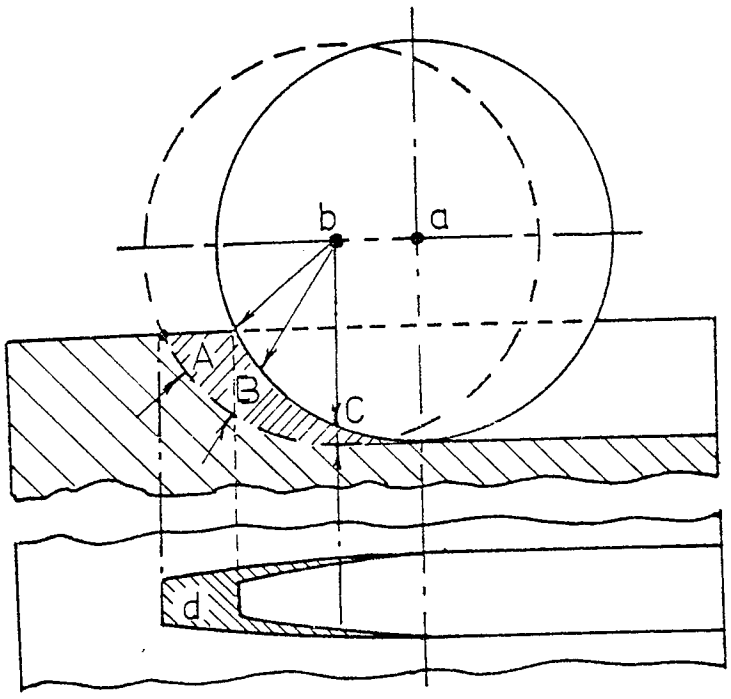

Fig. 6 CHIP THICKNESS DURING HOBBING

example, it is intended to assess the hob error on the gear produced.

In both cases the tooth form is produced by the hob representing a traversing rack against which the blank is rotated. The basic difference lies in the fact that with the tangential method each cutting face actually moves with the rack, whilst with axial feed method the traverse of the rack is only imaginary, each cutting face maintaining its position relative to the rack. Its travel is hereby merely the sequence of a row of hob teeth, each of which assumes a single enveloping position of the rack.

When hobbing worm wheels by the tangential method, each tooth of the hob cuts the complete profile from tip to root, whilst when hobbing spur and helical gears, the profile is produced by enveloping cuts from a complete row of teeth. Each individual hob tooth only cuts a short, definite portion of the profile.

The rule that a hob requires axial adjustment between sharpening to increase its useful life is not solely based on the fact that it is longer than required by the depth of engagement, but also on the realization that the element of wear on the hob teeth over the depth of engagement varies.

Fig. 6 shows the hob when advanced in the direction of the gear axis from position a to b, a comma shaped chip d will be produced in the section planes A, B and C removed by the individual teeth of the hob, shown in Fig.7 .

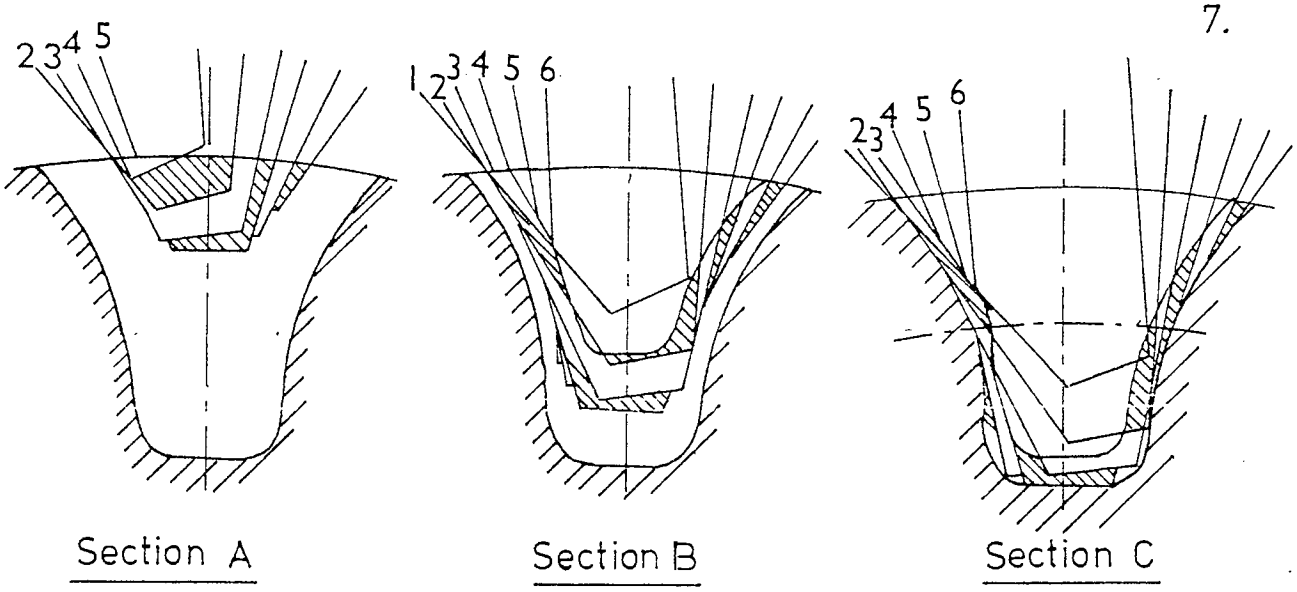

Fig. 7 SECTIONS A, B AND C IN FIG. 6

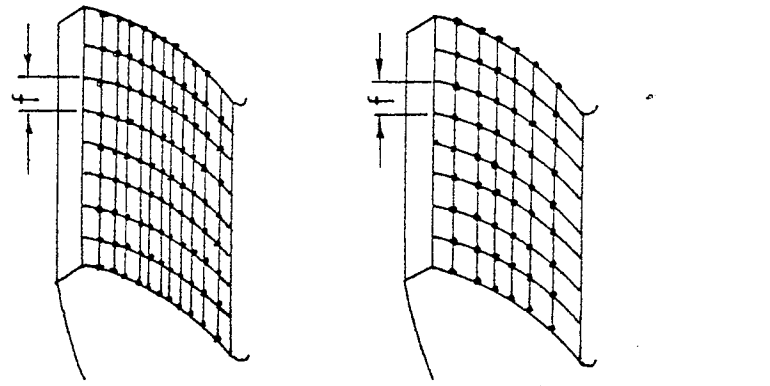

Fig. 8 Effect of number of starts on bedding points

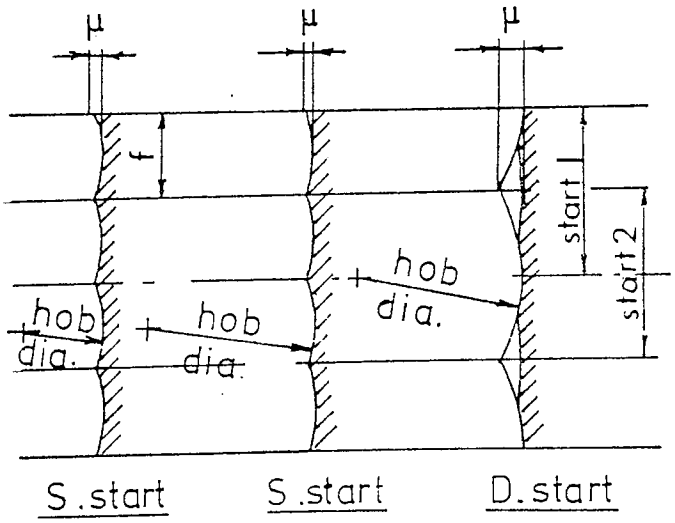

Fig. 9 Effect of number of starts on roughness

1.5 Multi-start Hobs

In the quest for shorter cutting times, spur and helical gear hobs made with more than one thread have always appeared attractive and hobs are sometimes made having two or even three threads. It has already been stated that in a single start hob one tooth only does the maximum amount of work for any particular axial position of the hob.

With a two-start hob, two teeth will carry the maximum load, provided that the hob has been mounted correctly and that the accuracy of single and multi-start hobs is the same. Multi-start hobs are not usually as accurate as single-start hobs owing to increased manufacturing difficulties though the effect on the work may be of little importance if a subsequent finishing process is applied. It is observed that for a specified cutting speed a two-start hob requires the hobbing machine table to rotate twice the speed when a single-start hob of the same diameter is used. This means that the machine must be capable of running at the increased speed without introducing excessive vibration.

The main point of interest in multiple-start hobs is that the number of facets on a tooth profile produced with a given feed is fewer than that obtained with a given feed is fewer than that obtained with a single-start hob as shown in Fig.8 . As a result the tooth profile is not such a smooth curve and in order to cut an acceptable shape, the feed per revolution of the work is made smaller than with a single start hob. Consequently, the advantage of the rate of production is not directly proportional to the number of threads in a multi-start hob.

Another point that affects the use of such hobs is that because fewer cuts are taken to generate an approximate involute curve, the amount of metal removed per cut is larger and this tends to reduce the period before resharpening becomes necessary.

It is clear from Fig. 9. that the tooth flank surface roughness increases with the increase in number of starts in the hob, providing the hob diameter and feed per revolution, f, are maintained constant, also by choosing a larger hob diameter, surface roughness will decrease, the permissible value of surface roughness before finishing is usually 1.8 microns.

Multi-start hobs have the same pitch accuracy as single-start hobs, and this eliminates a possible reason for not using them. Multi-start hobs may make a useful contribution to gear production.

1.6 Wear in Hobbing

The entering teeth of a generating hob are not involved in generating the tooth form as can be seen in Fig. 10. These entering teeth cut only 50 to 60 per cent of the material in the tooth valley.

The generation of involute form only occurs on the line of action. In practice, an even wear of the hob teeth is visible, therefore, the wear of the entering hob teeth is a factor larger than that of the involute generating teeth.

At tooth A, the hobbing work has been finished for about 50 per cent, whilst the cutting edge essentially has worked over

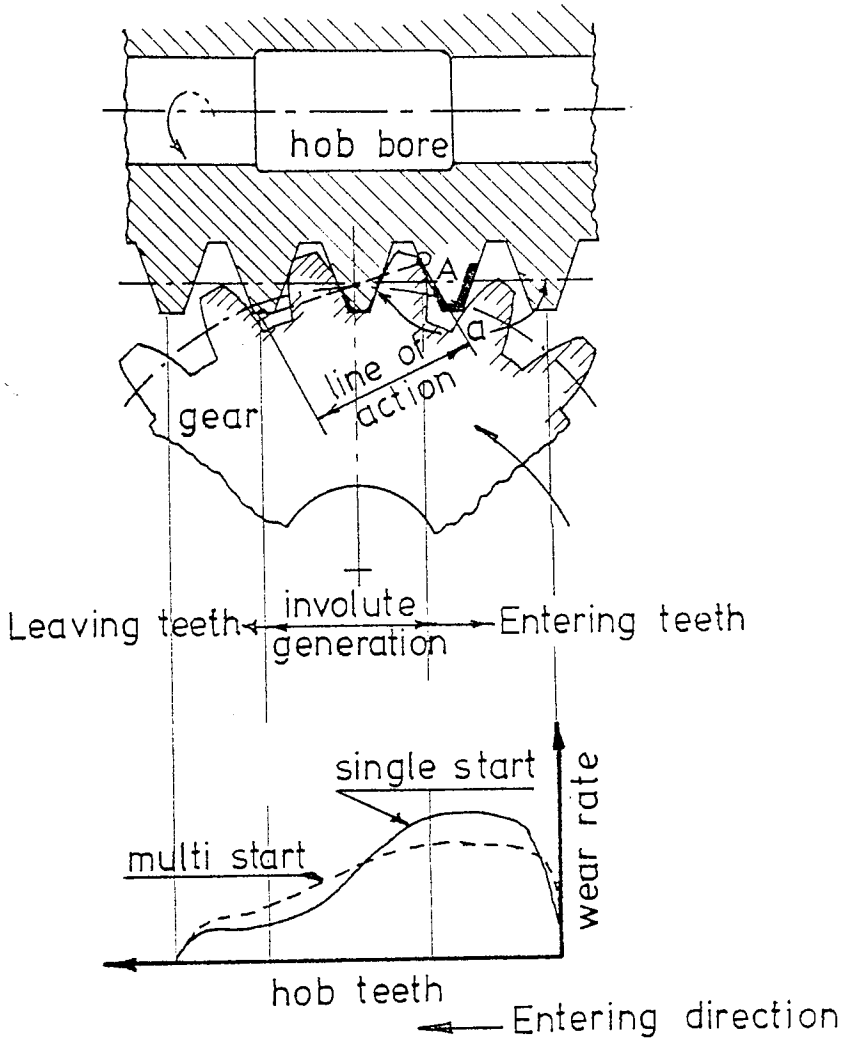

Fig.10 DISTRIBUTION OF HOB WEAR

the length a. This length a is worn most as shown in the bottom sketch of Fig. 10 .

With multi-start hobs "entering" occurs much faster, and the involute generating teeth are engaged more heavily in cutting work as well. This means a better wear distribution than with single-start hobs.

Practice has shown that the working life of a multi-start hob is longer than that of a single-start hob, as wear is less. A double-start hob, with the same feed and hob speed, will cut the gear twice as fast as a single start hob.

1.7 Methods of Hobbing

A number of methods in which gears can be produced by means of hobbing machines. These techniques are briefly described as follows:

a - climb/conventional hobbing

b - axial, tangential and radial feed

c - diagonal hobbing

d - oblique hobbing

e - worm generation

f - non-differential method

g - high speed hobbing

h - prime numbers of teeth

i - helical gears with prime number of teeth

j - cutting low helix angles

k - fly cutting

1.8 Why Hobbing as a Gear Cutting Process?

It was decided in this research to study hobbing as a gear cutting process for the following reasons:

i hobbing is versatile in that it can cover a variety of work including spur gears, helical gears, worms and worm wheels, splines and serrations and a variety of special forms.

ii there is no intermittent motion to give rise to errors, as the indexing is continuous.

iii there is no loss of time due to non-cutting on the return stroke.

iv there is no problem due to reversal of masses.

v it is possible to generate internal gears in a very limited application which involves a special hob head and cutting tools, and the gear diameter must be reasonably large.

vi the author felt as indicated in the literature survey that little work was done in the improvement and development in performance of gear-hobbing machines, from cutting and economy points of view.
There have been some contradictions in different reports which the author wanted to investigate, clarify and compare.

1.9 The Need for Investigation into the Hobbing Process

The exacting demends for producing accurate gears make it necessary to determine the cutting torques and forces coming on the hob shaft. Further, recent researches have indicated

that the determination of the cutting force behaviour is essential for analysing the produced gear teeth accuracy and surface finish[2] , and the stability of hobbing machine[9] , particularly the nature of variation of torques with respect to principle variables.

Literature research[1] indicates that the process of hobbing has been invented over a hundred years ago, and since then many investigations have been carried out for developing gear cutting machines on hte hobbing principle. However, not much work has been found until recently in the field of mechanics of hobbing during gear cutting process.

Ueno [28], Padham [4] and Severilov [12] have investigated the torque coming on the hob shaft. Rozenberg and Adam [21] also attempted to experimentally determine an expression for the torque in hobbing process.

Bhattacharyya [2] and Cook [6] have investigated the magnitude and nature of the tangential and radial components of the cutting force during conventional and the climb hobbing process.

In these reports the effect of cutting parameters on torques and forces has been studied, but nowhere in any of these references has the significance of the cutting parameters been tested statistically, and it was also reported that cutting speed has little or no effect on torques and power consumed during hobbing.

The first part of this work is being carried out in order to assess readily a method of determining cutting torque encountered by hob shaft during hobbing gears, a specially designed torque dynamometer [2] was used for this purpose.

A Wattmeter was used to evaluate power consumed during the hobbing of spur and helical gears, torques and power observations occurred by changing various cutting parameters measured according to a statistically designed experiment.

The results were analysed, compared with previous researches and tested,; the relationship between maximum cutting torque, average power consumed and various cutting parameters were established.

Unlike others, the effect of cutting speed was shown to have a significant effect both upon cutting torques and power consumed in conventional hobbing. This conclusion resulted in the publication of reference [20].

There are, of course, many different gearing arrangements depending upon the angular relationships between the shafts to be geared together, and the tolerances acceptable in manufacture vary greatly. In clock manufacture, one is interested in the number of teeth on the gear wheel and the tooth form is not important. Gears for armaments and transmissions depend upon gears that are accurate in every respect.

Most gear teeth, when they are in mesh, have line contact and, as can be imagined, the pressure on the line of contact is very large. Combine this with the condition that the gear teeth slide along each other and it can be seen that surface

roughness is a very important factor in gear production.

The nature of gear teeth surface texture is discussed in the second part of this investigation and tests were conducted on four different steel blanks in order to observe the effect of cutting parameters on gear teeth surface roughness in the direction of axial feed.

It is important to distinguish how the chips are removed in the process of hobbing. Like milling, there are two methods, the first one being the conventional manner of hobbing, the other being the climb-hobbing. In the conventional hobbing, the so-called "comma-chip" is obtained from the thin end, while in climb hobbing, the chip starts at its thicker end.

In metal cutting practice, it is assumed that the cutting forces primarily vary in milling and similar processes because of the variation of chip thickness. However, the variation of cutting forces also depends upon many other parameters involved with the type of process itself. In turning and similar operations, the width and depth of cut are clearly defined and measured. However, in hobbing both quantities of width and depth of cut vary during the cutter rotation in hobbing, chips are being removed from the periphery as well as from both the flanks of the tooth profile. Hence, the chips are non-uniform and irregular in shape.

Generally, it is assumed that relative vibration between the tool and workpiece causes variation of cutting force. Mostly it is further assumed that the cutting force varies because of the variation of chip thickness.

In hobbing machines, chatter may often be encountered which strongly limits the rate of production. Chatter in hobbing has some special features distinguising it from chatter on other kinds of machine tools. Direct application of the published methods of chatter analysis, as in refs.[25], [26] and [27] on hobbing is difficult. Slavicek[9] modified the theory of chatter with respect to the special aspects of hobbing.

The report concluded that stability of hobbing depends strongly on the parameters of the cutting process, namely, on the number of teeth of the blank, module, axial feed rate and the diameter and the number of hob gashes. The report, however, did not consider hob speed as a factor affecting vibration, and the analysis was conducted under the following assumptions:

a) the mean width of chip on both side edges is equal

b) the mean width of chip on one side is approximately equal to that on the peripheral edge[39].

These assumptions were obtained from experimental data without any theoretical background.

The third part of this work concerns an investigation which was carried out into the effect of cutting parameters upon the machine tool structure vibration, where cutting speed was found to have a significant influence on machine vibration.

In hobbing, the influence of cutting conditions is more complex than in orthogonal cutting, many teeth of the

the hob cutting simultaneously with very different width and thickness of chip, these varying also during the rotation of the hob. It is difficult to determine the total width of chip on the bottom and the flank, which have an essential influence on torque, surface finish and stability. Moreover, both these values significantly depend on the parameters of the cutting process, e.g. on the blank diameter, D.P., hob diameter and number of gashes, axial feed rate, depth of cut, etc.

Principally, however, the analysis of the influence of these parameters on the width and thickness of chips enables one to determine their influence on torques and stability, and to explain certain experimentally obtained results.

In part four of this investigation a practical method is presented to calculate the volume of metal removed during hobbing, the theory of action of peripheral and side edges of the hob is attempted as well as a theoretical evaluation of hob wear, and an analytical method of calculating uncut-chip width created by top and side cutting edges during hob rotation is presented.

Tool-life is an important parameter in assessing manufacturing costs in metal cutting operations. It has a direct influence on the physical operation of the plant as well as on the economic and profitability of cutting.

In recent years, the number of people involved with the development and evaluation of improved cutting tool materials has grown considerably. But very little work was done in the field of gear hobbing mainly in Japan and the USSR.

In part five of this work, the wear mechanism in hobbing is discussed, the cutting parameters affecting hob life are analysed and a general mathematical model to describe hob life in terms of six independent variables is established together with the estimated error variance.

Finally, part six combines all the previous effects of cutting parameters to give a general viewpoint into the economic problem in gear hobbing where at least the fundamental variables are included in the analysis in terms of the reduction in machining cost. The concept of chance-constrained programming is used to determine the optimum cutting conditions considering the probalistic nature of the objective function and constraints.

CHAPTER II

PREVIOUS RESEARCH INTO THE SUBJECT

2.1 General Introduction

Hobbing as a method of gear production seems to have had a long struggle before it became accepted. The earliest recorded hobs were made by Bodmer before 1840.[47]

Prior to the introduction of hobbing machines, Germany had not made a major contribution to practical methods of gear production, though development of known methods have received considerable attention. The man who separately first designed and made successful special purpose hobbing machines capable of cutting helical gears were Jungst and Reinecker while a few years later in 1897, Hermann Pfauter patented the first universal gear hobbing machine.[42]

A literature survey [1] on the hobbing process shows that earlier work has been concentrated upon finding the cause of the periodic errors resulting from kinematic and transmission drive.

As early as 1905, Parsons determined periodic errors in the drive system of the machine table. Kinematic errors, owing to transmission drive, were in the worm reduction gear which gave rise to errors in gear blanks during hobbing.

A creep mechanism was then designed which overcame these errors and distributed them uniformly around the blank during cutting.

There are other factors which cause errors in hobbing. The obvious and wellknown factor in the machine-tool is the deflection of the machine's structure caused by the dynamic behaviour of the cutting forces. However, not much work has been found until recently in the field of mechanics of hobbing during the gear cutting process.

2.2 Assessment of Torques and Forces during Hobbing

To meet the increasing demands for raising productivity as well as for cutting harder gear materials with reasonable accuracy, it is necessary to determine the different cutting forces and torques.

It is important to distinguish how the chips are removed in the process of hobbing. Like milling, there are two methods, the first one being the conventional manner of hobbing, the other being the climb hobbing. It is assumed that the cutting forces primarily vary in milling and similar processes because of the variation of chip thickness. However, the variation of cutting forces also depends upon many other parameters involved with the type of process itself.

During hobbing, both peripheral and side edges of the hob remove the chips. However, the main part of the chip volume is cut off by peripheral edges. The side edges merely shape the teeth. The edges do not cut simultaneously, and the width

of cut is different at the different positions of the cutting edge. Work by Bhattacharyya [2] showed that the forces on the plane of the basic rack can be obtained by simulation with respect to the metal cutting process. The tangential components of the cutting force was estimated as follows:

$$P_T = \bar{K} \cos \eta \frac{\Sigma \Sigma}{z_n \; i} A_i \qquad (1)$$

where; P_T is the tangential component of the cutting force

$\bar{K}$ is a constant

Z_n is the number of teeth in actual contact

A_i is the area of cut at the i^{th} side

i is the number of starts in the hob

η is the friction angle

The report suggested that it was very difficult to estimate the instantaneous variation of the area of cut of equation (1) and a convenient approach for estimating the tangential cutting force P_T is to be obtained from the specific energy of cutting.

An interpolation of maximum torque, average of maximum torque and average cutting torque from the energy principle can be obtained from [3].

P.E.R.A. [4] in its survey outlines the theoretical method of estimating the cutting forces by measuring the power during the hobbing process.

2.3 Measurement of Cutting Forces and Torques

Determination of cutting forces and torques in magnitude and direction is important to analyse the metal cutting operations quantitatively; certain observations must be made before, during and after a cut.

The number of observations that can be made during the cutting process is rather limited, one of the more important measurements of this type being the determination of magnitude and direction of the cutting force components.

Dynamometers are used to measure forces and torques exerted upom a cutting tool or the workpiece. The two main requirements which must be satisfied in the dynamometer design are sensitivity and rigidity.

The main three cutting force components in hobbing are, the tangential component (P_T), the radial component (P_R) and the vertical component (P_V).

2.3.1 Torque Dynamometers

The principle of torque dynamometers is to measure the tangential component of hobbing force from the twisting moment of the hob shaft by means of four active strain gauges which are cemented at right angles to each other, the gauges rotating while the measuring instruments are stationary. A form of collector rings or slip rings assembly will be necessary to maintain electrical contact between the instrument and gauges. The slip ring contact resistance variation must be minimised

during electrical installation of the system. The most efficiently designed dynamometer will be of little value if the measuring instrument used with it is not accurate or sensitive enough, or does not have a frequency response that is sufficiently high to follow significant fluctuations of torques. Examples of Torque Dynamometer and the relevant instrumentation are shown in detail in references [3], [4] and [5].

2.3.2 Three-component Force Dynamometers

The principle of the three component dynamometers is to measure the magnitude of the cutting forces in three directions, the gear blank mounted on the dynamometer which could be fixed on the machine, or to rotate with the gear blank. Many special types of three component force dynamometers were designed. A top hat dynamometer is one where the measuring section is a thin cylindrical shell attached to rigid top and bottom plates. The reaction is conveyed by the dynamometer and recorded on an electrical recorder [6] and [7]. A three-component ring-type dynamometer has been designed [27], where strain-rings were fixed on the work table surface, a thrust bearing separates the gear blank and the dynamometer.

The principle of strain-rings is well known and can be seen from references [18] and [19].

Khardin [8] has measured the three force-components on a dynamometer using the strain-gauge technique, the strain-gauges mounted in tailstock and bottom centre of the work mandrel and the signal transmitted by means of slip-rings.

2.4 Assessment of Power Consumed During Cutting

To determine whether the maximum cutting torques or average cutting power used in hobbing were proportional to the rate of metal removal of workpiece, necessitates the investigation of input power to the main drive motor. The cutting power can be calculated theoretically from the cutting torque relationship and the work done by the hob. The following equation describes the relationship between average power consumed and the average cutting torque:

$$W_p = \frac{N_h \cdot T_{av}}{1.95} \qquad (2)$$

where: W_p is the average power consumed during cutting, watts.

N_h is the hob speed, r.p.m.

T_{av} is the average cutting torque, lb.in.

The procedure for measurement of power consumed during cutting depends on the machine drive system, for the induction type main drive motor operates at main voltage of 440 volts, 3-phase A.C. circuit. The measurement of power can be carried out by using the following methods:

a) Star connected balanced load with neutral point accessible, where a wattmeter is connected with its current coil in one line and the voltage circuit between that line and the neutral point. Or a single phase wattmeter is used in conjunction with "Y" box or key type series plug.

b) Balanced or unbalanced load, star or delta connected. "The two wattmeter method".

Where the total power is the algebraic sum of two readings under all conditions of load and power factor [4].

2.5 Variation of Torques, Forces and Power During Hobbing

To meet the increasing demands for raising productivity as well as for cutting harder gear materials with reasonable accuracy, it is necessary to analyse the variation of torques, forces and power consumed during cutting with respect to the cutting parameters.

In metal cutting practice, it is assumed that the cutting forces primarily vary in milling and similar processes because of the variation of chip thickness. However, the variation of cutting torques and forces also depends on many other parameters involved with the type of process itself, like changing tool Geometry, changing cutting parameters, speed, feed and so forth.

Bhattacharyya[2] has observed the components of cutting forces during the process of hobbing for different feeds and modules for finding the tangential and radial components of the hobbing force P_T and P_R respectively, his analysis showed that the effect of module and feed on the force components were given by:

$$P_T = 43\ m^{1.50}\ f^{0.75} \quad \text{kg} \qquad (3)$$

$$P_R = 40\ m^{1.96}\ f^{0.55} \quad \text{kg} \qquad (4)$$

It was seen that the exponent of module agrees well with the analytical estimated exponent, but the author did not consider

the cutting speed in his research as well as other cutting parameters such as the number of teeth in the blank and material hardness.

Cook and Welbourn [6], [7] suggested in their investigation on the variation of peak cutting force components when varying the cutting parameters for spur and helical gears, that the peak vertical force component is proportional to: axial feed$^{0.8}$ X Diametral Pitch$^{-1.3}$ X blank hardness (approximate formula). The report also suggests that cutting speed had little effect on the peak cutting force within the range covered.

Inozemtsev [11] in an attempt to observe the effect of changing the hob cutting edge geometry on the cutting forces, measured all three components of the cutting force. However, only the tangential component was considered. His analysis made it possible to draw the following conclusions:

1. Radial rake has a great effect on the cutting force, and positive radial rake considerably reduces the cutting forces.
2. The peripheral clearance angle has a greater effect on the cutting force than radial rake.
3. The hobs with positive radial rake and greater clearance angle give better dynamics of cutting.
4. The two-start hob with improved cutting edge geometry cuts almost as easily as a single-start conventional hob.
5. Straight gashes reduce cutting force and increase uniformity of cutting. Therefore, from the point of view of dynamics of cutting it is advisable to manufacture

hobs with straight gashes.

The author based his conclusions on constant cutting conditions, where, cutting speed was 75,4 ft/min., axial feed 0.059 in/rev., number of teeth 35 and depth of cut 0.338 in., which make his results very limited.

A report by the Japanese Government mechanical laboratory [3] was the first and foremost step in measurement of maximum and average cutting force acting tangentially to the hob. The report shows clearly, backed by experimental results the variation of tangential force and power consumed in both climb and conventional hobbing, with and without the use of coolant, for different gear blank materials. A theoretical evaluation of ship thickness was attempted, but not compared with experimental results, the report also related the force and power variation to one cutting parameter at a time, which shows only the individual effect on the response.

Padham[4] studied the relationship between maximum cutting torque, average power consumed during cutting and a host of variable cutting parameters v.i., axial feed, cutting speed and material hardness. Different hob sizes were used to conduct tests to generate spur gears in a conventional hobbing method.

The thesis dissertation describes fully the relationship between torques and power versus axial feed, module, cutting speed and material hardness, one variable at a time, and the following observations were recorded:-

1. The cutting torques were found to drop with increasing the cutting speed and to increase less than linearly with axial feed.
2. The magnitude of cutting torques increased considerably with increase in gear module.
3. The cutting power (in watts) increases sharply with increase in module, and rises rapidly with an increase in hob speed.

Severilov [12] describes that Donetsk Engineering Works had carried out complex investigations into the power relationships when cutting spur gears with relieved (standard) and non-relieved hobs. As a result, general relationships were established between average and maximum cutting torques on the one hand, and the main ancillary parameters of the process on the other. The results showed that no monotic function exists for average torque as a function of the Brinell number in a wide range of hardness variation; the module was found to have a substantial effect on the torque.

In an attempt to explain the effect of the number of teeth on the torque, many authors have come to contradictory conclusions; this is connected with the complex influence of the number of teeth on the cutting parameters.

Sheryshev [14] investigated force and temperature relationships in hobbing Titanium alloy steel gears. The report indicated that when hobbing with cutting fluid the cutting force is reduced by 20 to 30%, cutting speed has a greater influence on the cutting temperature than the feed rate, gear module has a great effect on the cutting force, and the number of teeth in the gear had no influence on cutting temperature and force.

2.6 Stability of Hobbing Machines

In hobbing machines chatter may often be encountered which strongly limits the rate of production. Chatter in hobbing has some special features distinguishing it from chatter on other kinds of machine tools.

The hobbing process itself differs considerably from other kinds of machining. In orthogonal cutting the width and thickness of cut are clearly defined, In hobbing, however, both quantities vary in a wide range during the revolution of the tool. Generally it is assumed that relative vibration between the tool and workpiece causes vibration of the cutting force. Mostly it is further assumed that the cutting force varies because of the variation of the chip thickness[3] .

In hobbing, chips being cut from the bottom as well as from both flanks of the hob profile. Consequently, vibrations of any direction in the plane perpendicular to the cutting speed will influence the cutting force.

The theory of chatter was modified with respect to the special aspects of hobbing[9] , and the role of the structure of the hobbing machine as based on experimental results was described[10] .

Slavicek[9] indicated in his paper that the determination of the cutting force behaviour is essential to analyse the stability of the hobbing machine, and has further described the influence of cutting parameters of the process on stability where the maximum width of the contact area, L depends upon: the number of teeth in the blank, Zg, module, m, and the axial feed rate, f, as follows:

$$L = 0273\ f^{0.17}\ Zg^{0.61}\ m^{1.18} \qquad (5)$$

Then the total width of chip on the peripheral edges, b was approximated as a portion of the width, L as follows:

$$b = 0.22\ L \qquad (6)$$

The limits of stability were determined from Eq. (6), and the results showed that stability of hobbing depends strongly on module, axial feed rate, number of teeth in the blank, hob diameter and number of gashes in the hob; it was also suggested that with the increase of module, the width of chip increases and therefore, stability decreases.

It is not evident however, from the results as to what effect speed has upon the stability or other parameters as Eqs. (5) and (6) are empiric and the significance of the parameters is not clear.

2.7 The Mechanics of uncut-chip during Hobbing

Principally, the anlysis of the influence of the parameters of the cutting process on chip width and chip thickness enables one to determine their influence in order to explain certain experimentally obtained results. Russian and Japanese researchers have been most active in this field and many papers giving lengthy calculations and formulae have been put forward. Although a wide range of actual references has been collected only a limited number have been fully translated, owing to

translation difficulties, time and expense. Others have been partly translated and relevant information subtracted.

Fundamental distinction was found between the work of the peripheral cutting edges of the hob and the work of the edges cutting the flanks of the gear teeth. Peripheral edges cut off a major part of the gear blank material while side edges merely shape the flanks. The ratio of the work of both kinds of edges is shown by Sidorenko[39].

The traces of the top cutting edges in action and the profile of the generated root surface of the gear was calculated by Wakuri [28] and thickness S and length L of the chips created by the top cutting edges of the hob was estimated.

Most researchers concentrated on the theory of action of the top cutting edges of hob teeth under the assumption that it cuts off the major part of material, and side edge chips is not of interest from the production and wear point of view. It is clear, however, that the chip width and thickness on the side edges have the same influence on stability as those on the peripheral edges.

2.8 Tool Wear and Tool-life in Hobbing

In recent years, the number of people involved with the development and evaluation of improved cutting tool materials has grown considerably. But very little research work was carried out in the field of gear hobbing, and the present trend goes towards the development of hobs with sintered carbide blades.

Description of tool wear is important as the practical consequences of tool wear, vary from both cutting conditions and the quality specifications of the material being machined. As a result, tool-life will have different meanings in different contexts.

Early work by Rapp [15] suggested a controlling factor in determining hob life is the rapid breaking down of the corners of the hob teeth. The following statements were made, based upon his results:

1. Any low-carbon steel, with hardness under 225 Brinell, can be hobbed at speeds of 275 to 300 ft/min and feeds of 0.090 to 0.100 ipr, with excellent tool life and quality.
2. The limiting factor in hobbing the heavier pitches is not the tool wear, but the hobbing machines themselves.
3. Relatively small changes in speed can affect hob life greatly, especially above 300 ft/min.
4. Climb hobbing in almost every instance results in greater tool life and improved surface finish.
5. The development of high positive rake angle allows speeds between 300 and 350 ft/min which, with light feeds, will produce gears having a high degree of accuracy and surface finish.

Inozemtsev [11] observed the influence of changed cutting geometry on the hob life; the wear was measured on the clearance and rake faces. In all cases the right sides of the tooth tips located in a plane at right angles to the centre axis

were subject to greater wear. The analysis of the report showed that increase of the clearance angle reduces hob wear, as well as for positive radial rake. Results also indicated that backed off hobs with modified cutting edge geometry have 3 to 4 times greater life compared with conventional hobs.

It is noted here that the above conclusions were based upon constant cutting conditions, and a different cutting speed was selected when testing each hob. Therefore there is no correlation between the results.

To meet the increasing demands for cutting harder gear materials, the development of hobs with sintered carbide blades has been urged. This kind of hob, however, has not come into practical use yet for steel gears except with those of fine modules because of technical and economic difficulties. From the technical view, chipping, which occasionally occurs at the cutting edges results in the distrust of users on the sintered carbide hobs.

Investigations have been made with sintered carbide hobs, in which only finishing of hardened gears has been carried out.

Fujikawa [13] attempted to find out the optimum cutting conditions experimentally for hobbing carbon steel gears with sintered carbide hobs. Tool-life criteria was determined by the values of flank wear at the corner and top edges of each cutting tooth (including chipping) exceeding the masimum value of 1mm. The report suggests that the progress

of flank wear is decreased with an increase in feed rate, and a better result may be expected with higher cutting speed and larger feed rate on a specially designed hobbing machine. It was also believed that productivity in hobbing will be raised several times by utilizing sintered carbide hobs.

In the investigation, the author varied one cutting parameter at a time while the other parameters were kept constant. Therefore the obtained optimum cutting conditions is just a special case and cannot be generalised.

CHAPTER III

GENERAL SET UP

3.1 Machine Set-up

A HV-14 type "SYKES" Universal Gear Hobbing Machine has been employed in the present study, conventional hobbing method being employed, where the hob is fed axially in a direction the same as that in which the cutting edge approaches the work. The machine is not equipped for climb hobbing.

Some of the main specifications of "SYKES" HV-14 are shown in table 1.

Table 1 Machine Specifications

Outside diameter:	Maximum with steady column	14 in.
	without steady column	15 in.
	Face width without steady column	9 in.
Feeds:	Variation by means of pick-off gears Maximum 0.160 i.p.r.	
Hob speeds:	6 obtained by means of pick-off gears. With standard 2 H.P., 1425 r.p.m. motor: 74, 92, 115, 143, 178, 224 r.p.m.	
Pitch:	Spur gears 6 D.P. 4.2mm Module. 0.525 in. C.P. Helicals, 45-deg., 7 D.P. Depending on material and type of hob head.	
Number of teeth:	Minimum 6. Maximum 600 approx.	
Work table:	Diam. 11 in. (280mm), Bored 2.75 in. reducing to 1.75 in.	
Centres:	Hob spindle to work table, Max. 9 in., Min. 1¼ in.	
Height:	Work table to arbor support, Max. 17¼ in.	

* For full details see capacity charts in "Sykes" operators Handbook.

Cutting conditions, type of material and type of tooling determine the appropriate setting up of cutting speeds and rate of metal removal.

3.2 Setting the hob

When cutting a tooth space there is normally one tooth only in a hob that cuts the full tooth space. The question then arises whether the hob should be so located axially that this tooth lies on the common normal between the hob and the work axis. In practice, this is of no importance for numbers of teeth exceeding eleven, since the process of generation produces a smooth curve that approximates closely to the theoretical involute.

When setting up each hob, the taper and locating diameter of the hob arbor and spindle were carefully cleaned and fitted to the machine, checking with a dial indicator showed true running.

The hob axis must be aligned relative to the gear axis and consideration must be given to the hob helix angle. When a spur gear is cut the hob head is set at the helix angle of the hob, and for helical gears it is set at the helix angle of the gear plus or minus the helix angle of the hob. The correct setting of the hob head relative to the gear for various combinations of hand of helix is shown in Fig. 11.

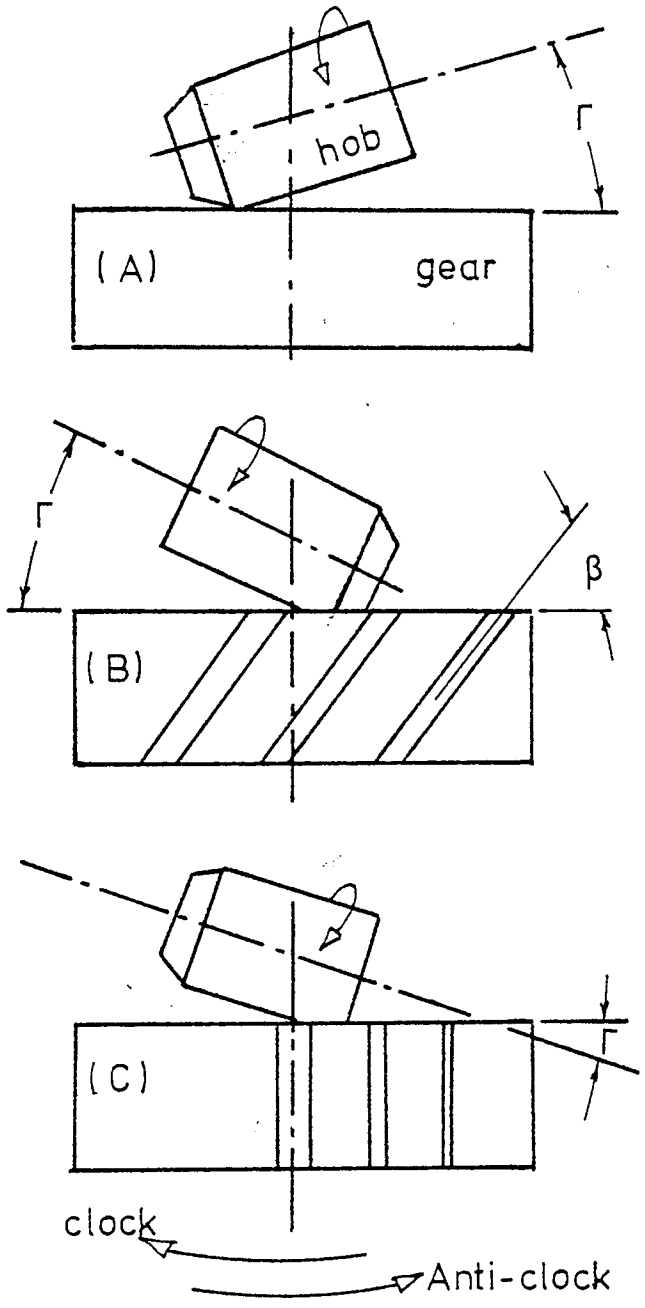

Type of gear		hob	Diag. Table		Γ
Spur gears		RH	C	Anti-clock	γ
		LH	A	clock	γ
Helical gears	RH	RH	A	Anti-clock	β-γ
		LH	A	clock	β+γ
	LH	RH	B	Anti-clock	β+γ
		LH	B	clock	β-γ

Fig.11 SETTING OF THE HOB HEAD

3.3 Selection of hobs

Single start hobs conforming to BS 2062/1963 (Grade B) specification have been used in the present study, The particulars of the three hobs used are shown in Table 2.

Table 2 Hob Specifications

Hob number	1	2	3
Normal D.P.	8	10	12
Module, mm	3.1749	2.540	2.117
Rake angle	0	0	0
Helix angle	2° 40′	2° 6′	1° 53′
Addendum	0.1250 in. (3.175 mm)	0.1000 in. (2.540 mm)	0.0833 in. (2.1158 mm)
Dedendum	0.1563 in. (3.970 mm)	0.1250 in. (3.175 mm)	0.1041 in. (2.644 mm)
Pressure angle	20°	20°	20°
Bore	1.250 in. (3.175 mm)	1.250 in. (3.175 mm)	1.250 in. (3.175 mm)
Type	S.S.R.H.	S.S.R.H.	S.S.R.H. *
Sykes number	HP 132-9/RN	HP 368-20/VZE	HP 32/AG
Cutting depth	0.2813 in. (7.145 mm)	0.2250 in. (5.715 mm)	0.1875 in. (4.762 mm)

* S.S.R.H. is single start Right Hand Hobs
Conform to BS 2062/1963 (Grade B).

From the manufacturing practice of hobs, a relationship between the outside diameter of the hobs and their module is often observed. By plotting the Sykes' data per size of hobs,

a relationship of the form:

$$D_h = 43\ m^{0.48} \quad \text{mm} \qquad (26)$$

has been obtained. This relationship has been used in the theoretical calculations and analysis for cutting forces and energy consumption during the hobbing process.

3.4 Gear Blank Materials

It was decided in the present study to investigate the variation in dynamic effects when using different types of blank material. Upon this decision and to improve the statistical design of experiment to cover a wider range of material hardness [20], four types of steel, namely, En 1A, En 8, En 34 and En 16T were used. The choice of these steels was determined by the tensile strength and hardness. The chemical compositions and mechanical properties of the blank materials conform to BS 970:1955 and are shown in Table 3.

En 1A and En 8 steels were ordered in 5in. O.D. bright finished hot rolled bars, En 34 was available in 5¼ in. O.D. black steel bars, and En 16T was available in 4½ in. steel bars.

The blanks were cut off from the bars, drilled and reamed, faced and turned to size. It was decided to keep the blank diameters constant in order to observe and analyse the effect of cutting parameters on the mechanics of gear hobbing. The blank specifications are given in Table 4.

Table 3 The Material Properties

Specification	Type of Steel	Chemical Composition, per cent								Tensile strength, min tons/sq.in.	Elongation %
		C	Si	Mn	Ni	Cr	Mo	S	P		
En 1A	Free-cutting steel	0.07/0.015	0.10 max	0.80/1.20	-	-	-	0.20/0.30	0.070 max	32	26
En 8	40 Carbon steel or mild steel	0.35/0.45	0.050/0.35	0.60/1.00	-	-	-	0.060 max	0.060 max	35	20
En 34	2 per cent nickel -molybdenum (low C)	0.14/0.20	0.10/0.35	0.30/0.60	1.50/2.00	-	0.20/0.30	0.050 max	0.050 max	45	18
En 16T	Manganese-moly -bdenum	0.30/0.40	0.10/0.35	1.30/1.80	-	-	0.20/0.35	0.050 max	0.050 max	65/75	11

Table 4 Gear blank specifications

Gear blank number	1	2	3
Number of teeth	29	36	44
D.P.	8	10	12
Pitch diam., in.	3.375 (85.725 mm)	3.600 (91.44 mm)	3.666 (93.12 mm)
Outside diam., in.	3.875 (98.425 mm)	3.800 (96.52 mm)	3.833 (97.358 mm)
Width of blank, in.	1.000 (25.4 mm)	1.000 (52.4 mm)	1.000 (52.4 mm)

It is observed that the blank outside diam. varied between 1.067 mm and 1.905 mm., this variation, however, was unavoidable in order to maintain the finished gear dimensions, but has no significant effect on the results.

Measurement of hardness

Readings of Brinell Hardness Number (H_B) were taken at three different positions on the machined blanks for each type of steel, the average (H_B) readings are given below.

Material	Avg. H_B
En 1A	115
En 8	183
En 34	164
En 16T	269

3.5 Feed and Speed Gears

For a complete range of feeds, the necessary gears, which are 1.25mm. module, are as follows:

20, 24, 30, 40, 60, 80 and 90 teeth.

The axial feed in inches per table revolution is obtained from a graph and multiplied by correction factor. The available axial feeds are as follows:
0.024, 0.030, 0.036, 0.040, 0.043, 0.047, 0.050, 0.053, 0.058, 0.060, 0.068, 0.078 and 0.090 i.p.r.

It is normal practice to finish the gear in one cut excepting for very high tensile steel when a high degree of surface finish is required.

The speed gears are located at the right hand side of the machine, the hob speeds in r.p.m. are given as follows,

74, 92, 115, 143, 178 and 224 r.p.m.

3.6 Helical Hobbing

It is possible to hob helical gears without using the differential. There may be, however, some difficulty in obtaining the ratio with required accuracy.

The following formula gives the required ratio,

$$\text{ratio} = \frac{\text{Lead/feed}}{(\text{Lead/feed}) \pm 1} = \frac{12}{Z_g} \qquad (7)$$

The + sign is used where hob and gear are of opposite hand, and - sign when of the same hand.

The differential is normally used when hobbing accurate helical gears; small errors were observed when the helix angle was 30°. An error of 0.033 mm. appeared in the lead of 80 cm. and an error of 0.104 mm. was observed in the lead of 125 cm. when the helix angle was 45°.

CHAPTER IV

ASSESSMENT OF TORQUES AND POWER CONSUMED DURING HOBBING

4.1 Introduction

The measurement of cutting forces coming on the hob shaft have recently become essential to evaluate its effect on the accuracy of the gears produced and the structural variations of the machine. Furthermore, these forces help in determining the effects of gear train dynamics of the machine. Slavicek has indicated in his report that the determination of the cutting forces behaviour is essential for analysing the stability of the hobbing machine.

The object of investigation and execution of this section is as follows:-

1. To measure, record and assess readily the magnitude of cutting torques coming on the hob arbor shaft during hobbing by means of a specially designed torque dynamometer.

2. To observe the effect of cutting parameters on the variation of torques and power consumed, test the significance of their effect and compare the results with previous investigations.

3. To establish a generalised mathematical model in order to describe maximum torque and average power consumed in terms of the following cutting parameters: axial feed rate, blank material hardness, hob D.P., cutting speed and gear helix angle.

4.2 Analysis of Forces During Hobbing

In hobbing, the directions and values of the cutting forces on all edges in cut vary during the rotation of the hob. This variation, however, will be neglected and mean values and directions of the cutting forces will be established.

The forces on the plane of the hob basic rack can be obtained by simulation with respect to fundamental metal cutting process. The hob basic rack plane ($X_H Y_H$) is shown in Fig. 12 and it is assumed that displacements in this plane only influence the variation of the cutting force [9] .

The hob removes chips from the gear blank at the periphery and the sides of hob teeth, if equal width of chip on the left and right flanks is assumed, P_{XH} has the X- direction and P_{YH} lies in the YZ-plane and is inclined by the angle β_y to the Y-axis.

From the schematic force diagram shown in Fig. 12(a)

$$\bar{P}_{XH} = \bar{P}_1 - \bar{P}_2 \qquad (8)$$

It is observed that under the assumption of equal cutting at the sides, resultant P_{XH} is zero, while the total P_{XH}, shown in the YZ-plane of basic rack Fig. 12(b) is equal to

$$P_{YH} = (P_4 \sin\beta_4 + P_5 \sin_{\beta_5}) \sin\alpha + P_3 \sin\beta_3 \qquad (9)$$

Similarly,

$$P_T = P_{ZH} = \Sigma P_i \cos\beta_i \qquad (10)$$

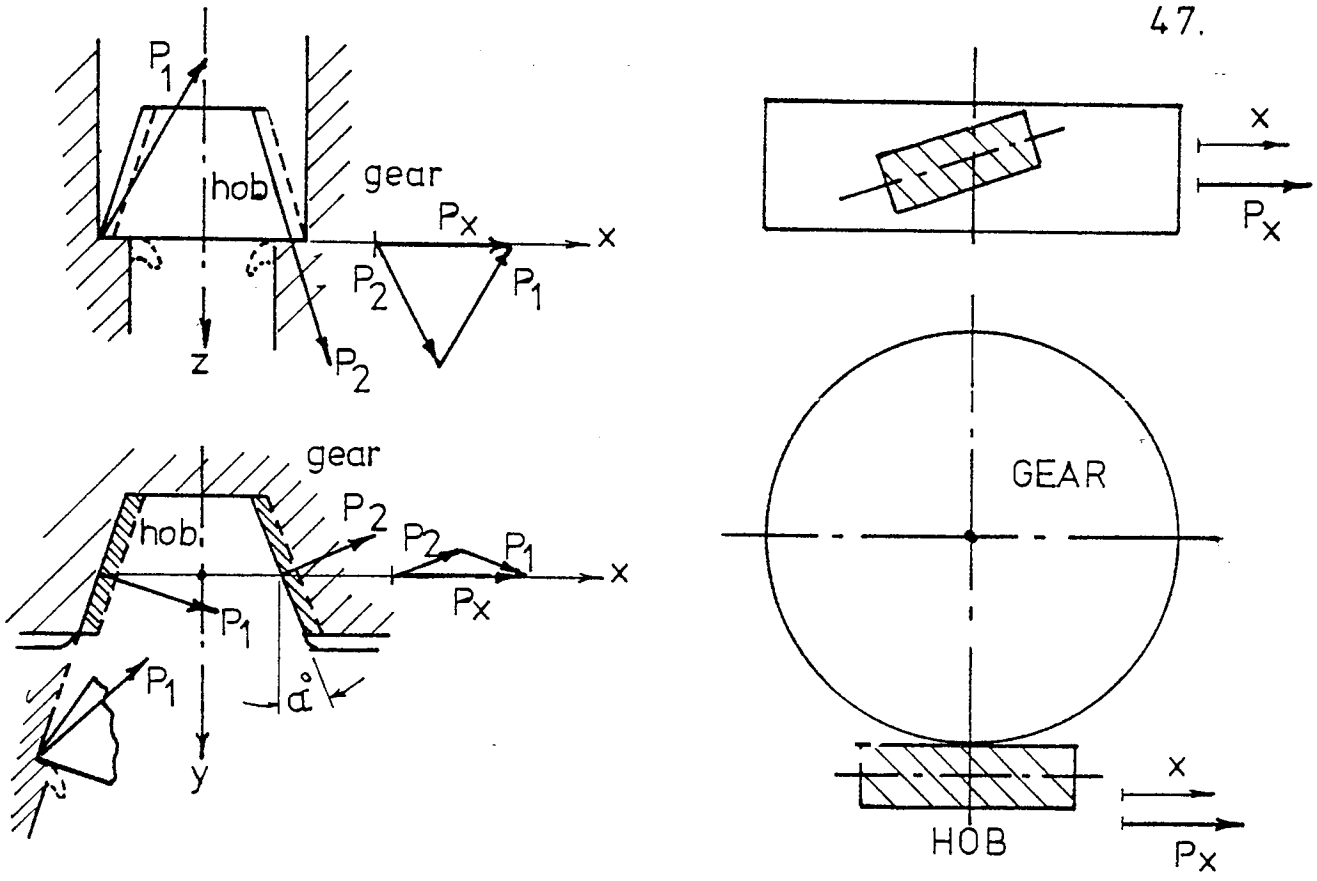

a) Geometry of chip formation and forces acting at the X - direction

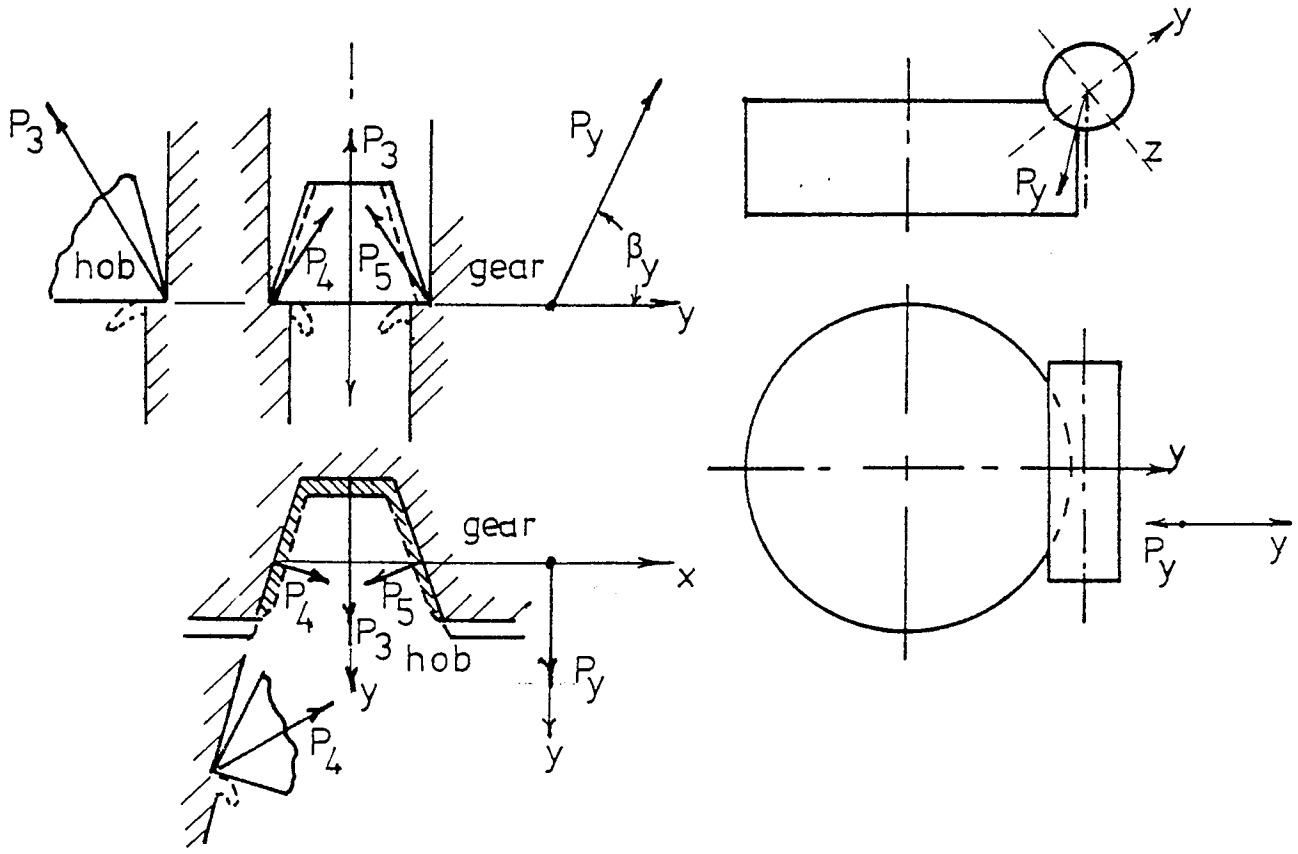

b) Geometry of chip formation and forces acting at the Y - direction

Fig.12 GEOMETRY OF CHIP FORMATION AND FORCES IN HOBBING

where,

P_T is the tangential cutting force

P_i is the resulting cutting load at the ith side

β_i is the friction angle at the ith side

α is the pressure angle

The resulting cutting load on hob teeth is directly related to the area of cut at the ith side. However, it is very difficult to estimate the instantaneous variation of the area of cut. An alternative method is described below.

4.3 Assessment of Tangential Cutting Force

A convenient approach for estimating the cutting torque is to find it from the specific cutting energy, as follows.

Work done "W" per revolution of the hob is given by

$$W = 2 \pi T_{av} N$$

where, $N = \frac{Z_g}{S_h}$ = revolution of hob per revolution of blank

T_{av} is the average cutting torque

Thus

$$W = 2 \pi T_{av} \frac{Z_g}{S_h} \qquad (11)$$

Also during this period, when the blank has rotated once, the volume of material removed is given by,

$$V_m = \frac{\pi}{2} \text{ d. m. Zg. f} \qquad \text{mm}^3/\text{rev} \qquad (12)$$

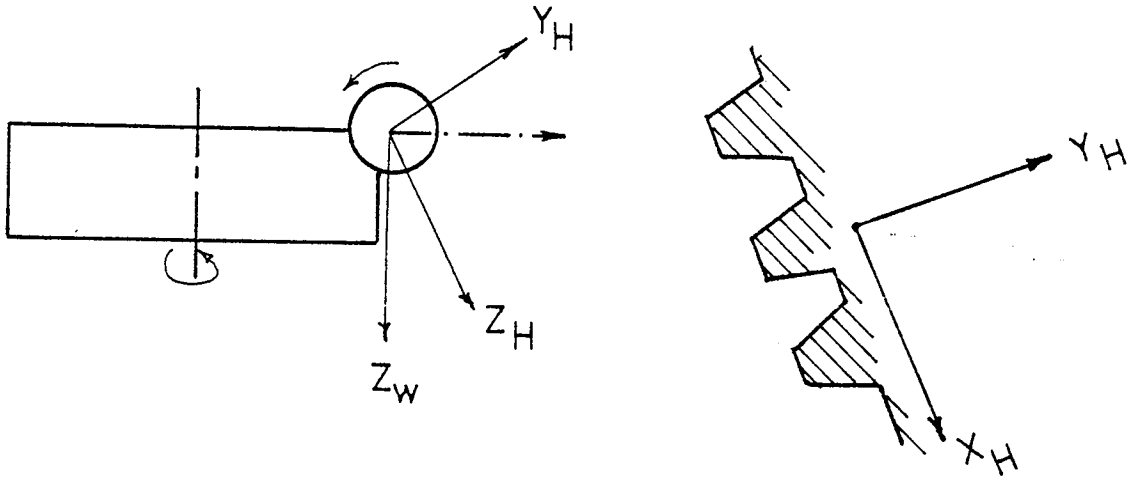

Basic rack

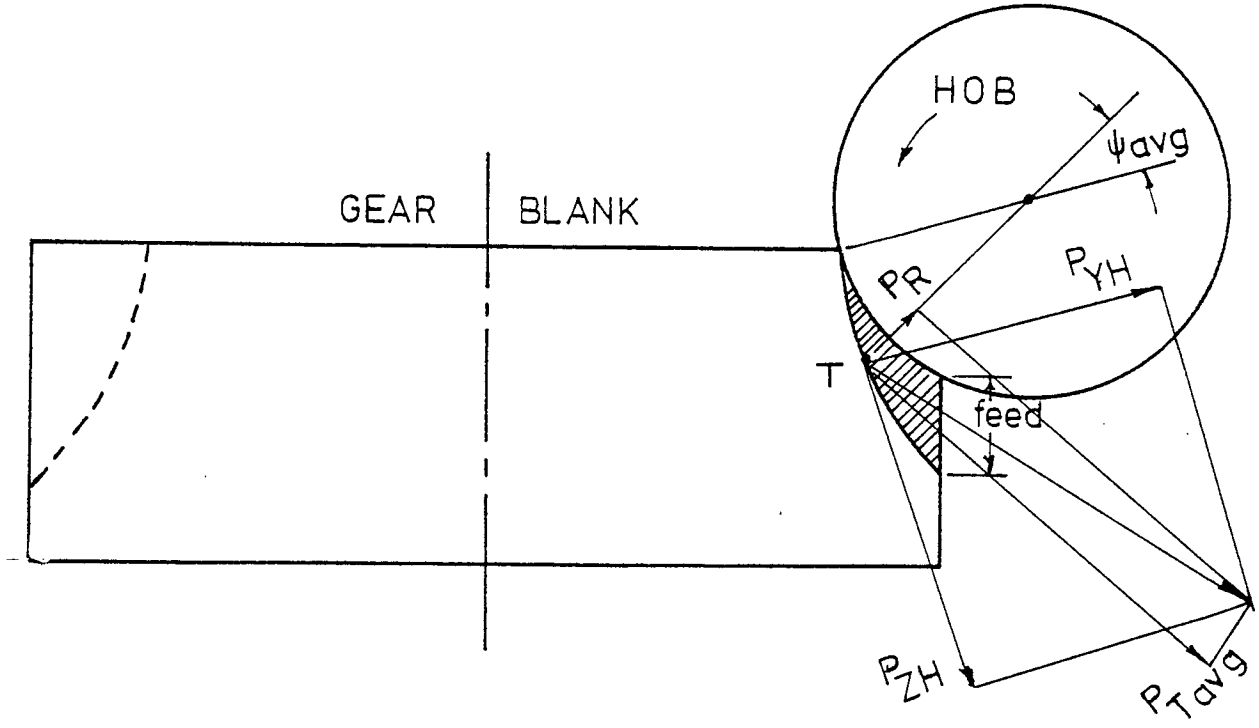

Fig.13 TANGENTIAL AND RADIAL COMPONENT OF FORCES ACTING AT THE MEAN CONTACT ANGLE

where,

d is depth of cut, mm

m is gear module, mm

f is axial feed, mm/rev

When full of depth of cut is applied, depth of cut is given by,

$$d = 2.157\ m \qquad mm$$

The volume of metal removed becomes,

$$V_m = 1.078\ \pi\ m^2\ Zg.\ f \qquad mm^3/rev \qquad (13)$$

Now the specific energy during hobbing is,

$$U = \frac{W}{V_m} = \frac{1.854\ T_{av}}{m^2.f.\ S_h} \qquad (14)$$

And average torque acting on the hob shaft at full depth of cut is obtained as follows

$$T_{av} = \left(\frac{U}{1.854}\right)\ m^2\ S_h \qquad (15)$$

The expression for the tangential component of average cutting force P_{Tav} is given by,

$$P_{Tav} = \frac{2\ T_{av}}{D_h} \qquad (16)$$

where, D_h is hob diameter.

From manufacturers hob data,

$$D_h = 43\ m^{0.48} \qquad mm \qquad (17)$$

hence,

$$P_{Tav} = \frac{2\,U_i}{1.854}\; m^2 . f . \left(\frac{1}{43\; m^{0.48}}\right)$$

$$= C_m . m^{1.52} . f \qquad (18)$$

Equation (18) shows that the tangential average force acting on the hob shaft is directly dependent on feed, while with module the effect is more pronounced. The tangential force component is shown in Fig. 13.

4.4 Interpolation of Cutting Torques from the Energy Principle

Direct measurement of the tangential force, P_T is difficult as it is oscillating rapidly during cutting; the dynamometer must be capable of measuring the fluctuation on a time base. From general principles which can be deduced from the cutting test data obtained from peripheral milling, it is possible to deduce the approximate form of the force fluctuations which occur in gear hobbing.

The undeformed chip length and thickness in the case of gear hobbing is compared with peripheral milling as shown in Fig. 14.

The cutting edge (II) of the hob begins to cut in from point, A, that is the cross point of the curves traced by the preceding edge (I) as shown in Fig. 14(a). It was observed that the tangential cutting force increased linearly in relation to the undeformed chip length[3], between points A and E, and remained constant between E and B at the maximum value of tangential force for one hob tooth during cutting.

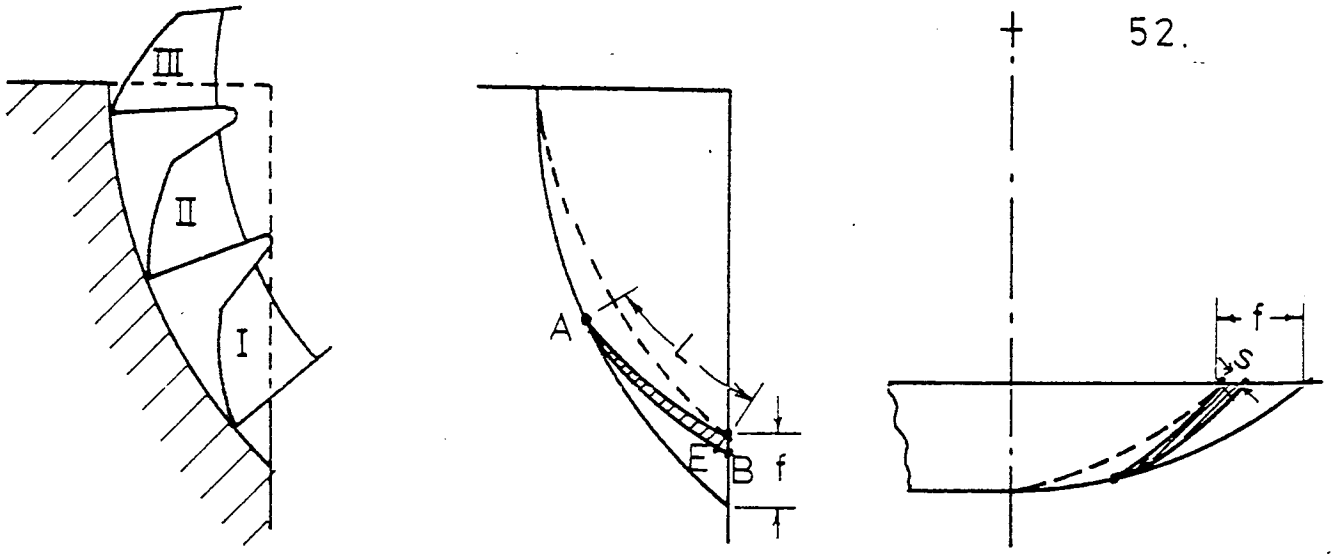

a) Hob teeth action b) Hobbing c) Milling

Fig.14 UNDEFORMED CHIPS

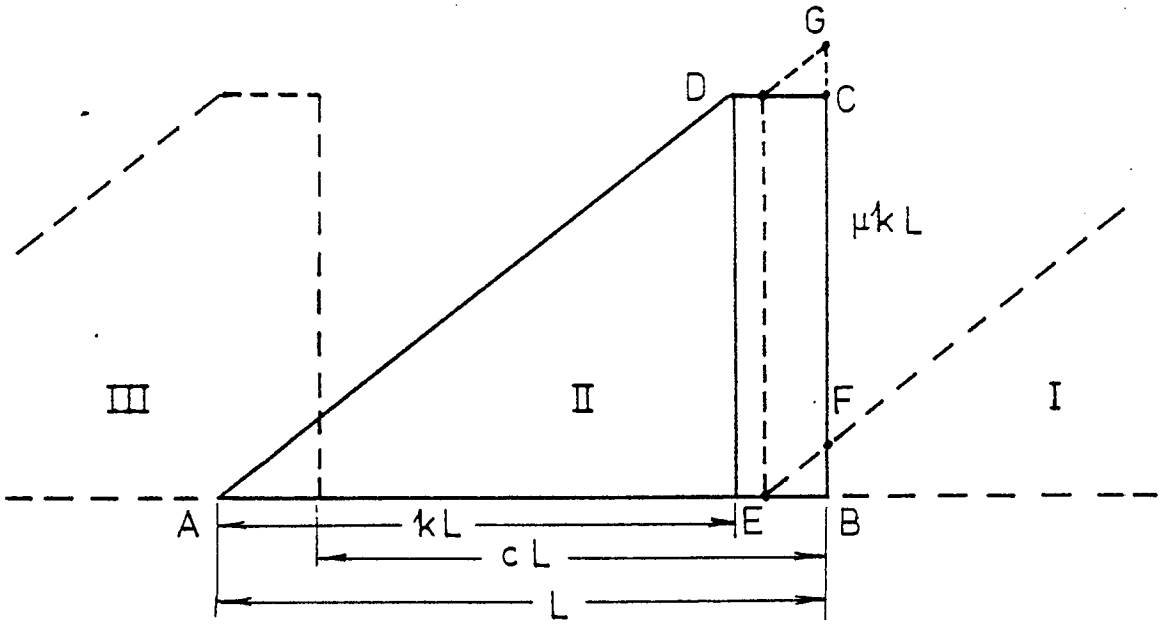

Fig.15 PRINCIPLE ENERGY DIAGRAM

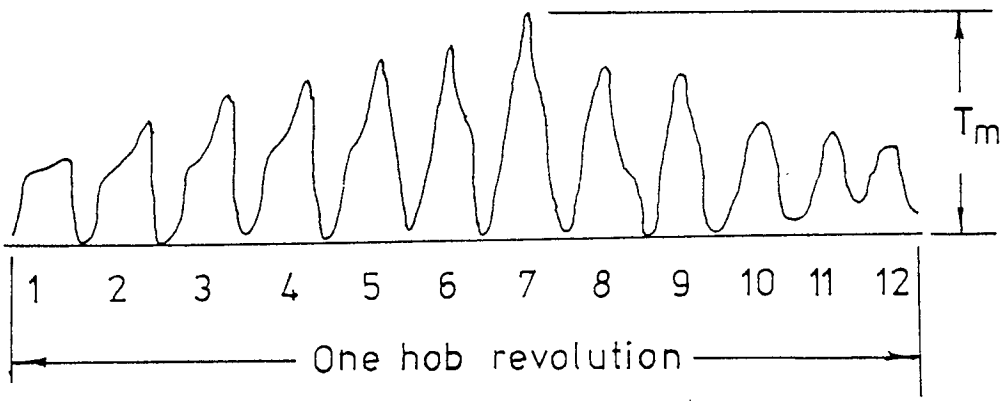

Fig.16 EXAMPLE OF TORQUE TRACINGS

Fig. 15 shows in an ideal form the relationship between the tangential cutting force acting on the hob teeth and the distance traversed by the tooth during cutting, the tangential force at point E is given by,

$$P_{Tj} = \mu_j \; k \; L \tag{19}$$

where,

L is the total length of the underformed chip

k is constant depending on chip thickness

μ is the value of slope, AD, and has a value which includes the frictional resistance of the tooth to slide over the material

j represents the cutting tooth number with respect to the number of flutes in the hob, Z_h

Work done by tooth II in the cutting action shown in Fig. 15 is obtained as follows,

$$\begin{aligned} W_{II} &= \triangle \text{ ADE} + \square \text{ EBCD} \\ &= \tfrac{1}{2} \; \mu_{II} \; k^2L^2 + \mu_{II} \; kL(1-k)L \\ &= \mu_{II} \; k \; L^2 \; (1-k/2) \end{aligned} \tag{20}$$

Work done by jth tooth is,

$$W_j = \mu_j \; k \; L^2 \; (1-k/2) \tag{21}$$

The total work done during one hob revolution is obtained as follows,

$$W = \sum_{j=1}^{z_h} W_j$$

$$= \sum_{j=1}^{z_h} \mu_j \cdot k. L^2 (1-k/2)$$

$$= k. L^2 (1-k/2) \sum_{j=1}^{z_h} \mu_j$$

If $\mu = \sum_{j=1}^{z_h} \mu_j$

then $W = \mu .k.L^2 (1-k/2)$ (22)

The expressions for average torque T_{av}, maximum torque T_m, and average of maximum torque $\bar{T}_m$ are obtained as follows,

the average tangential force, $(P_T)_{av}$ is expressed as,

$$P_{Tav} = \frac{W}{Z_h . c . L}$$

$$= \frac{\mu .k.L}{Z_h . c} (1-k/2)$$

where,

Z_h is number of flutes in the hob

c is constant depending on hob diameter, number of flutes in the hob, depth of cut, and number of starts in the hob.

The average cutting torque, T_{av} is then obtained,

$$T_{av} = (D_h/2) \frac{\mu .k.L}{z_h . c} (1-k/2) \quad (23)$$

where D_h is the hob diameter.

The maximum cutting force (P_{mj}) for one tooth is obtained from the algebraic sum of intersecting forces when more than one tooth is engaged simultaneously as follows,

$$P_{m.j} = \overline{BG} = \overline{BF} + \overline{BC}$$

where,

$$\overline{BF} = \mu_{j+1}(1-C)L$$

$$\overline{BC} = \mu_{j}.k.L$$

then

$$P_{mj} = \mu_{j}.k.L + \mu_{j+1}(1-C)L$$

The maximum cutting force acting on the hob during one revolution, P_m is obtained from,

$$P_m = \sum_{j=1}^{z_h} P_{mj}$$

$$= \sum_{j=1}^{z_h} \{\mu_j.k.L + \mu_{j+1}(1-C)L\}$$

$$= L\{k \sum_{j=1}^{z_h} \mu_j + (1-C) \sum_{j=1}^{z_h} j+1\}$$

$$P_m = \mu.L\{k+(1-C)\}$$

the maximum cutting torque, T_m is thus obtained,

$$T_m = (D_{h/2})\ \mu\ .L\ \{k+(1-C)\} \qquad (24)$$

Average of maximum cutting force, $\overline{P}_m$ is obtained as follows,

$$\bar{P}_m = \frac{P_m}{z_h} = \mu.L \{k+(1-C)\} / z_h$$

and average of maximum torque $\bar{T}_m$ is therefore,

$$\bar{T}_m = (D_h/2)\ \mu.L \{k+(1-C)\} / z_h \qquad (25)$$

4.5 Interpretation of data

Data is interpreted from the tracings obtained from the oscillograph in relation with the theoretical analysis as follows:

Fig. 16 shows an example of torque tracings during one revolution of the hob, the numbers 1,2,.....,12 indicate the hob gashes.

Maximum torque T_m is obtained by measuring the torque at peak number 7 for the example given.

Average of maximum torque $\bar{T}_m$ is obtained as follows,

$$\bar{T}_m = \frac{\text{sum of 12 peaks}}{\text{number of peaks}}$$

Average torque, T_{av} is calculated from the work done by the hob as follows,

Work done by the hob in 1 sec. $= \frac{6600}{746} W_p$ lb.in.

$= 8.85\ W_p$ lb.in.

$= 0.999\ W_p$ Nm

where

W_p is the average power consumed during cutting, watts

Work done by the hob during one cycle $= (\frac{0.999 \times 60}{N_h}) W_p$ N_m

where,

N_h is the hob speed, r.p.m.

Average work done by the hob during one rotation = $2 \pi T_{avg}$

$$2 \pi T_{av} = \frac{0.999 \times 60 \times W_p}{N_h} \qquad (26)$$

Average torque, T_{av} is then obtained,

$$T_{av} = \frac{0.999 \times 60 \times W_p}{2 \pi N_h} \quad (Nm) \qquad (27)$$

For N_h = 115 r.p.m.

$T_{av} = 0.0829 \ W_p$ (Nm)

For N_h = 74 r.p.m.

$T_{av} = 0.129 \ W_p$ (Nm)

For N_h = 178 r.p.m.

$T_{av} = 0.0536 \ W_p$ (Nm)

4.6 Dynamometry

It was decided in this study to measure the torque acting to the hob arbor, one of the more important measurements of this type being the determination of tangential cutting force components.

The two main requirements to be satisfied in dynamometer design are, sensitivity of measuring a minimum load or force, and rigidity of allowing a minimum deflection under the maximum applied load or the desired natural frequency.

There are many other special dynamometer requirements as follows:

(i) Must be rigid enough so as not to interfere with the cutting operation by causing the excessive vibration and chatter.

(ii) The natural frequency of the dynamometer must be at least four times the maximum exciting frequency to which the tool is subjected.

(iii) Cross sensitivity between the different components of forces during deformation must be either negligible or kept as minimum as possible.

(iv) A dynamometer must be stable with respect to time, temperature and humidity.

Some of the instruments to measure force components which involve the measurement of deflections are as follows:

(a) Dial indicator
(b) Hydraulic Pressure Cell
(c) Optical Interfermometer
(d) Pneumatic Solex Micrometer and other devices
(e) Piezoelectric Crystal
(f) Electric Transducers

The advent of the wire resistance strain gauge has made it possible to design simplified metal cutting dynamometers which are stiff, sensitive, easily portable and readily applied to provide a continuous chart record of cutting forces.

The design of dynamometer used in the study involves the use of electrical strain gauges (torque gauges) bonded to the hob arbor to measure the shear strain, the torque is then interpreted from the recorded charts.

4.7 Design of Torque Dynamometer

Fig. 17 shoes the dynamometer designed. The four principle components are the strain gauges on the shaft, the power supply to the gauges, the electrical circuit and the slip ring unit on the shaft which provides the contacts between the rotating gauges and the electrical circuits.

It was decided to design a new hob arbor as shown in Fig. 18 due to some difficulties in locating the electrical leads from the strain area to join slip ring contacts as the existing hob shaft arbor was hardened and ground.

ARNE Steel (high speed tool steel) was used as shaft material. The necessary machining operations in the preparation of shaft were carried out, the shaft was then hardened to 62 HRC and later ground to conform to the design.

ARNE Steel has the following specifications :

HRC	U.T.S.	E	G
62	2255 KN/m^2	190 x 10^6 KN/m^2	73.08 x 10^6 N/m^2

The design calculations are shown in Appendix I.

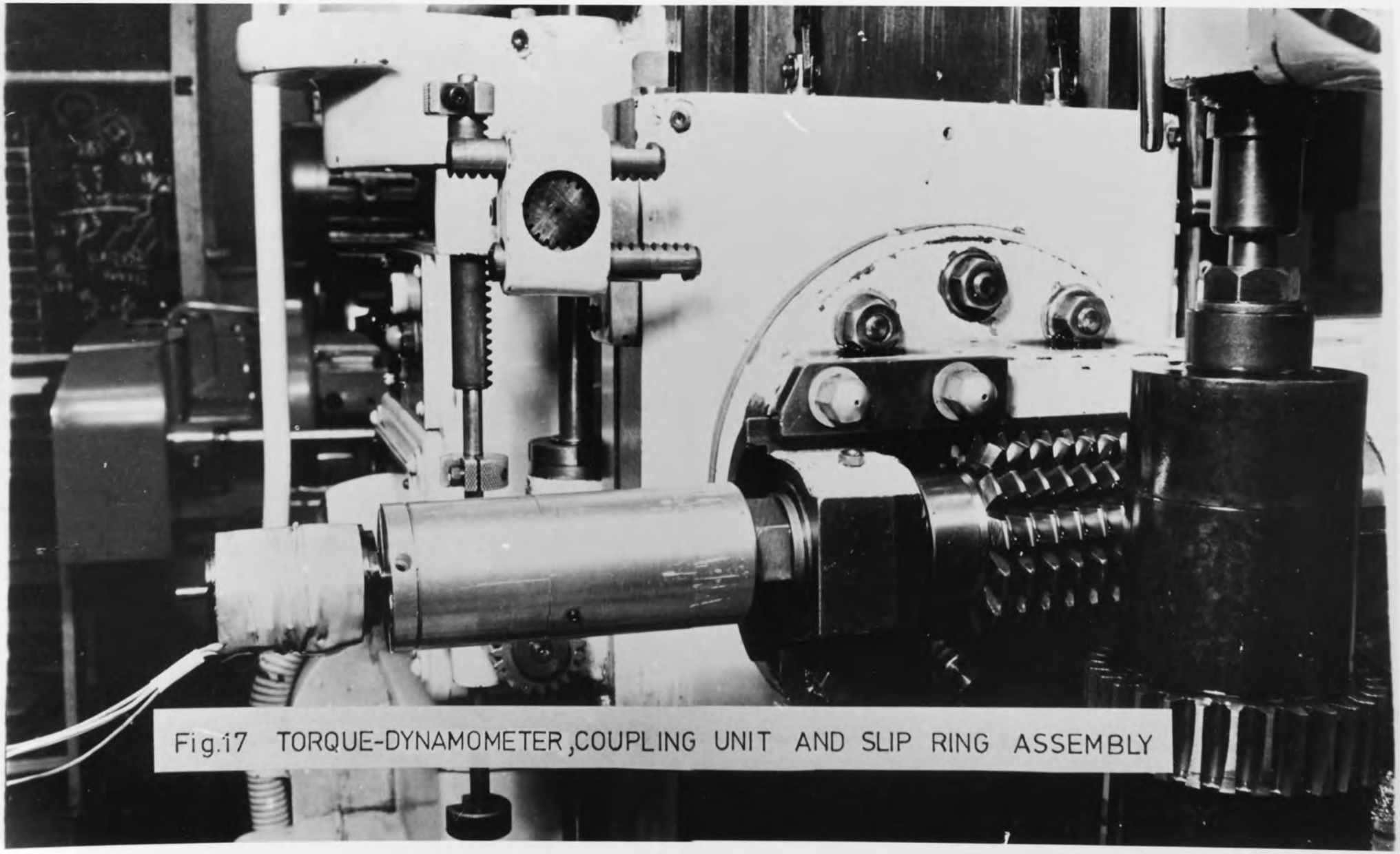

Fig.17 TORQUE-DYNAMOMETER, COUPLING UNIT AND SLIP RING ASSEMBLY

4.7.1 Strain Gauge Installation

The method of measurement of torsion on a circular shaft by means of four active strain gauges which are cemented at right angles has been employed.

The method of affixing, glueing and moisture proofing electrical strain gauges to metallic surfaces and other factors which determine the choice of adhesives have been described in great detail by the gauge manufacturers [40] and other authors [41].

The special two double pair (nominal resistance 100 ohms) of Tinsley Torque gauges were located and orientated on the shaft as shown in Fig. 19 and Fig. 20. This procedure results in automatic temperature compensation and elimination of axial and bending strains.

Before fixing the gauges, the shaft diameter (d) over which the gauges would be affixed was cleaned and degreased with carbon tetra-chloride (Inhinbisol). The gauge was then cemented in position on the shaft diameter by placing the gauge on sellotape strip, pouring a drop of gauge bonding glue (Permabond) on the diameter; the gauge was quickly located on the glue surface.

The procedure was repeated for the second double pair gauge, then the gauges were covered with Phillips Silicon Wax to provide some mechanical protection and also to prevent atmospheric moisture from causing damage.

Installation of electrical leads is shown in the wiring diagram Fig. 20, and different colours of wires were used to distinguish D, E, F and G.

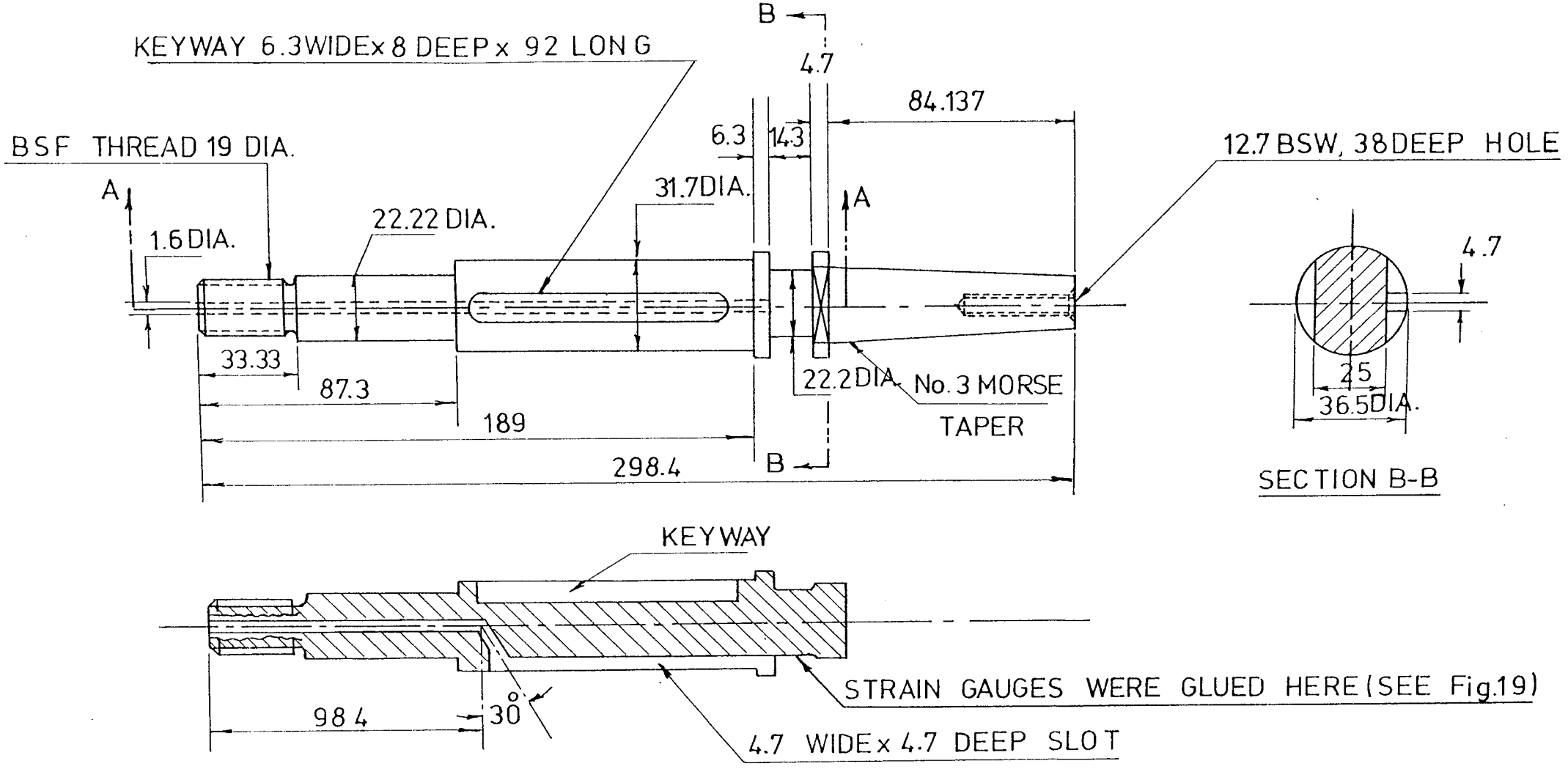

Fig. 18

HOB ARBOR (DYNAMOMETER)

MATERIAL: ARNE TOOL STEEL

ALL DIMENSIONS IN mm

TOLERANCES ARE ± 0.076 mm

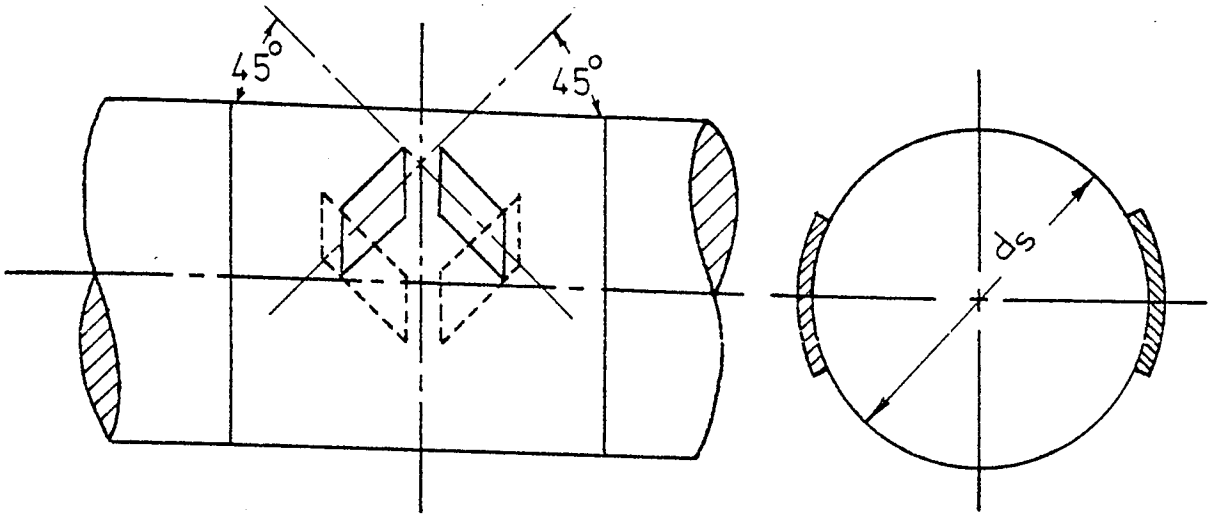

Fig.19 LOCATION OF TORQUE GAUGES ON THE HOB SHAFT

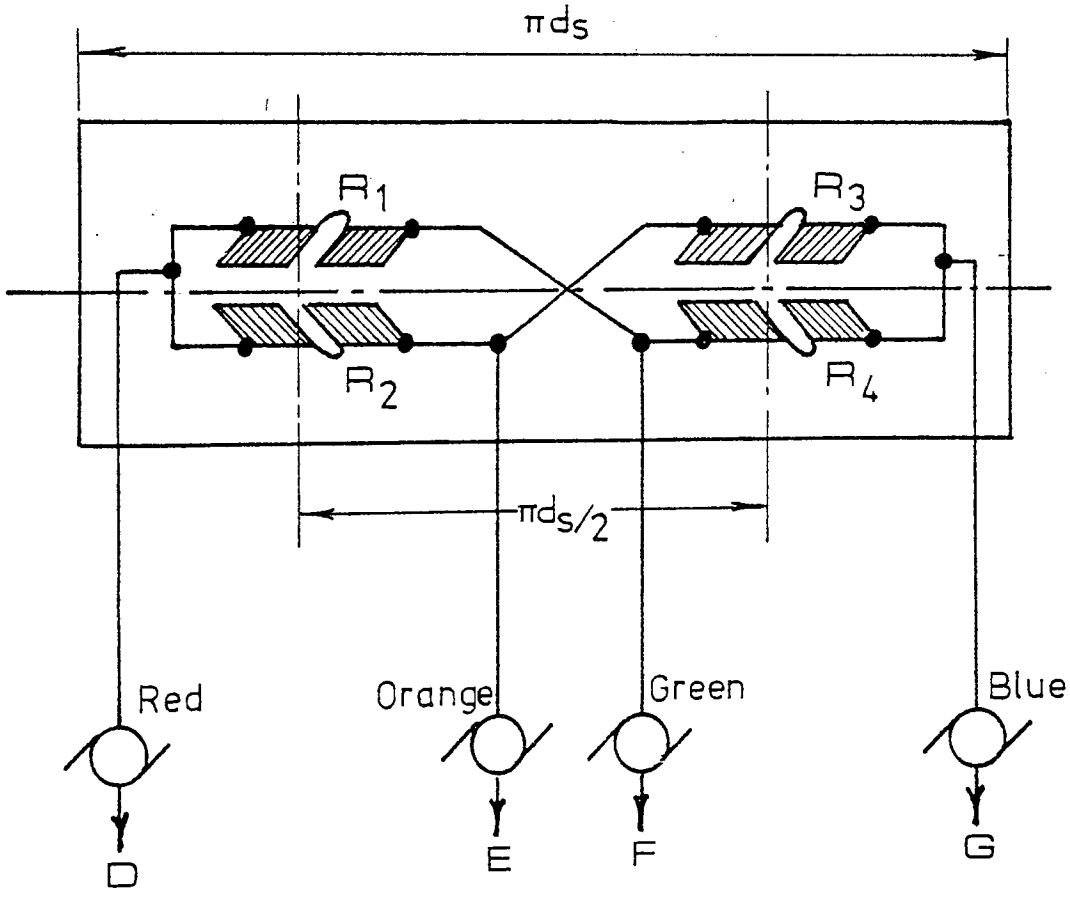

Fig. 20 TORQUE GAUGES WIRING DIAGRAM

4.7.2. Collector Ring Assembly

It is obvious that some form of collector rings or slip rings assembly will be necessary to maintain electrical contact between the instruments and gauges. I.D.M. slip ring assembly was employed, where the rings are formed by a special process of electrodeposition of fine silver. The specification and other details of I.D.M. slip ring assembly can be obtained from the manufacturer manual. The slip ring assembly has low electrical noise and the device was found to be suitable for the dynamometer.

A coupled mounting was necessary to join conveniently and safely, the connection of leads from the gauges through the shaft to the contacts of slip rings. Fig. 21 shows the design of slip ring coupling made in Aluminium, Fig. 22 also shows the coupling and slip ring assembly. The slip ring contact resistance variation was kept to a minimum during electrical installation of the system.

A conventional arrangement of strain gauge system employed is shown in Fig. 22. It has the advantage of temperature compensation, elimination of strains other than torsional strains, and comparative freedom from inaccuracies due to slip ring contact resistance variation. R_5 is a balancing resistor for null balancing operation of the bridge which is varied by the dial of the instrument.

4.8 Selection of Instruments

The most efficiently designed dynamometer will be of little value if the measuring instruments used with it is not accurate or sensitive enough, or does not have a frequency

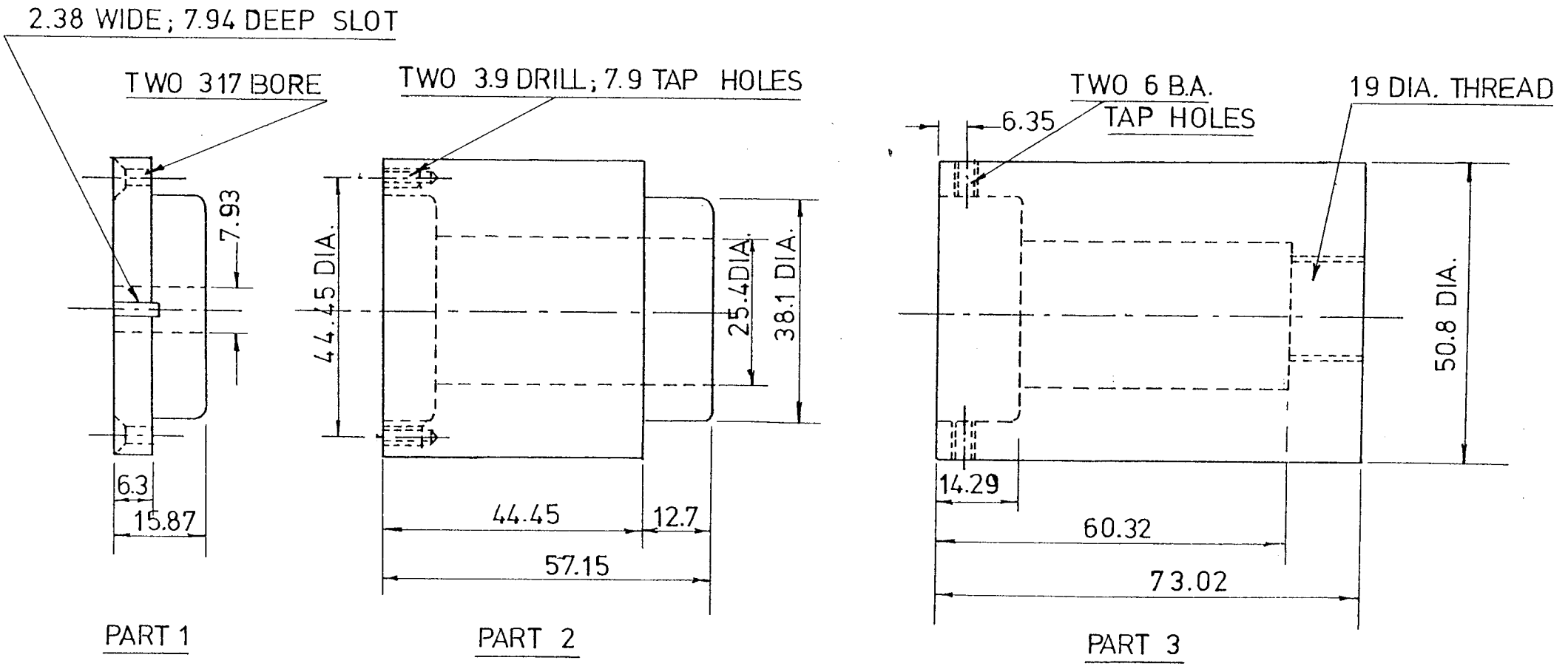

SHAFT SLIP RING COUPLING

MATERIAL: ALUMINIUM

ALL DIMENSIONS ARE IN mm

TOLERENCES ARE ± 0.127 mm

Fig. 21

response that is sufficiently high to follow significant fluctuations of torques.

One of the items which all these instruments has in common is an amplifier, since strain gauge output voltages are so minute. In other respects, the several instruments differ widely.

A decision which must be made concerns the choice between AC and DC bridge circuits. The AC circuit has an advantage of eliminating the possibility of thermo-electric effects in the circuit wiring and generally offers a greater range of stable amplification than the DC bridge circuit. On the other hand, DC circuit requires no shielding and it is free from 50 cycle pick up.

It was first decided to use a B.P.A. Transducer Meter, series C51, where the amplified signal-modulated carrier is fed to a phase-sensitive, transistor demodulator, the D.C. output of which actuates the indicating meter. This output is also brought to a jack-socket and may be observed on a direct-writing recorder. However, the recording unit showed a high level of noise in the output signals.

The second choice was the Thorn Stabilised Power Supply Type V.21, with Output 3-30V, D.C. and 0-1 Amp. It has a Voltage control to balance the bridge resistively and also capacitatively; the bridge proved sensitive enough, although no indicators to measure the strain, but the output signals were very clear.

For recording purposes, several instruments were available, the ABEM ULTRALETTE-12 was selected as an advanced

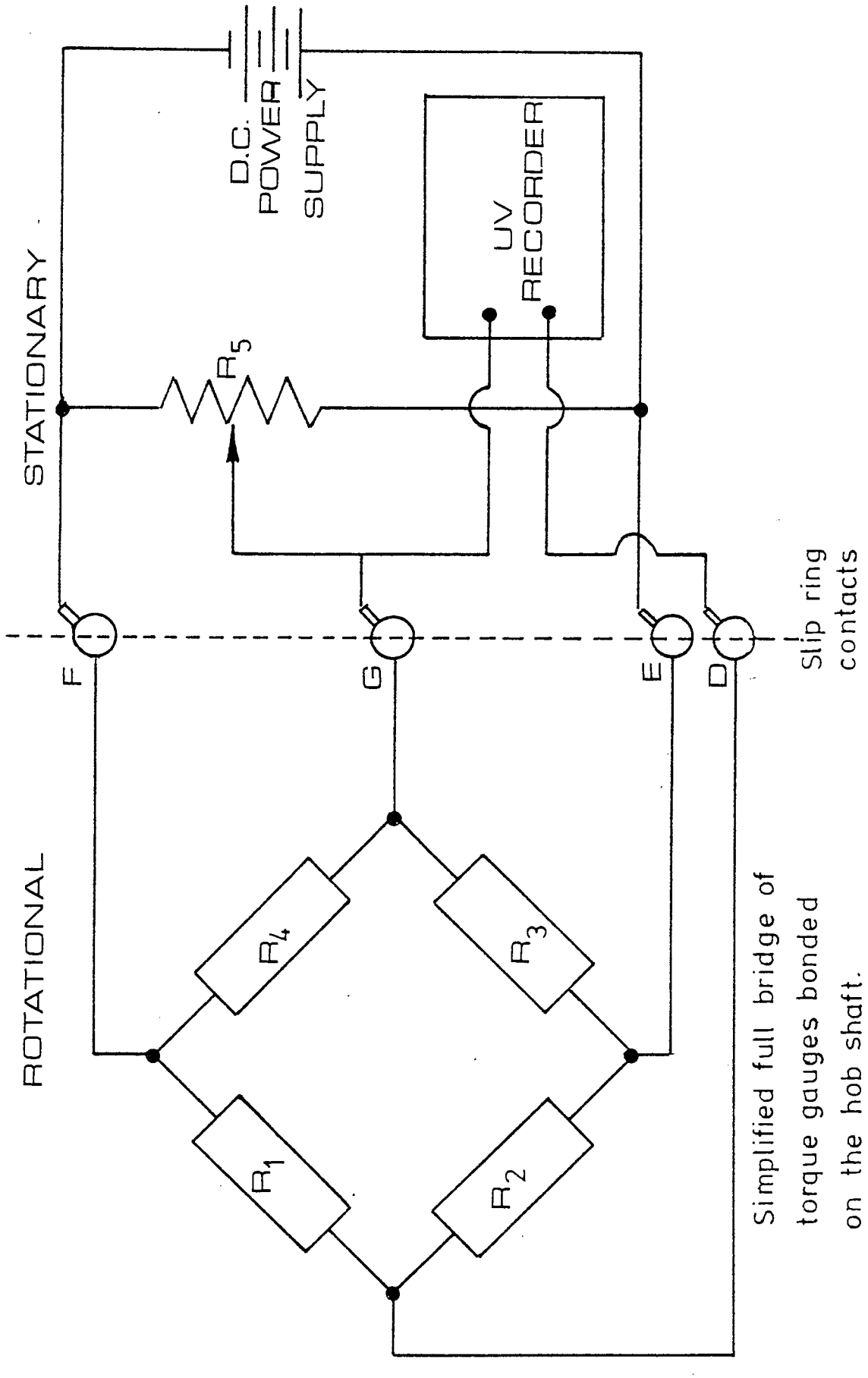

Fig. 22 TORQUE MEASUREMENT INSTRUMENTATION

mirror galvanometer direct recording oscillograph is an advantage, the light source is a high pressure mercury vapour lamp, and the recording paper used is sensitive to ultra-violet light. At slow writing speeds the traces become visible immediately. A wide range of standard galvanometers is available with natural frequencies from 60 to 8000 C/S, sensitivities from 4000 to 0.11 mm/mA, and internal resistance from 85 to 3.5 ohms.

Fig. 22 shows the sketch of instrumentation involved in measurement of torque.

4.9 Measurement of Cutting Power

It was decided to measure the power consumed during cutting at the same time when measuring the torque.

"SYKES" Gear Hobbing Machine HV-14 is driven by main drive motor, rated at 2 h.p., 1450 r.p.m. and operates at mains voltage of 440 volts. The motor is of induction type, and input is by three-phase A.C. circuit.

It was feasible that the measurement of power in this three-phase, three-wire system can be carried out using a "Star Connected balanced load with neutral point accessible" method as shown in Fig. 23.

A wattmeter (W) is connected with its current coil in one line, and the voltage circuit between that line and the neutral point; the reading on the wattmeter gives the power per phase, where :

$$\text{Total power} = 3 \times \text{wattmeter reading}$$

In the experiment, Cambridge Single Phase Wattmeter (cat. No. 44371/2) was used to measure power in the range (0 to 1250 watts) in one phase of the drive motor circuit, assuming the load in each phase to be equal.

4.9.1. Procedure for Measurement

The determination of whether the maximum cutting torques or average cutting power consumed during cutting were proportional to the cutting parameters, necessitates the investigation of input power to the main drive motor under different combinations of machining conditions. In general, the power was measured for the same cutting conditions as in unison with cutting torques measurement.

When measuring cutting power, two readings were taken; one with machine running idle (no load power) and the other with hob cutting at full depth, total power.

The power consumed during cutting is obtained by the following relationship.

Power Consumed = full load power - no-load power

An attempt was made to discover if there was any variation in cutting speed under varying load conditions. "Hasler Tachometer" and "Solarton Tachometer" were used to measure hob speed and for a series of tests, the variation of hob speed under cutting conditions appeared to be less than 1%, and is thus neglected.

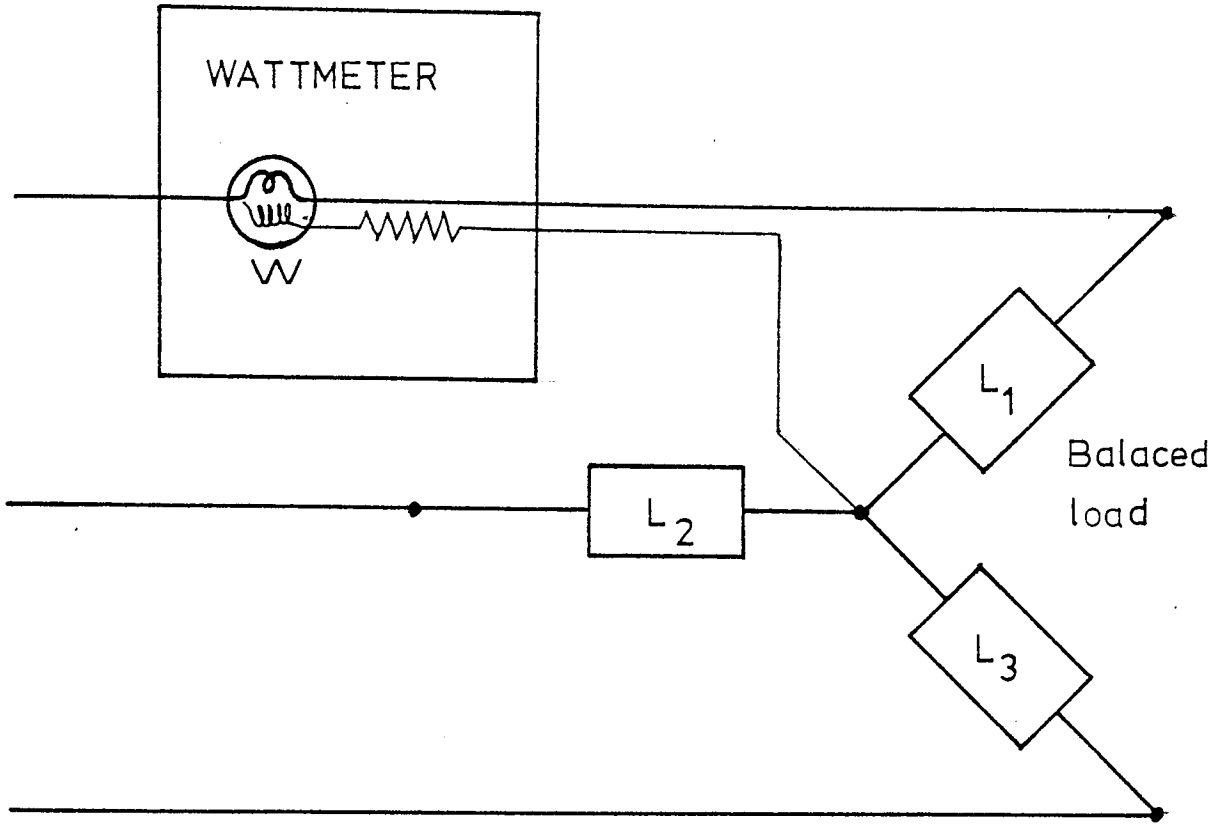

Fig. 23 MEASUREMENT OF POWER

4.10 Torque and Power Experimental Procedure

The machining action was carried out to cut spur and helical gears, the test initiated by choosing En 1A material blank, mounting it securely in the workpiece holding mandrel. The blank was set correctly with respect to the hob to attain full depth of cut for one hob travel during axial feed. The machine was started up and the hob fed axially by engaging the feed lever.

At full depth, the torque output from the dynamometer was recorded on the oscillograph, then the machine was stopped after disengaging the feed lever.

The feed gears were changed to a new feed rate and the procedure was repeated. During the experiment the hob speed was kept constant for a range of different feeds, then the speed was varied for the same range of feed rates. By this procedure, it was possible to record torque tracings at full depth of cut for different combinations of speeds and feeds.

The whole test was repeated by replacing En 1A blanks with En 8, En 34 and En 16T in turn.

The tests performed in each of the different combinations between speed, feed and material hardness while the hob was kept in a reasonable sharp condition to avoid the effect of tool wear on the results. It was assumed that the blank diameters are constant, and the module of gear was altered with the change of hob only at different cutting conditions.

4.10.1 Design of Experiment

A well-designed experiment can substantially reduce

the number of tests, and yet provide all of the essential information for a statistical analysis which will yield useful inferences.

The analysis of the gear hobbing process can be viewed as a problem to determine the relationship between the process input (cutting parameters) and output (torques, power, ...etc) for the purpose of prediction and/or control. The problem is to determine which of a host of variables have significant effect on the output, and then to determine a mathematical model to describe how they influence the response.

The approach taken by the author in building a model to describe the process will depend on the degree of a priori information available about the process.

Preliminary investigation by the author [20] indicates that the cutting speed has a significant effect on both maximum torque and average power. However, in the present design of experiment, the effect of cutting speed will be observed more accurately as well as other cutting parameters for hobbing both spur and helical gears.

4.10.2 Spur Gears

A four-factor design of experiment to investigate the effect on cutting torques and average power consumed when hobbing spur gears was used. The axial feed rate was at four levels as follows:

$$f = 0.024, 0.036, 0.050 \text{ and } 0.078 \text{ i.p.r.}$$
$$(0.609, 0.914, 1.270 \text{ and } 1.987 \text{ mm})$$

and the hob speed was at three levels as follows:

N_h = 74, 115, 178 r.p.m.

Four different materials were cut in this experiment, the materials and hardness (H_B) are as follows:

En 1A (115), En 34 (164), En 8 (183) and En 16T (269)

Three types of hobs were used to cut the materials,

8, 10 and 12 D.P.

Maximum, average of maximum and average torques were measured as well as power consumed during cutting at each different combination of cutting parameters.

4.10.3 Helical Gears

A four-factor design of experiment to investigate the effect on cutting torques and average power consumed during hobbing helical gears was used. The axial feed rate was at four levels as follows:

f = 0.024, 0.036, 0.050 and 0.078 i.p.r.

(0.609, 0.914, 1.270 and 1.987 mm)

and the hob speed was at three levels as follows :

N_h = 74, 115 and 178 r.p.m.

The gear helix angle was selected at three levels as follows

= 0^o, 31^o and 45^o.

Three types of hobs were used in this experiment,

8, 10 and 12 D.P. The material hardness was kept

constant, where only one type of steel was chosen, En 34 (H_B=164).

Measurements of torques and power were carried out.

4.10.4 Measurement of cutting power

Power consumed during machining spur and helical gears of different module at different combinations of cutting parameters, was measured at the same time when torques were measured. The procedure for measuring power by wattmeter is described fully in 4.9.

4.11 Calibration of Torque Dynamometer

4.11.1 Introduction

The calibration of transducers is normally carried out by applying a series of known loads or torques, measuring the corresponding linear or angular deflections and then putting the 'best' straight line through the results.

The 'best' straight line is often determined by applying a regression technique, by minimising the sum of squares of the deviations of the experimental points from a straight line. A refinement sometimes employed is the use of a computer to reject experimental points which lie more than an arbitrary distance from the computed line, followed by a re-calculation of the line position.

4.11.2 Method of Calibration

A "Lever-method" was used to calibrate the dynamometer. A standard spanner with a span of 11 in. was fitted on the locking nut of the hob shaft. The hob shaft was restrained

from moving or rotating by holding the flywheel rigidly.

It was intended to carry out the calibration in the same direction of the torque acting upon the hob shaft; a strong rope was attached to the end of the spanner and passed round a free running pully placed on the column handle, the other end of the rope attached to the weights. Thus the friction was minimal.In this manner, weights up to 50 lb in steps of 5 lb at a time were applied, and static torque readings taken on an oscillograph recording. Then the loads were removed in steps of 5 lb and the results recorded. The stabilised power supply was adjusted at 7 volts and 0.075 Amps.

4.11.3 Curve shape

The inherent assumption in this form of calibration is that the points would lie on a straight line if there were no measuring errors but that there are statistically distributed errors on either side of this line. This assumption is not always true since in practice there may be hysteresis in the system; metal internal hysteresis accounts for some of the observed energy absorption but the majority of energy absorption usually comes from friction at joints in the system.

A typical level of hysteresis is about ±0.2%, the dynamometer calibration curve has the level of ±0.15%. This corresponds to a resonance dynamic magnification factor of the order of many hundreds and is unusual in a mechanical system. The effect of hysteresis is shown exaggerated in Fig. 24. The hysteresis loop is approximately a parallelogram.

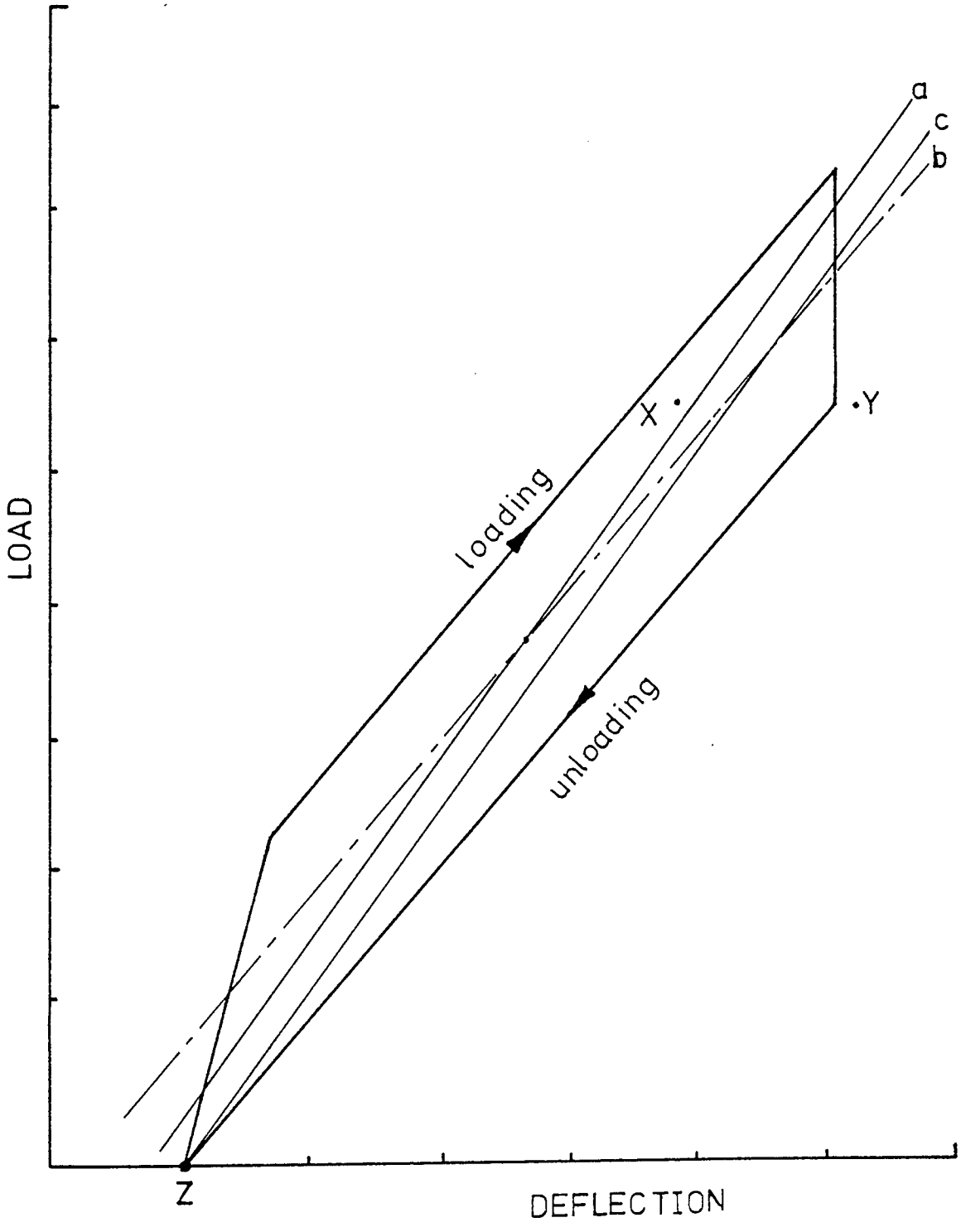

Fig. 24 POSSIBLE "BEST" LINES THROUGH EXPERIMENTAL POINTS

4.11.4 Selection of line

The use of a 'least squares' optimisation has the effect of biasing the line towards a steeper slope, as shown by line a in Fig. 24 due to the basic shape of the hysteresis curve. If line a is taken as the calibration curve for the transducer, the maximum measurement errors in the system will be significantly increased compared with those associated with line b which has been made parallel to the long sides of the parallelogram. The increase in maximum error depends upon whether the zero and 100% load points are computed as single or double experimental points; the increase in error may be estimated on simple assumptions and can be as great as 20%.

A more serious effect occurs if a computational approach is used to reject suspect experimental points. Two such points X and Y, obtained with decreasing load, are shown in Fig. 24. Point Y is nearer to the hysteresis loop than point X but the computer will reject point Y first since it is further from the 'best' line a.

4.11.5 Zero effects

The hysteresis loop shown in Fig. 24 poses yet another problem due to the fact that the 'least squares' line a and the minimum error line b do not pass through Z, the zero load point.

In practice, zero is normally set at point Z, then the given slope corresponding to line a is used, so that the line of calibration is c. This gives high errors at about 20% of the full strain range.

However, if a line is put through Z with the slope of the minimum error line b, the errors will be even higher.

4.11.6 Alternative approach

Since the use of a 'least squares' approach will give errors and possible rejection of valid instead of invalid experimental points, it is worth while using an alternative approach which allows a better assessment of the experimental results.

In practice it can be seen from the exaggerated hysteresis loop in Fig. 24 which points are valid and which are not. However narrow the actual hysteresis loop, the results can be plotted with an increased horizontal scale to define the loop more clearly. In practice the easiest method of doing this is to deduct an arbitrary amount per unit load from the experimental readings e.g. deflections are about 7.5 mm per 110 lb.in torque could be deducted from all readings, and the residual small deflection plotted. Any faulty points are then easily seen and the 'best' line may be put through by eye; the slope so determined is then added to the base slope of 7mm per 110 lb.in torque. The dynamometer calibration curve, shown in Fig. 25.

The zero problem may be solved by adjusting the observed zero by an amount equivalent to half the width of the hysteresis band.

A comparison between "least squares" line and best line is shown below:

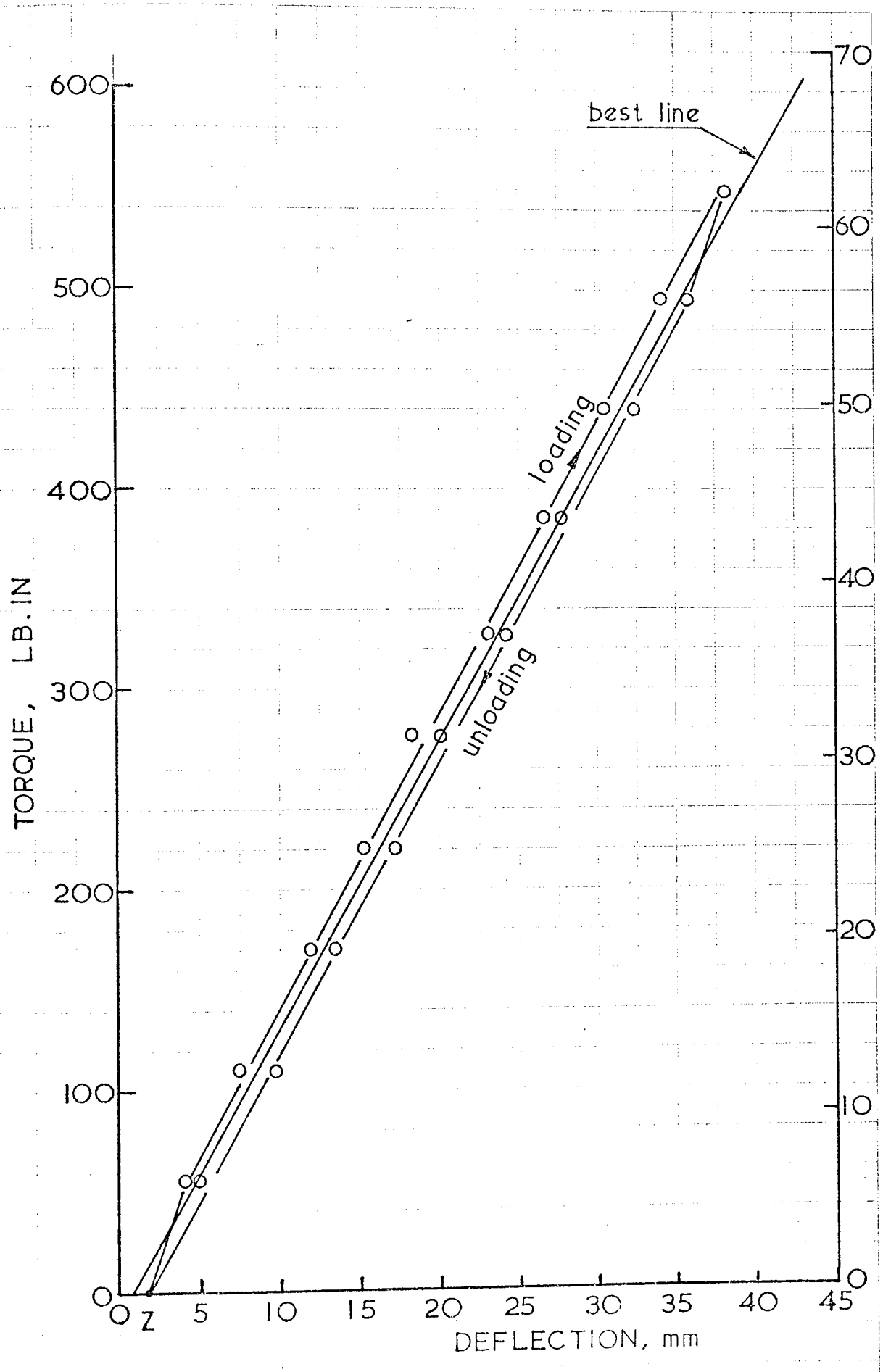

Fig.25 THE DYNAMOMETER CALIBRATION CURVE

Least Squares: slope = 14.8964 lb.in/mm deflection

Zero set = 1.4 mm

Best line: slope = 14.3333 lb.in/mm. deflection

Zero set = 1 mm.

4.12 RESULTS, (Tables and Graphs)

TABLE 5

SPUR GEAR TORQUE RESULTS

Axial feed f , mm/rev	MTRL (HB)	HOB D.P.	T_m (Nm) Hob speed, N_h, rpm			$\bar{T}_m$ (Nm) Hob speed, N_h, rpm		
			74	115	178	74	115	178
0.609	En1A (115)	8	52.54	42.93	34.46	41.24	33.89	28.24
		10	29.37	27.12	22.93	23.16	20.33	17.51
		12	26.89	23.95	21.47	20.33	17.51	16.38
	En34 (164)	8	56.49	51.52	43.61	42.93	38.41	31.63
		10	38.98	32.76	28.25	29.94	24.85	20.33
		12	32.20	24.85	22.82	25.42	20.33	16.95
	En 8 (183)	8	44.29	37.85	32.20	35.02	30.50	23.72
		10	29.37	27.68	22.70	24.85	20.33	16.95
		12	22.03	18.64	15.82	18.08	14.68	11.86
	En16T (269)	8	58.18	52.53	36.15	48.01	40.67	29.93
		10	44.63	37.28	29.37	36.15	28.24	23.72
		12	32.99	28.02	22.82	27.11	21.46	18.07
0.914	En1A	8	68.92	56.49	45.19	56.49	47.45	37.28
		10	39.54	37.28	31.40	32.76	29.37	24.29
		12	33.89	30.89	27.68	27.68	23.72	20.90
	En34	8	71.18	64.62	66.66	55.36	50.34	42.93
		10	49.71	41.80	36.15	41.24	33.89	30.50
		12	41.24	31.65	29.37	33.90	27.11	23.72
	En 8	8	59.31	51.40	43.61	49.71	41.24	33.89
		10	36.60	34.46	28.24	31.63	27.11	22.03
		12	27.68	23.38	19.77	23.16	19.20	15.81
	En16T	8	73.44	66.09	47.45	63.27	55.36	38.98
		10	54.79	46.32	36.15	46.32	37.28	29.37
		12	42.93	36.15	29.37	36.15	29.37	24.29
1.270	En1A	8	85.86	71.18	57.62	74.56	61.00	48.01
		10	51.97	47.45	40.67	42.93	39.54	33.89
		12	40.11	36.72	33.33	35.02	30.50	27.11
	En34	8	86.20	77.95	66.66	70.61	64.39	53.66
		10	62.14	51.97	44.63	53.10	44.06	37.28
		12	50.28	38.41	35.59	44.08	33.89	29.94
	En 8	8	76.26	66.09	55.36	65.53	55.36	46.35
		10	43.49	40.67	33.89	38.41	34.45	27.68
		12	33.33	28.02	23.72	28.81	24.29	22.59
	En16T	8	88.69	77.96	56.49	79.08	67.78	48.58
		10	64.96	54.23	42.37	57.05	46.32	36.15
		12	53.66	45.19	37.28	46.88	39.54	31.63
1.987	En1A	8	122.02	96.03	77.95	107.33	89.25	68.92
		10	71.18	66.66	57.62	63.27	59.88	49.71
		12	52.19	46.88	42.93	46.88	40.67	36.72
	En34	8	110.72	100.32	85.86	97.16	89.25	77.39
		10	83.60	70.05	59.88	75.13	63.27	55.36
		12	65.53	49.71	46.32	62.14	46.32	43.49
	En 8	8	106.20	91.10	77.39	96.03	81.34	69.48
		10	54.90	51.40	42.93	50.27	46.88	38.41
		12	42.36	36.15	31.07	38.41	33.89	27.11
	En16T	8	112.86	102.81	77.13	107.31	94.90	67.77
		10	81.34	68.69	53.10	74.56	63.27	47.45
		12	72.30	61.57	50.84	66.66	56.49	44.63

TABLE 6

SPUR GEAR POWER AND AVERAGE TORQUE RESULTS

Axial feed f, mm/rev	MTRL (HB)	HOB D.P.	W_p (watts) Hob speed, Nh, rpm			T_{av} (Nm) Hob speed, N_h, rpm		
			74	115	178	74	115	178
0.609	En1A (115)	8	108	145	200	13.89	11.97	10.73
		10	62	94	140	8.02	7.79	7.45
		12	52	62	80	6.66	5.08	4.29
	En34 (163)	8	110	155	240	14.23	12.88	12.88
		10	60	90	115	7.68	7.45	6.10
		12	44	68	92	5.65	5.64	4.97
	En 8 (183)	8	90	110	160	11.63	9.15	8.58
		10	70	98	140	9.04	8.13	7.45
		12	60	80	100	7.68	6.66	5.31
	En16T (269)	8	94	145	230	12.09	11.97	12.31
		10	80	120	170	10.28	9.94	9.15
		12	54	80	118	7.00	6.66	6.32
0.914	En1A	8	160	220	300	20.67	18.19	16.04
		10	94	140	200	12.09	11.63	10.73
		12	78	94	120	10.05	7.79	6.44
	En34	8	180	240	380	23.16	19.88	20.33
		10	100	140	175	12.88	11.63	9.38
		12	65	100	140	8.36	8.24	7.45
	En 8	8	160	180	280	20.67	14.91	15.02
		10	94	140	200	12.09	11.63	10.73
		12	77	100	130	9.94	8.24	7.00
	En16T	8	160	260	410	20.68	21.58	22.03
		10	120	180	250	15.48	14.91	13.44
		12	84	120	180	10.84	9.94	9.72
1.270	En1A	8	220	305	440	28.36	25.30	23.61
		10	130	185	290	16.72	15.36	15.59
		12	108	130	170	13.89	10.73	9.15
	En34	8	250	340	540	32.20	28.24	28.92
		10	140	205	250	18.07	17.06	13.44
		12	90	150	200	11.63	12.42	10.73
	En 8	8	240	280	420	30.95	23.27	22.48
		10	130	185	285	16.72	15.36	15.25
		12	100	120	160	12.88	9.94	8.58
	En16T	8	260	420	660	30.50	34.91	35.36
		10	170	240	340	21.92	19.88	18.19
		12	115	180	250	14.80	14.91	13.44
1.987	En1A	8	360	480	680	46.43	39.88	36.49
		10	200	300	445	25.76	24.85	23.84
		12	170	205	260	21.92	17.06	13.89
	En34	8	400	580	880	51.63	48.13	47.22
		10	230	330	420	29.71	27.34	22.48
		12	140	220	300	18.07	18.30	16.04
	En 8	8	430	500	720	55.36	41.46	38.64
		10	200	300	450	25.76	24.85	24.17
		12	170	160	200	21.92	13.22	10.73
	En16T	8	460	760	1040	59.31	63.04	75.81
		10	260	400	540	30.50	33.21	28.92
		12	180	280	390	23.16	23.27	20.90

TABLE 7

HELICAL GEAR TORQUE RESULTS

MACHINING DATA: Blank; helical, En34 steel (HB 164)

Helix Angle	Axial feed f, mm/rev	Hob D.P.	T_m (Nm) Hob speed, N_h, rpm			$\bar{T}_m$ (Nm) Hob speed; N_h, rpm		
			74	115	178	74	115	178
0°	0.609	8	56.49	51.52	43.61	42.93	38.41	31.63
		10	38.98	32.76	28.24	29.94	24.85	20.33
		12	32.20	24.85	22.82	25.42	20.33	16.95
	0.914	8	71.18	64.62	55.36	55.36	50.84	42.93
		10	49.71	41.80	36.15	41.24	33.89	30.50
		12	41.24	31.63	29.37	33.89	27.11	23.72
	1.270	8	86.20	77.95	66.66	70.61	64.39	53.66
		10	62.14	51.97	44.62	53.10	44.06	37.28
		12	50.27	38.41	35.59	44.06	33.89	29.93
	1.987	8	12.51	99.91	85.86	97.16	89.25	77.39
		10	83.60	70.04	59.88	75.13	63.27	55.36
		12	65.52	49.71	46.32	62.14	46.32	43.50
15°	0.609	8	68.24	58.75	51.97	58.75	49.71	40.67
		10	40.67	37.28	35.02	33.89	30.50	27.11
		12	36.15	31.06	24.85	29.37	27.11	21.46
	0.914	8	81.68	68.69	58.75	70.05	59.88	50.84
		10	48.58	46.32	42.93	42.93	39.54	35.58
		12	42.93	37.28	29.37	37.28	32.20	25.98
	1.270	8	90.94	78.52	67.79	83.60	68.92	59.88
		10	58.74	55.36	51.97	53.10	50.84	45.19
		12	50.84	42.93	33.89	44.06	39.54	31.07
	1.987	8	109.60	92.64	79.31	99.98	88.12	78.69
		10	74.56	71.74	65.52	70.05	67.79	61.00
		12	61.00	53.10	42.36	56.49	50.84	38.41
30°	0.609	8	81.34	68.91	59.88	67.79	57.05	49.71
		10	56.49	49.71	41.80	47.45	42.93	36.15
		12	37.28	31.63	28.80	30.50	25.98	22.03
	0.914	8	96.03	82.47	70.04	81.34	71.18	61.00
		10	64.39	56.49	46.32	55.36	49.71	42.93
		12	47.80	41.80	36.15	41.80	36.72	29.37
	1.270	8	108.46	92.07	81.12	99.42	83.60	71.17
		10	69.48	58.75	51.40	65.53	56.49	48.58
		12	59.87	51.97	45.19	50.84	45.19	38.41
	1.987	8	115.23	112.98	97.16	112.98	99.99	90.38
		10	81.34	68.92	57.39	76.82	67.79	56.49
		12	79.08	67.78	58.75	72.87	55.36	55.36

TABLE 8

HELICAL GEAR POWER AND AVERAGE TORQUE RESULTS

MACHINING DATA: Blank; helical, En34 steel (HB 164)

Helix Angle	Axial feed f, mm/rev	Hob D.P.	W_p (watts) Hob speed; N_h, rpm			T_{av} (Nm) Hob speed; N_h, rpm		
			74	115	178	74	115	178
0°	0.609	8	110	155	240	14.23	12.88	12.88
		10	60	90	115	7.68	7.45	6.10
		12	44	68	92	5.65	5.65	4.97
	0.914	8	180	240	380	23.16	19.88	20.34
		10	100	140	175	12.88	11.64	9.38
		12	65	100	140	8.40	8.36	7.45
	1.270	8	250	340	540	32.20	28.24	28.92
		10	140	205	250	18.07	17.06	13.44
		12	90	150	200	11.64	12.43	10.73
	1.987	8	400	580	880	51.63	48.13	47.22
		10	230	330	420	29.71	27.34	22.48
		12	140	220	330	18.07	18.30	16.04
15°	0.609	8	120	170	285	15.48	14.12	15.25
		10	80	130	212	10.28	10.84	11.41
		12	54	72	105	7.00	5.98	5.65
	0.914	8	190	270	450	24.51	22.37	24.18
		10	110	175	280	14.23	14.57	15.02
		12	83	110	157	10.73	9.15	8.36
	1.270	8	280	390	660	36.15	32.42	35.36
		10	150	220	360	19.32	18.30	19.32
		12	117	165	200	15.14	13.67	5.59
	1.987	8	460	650	1040	59.31	54.00	55.81
		10	240	320	490	30.95	26.55	26.32
		12	190	250	350	24.51	20.79	18.75
30°	0.609	8	140	200	375	18.07	16.61	20.11
		10	110	160	240	14.23	13.22	12.88
		12	65	100	140	8.36	8.24	7.45
	0.914	8	230	320	600	29.71	26.55	32.20
		10	145	215	320	18.64	17.85	17.17
		12	106	170	230	13.67	14.12	12.31
	1.270	8	330	460	880	42.59	38.18	47.22
		10	185	270	410	23.84	22.37	22.03
		12	160	245	340	20.67	20.33	18.19
	1.987	8	550	760	1160	70.95	63.04	62.25
		10	255	370	570	32.87	30.73	30.62
		12	270	420	570	34.80	34.91	30.62

TABLE 9

ANALYSIS OF VARIANCE FOR MAXIMUM TORQUE (T_m)

Source of Variation	Degrees of Freedom	Sum of Squares	Variance	Variance ratio, F
f	3	0.1376E7	0.4586E6	39.345††
HB	3	0.2857E6	95252.89	8.172††
D.P.	2	0.1385E7	0.6931E6	59.425††
N_h	2	0.2582E6	0.1291E6	11.076††
f.HB	9	0.7875E5	8750.315	0.732n.s.
HB.(D.P.)	6	0.8510E5	14183.53	1.187n.s.
f.(D.P.)	6	0.3785E5	6308.38	0.528n.s.
f.N_h	6	0.9917E5	16258.25	1.383n.s.
HB.N_h	6	0.7098E5	11850.09	0.990n.s.
(D.P.).N_h	4	0.3114E5	7785.88	0.651n.s.
f.(D.P).HB	18	0.2466E6	13699.97	1.532n.s.
HB.(D.P).N_h	12	0.1131E6	9425.22	1.054n.s.
f.HB.N_h	18	0.1592E6	8842.55	0.989n.s.
f.(D.P).N_h	12	0.3065E6	25542.05	2.856†
RESIDUAL	36	0.3219E6	8942.513	
TOTALS	143	0.4855E7	33955.0205	

f; Axial feed rate, mm/rev

HB; Brenil Hardness Number "Blank"

D.P.; Normal Diametral Pitch

N_h; Hob speed; rpm

†† Significant at the level of 0.01

† Significant at the level of 0.05

n.s. Not significant.

TABLE 10

ANALYSIS OF VARIANCE FOR AVERAGE OF MAX. TORQUE ($\bar{T}_m$)

Source of Variation	Degrees of Freedom	Sum of Squares	Variance	Variance ratio; F
f	3	0.8483E6	0.2827E6	42.284 ††
HB	3	0.7644E5	25480.02	3.810 †
D.P.	2	0.5585E6	0.2792E6	41.759 ††
N_h	2	0.2928E7	0.1464E7	218.942 ††
f.HB	9	0.6334E4	703.762	0.787n.s.
HB.(D.P)	6	0.4643E4	773.777	0.865n.s.
f.(D.P)	6	0.6738E5	11231.00	12.555 ††
$f.N_h$	6	0.3897E6	64962.49	72.621 ††
$HB.N_h$	6	0.5138E5	8563.74	9.573 ††
$(D.P.)N_h$	4	0.2840E6	71006.38	79.378 ††
f.HB.(D.P)	18	0.1842E5	1023.34	2.693 ††
$HB.(D.P).N_h$	12	0.3725E4	310.41	0.817n.s.
$f.(D.P).N_h$	18	0.1036E5	575.62	1.515n.s.
$f.HB.N_h$	12	0.3968E5	3307.2	8.702 ††
RESIDUAL	36	0.1368E5	380.07	
TOTALS	143	0.5301E7	37069.77	

TABLE 11

ANALYSIS OF VARIANCE FOR AVERAGE POWER (W_p)

Source of Variation	Degrees of Freedom	Sum of Squares	Variance	Variance ratio; F
f	3	0.9196E6	0.3065E6	27.744 ††
HB	3	0.9624E5	32081.43	2.903 †
D.P.	2	0.6059E6	0.3029E6	27.417 ††
N_h	2	0.1692E7	0.8460E6	76.569 ††
f.HB	9	0.3960E5	4400.53	2.061 n.s.
HB.(D.P)	6	0.3278E5	5463.02	2.559 †
f.(D.P)	6	0.1921E6	3202.25	14.997 ††
$f.N_h$	6	0.5983E6	99721.66	46.704 ††
$HB.N_h$	6	0.3586E5	5977.15	2.799 †
$(D.P).N_h$	4	0.3658E6	91468.74	42.839 ††
f.HB.(D.P)	18	0.2016E5	1120.14	1.279 n.s.
$HB.(D.P).N_h$	12	0.2138E5	1781.790	2.035 n.s.
$f.(D.P).N_h$	12	0.1153E6	9611.52	10.977 ††
$f.HB.N_h$	18	0.2138E5	920.67	1.051 n.s.
RESIDUAL	36	0.3152E5	875.59	
TOTALS	143	0.4783E7		

TABLE 12

ANALYSIS OF VARIANCE FOR HELICAL MAX. TORQUE (T_m)

Source of Variation	Degrees of Freedom	Sum of Squares	Variance	Variance ratio; F
β	2	0.1136E6	56789.06	4.141 †
f	3	0.9435E6	0.3144E6	22.931 ††
D.P.	2	0.1382E7	0.6911E6	50.392 ††
N_h	2	0.2275E6	0.1137E6	8.294 ††
β.f	6	0.1021E6	17022.69	1.049 n.s.
f.(D.P)	6	0.1879E5	3132.39	0.193 n.s.
β.(D.P)	4	0.5815E5	14537.37	0.895 n.s.
β.N_h	4	0.2240E5	5599.995	0.345 n.s.
f.N_h	6	0.2513E5	4189.38	0.258 n.s.
(D.P).N_h	4	0.1354E5	3385.67	0.209 n.s.
β.f.(D.P)	12	0.3637E6	30310.6	2.387 †
f.(D.P).N_h	12	0.1549E6	12911.47	1.017 n.s.
β.f.N_h	12	0.1598E6	13317.64	1.049 n.s.
β.(D.P).N_h	8	0.1207E6	15091.09	1.189 n.s.
RESIDUAL	24	0.3047E6	12695.61	
TOTALS	107	0.4011E7	37484.665	

β ; Helix angle, degrees

TABLE 13

ANALYSIS OF VARIANCE FOR HELICAL AVERAGE TORQUE ($\bar{T}_m$)

Source of Variation	Degrees of Freedom	Sum of Squares	Variance	Variance ratio; F
β	2	0.4612E5	23060.19	1.212 n.s.
f	3	0.3012E6	0.1004E6	5.277 ††
D.P.	2	0.1608E6	80396.03	4.225 ††
N_h	2	0.3205E7	0.1602E7	84.220 ††
β.f	6	0.2146E6	35776.92	2.630 †
f.(D.P)	6	0.3063E6	51052.75	3.753 ††
β.(D.P)	4	0.1629E6	40731.72	2.995 †
f.N_h	6	0.1357E6	22928.54	1.686 n.s.
(D.P).N_h	4	0.8792E5	21981.30	1.616 n.s.
β.f.(D.P)	12	0.4022E6	33515.49	3.704 ††
f.(D.P).N_h	12	0.1329E6	11075.44	1.224 n.s.
β.f.N_h	12	0.9183E5	7652.80	0.846 n.s.
β.(D.P).N_h	8	0.8080E5	10100.33	1.116 n.s.
β.N_h	4	0.3043E5	7607.55	0.559 n.s.
RESIDUAL	24	0.2172E6	9049.28	
TOTALS	107	0.55779E7	52130.09	

TABLE 14

ANALYSIS OF VARIANCE FOR HELICAL AVE. POWER (W_p)

Source of Variation	Degrees of Freedom	Sum of Squares	Variavce	Variance ratio; F
β	2	0.1423E6	71149.84	4.659 †
f	3	0.9627E6	0.3209E6	21.016 ††
D.P.	2	0.7494E6	0.3747E6	24.539 ††
N_h	2	0.2175E7	0.1088E7	71.229 ††
β .f	6	0.1979E5	3298.49	1.315 n.s.
f.(D.P)	6	0.1816E6	30310.18	12.085 ††
β.(D.P)	4	0.1191E5	2978.48	1.188 n.s.
$\beta.N_h$	4	0.9195E5	22988.04	9.166 ††
$f.N_h$	6	0.5083E6	84725.16	33.782 ††
$(D.P).N_h$	4	0.5121E6	0.1280E6	51.048 ††
β.f.(D.P)	12	0.1456E5	1213.41	1.662 n.s.
$f.(D.P).N_h$	12	0.1152E6	9599.41	13.152 ††
$\beta.f.N_h$	12	0.7255E4	604.56	0.828 n.s.
$\beta.(D.P).N_h$	8	0.1602E5	2002.44	2.743 †
RESIDUAL	24	0.1752E5	6563.13	
TOTALS	107	0.5526E7	51649.23	

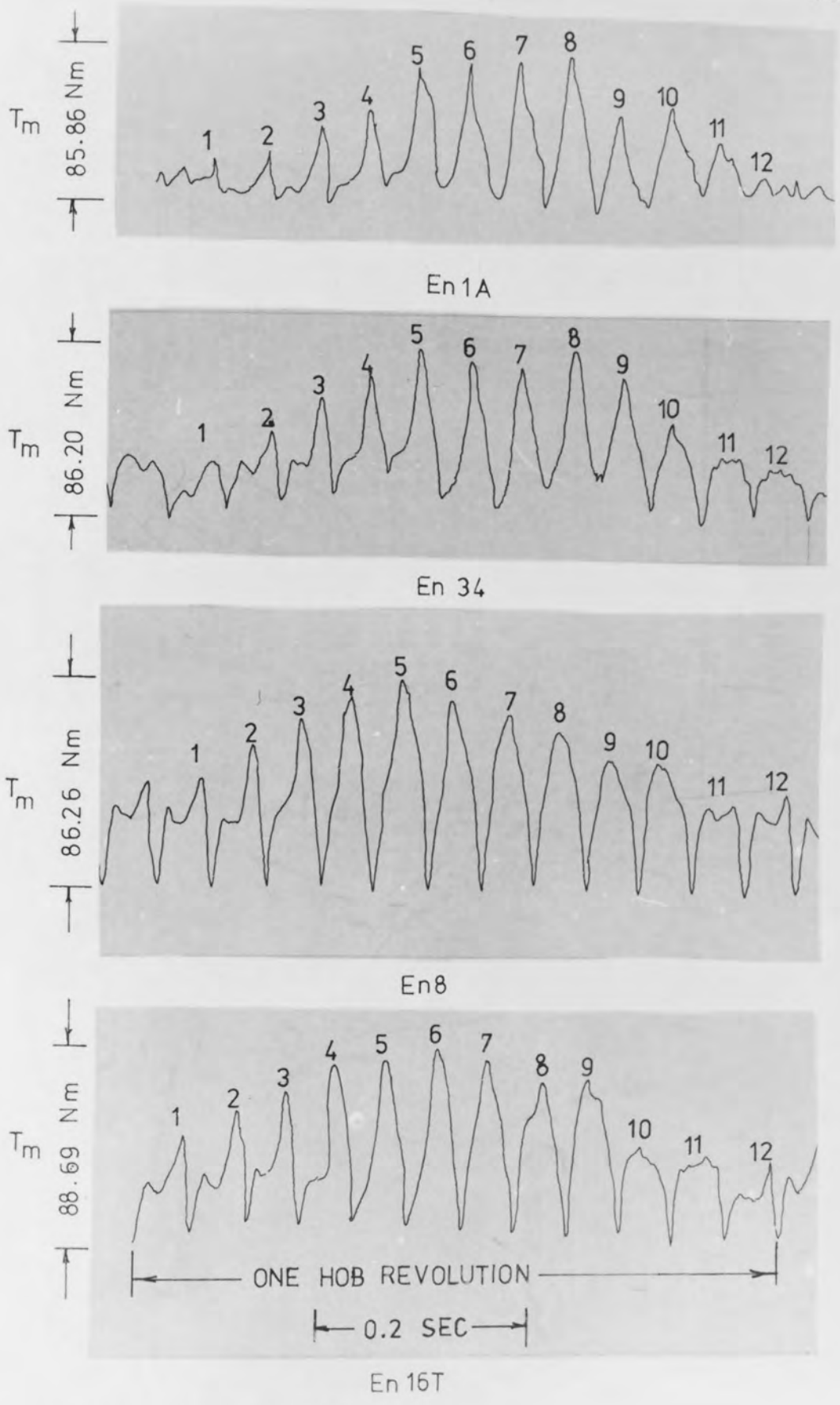

Fig. 26. MACHINING DATA:

HOB : 8 D.P., S.S.R.H., 12 GASHES
FEED : 1.270 mm/rev
SPEED : 115 r.p.m.

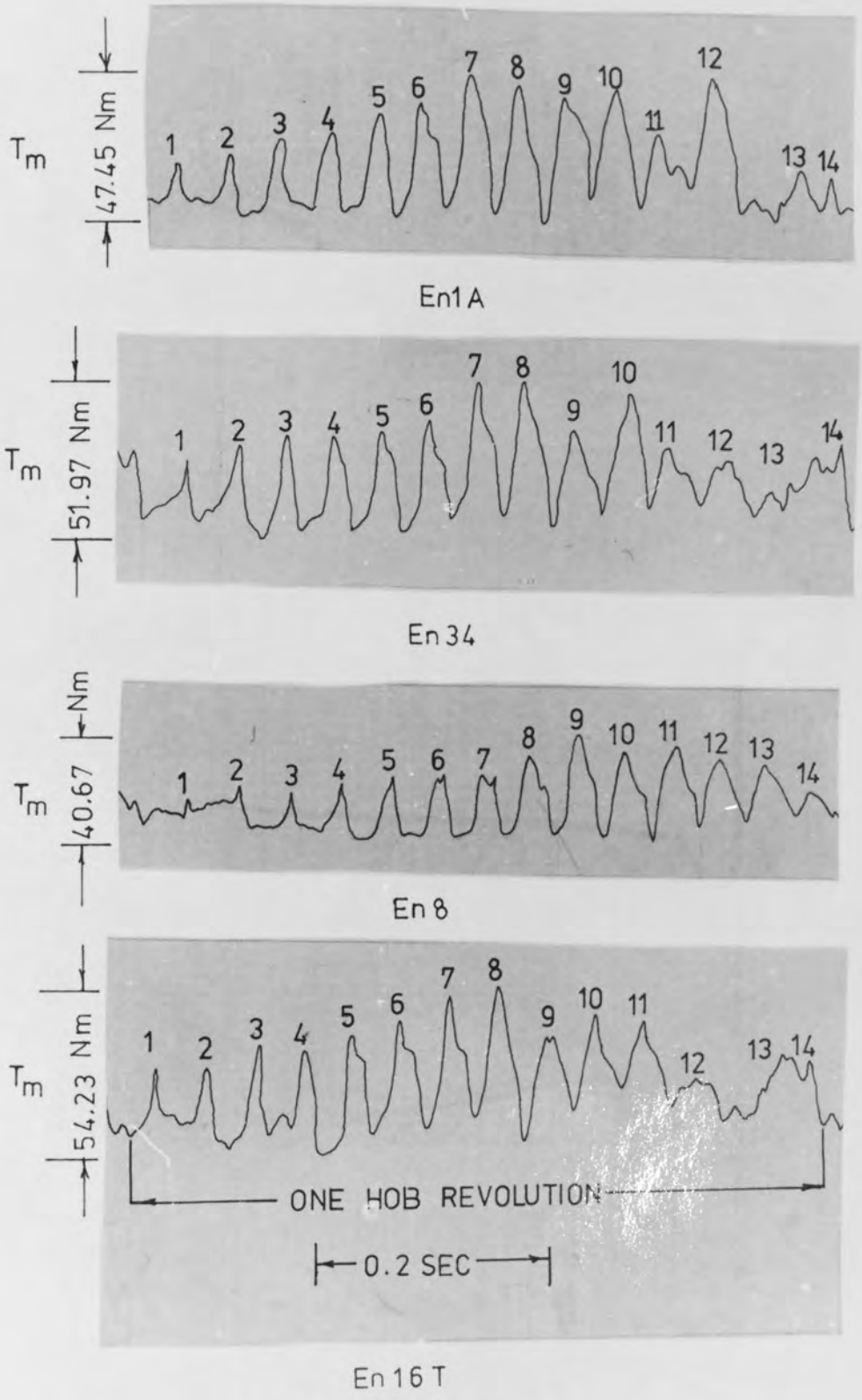

Fig. 27. MACHINING DATA:

HOB : 10 D.P. S.S.R.H., 14 GASHES
FEED : 1.270 mm/rev
SPEED : 115 r.p.m

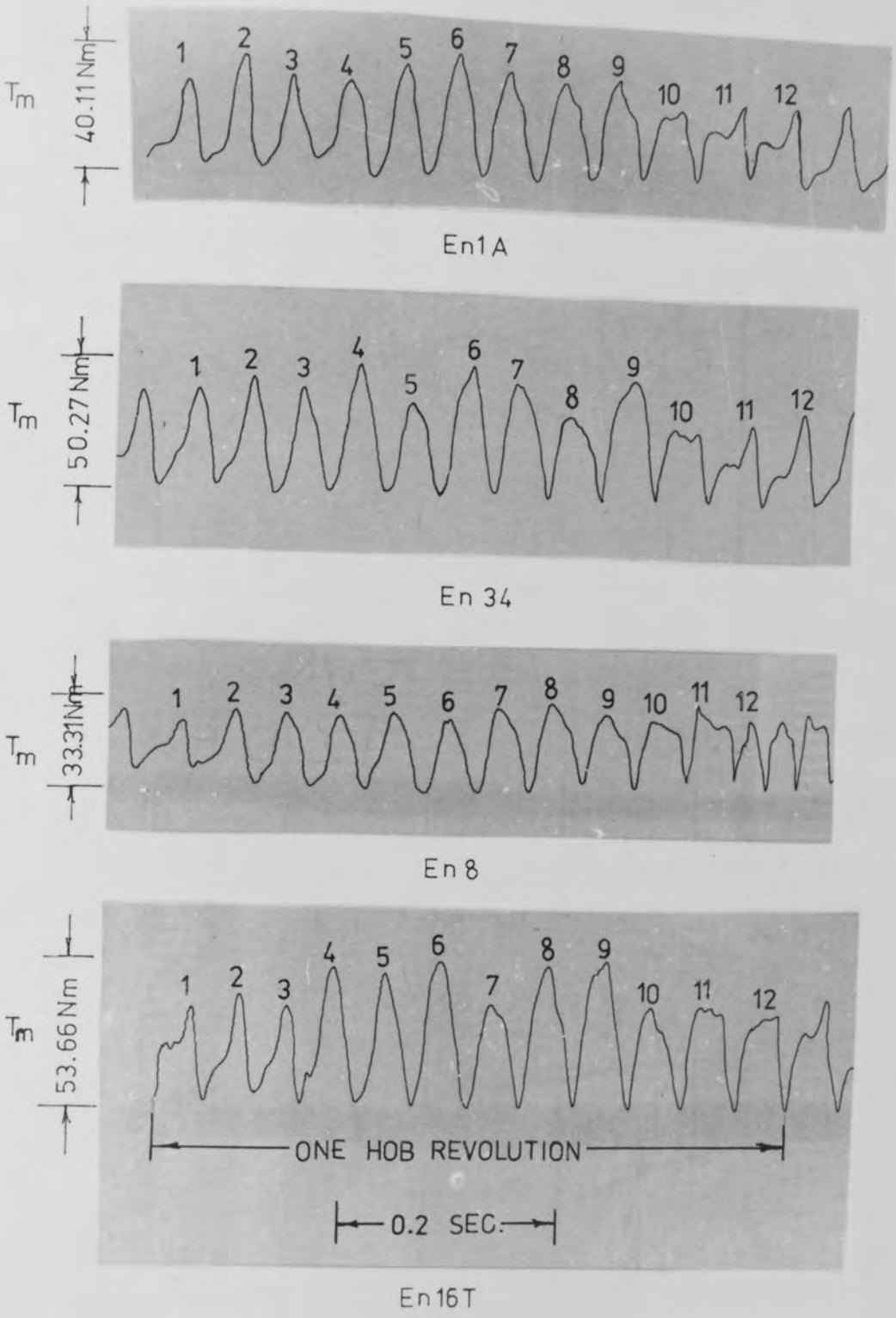

Fig.28. MACHINING DATA:

HOB : 12 D.P. S.S.R.H., 12 GASHES

FEED: 1.270 mm/rev

SPEED: 115 r.p.m.

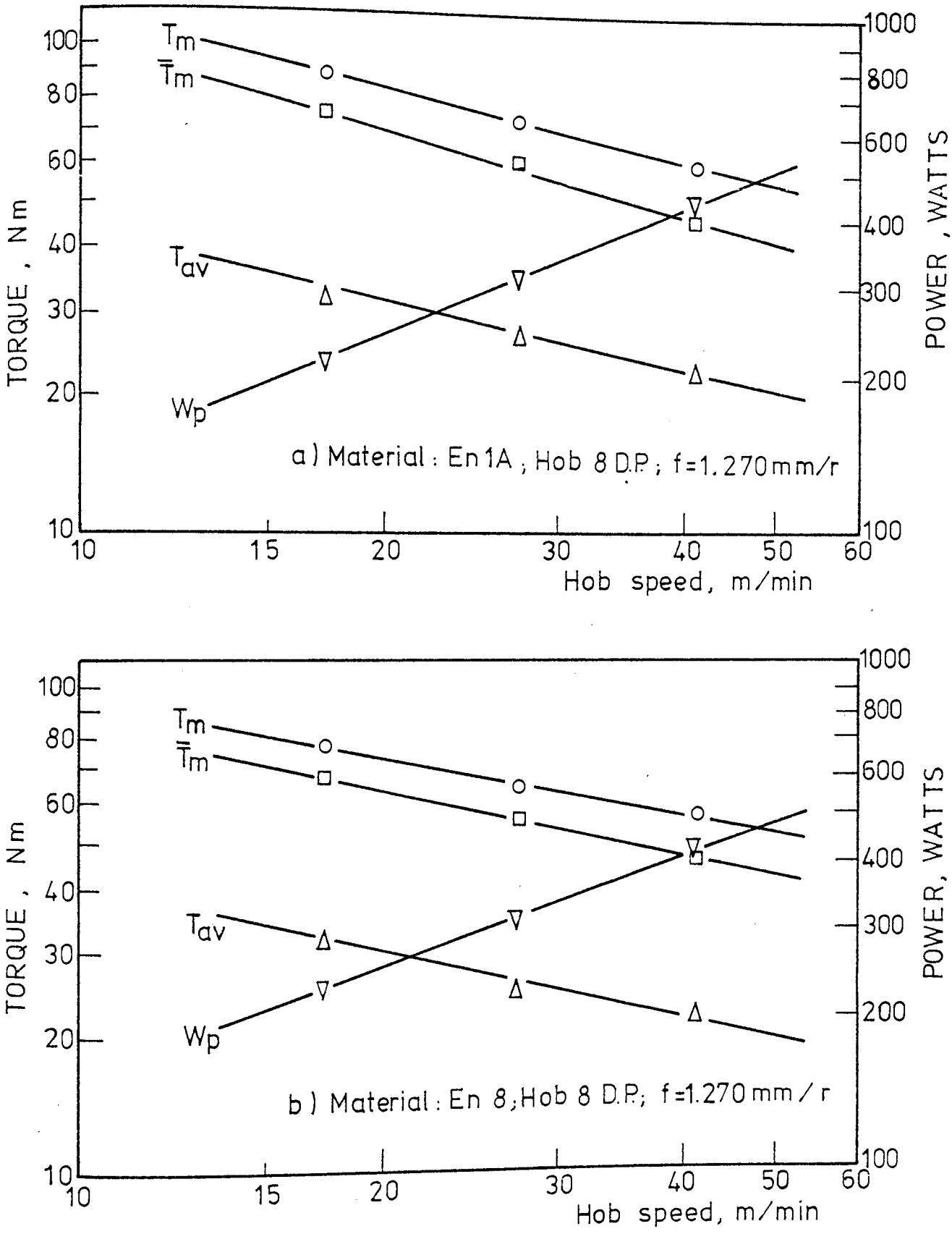

Fig. 29 EFFECT OF CUTTING SPEED ON TORQUES AND POWER

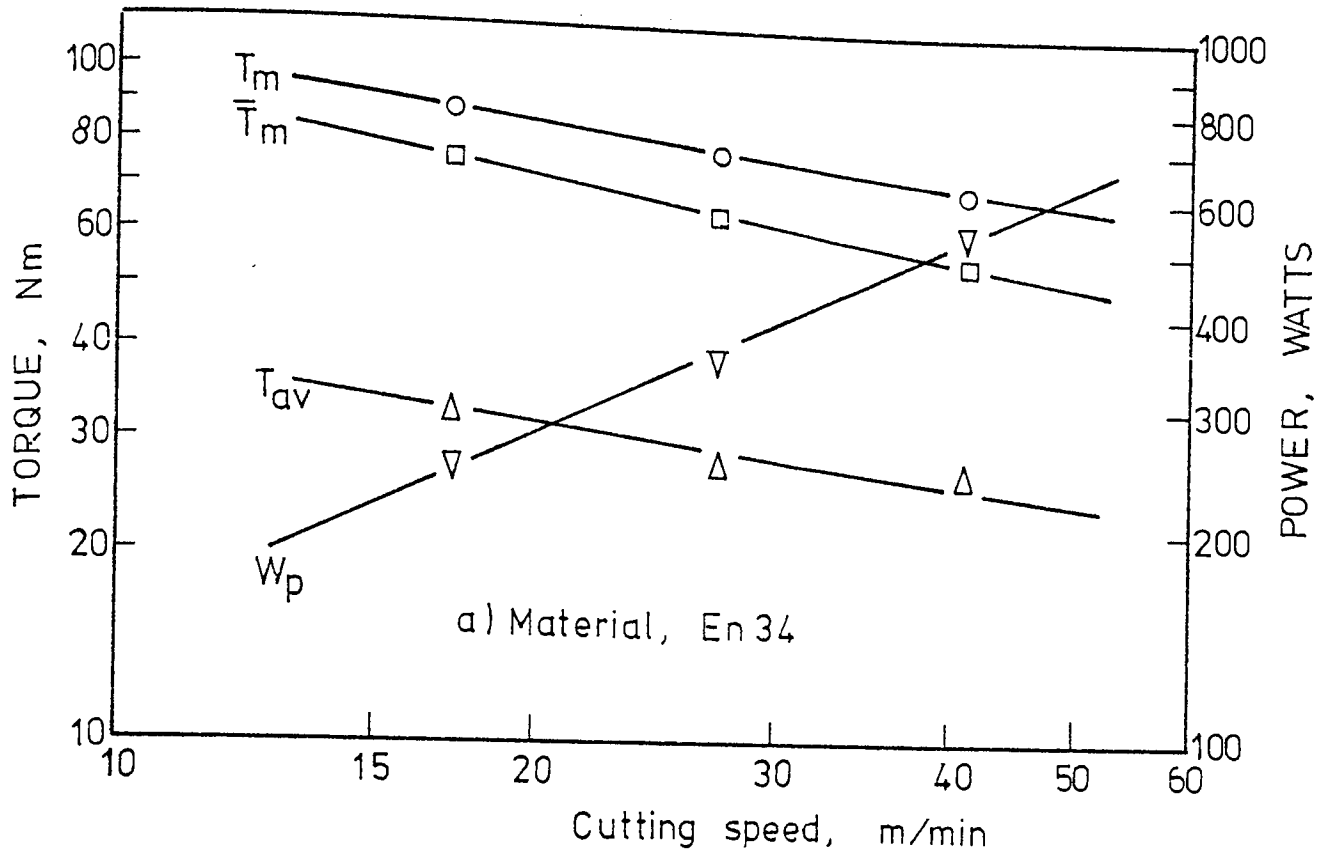

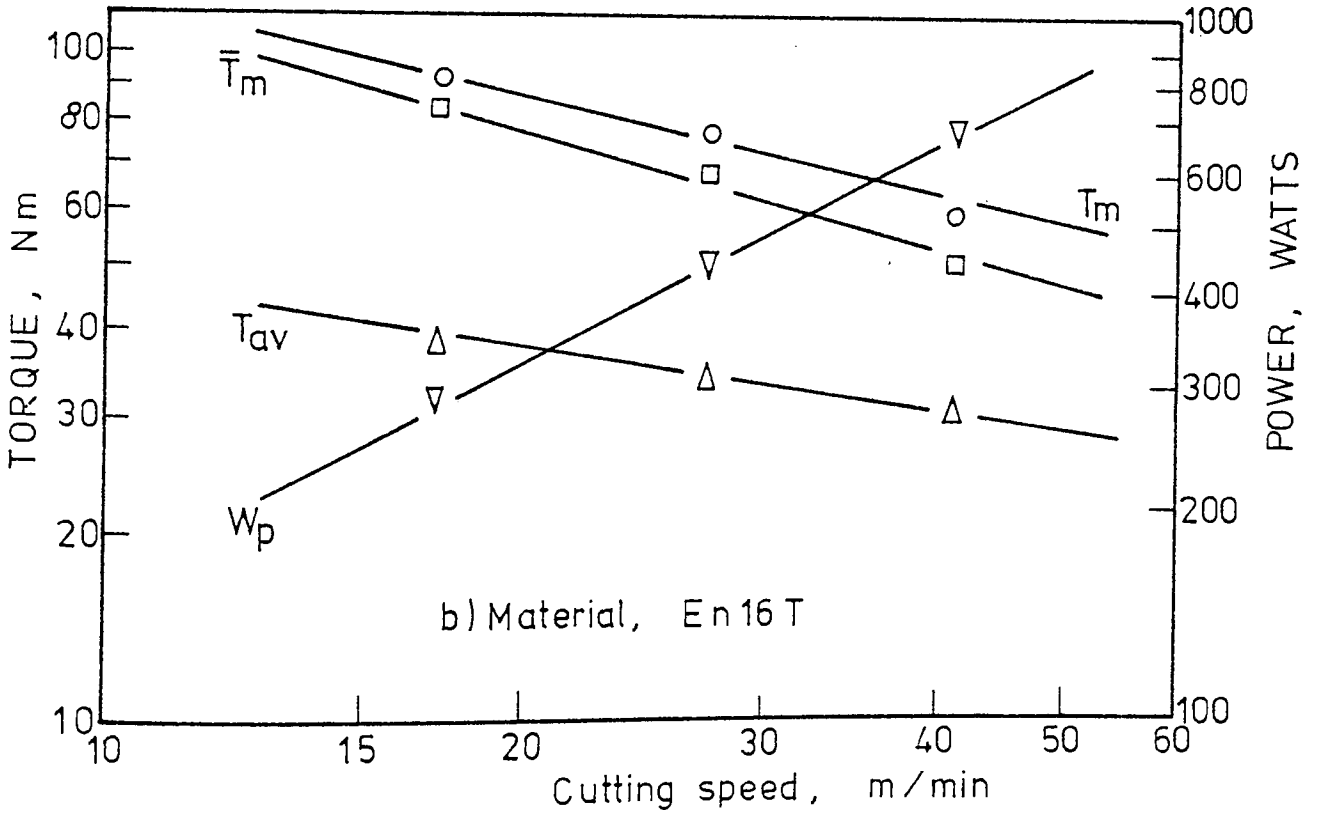

Machining Data:

Hob; 8 D.P., 12 gashes

f = 1.270 mm/rev

Fig. 30 EFFECT OF CUTTING SPEED ON TORQUES AND POWER

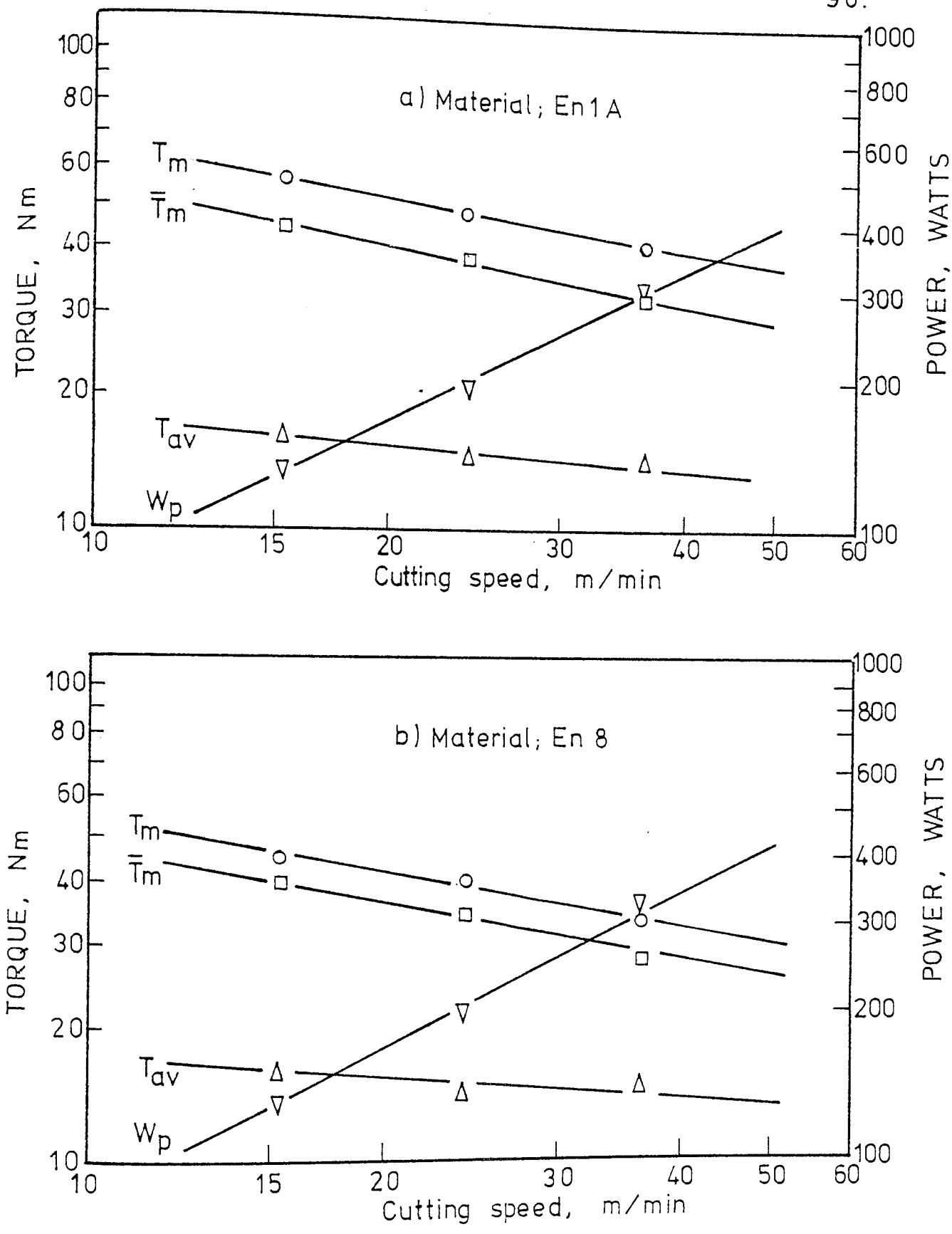

Machining Data:

Hob; 10 D.P., 14 gashes

f = 1.270 mm/rev

Fig. 31 EFFECT OF CUTTING SPEED ON TORQUES AND POWER

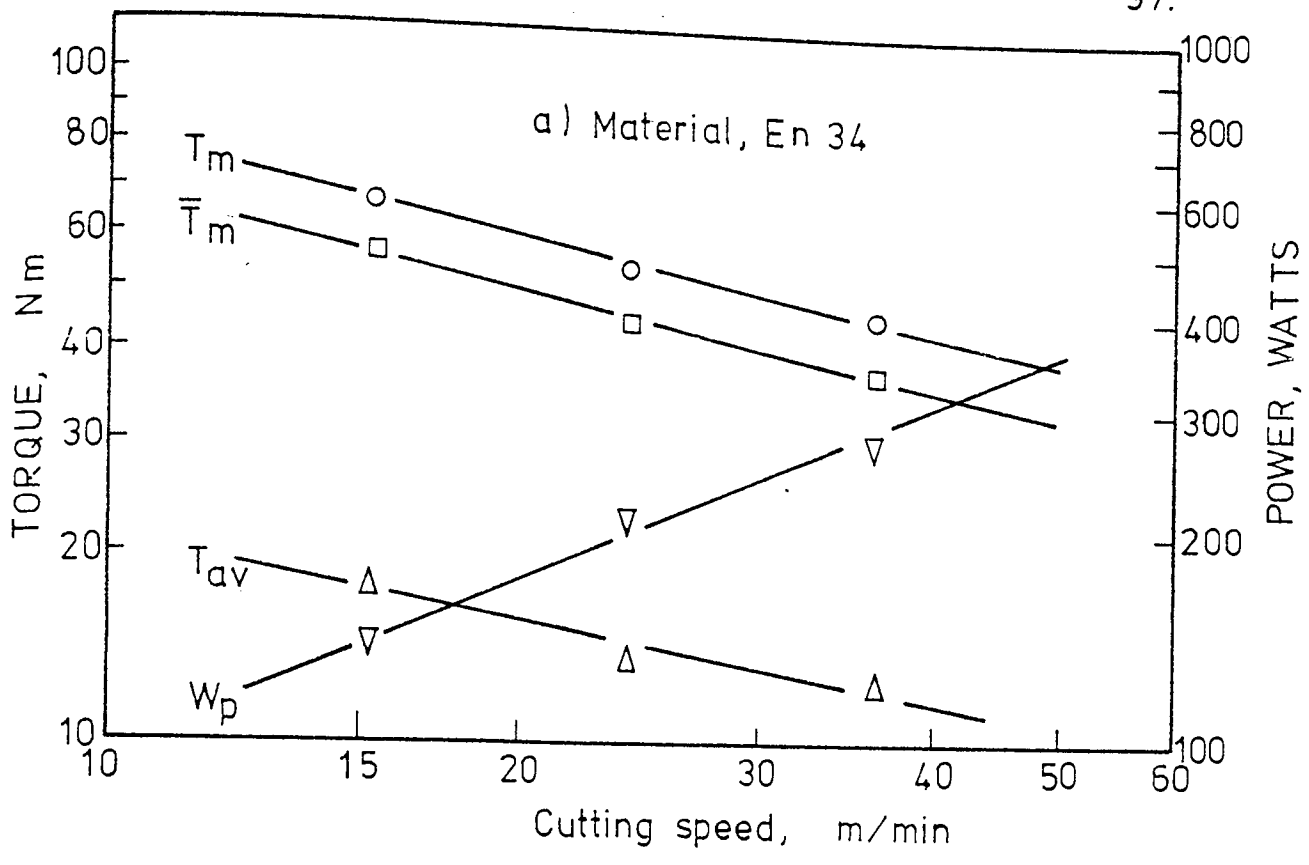

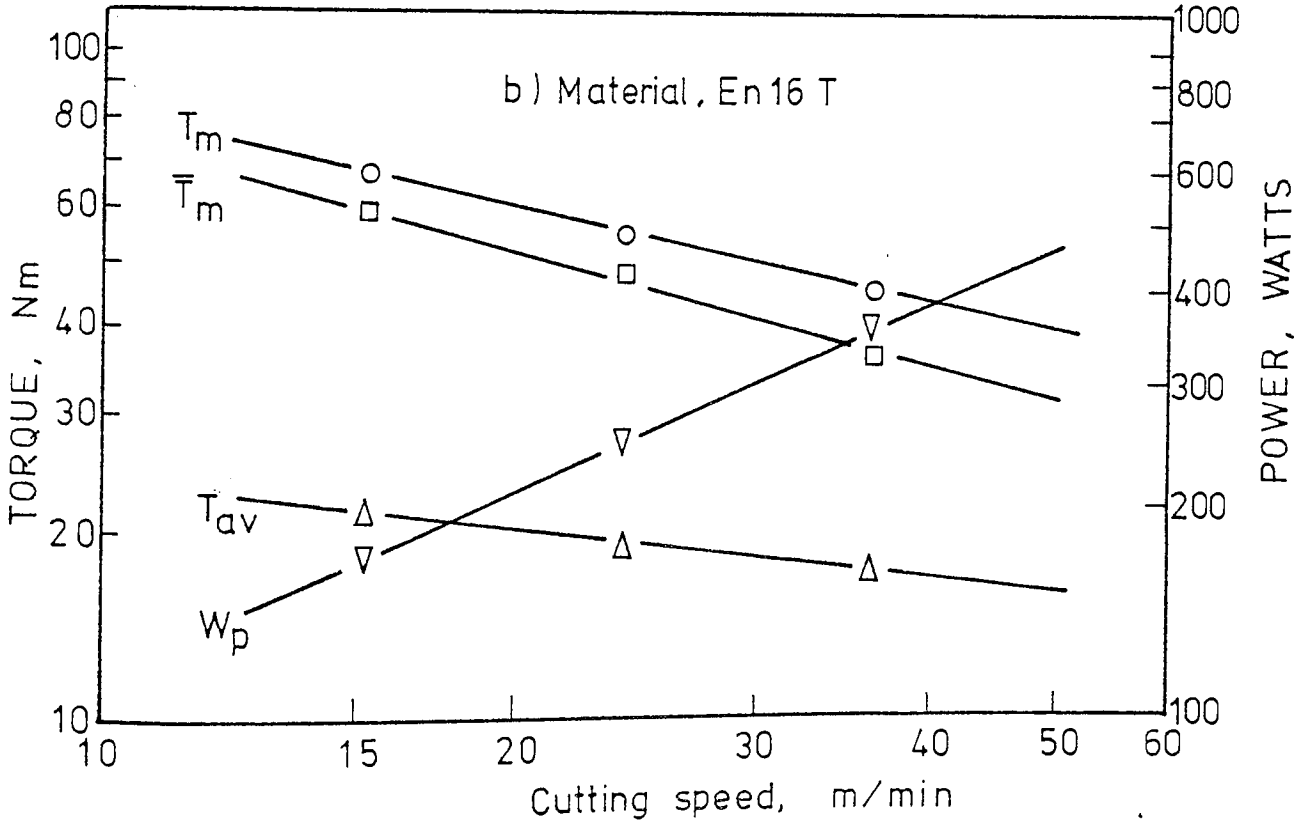

Machining Data:

Hob; 10 D.P., 14 gashes

f = 1.270 mm/rev

Fig. 32 EFFECT OF CUTTING SPEED ON TORQUES AND POWER

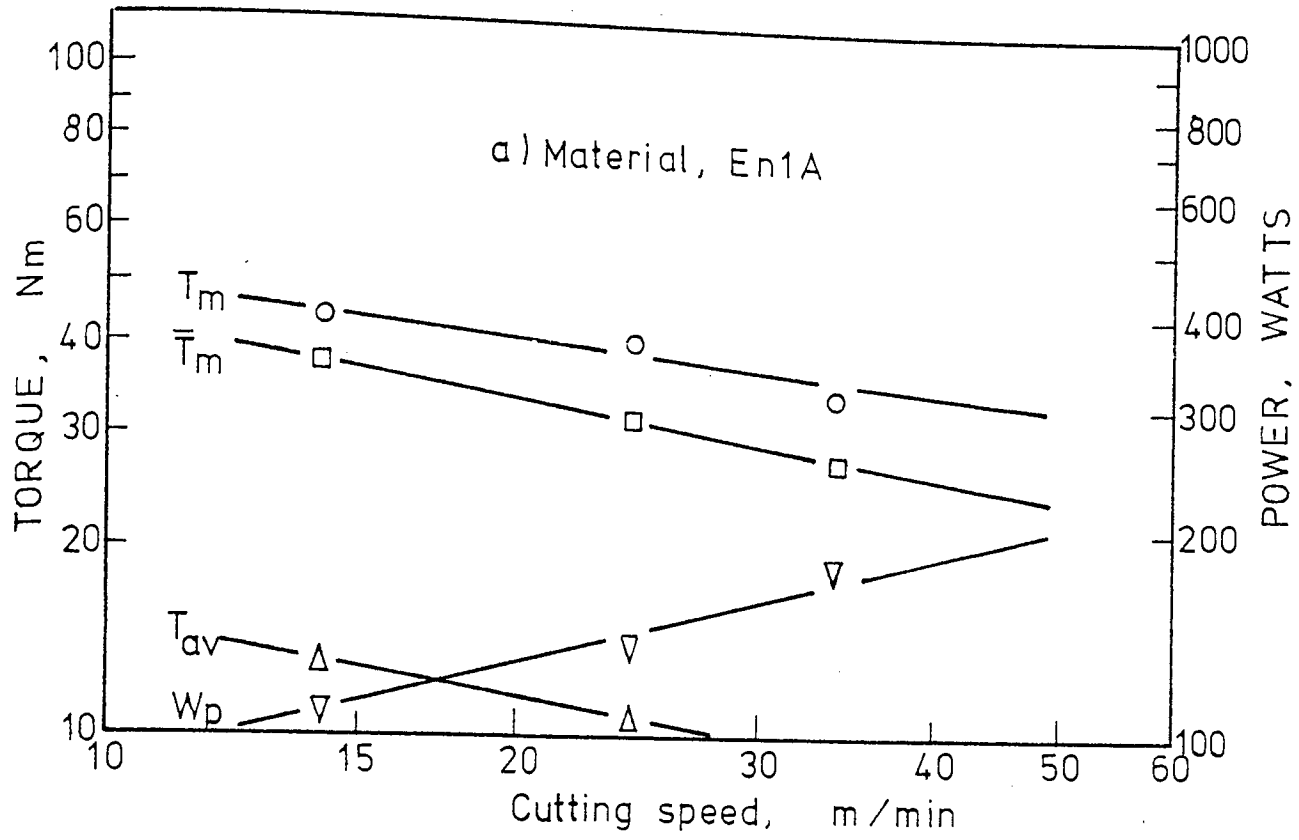

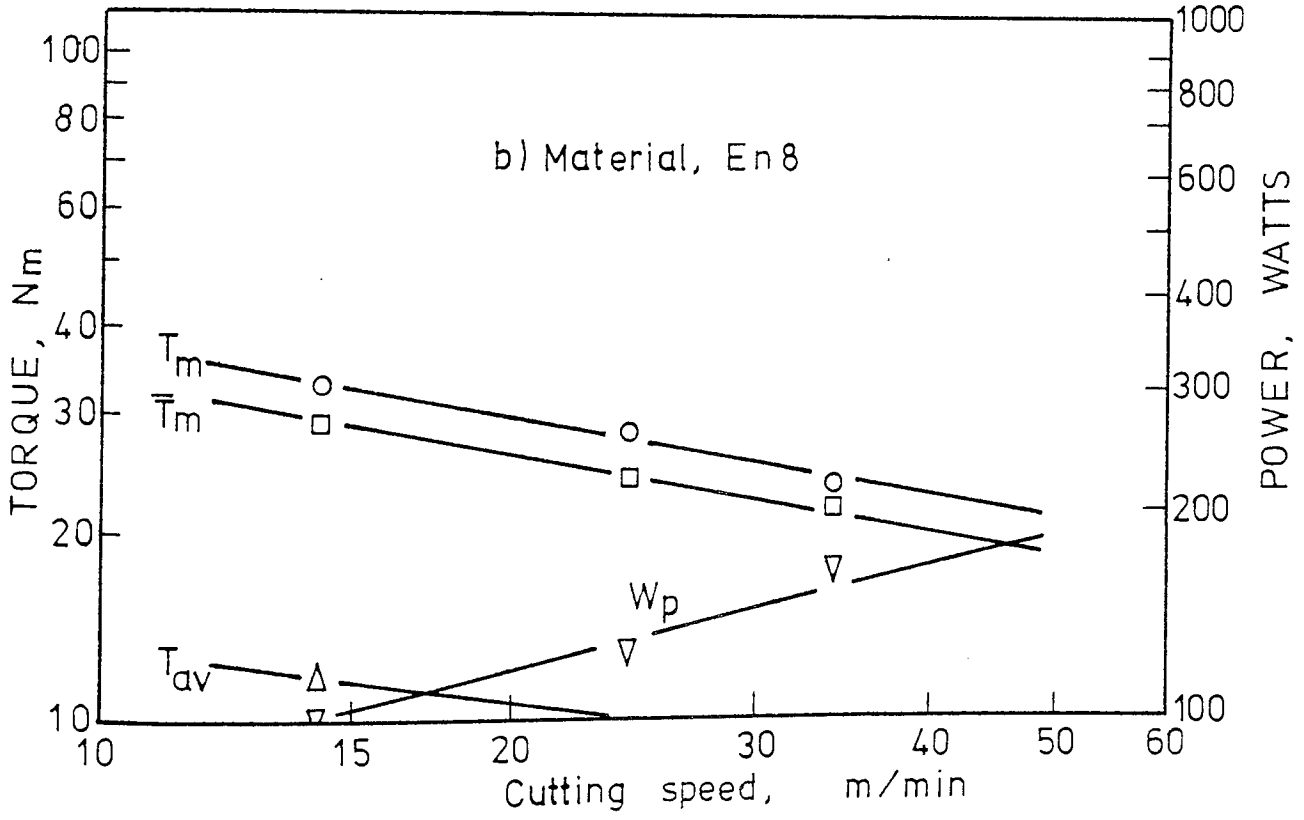

Machining Data:

Hob; 12 D.P., 12 gashes

f = 1.270 mm/rev

Fig. 33 EFFECT OF CUTTING SPEED ON TORQUES AND POWER

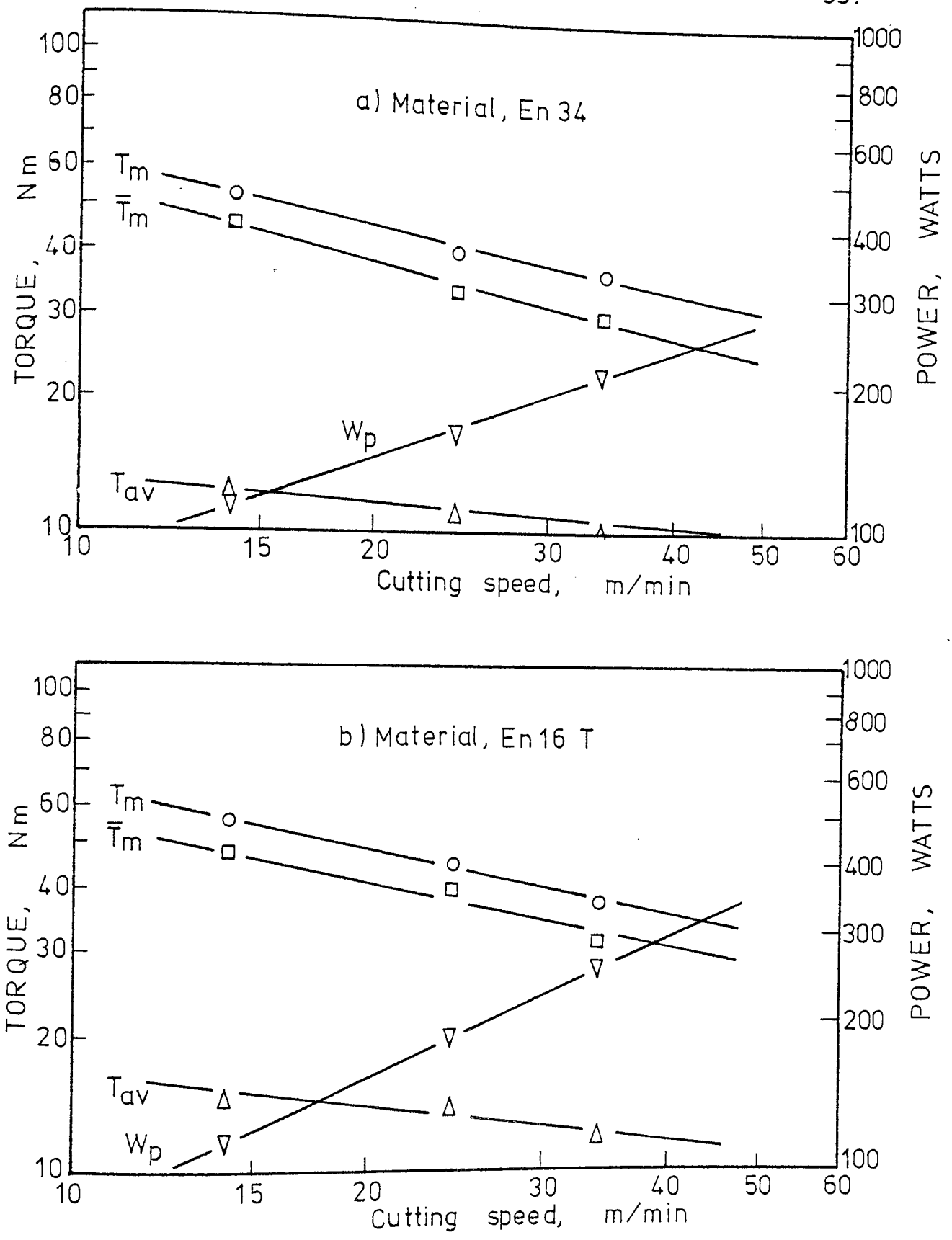

Machining Data:

Hob; 12 D.P, 12 gashes

f = 1.270 mm/rev

Fig. 34 EFFECT OF CUTTING SPEED ON TORQUES AND POWER

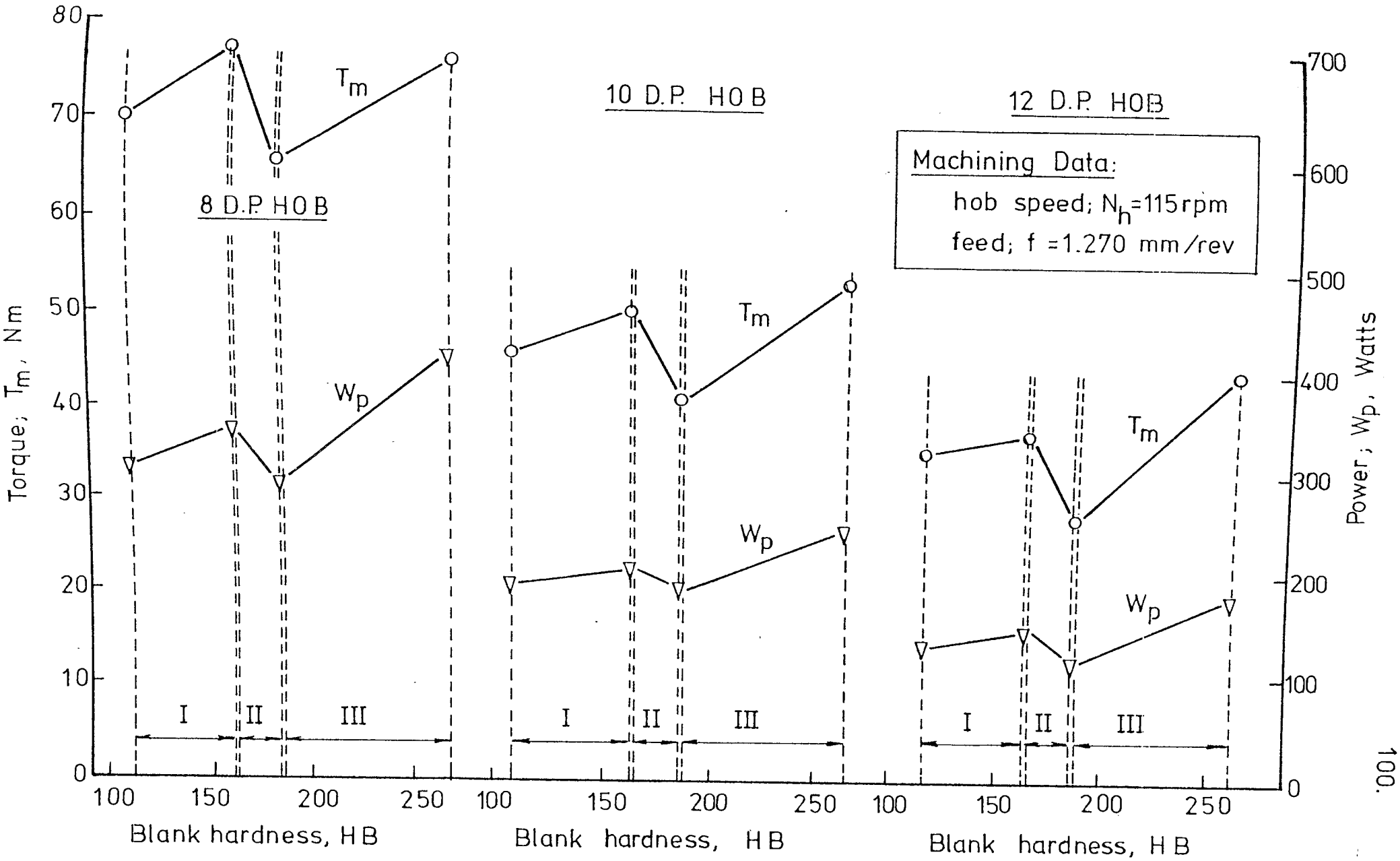

Fig.35 EFFECT OF HARDNESS ON TORQUE AND POWER

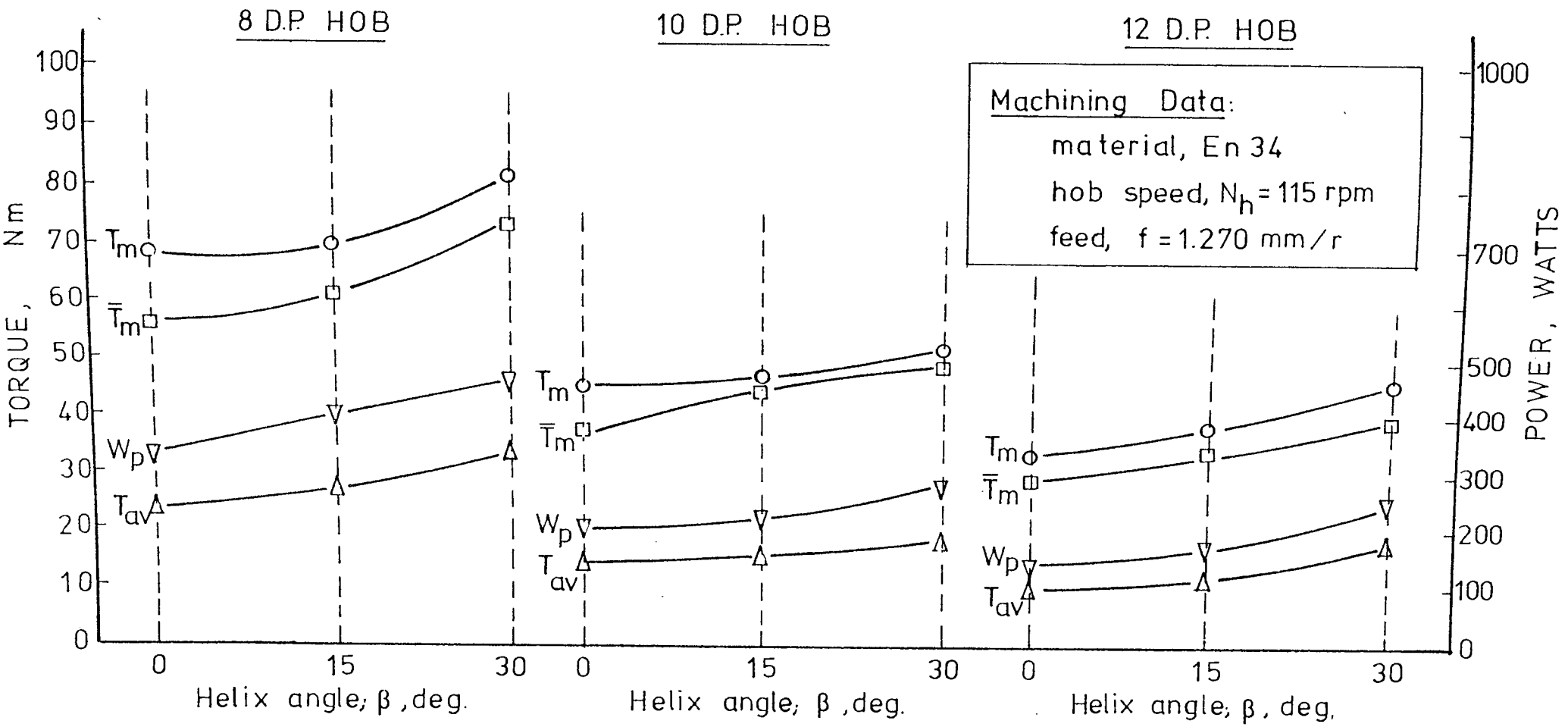

Fig. 36 EFFECT OF HELIX ANGLE ON TORQUES AND POWER

4.13 Discussion of Results and Comment

4.13.1 The Results

The simple hobbing process is assumed in all the following analyses, the rough hobbing of spur and helical gears with a single thread hob. Full depth of cut corresponding to the particular diametral pitch and conventional hobbing are concerned.

4.13.2 Recordings from Oscillograph

Figs. 26, 27 and 28 represent some recordings of the oberservations measured by the torque dynamometer. These graphical traces thus obtained express the electrical analogue of torque against distance circumscribed by the hob. Paper speed through the oscillograph was set at 200 mm./sec.

The values of cutting torques T_m and $\overline{T}_m$ were interpreted from the tracings by means of calibration graph shown in Fig. 25, and the results were tabulated in tables 5, 6 and 7.

The peaks on the traces correspond to the number of gashes in the hob; 12 gashes for 8 D.P. hob, 14 gashes for 10 D.P. hob and 12 gashes for 12 D.P. hob. The oscillograph traces were recorded at full depth of cut for each blank.

It is observed that the tooth trace rises from zero (datum) to a certain maximum almost linearly and proportional to torque encountered by a tooth and falls to zero after the cut has been accomplished. Another notable inference which can be drawn from the traces is that a following cut initiates well before a preceding cut for a tooth is completed. This can be explained by the fact that the hob is being fed axially

at constant rate and chances for preceding tooth to lose contact depend on hob diameter, the number of gashes in the hob and depth of cut.

4.13.3 Power and Average Torque Results

Readings of average power consumed during cutting were taken by the Wattmeter, and values of the average torque T_{av} were calculated from the power readings.

Results of average power, Wp and average torque T_{av} are tabulated in tables 6 and 8 for spur and helical gears respectively. Figures were rounded up to the nearest whole number.

4.13.4 Graphical representation of tabulated results

Some of the tabulated results are represented in graphical form as shown in Figs. 29 to 35 for spur gears, and Fig. 36 for helical gears.

4.13.5 Torques and Power versus Hob Speed

Figs. 29 to 34 show in graphical form, maximum torque; T_m, average of maximum torque; $\bar{T}_m$, average torque, T_{av} and the average cutting power, W_p have been plotted against hob speed, V (m/min) at constant feed of 1.270 mm/rev for spur gears of 8 D.P., 10 D.P. and 12 D.P. where four different types of steel blanks were used.

From each of the figures, it is observed that when hob speed is increased, cutting torques decrease linearly and the average power increase linearly on a Log.log scale, but do not pass through zero. This may be explained by the fact that the edge of the edge of the cutter could be deforming the surface

of the workpiece elastically, plastically, or both, without actually cutting it, as in normal rubbing.

4.13.6 Torque and Power versus Material Hardness

The work material is one of the major variables affecting cutting forces and power. The common variables considered are work-material composition and microstructure, its hardness and work hardening properties.

Fig. 35 shows in graphical form the variation of max torque and average cutting power for 8 D.P., 10 D.P. and 12 D.P. spur gears plotted against Brinell Hardness Number, (H_B) for constant speed and feed rate. From these graphs it is explicit that no monotonic function exists for torque, T_m or power, W_p as a function of (H_B) in the range covered, although in practice there is a general trend for torque and power to increase with the increase of hardness, because the range is divided into three different zones depending on the mechanical properties and structure of the material.

The hardness number shown has been measured on the blanks as obtained directly from the manufacturer and no heat treatment was given. More specifically, it can be observed from Fig. 35 that in zone I that torque and power rise with hardness. This is characterised by improved metallurgical and mechanical properties for En 1A and En 34 steel. Both types of steel have Low Carbon Content and fairly high ductility.

In Zone II, there is a sharp drop in both torque and power from En 34 to En 8 steel as hardness increases. This can be accounted for by the fact that in annealed and normalised form, a coarsely dispersed structure of lamellar pearlite

(En 8 steel) is present which produces a low strength and ductility.

In Zone III, torque and power increased again with the increase of hardness as expected between En 8 and En 16T (Manganese-molybdenum steel).

An important advantage of microstructure studies over the simpler average hardness method is that the various machining difficulties can be predicted from metallurgical observations.

4.13.7 Torques and Power versus Helix Angle, β

Fig. 36 shows in graphical form the variation of torques T_m, $\bar{T}_m$, T_{av} and power, W_p against the gear helix angle, β for 8 D.P., 10 D.P., and 12 D.P. hobs at constant speed and axial feed for En 34 steel. It is observed that torques and power increase with the increase of helix angle, and that D.P. of the gear to be cut has a substantial effect on torques, because with a large D.P., the thickness and perimeter of the undeformed chip will go up.

4.14 Statistical Analysis

A set of 144 tests based upon preliminary investigation was provided by combinational arrangement of 4X4X3X3 non-factorial experimental design in order to provide all the essential information about Torques, T_m, $\bar{T}_m$ and T_{av} and Power, W_p behaviour with respect to the cutting parameters when hobbing spur gears.

And a set of 108 tests were based upon a combinational arrangement of 3X4X3X3 non-factorial design of experiment to observe torques and power behaviour against cutting parameters

when hobbing En 34 steel helical gears.

I.C.L. 1904 series statistical analysis system was employed to compute the Analysis of Variance and Multiple Regression.

4.14.1 Effect of feed, hardness, D.P. and Hob Speed on max. torque, T_m

The analysis of variance is given in Table 9 and it follows that D.P., feed, H_B and hob speed have a highly significant effect on max. torque acting on the hob shaft. Also that the interaction between f, D.P. and speed is less significant. It can be observed that hob diametral pitch has the most significant effect on T_m, hence the assumption that speed has little or no effect on torque is rejected over this range of cutting conditions, and it should be considered as well as the other cutting parameters.

4.14.2 Effect of feed, hardness, D.P. and Hob Speed on av. of max. torque, $\bar{T}_m$

The analysis of variance presented in Table 10 shows average of max torque, $\bar{T}_m$ during spur gear hobbing for different materials, hobs, speeds and feeds given in Table 5. It can be seen that hob speed, feed and D.P. are highly significant, while material hardness is less significant, also the interactions between feed and D.P. and between feed and speed and between hardness and speed, and feed, hardness and D.P., and between feed, hardness and speed have a high significance level of 0.01 on average of hob max. torque. While the rest of the interactions have no significant effect. It should be noted that speed has the most significant effect on torque $\bar{T}_m$. Hence the assumption is again rejected.

4.14.3 Effect of feed, hardness, D.P. and Speed on Average Power, W_p

The average power consumed during cutting spur gears for the different materials, hobs, feeds and speeds are given in Table 6. The analysis of variance is presented in Table 11. It follows that speed, feed and D.P. are highly significant as well as the interactions between feed and hardness, feed and speed, hardness and speed and interaction between feed, speed and hardness have a highly significant effect on average power. Also the blank material hardness and interactions between hardness and D.P., and between hardness and speed are less significant at the level of 0.05, while the rest of the interactions have no significant effect. Again it is noticed that speed has the most significant effect on power.

4.14.4 Effect on maximum torque in helical hobbing

To observe the behaviour of maximum torque, T_m during cutting En 34 steel helical gears for different helix angles, feeds, hobs and speeds, the analysis of variance is presented in Table 12. It can be seen that D.P., feed and speed have high significance on maximum torque, while helix angle β and interaction between helix angle, feed and D.P. are less significant at the level of 0.05. All the other possible interactions are not significant. It is noticed here that D.P. has the highest significant effect.

4.14.5 Effect on Average of Maximum Torque in Helical Hobbing

Analysis of variance Table 13 shows that the helix angle has no effect on the average of maximum torque, $\bar{T}_m$ while speed has the highest significant effect. Feed and diametral pitch

are less significant. Interactions between feed and D.P. and between feed, helix angle and D.P. are highly significant, and the rest of the interactions are less or not significant.

4.14.6 Effect on average power in Helical Hobbing

The average power consumed during hobbing En 34 steel helical gears for different hobs, helix angles, feeds and speeds are given in Table 8. The analysis of variance is presented in Table 14. It can be seen that Speed, D.P. and feed are highly significant, helix angle is less significant. Interactions between feed and D.P., helix angle and speed, feed and speed, D.P. and speed and between feed, D.P. and speed are also highly significant, while the rest of the interactions are either less or not significant. It is noticed that speed is the highest significant parameter again.

4.14.7 Effect of Module and Feed on Average Torque

It was decided to obtain the relationship between average torque, module and axial feed for each gear blank material, En 1A, En 34, En 8 and En 16T at a constant hob speed of 115 r.p.m., then the results of previous work and analytical results are compared.

Three gear modules $\frac{1}{8}$, $1/_{10}$ and $1/_{12}$ inches were involved in the design of this experiment as well as four levels of feed,

$$f = 0.609,\ 0.914,\ 1.270 \text{ and } 1.987 \text{ mm/rev.}$$

The analytical expression is described as,

$$P_{Tav} = \frac{2\,T_{av}}{D_h} = C_m\ m^x . f^y . \qquad (28)$$

Equation (28) was described in Chapter II as follows:

$$P_{Tav} = C_m \; m^{1.52}.f$$

Table 15 represents the results of previous work to obtain the values of exponents x, y.

Table 15. Exponents x and y in Equation (28)

Exponents	Rozenberg[21]	Nekrasov[22]	Bhattacharyya[2]	Analytical
x	1.30	1.41	1.50	1.52
y	0.90	1.00	0.75	1.00

The results of the present analysis for each material is presented in Table 16 where torque in each case was related to axial feed and gear module by following the theoretical model (28).

Table 16 Results of Ave. Torque exponents

Material	Value of (x)	Value of (y)
En 1A	1.510	0.72
En 8	1.582	0.78
En 34	1.543	0.74
En 16T	1.495	0.68

The values of exponents (x) and (y) in Table 16 are closely related to the anlaytical values and agrees with the results of previous work.

4.15 Generalised Torque and Power Equations

In order to obtain a general relationship between Torque and/or Power as a dependent variable, and cutting parameters (i.e. feed, speed, hardness, etc) as independent variables, as can be seen in Fig. 29 to Fig. 34, the curves are non-linear and this may be considered in the statistical analysis, where the linearized model can be examined.

144 maximum torque and average power consumed results were considered as in table with the objective to establish equations for maximum torque and average power when cutting spur gears in terms of four independent variables; feed, hardness, diametral pitch and speed was based on the application of multiple regression analysis.

It was first assumed that both torque and power are related to the four parameters by relation of the form :

$$T_m,\ W_p = C\ f^{\beta_1}\ (D.P.)^{\beta_2}\ (HB)^{\beta_3}\ V^{\beta_4} \qquad (29)$$

or

$$\hat{y} = \ln T_m \text{ or } \ln W_p = b_o + b_1 \ln f + b_2 \ln(D.P) + b_3 \ln(HB) + b_4 \ln (V) \qquad (30)$$

Where $\hat{y}$ is the predicted value of maximum torque or average power on a logarithmic scale

$b_o, b_1 \ldots, b_4$ are parameters

The following generalised relationships were obtained

(i) when hobbing spur gears;

$$T_m = \frac{3795.645 \quad f^{0.624} \quad (HB)^{0.1138}}{(D.P.)^{1.662} \quad V^{0.372}} \quad Nm \qquad (31)$$

with error sum of squares = 0.25895, residual error = 0.1379 and multiple correlation = 0.947

$$W_p = \frac{329.238 \quad f^{1.067} \quad (HB)^{0.228} \quad V^{0.771}}{(D.P.)^{1.858}} \quad Watts \qquad (32)$$

with error sum of squares = 0.36702, residual error = 0.1636 and multiple correlation = 0.970

ii) when hobbing helical gears;

Another 108 readings of maximum torque and average power consumed during hobbing represented in Table 7 and Table 8 were considered. The following generalised relationships are similarly obtained when hobbing En 34 steel helical blanks,

$$T_m = \frac{6686.993 \quad f^{0.4995}}{(\cos\beta)^{1.356} \quad (D.P.)^{1.7027} \quad V^{0.324}} \quad Nm \qquad (33)$$

with error sum of squares = 0.6197, residual error = 0.078 and multiple correlation = 0.973

$$W_p = \frac{686.209 \quad f^{1.008} \quad V^{0.791}}{(D.P.)^{1.749} \quad (\cos\beta)^{3.0577}} \quad Watts \qquad (34)$$

with error sum of squares = 0.3058, residual error = 0.1732 and multiple correlation = 0.969

4.16 General Discussion

A purpose of this work has been to investigate the effect of cutting speed on cutting torques and average power consumed during hobbing spur and helical gears as well as other cutting parameters such as axial feed, material hardness, diametral pitch and gear helix angle. From a search of literature available it was discovered speed has little or no effect on cutting torques and power.

The results of the preceding analysis indicates that hob speed has the highest significant influence on average of maximum torque, and average power for both spur and helical hobbing, while a significance at the level of 0.01 on maximum and average torques, and it was noticed that cutting torques fall with a rise in hob speed as expected, and cutting power rises rapidly with an increase in hob speed.

Analysis of variance indicates that hob diametral pitch was found to have a substantial effect on maximum torque, T_m, because with a large D.P. the thickness and perimeter of the undeformed chip will go up.

Axial feed was also found to have a highly significant influence on cutting torques and power, the effect of feed on hobbing torques is more complicated in gear cutting than in turning. An increase of feed in gear hobbing leads to an increase in the depth of the undeformed chip, this increase is, however, not uniform along the length of contact (i.e. along the total perimeter of the cut) and is sharply

marked in the approach tooth machining zone. The length of contact increases proportionately as new approach teeth which move a thicker chip, come into operation.

To make the process more efficient, therefore, it would be advisable to vary the axial feed rate by applying a greater rate at the start of a pass and reducing it towards the end of full depth of cut.

Analysis of variance of helical hobbing proved that the gear helix angle has little or no effect on cutting torques and power when hobbing En 34 steel. It is generally useful to check the hardness as well as the microstructure when inspecting a work material. It has already been shown that for a given hardness the cutting torques and power will vary over a wide range by having different microstructures. This scatter can further increase if the hardness varies within and between workpieces. It would at least be useful to maintain the hardness within as small a tolerance as possible.

4.17 Conclusions

1. Cutting speed has a significant effect on cutting torques coming on the hob shaft and average power consumed during hobbing spur and helical gears, conventially.

2. It is advisable to vary the axial feed rate by applying a greater rate at the start and reducing it towards the full depth of cut.

3. The magnitude of cutting torques increased considerably with the increase of gear module from 12 D.P. to 8 D.P. An increase of 100% in feed produces an equivalent increase of 87% in maximum torque at constant hob speed.

4. It is useful to check the hardness as well as the microstructure when inspecting a work material, where it is explicit that no monotic function exists for cutting torques and power as a function of hardness.

5. The gear helix angle has little or no effect on cutting torques and power consumed when hobbing En 34 steel blanks.

CHAPTER V

THE STUDY OF THE VARIATION OF GEAR TEETH SURFACE ROUGHNESS

5.1 Introduction

The performance of every mechanism in which two surfaces are in sliding contact is affected by the texture of the surface. In toothed gearing the tooth flanks are in both sliding and rolling contact, and make either line or point contact with one another, depending upon which type of gear is being considered.

Although geometrical measurements are an important feature of the checking measures in the manufacture of accurate gears, microscopic geometrical measurements, like tooth flank roughness, are no less important. And as a parameter, surface roughness has some advantages, e.g. it may be seen as reflecting on the sub-surface layer condition in a way. This sub-surface condition is very important in relation to possible tooth failures.

Also surface roughness plays a role in the running in of gears; and surface quality is related to gear accuracy. Moreover, surface roughness relates to the tools, and the checking thereof; cutting edges, cutting angles and tool pitch errors.

One would like to point out that measurements on machined gears can never be improved upon too much. These measurements should be considered as of prime importance for controlling the cutting, finishing process, tools and hobbing machines. That is to say, the first and the best check on

the manufacturing process.

The irregular nature of the topography of a surface can arise from a number of process characteristics including inaccuracies in the machine tool, deformation under cutting force, vibration, geometry of the cutting action, metal tearing during chip formation, and metallurgical or heat-treatment effects. These factors will produce surface irregularities which can cause misalignment and part mal-functions, excessive loading over small areas, frictional and lubrication problems, general finishing and reflectivity problems as well as catastrophic failures. The purpose of this section is to investigate the effect of the cutting variables; e.g. axial feed, cutting speed, material hardness and gear diametral pitch on the machined gear tooth flank roughness along the feed line and to obtain a mathematical model to describe the relationship between surface roughness and cutting variables.

5.2 The Nature of the Surface

One of the basic problems in surface characterisation, apart from the determination of the numerical values by means of statistical moments (CLA, r.m.s., etc.), is to classify the type or family to which the surface belongs.

Three basic structural components may be evident in a typical surface profile, i.e.

1. Waviness or secondary texture
2. Roughness or primary texture
3. Surface lay or errors of form

The nature of the waviness component is dependent on

the overall process generating the surface. Surfaces generated by abrasive processes such as grinding often contain waviness structures which result more from the dynamics of the system (chatter, vibration) rather from the geometry of the generating operation. Such periodicities often have large wave-lengths relative to the primary texture which are not as readily perceivable unless a sufficiently long profile record is examined.

Surfaces generated by processes such as milling and gear hobbing will have shorter, more prominent periodicities arising from the tool geometry and progressive manner in which the surface are generated.

Roughness or primary texture defines the more localized irregularities in the surface profile. The nature of this component will depend primarily on the chip formation mechanism and the material properties of the workpiece and cutting tool combination.

The error of form defines the overall undulation of the surface and is related to the structure of the waviness component.

Peklenik [23] introduced in the proposal for a surface classification system the correlation functions as a comprehensive method of surface description, while Devor [24] developed a new technique for surface profile characterization which employs parametric stockastic models of the autoregressive-moving average (ARMA) class.

5.3 Preliminary Tests with 8 D.P. Hob

In order to investigate the variation of surface roughness of different parts of the spur gear tooth profile with axial feed and hob speed, preliminary tests were carried out using 8 D.P. hob on a SYKES HV-14 gear hobbing machine.

The cutting process in gear hobbing is considerably complicated compared with that in plain hobbing. The chip removal by each cutting tooth on a hob is different from one another, and the pulsating cutting force resulting from the intermittent cutting action of tooth blades. The nature of the machined gear tooth surface is very complicated in a unique way that the preliminary cutting tests were considered in order to observe graphically the variation of surface roughness with feed and speed for En 34 steel as an example.

Through the experiments, active type EP cutting oil was used, and the depth of cut was kept constant, to be 7.145 mm. for 8 D.P. hob.

5.3.1 The Experimental Conditions

Tool - 8 D.P. Hob; S.S.R.H.; 12 Gashes; 61.62 mm. O.D.

Work material - low carbon steel En 34 (HB = 164)

Feed rates - 0.609 mm/rev and 1.270 mm/rev

Hob speeds - 17.389, 27.024 and 41.828 m/min.

direction of feed - conventional

total space length of cut (= face width X number of teeth) -

2.54 X 29 = 73.66 cm

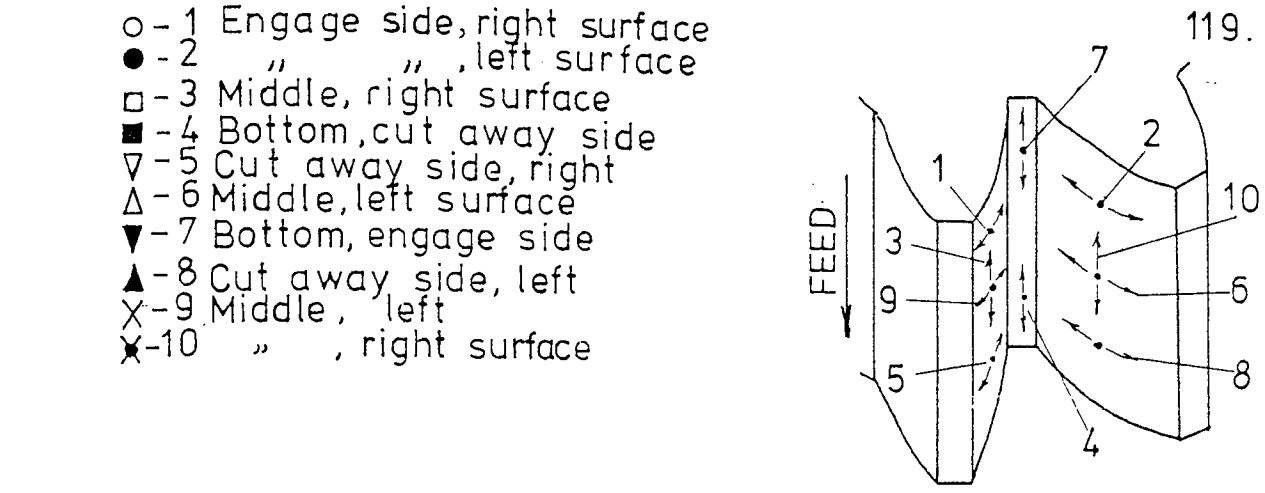

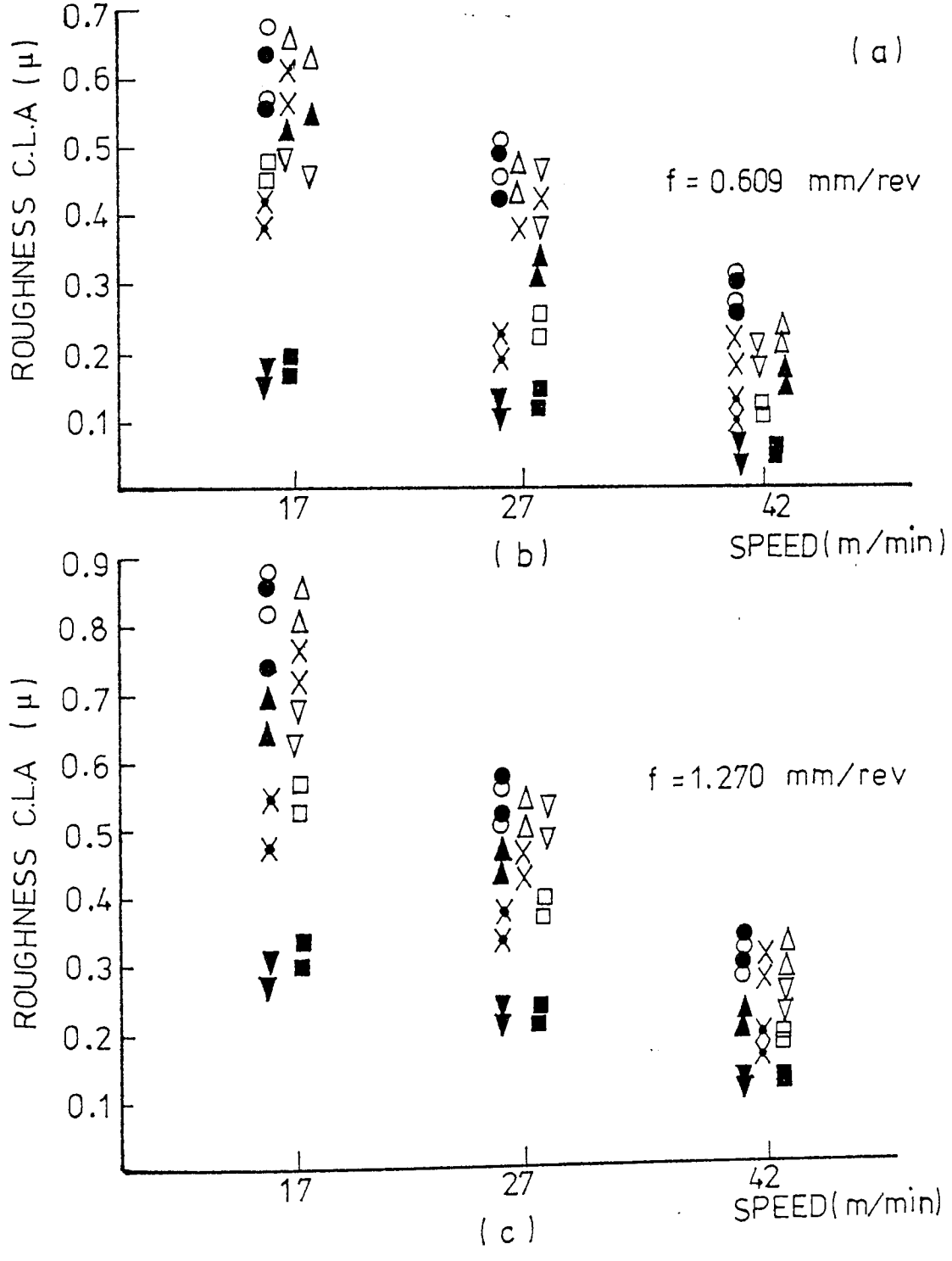

Fig.37. EFFECT OF SPEED AND FEED ON ROUGHNESS

Machining Data : hob; 8 D.P., S.S.R.H., 12 gashes
blank; En 34 steel, (HB 164)

The centre-line average (CLA) method of assessing surface texture is used where the values are expressed in microns.

5.3.2 Observations

The relations between surface roughness, cutting speed and axial feed are shown in Fig. 37. The surface roughness was measured at the bottom land and tooth surfaces of the gear cut in ten different positions. The positions and directions of measurement are shown in Fig. 37a.

It is clear that surface roughness decreases with the increase in hob speed, and increases with the increase in axial feed. Although it is shown in Fig.37 b ,and C that the surface roughness of the bottom land 4 and 7 and along the surface 3 and 10 are smaller than that of the tooth profile surfaces, this is not true. This is because the directions of motion of the tracer of the measuring instrument are different in both cases, in other words, the tracer is moved parallel to the direction of feed along the teeth, and perpendicularly to that on the tooth profile surface.

As far as preliminary tests are concerned, a higher cutting speed results in a less surface roughness, and more tests are needed in order to observe the significant influence of cutting parameter on surface roughness, and build a model to describe surface roughness in terms of feed rate, cutting speed, material hardness and hob D.P.

5.4 Experimental Set-up and Procedure

It was decided to measure surface roughness along the gear teeth, parallel to the feed direction at positions 3 and 10 as shown in Fig. 37a for different combinations of feed rate, hob speed, material hardness and hob diametral pitch. The definition and measurement of surface texture is covered by B.S. 1134: 1961. The centre-line-average (CLA) method.

5.4.1 Surface Measurement. The Taylor Hobson Talysurf

The Talysurf makes use of a sharply pointed stylus to trace the profile of the suface irregularities being measured. The nominal tip radius of the stylus point is made 0.001 in. (0.0025 mm) when a graphical record is needed, but for a CLA reading, a tip radius of 0.0005 in. (0.012 mm) is acceptable. Movement of the stylus as it follows the profile of the surface is measured relative to a skid. This is a block of large radius of curvature that follows the main form of the surface and provides a datum.

In its motion along a defined sampling length of the profile the vertical movement of the stylus causes electrical impulses to be fed into the instrument. From these a mean line is determined such that the nominal shape of the surface is defined and on each side of it the sums of the areas outlined by the surface are equal. Electrical integrating instruments refer to the mean line in evaluating the roughness. The actual surface texture reading is derived from the measurement of several sampling lengths taken consecutively along the surface. These cut-off values are chosen to suit the type of surface being measured.

The Taylor Hobson Talysurf instrument provides one of the most satisfactory means of determining surface texture on the CLA scale, particularly under workshop inspection conditions.

The instrument was set as follows:

Diamond stylus tip dimension; 0.0001 in. (0.0025mm)
Stylus bearing force; 0.1 gram.
Graphical magnification along surface; x 100
Graphical magnification normal to surface; ~ 2000
Average meter cut-off; 0.10 in. (2.54mm)
Operational traverse; 0.30 in. (7.62 mm)

5.4.2 Modifications and Addition to Equipment

A special jig was set up to enable the gear tooth surface to be measured quickly, efficiently and accurately by the Talysurf. This comprised of a 1 in. diameter arbour being clamped horizontally in a Vee block, bolted to a mount which was itself bolted to the Talysurf table as shown in Fig. 38a and b.

The gear was positioned on the arbour and a gear tooth positioned accurately in line with the stylus by means of a 0.750 in. slip gauge. This saved setting the Talysurf datum each time a reading was taken.

5.4.3 Surface Measurement

Each gear was mounted upon the arbour on the jig, and the slip gauge positioned beneath a gear tooth. The stylus was then brought forward to the tooth and the graph indicator pointer zeroed. The stylus was traversed across

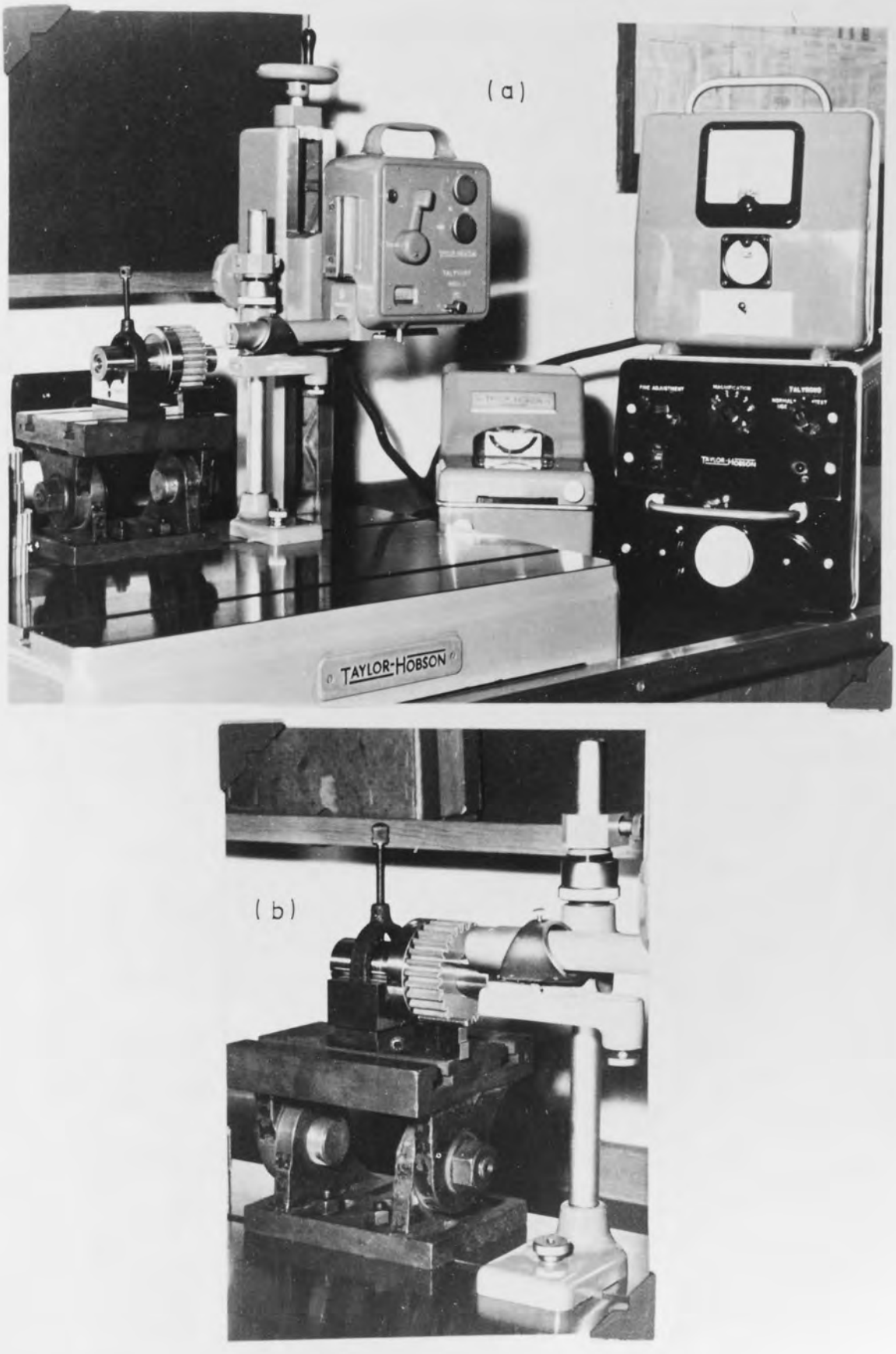

Fig.38. SURFACE ROUGHNESS MEASURING EQUIPMENTS

the gear tooth at positions 3 and 10 as shown in Fig. 37a, the CLA meter being read.

Two readings were taken on each side of a tooth, the average noted. This was repeated for three teeth on each gear, the average of each being noted. The grand CLA average for each gear and standard deviation was then computed.

Figs. 39 to 41 show some graphs of surface topography for 8, 10, and 12 D.P. gear teeth at different cutting speeds, taken at a magnification giving a 0.10 mm full scale.

5.4.4 Design of Experiment

The most simple hobbing process is assumed in all the following analysis, the rough hobbing of spur gears with a single thread hob. Full depth of cut corresponding to the particular diametral pitch and conventional hobbing are concerned.

The gears being measured are the same gears cut previously when torques and power were measured.

A 4x4x3x3 non-factorial design of experiment was used in order to investigate the variation of surface roughness with the cutting variables as follows:

Axial feeds; 0.609, 0.914, 1.270 and 1.987 mm/rev.

Hob Speeds; 74, 115 and 178 r.p.m.

Gear blank materials, En 1A (HB 115), En 34 (HB 164), En 8 (HB 183) and En 16T (HB 269)

Hobs; 8 D.P. (12 gashes), 10 D.P. (14 gashes) and 12 D.P. (12 gashes), S.S.R.H.

Cutting fluid; Active type EP cutting oil containing Sulphur, chlorine and fat.

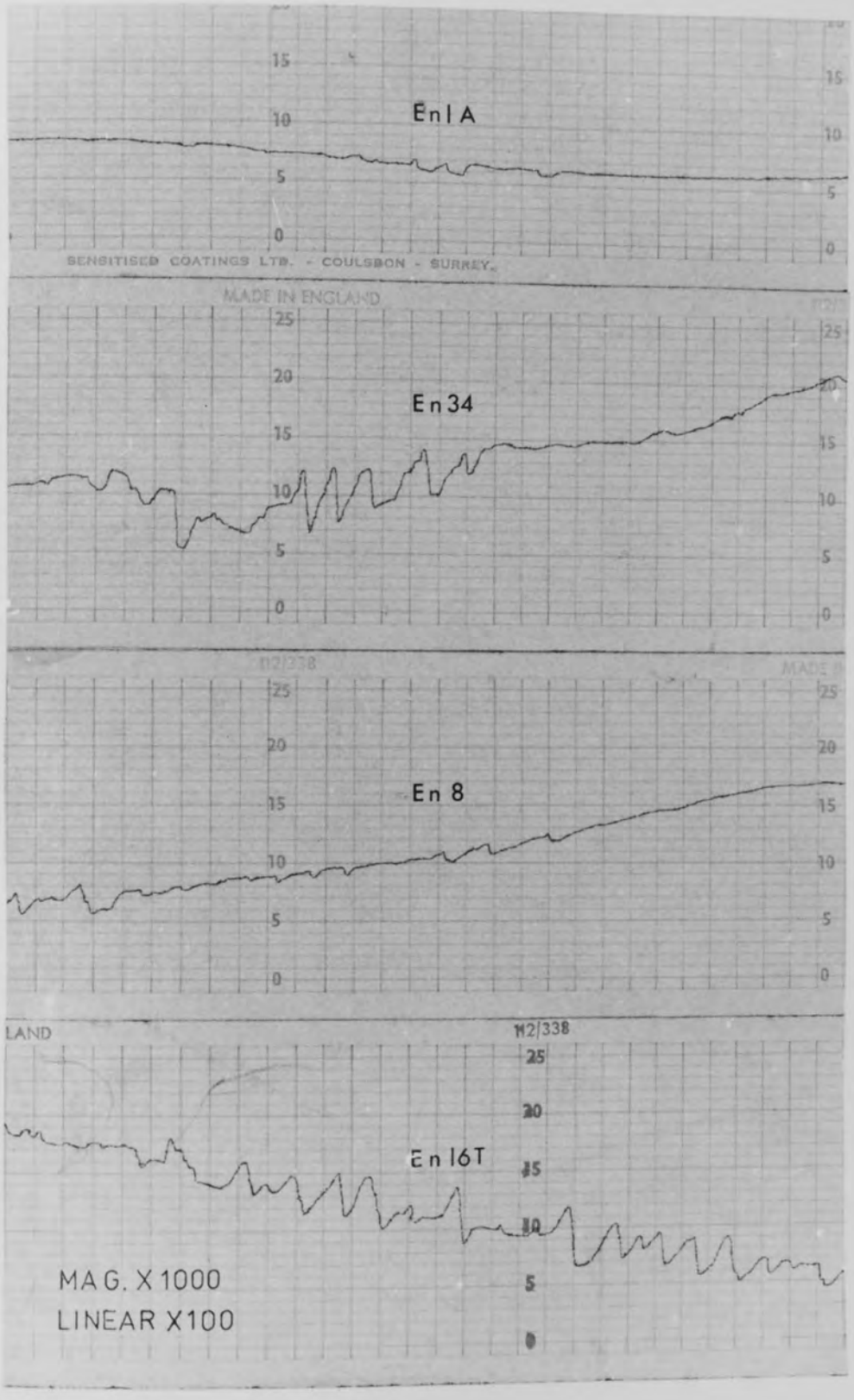

Fig.39. SURFACE FINISH TRACES

Machining Data: hob 8 D.P., 12 gashes
f = 1.270 mm / rev
N_h = 115 r.p.m.

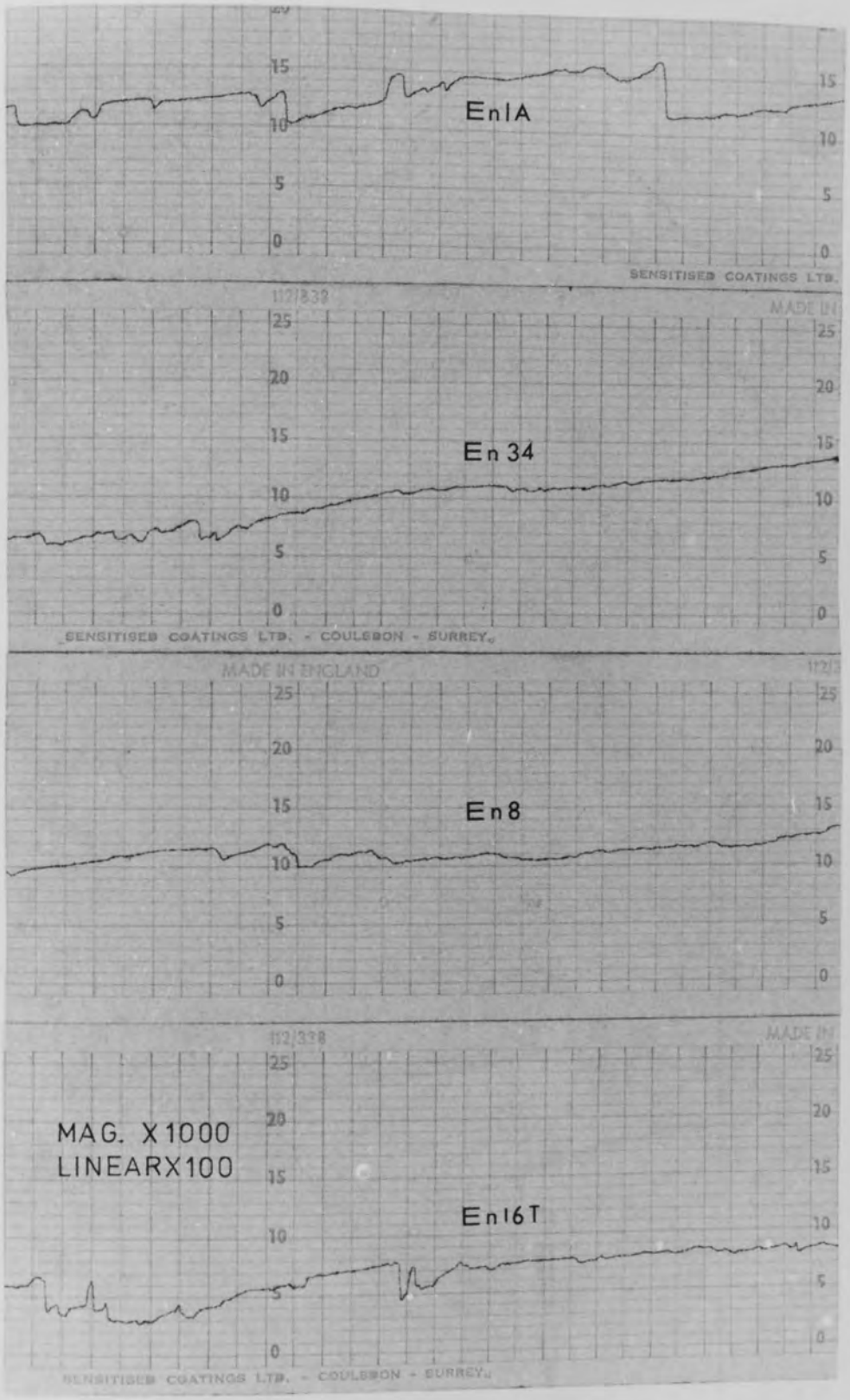

Fig. 40. SURFACE FINISH TRACES

Machining Data: hob 10 D.P., 14 gashes
f = 1.270 mm/rev
N_h = 115 r.p.m.

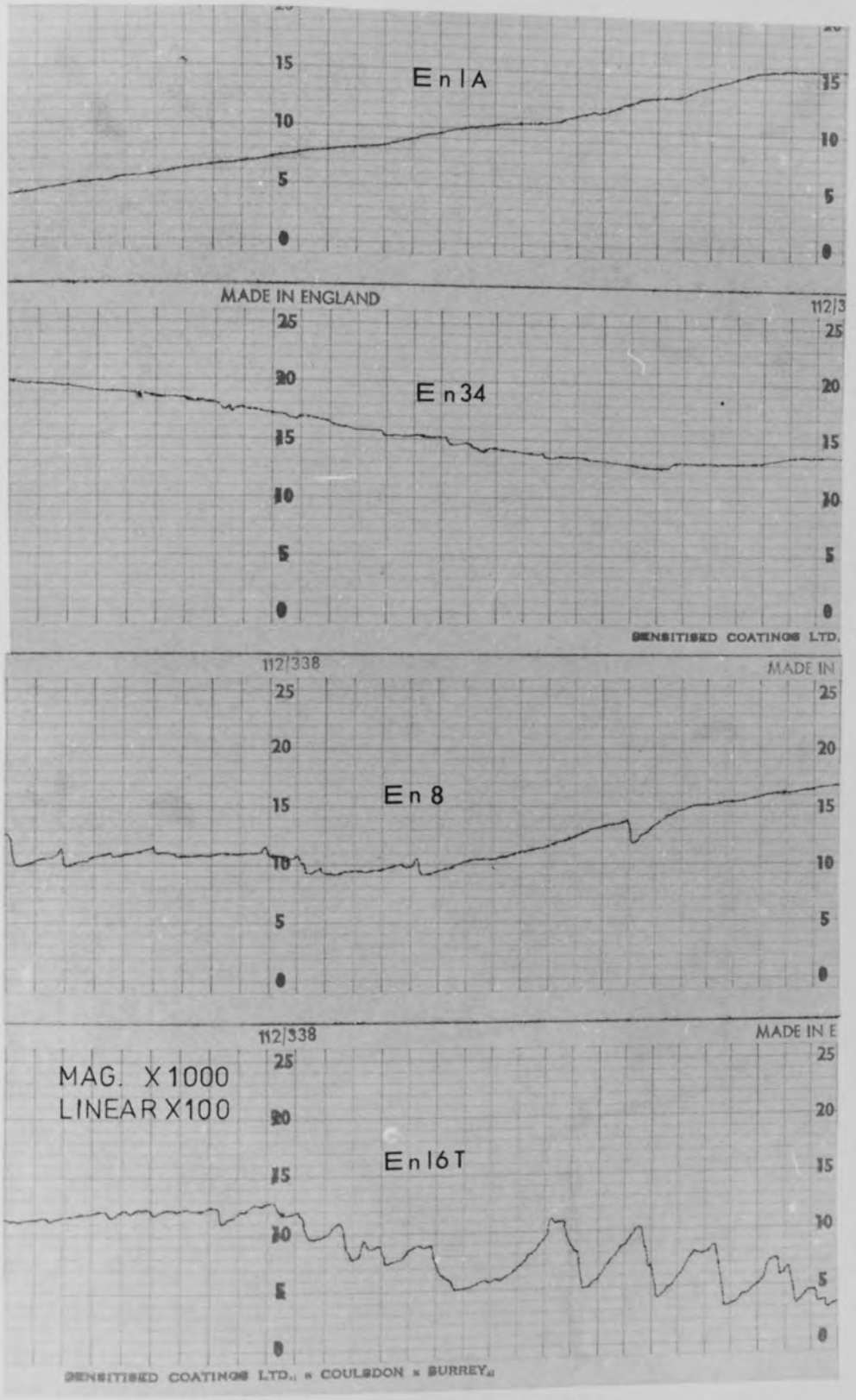

Fig. 41. SURFACE FINISH TRASES

Machining Data: hob 12 D.P., 12 gashes

f = 1.270 mm / rev

N_h = 115 r.p.m.

5.5 Test Results and Discussion

5.5.1 The Results

The average CLA value for each gear was computed together with standard deviation and presented in Table 17 against different combinations of axial feed, material hardness, hob diametral pitch and hob speed.

5.5.2 Graphical representation of tabulated results

Some of the tabulated results are represented in graphical form as shown in Figs. 42 to 46 in order to observe the variation of surface roughness with hob speed, axial feed, hob diametral pitch and material hardness.

5.5.3 Surface roughness versus hob speed

Figs. 42 and 43 show in graphical form the average gear CLA values plotted against hob speed at four different feeds, for 8 D.P. spur gears. It can be seen that in the case of each material, increasing hob speed from 74 r.p.m. to 178 r.p.m. resulted in a decrease in the values of CLA. A family of identical curves shows that better results of surface roughness are obtained at lower feeds.

5.5.4 Surface roughness versus Axial feed

The variation of surface roughness with axial feed at three different speeds is shown in Fig. 44 for 8 D.P. hob.

It can be seen that in the case of each gear material , increasing axial feed from 0.609 mm/rev to 1.987 mm/rev

TABLE 17

SURFACE FINISH MACHINING DATA: Hmax average ± S.D. (C L A)

Axial feed f, mm/rev	MTRL (HB)	HOB D.P.	HOB SPEED, N_h, rpm		
			74 rpm	115 rpm	178 rpm
0.609	En 1A (115)	8	0.55± .04	0.42± .01	0.35± .01
		10	0.42± .03	0.30± .00	0.26± .01
		12	0.51± .03	0.44± .02	0.38± .01
	En 34 (164)	8	0.50± .05	0.45± .02	0.29± .01
		10	0.40± .04	0.32± .02	0.25± .01
		12	0.66± .08	0.50± .03	0.40± .03
	En 8 (183)	8	0.60± .08	0.42± .03	0.40± .04
		10	0.40± .02	0.30± .02	0.26± .03
		12	0.60± .05	0.46± .03	0.38± .04
	En16T (269)	8	0.76± .06	0.50± .03	0.44± .05
		10	0.36± .02	0.30± .01	0.22± .01
		12	0.60± .05	0.51± .03	0.43± .02
0.914	En 1A	8	0.64± .06	0.48± .03	0.42± .03
		10	0.49± .03	0.38± .02	0.32± .02
		12	0.58± .03	0.52± .03	0.44± .03
	En 34	8	0.62± .04	0.53± .03	0.42± .03
		10	0.50± .03	0.40± .03	0.34± .02
		12	0.72± .06	0.58± .04	0.48± .03
	En 8	8	0.72± .07	0.50± .03	0.48± .04
		10	0.52± .03	0.32± .02	0.35± .02
		12	0.68± .04	0.54± .03	0.46± .03
	En16T	8	0.88± .09	0.60± .04	0.54± .04
		10	0.47± .06	0.34± .02	0.28± .01
		12	0.68± .07	0.57± .03	0.51± .02
1.270	En 1A	8	0.65± .05	0.52± .03	0.48± .03
		10	0.56± .02	0.44± .02	0.39± .02
		12	0.65± .04	0.58± .03	0.50± .03
	En 34	8	0.72± .06	0.64± .04	0.53± .03
		10	0.59± .05	0.49± .03	0.42± .02
		12	0.81± .06	0.65± .04	0.59± .04
	En 8	8	0.70± .04	0.62± .03	0.51± .03
		10	0.58± .03	0.48± .02	0.44± .03
		12	0.75± .05	0.60± .04	0.52± .03
	En16T	8	1.02± .08	0.74± .05	0.66± .05
		10	0.61± .04	0.50± .03	0.42± .03
		12	0.81± .06	0.68± .04	0.58± .03
1.987	En 1A	8	0.76± .06	0.60± .04	0.52± .03
		10	0.65± .05	0.51± .02	0.46± .02
		12	0.74± .06	0.66± .04	0.56± .03
	En 34	8	0.85± .07	0.75± .05	0.65± .04
		10	0.69± .06	0.57± .03	0.50± .03
		12	0.91± .05	0.75± .05	0.60± .04
	En 8	8	0.90± .06	0.71± .04	0.65± .04
		10	0.74± .05	0.55± .03	0.52± .03
		12	0.85± .05	0.68± .03	0.60± .04
	En16T	8	1.20± .08	0.97± .06	0.85± .06
		10	0.76± .06	0.58± .05	0.50± .04
		12	0.88± .06	0.74± .06	0.68± .05

TABLE 18

ANALYSIS OF VARIANCE FOR SURFACE ROUGHNESS

Sourse of Variation	Degrees of Freedom	Sum of Squares	Variance	Variance ratio, F
f	3	0.1131E1	0.3770	39.803††
HB	3	0.7745E-1	0.0258	2.725†
D.P.	2	0.7009E0	0.3504	36.996††
N_h	2	0.6767E0	0.3384	35.721††
f.HB	9	0.5640E-1	0.0063	0.631
HB.(D.P.)	6	0.5822E-1	0.0097	0.977
f.(D.P.)	6	0.2908E-1	0.0048	0.488
f.N_h	6	0.3351E-1	0.0056	0.562
HB.N_h	6	0.8668E-1	0.0144	1.455
(D.P.).N_h	4	0.4271E-1	0.0107	1.075
f.HB.(D.P.)	18	0.1213E-1	0.0067	0.712
HB.(D.P.).N_h	12	0.2125E-1	0.0177	1.870
f.HB.N_h	18	0.1568E0	0.0087	0.919
f.(D.P.).N_h	12	0.1215E0	0.0101	1.069
RESIDUAL	36	0.3410E0	0.0095	
TOTALS	143	0.3846E1	0.0269	

†† Significant at the level of 0.01

† Significant at the level of 0.05

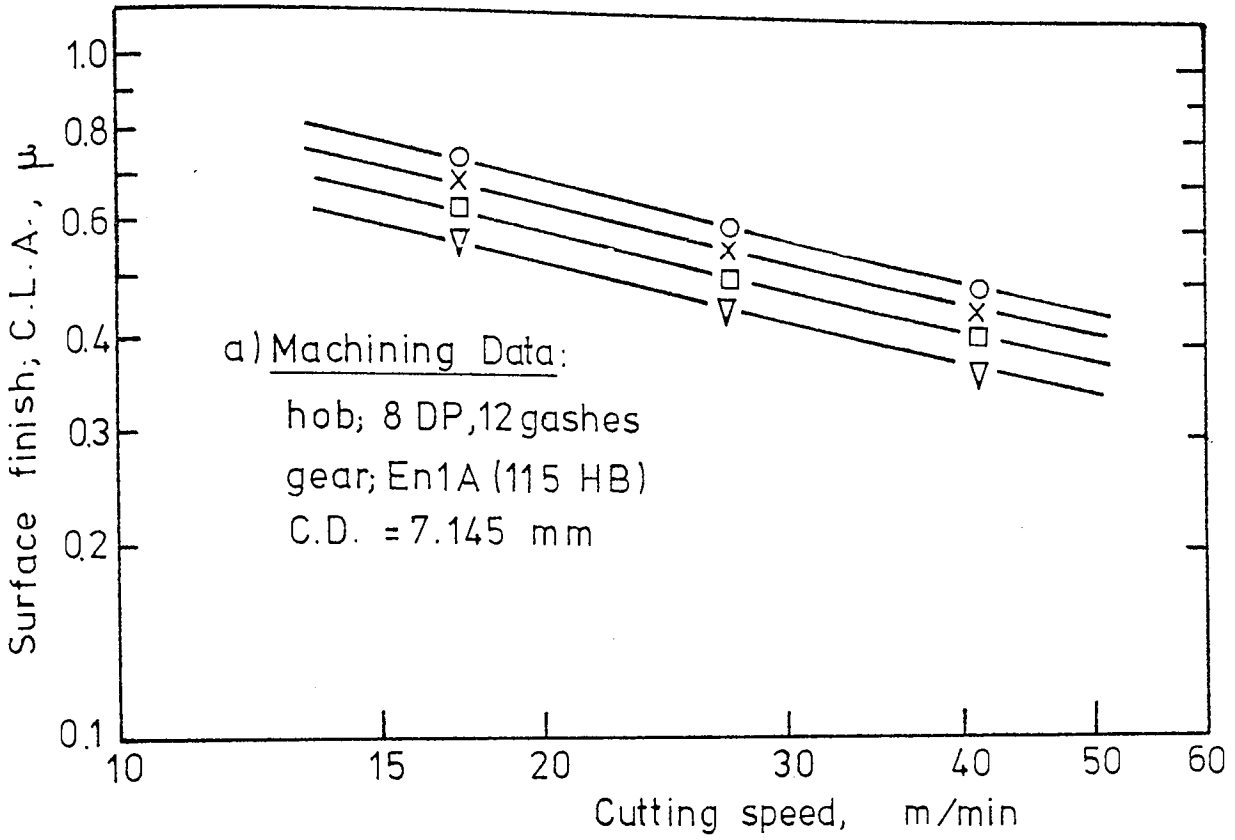

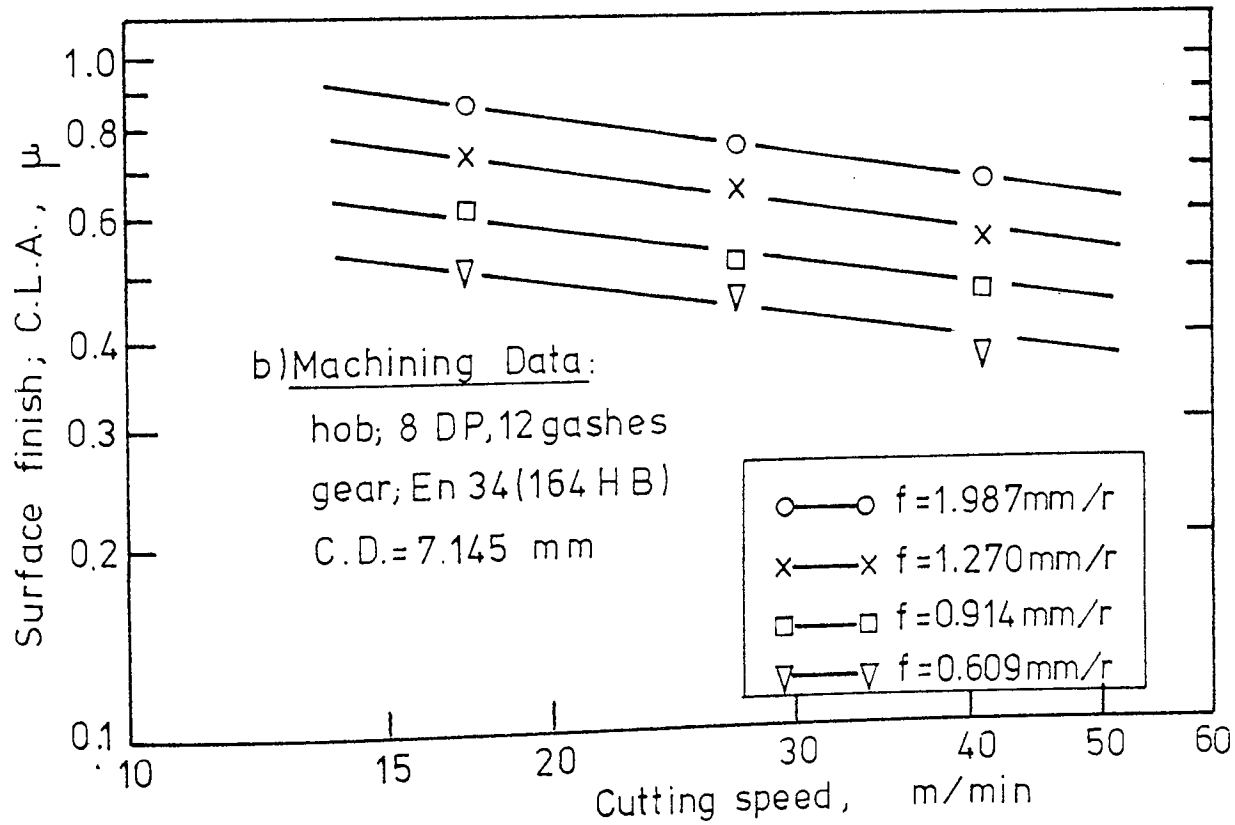

Fig. 42 EFFECT OF SPEED ON SURFACE FINISH

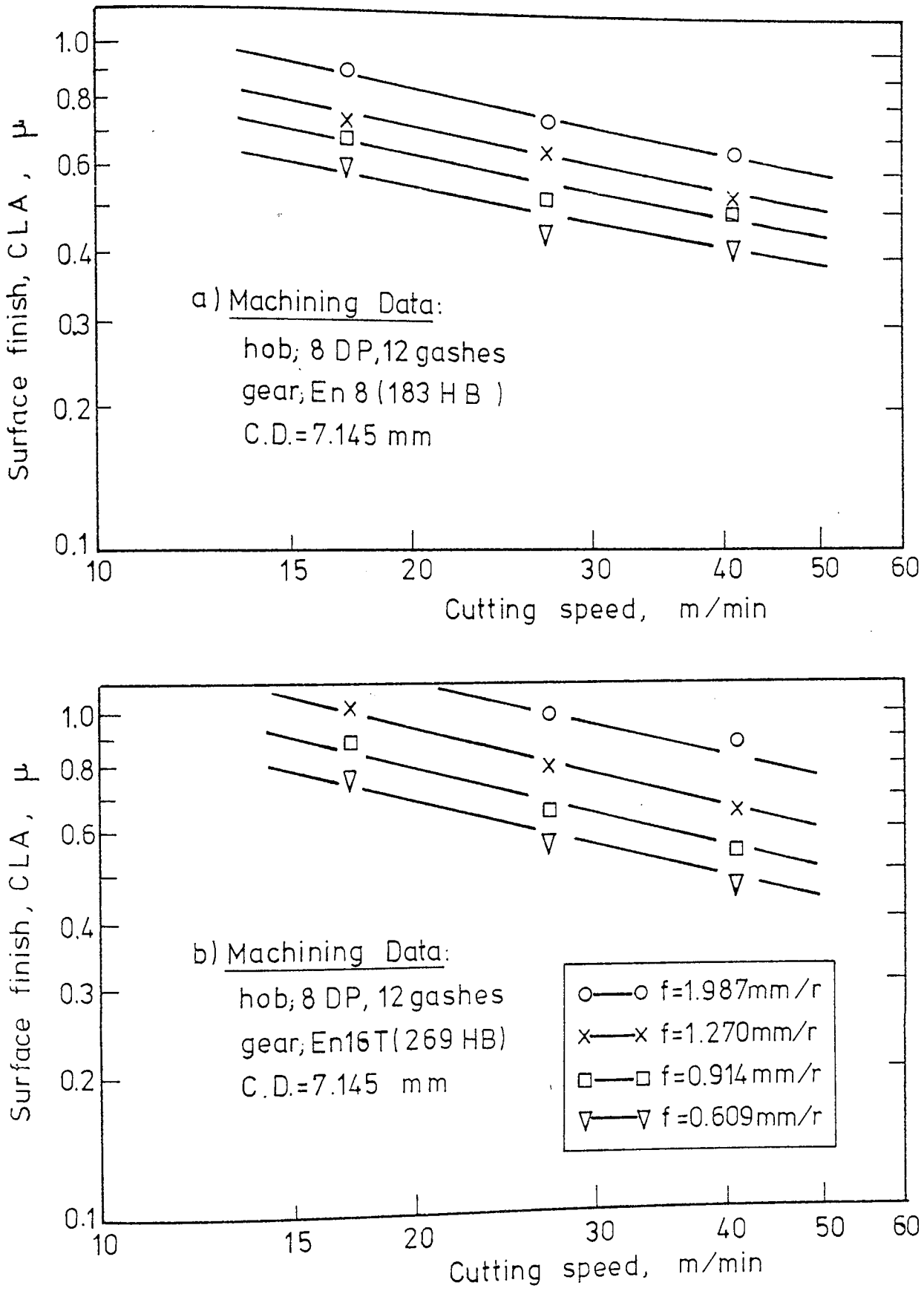

Fig. 43 EFFECT OF SPEED ON SURFACE FINISH

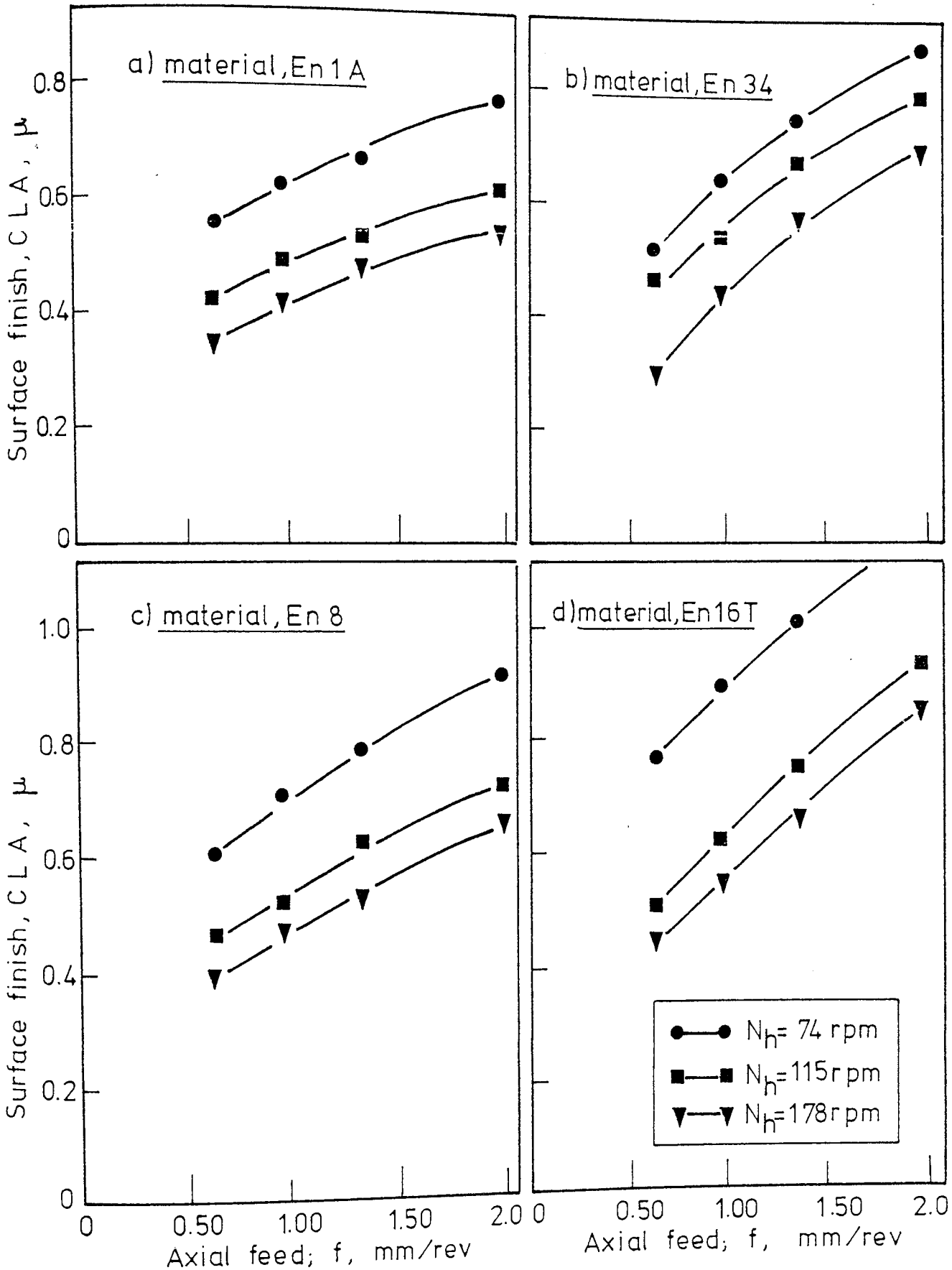

Fig. 44 EFFECT OF FEED ON SURFACE FINISH FOR 8 D.P HOB

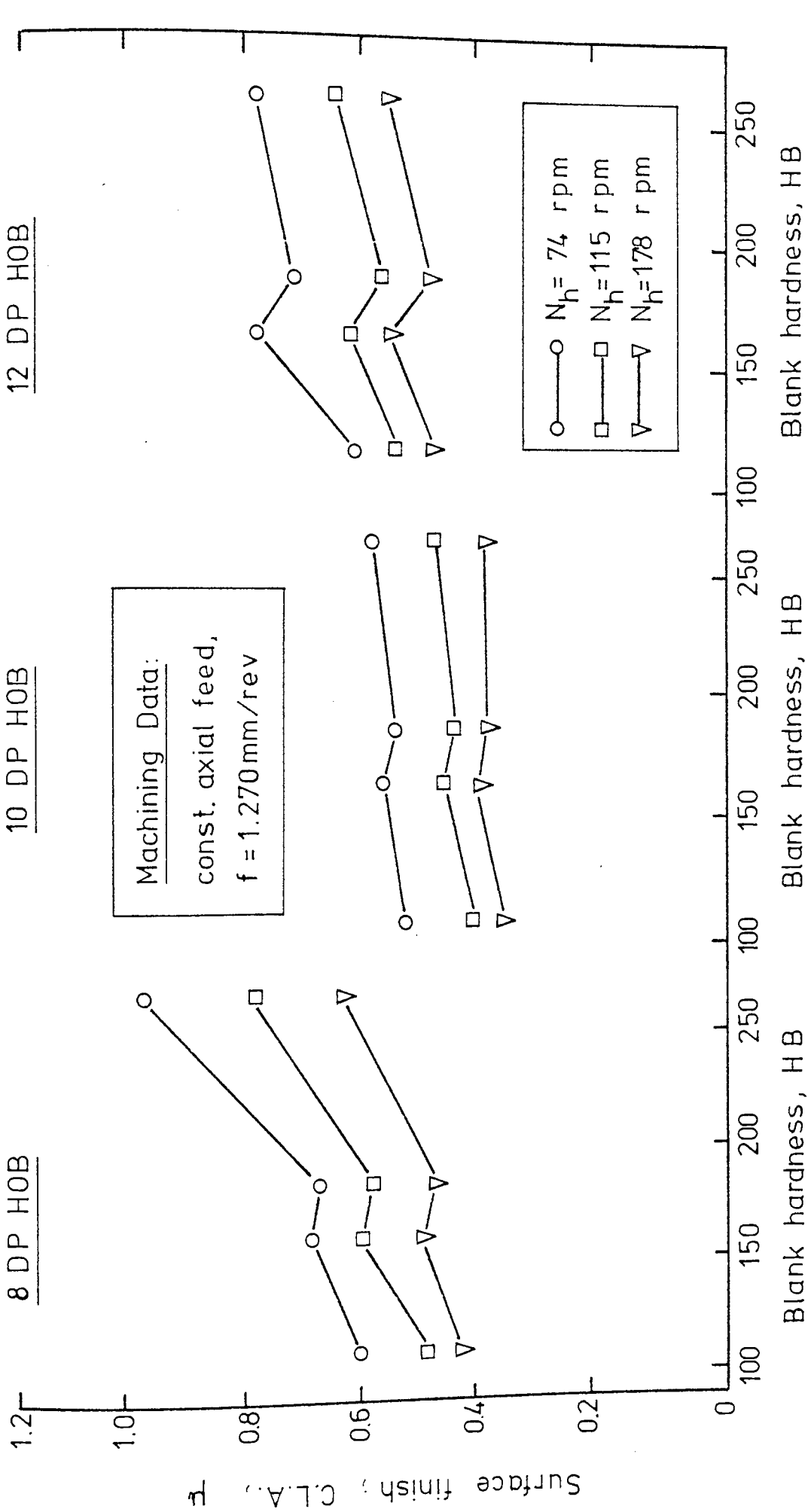

Fig. 45 EFFECT OF HARDNESS ON SURFACE FINISH AT CONSTANT FEED

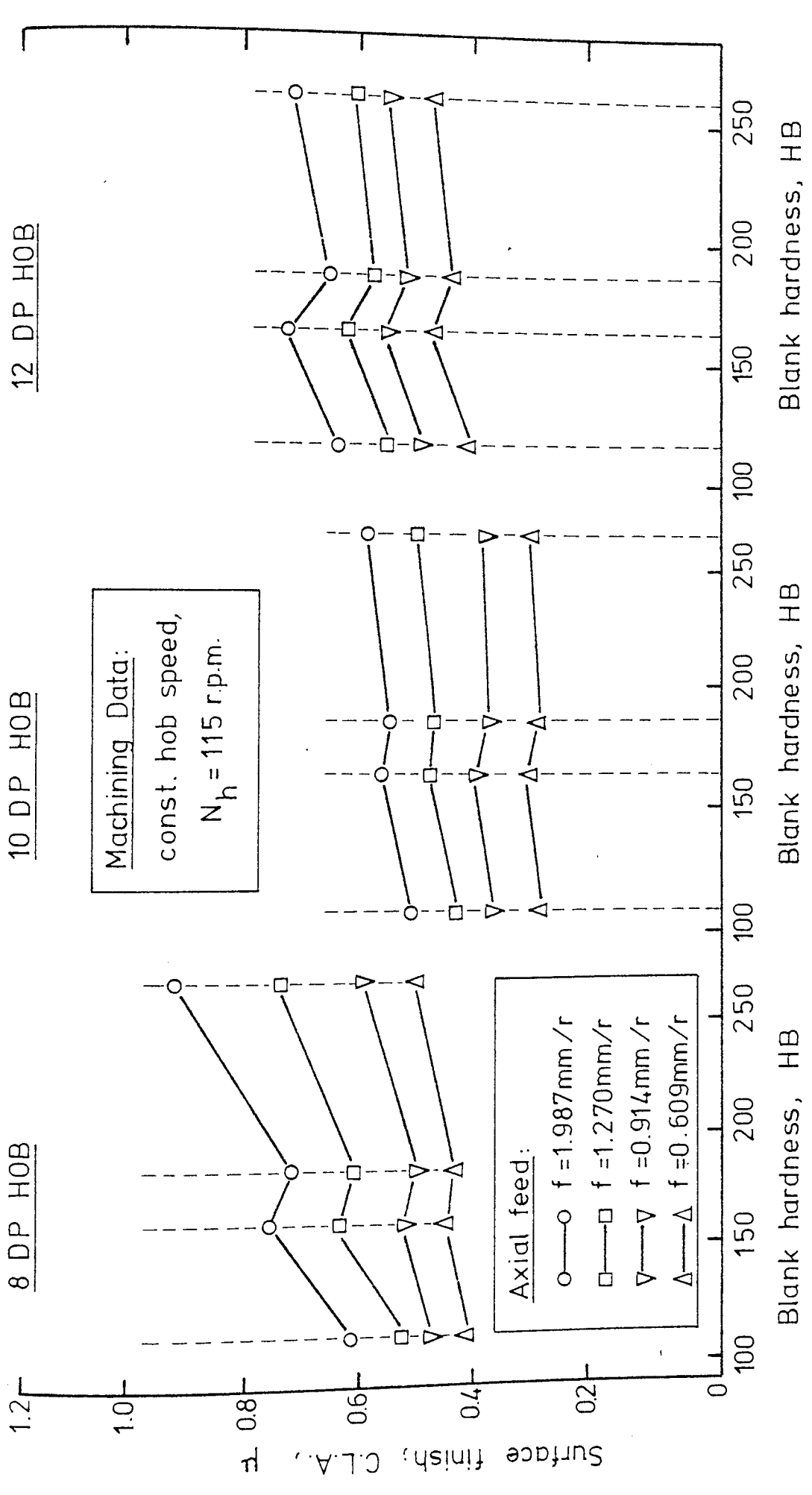

Fig.46 EFFECT OF HARDNESS ON SURFACE FINISH AT CONSTANT SPEED

resulted in an increase in the values of CLA. Best results are obtained with the smallest axial feed and highest hob speed.

5.5.5 Surface roughness versus material hardness

Fig. 45 shows in graphical form the variation of gear teeth surface roughness, H_{max} plotted against gear material hardness at three different hob speeds for three types of hobs, feed rate was kept constant at 1.270 mm/rev.

The hob speeds being 74, 115 and 178 r.p.m., the material Brinell hardness being, En 1A (115), En 34 (164), En 8 (183) and En 16T (269) and hobs 8, 10 and 12 D.P.

It can be observed that in the case of each speed level, increasing material hardness from (HB 115) to (HB 164) and from (HB 183) to (HB 269), resulted in an increase in the values of CLA. It is also observed that a slight drop in surface roughness while material hardness increased from (HB 164) to (HB 183).

Fig. 46 shows the variation of surface roughness against gear material hardness at four different feed levels for three types of hobs, hob speed was kept constant at 115 r.p.m.

The axial feeds being 0.609, 0.914, 1.270 and 1.987 mm/rev. It can be observed that in the case of each feed level, surface roughness increases with the increase of axial feed, it is also explicit that no monotonic function exists for surface roughness as a function of material hardness.

Surface roughness graphs shown in Fig. 42 and Fig. 46 appear to follow a pattern, it is noticed that maximum surface roughness is obtained by 8 D.P. hob while minimum is obtained by 10 D.P. and best surface roughness results are observed with the smallest axial feed and highest hob speed for 10 D.P. hob.

Although surface roughness graphs shown in Figs. 42 to 46 provided useful information about the effect of different cutting parameters on surface roughness, further analysis is still needed to observe the significance of these effects.

5.5.6 Analysis of Variance

A set of 144 tests was provided by combinational arrangement of 4x4x3x3 non-factorial experimental design shown in Table 17 in order to observe surface roughness behaviour against the cutting parameters when hobbing spur gears of four different steels with three different types of hobs.

5.5.7 Effect of feed, hardness, D.P. and hob speed on Surface roughness

The analysis of variance is given in Table 18 and it follows that axial feed, hob diametral pitch and hob speed have a high significant effect on gear teeth surface roughness at the level of 0.01 while material hardness is less significant at the level of 0.05 . Interactions between feed, hardness, D.P. and hob speed have no significant effect on surface roughness.

5.6 Generalised Surface Roughness Equation

In order to obtain a general relationship between surface roughness, H_{max} as a dependent variable, and cutting parameters (i.e. feed, hob speed, hardness and D.P.) as independent variables. As can be seen in Figs.44 to 46, surface roughness graphs are non-linear and this may be considered in the statistical analysis, where the linearized model can be examined. 144 surface roughness results were considered as in the table with the objective of establishing a general mathematical model for gear teeth surface roughness when hobbing spur gears in terms of four independent variables.

It was assumed that the relationship is of the form:

$$H_{max} = C_m \, f^{\alpha_1} (D.P.)^{\alpha_2} \, (HB)^{\alpha_3} \, . \, V^{\alpha_4} \qquad (35)$$

where, C_m is constant

$\alpha_1, \alpha_2, \alpha_3, \alpha_4$ are parameters.

The following generalised relationship was obtained for hobbing spur gears,

$$H_{max} = \frac{0.928 \quad f^{0.398} \qquad HB^{0.188}}{DP^{0.147} \qquad V^{0.460}} \; \mu(CLA) \qquad (36)$$

with error sum of squares = 0.023, residual error = 0.126 multiple correlation = 0.973

5.7 Discussion of Results

From Figs. 42 to 46, together with analysis of variance it can be seen that feed, hob speed and hob diametral

pitch have high significant effect on surface roughness where an increase in hob feed rate promotesa rougher surface finish on gear teeth machined from En 1A, En 34, En 8 and En 16T steels. An increase in hob speed results in a smoother surface finish.

The expected sequence of the effect of hob diametral pitch on surface roughness was broken when 10 D.P. hob resulted in a smoother surface finish than that produced by 12 D.P. and that is because 10 D.P. hob contains 14 gashes while 12 D.P. and 8 D.P. hobs have 12 gashes, therefore the number of gashes in the hob has an effect on surface roughness, i.e. an increase in the number of hob gashes results in a smoother surface finish.

It is apparent that Brinell hardness, which gives an average hardness measurement is not the only work-material variable to account for the effect of work-material properties on surface roughness. The hardness of the work material constituents and their properties will influence the average hardness and surface hardness. The observed drop in CLA values between En 34 and En 8 in Figs. 45 and 46 can be related to the drop in torques and power in the same hardness region Fig. 35 which explains the behaviour of surface roughness for An 8 steel and stresses the point of the need for microstructure studies.

5.8 Conclusions

1. Increase in axial feed rate within normal Universal hobbing machine ranges promotes a rougher surface finish on spur gear teeth.
2. Increase in hob speed results in a smoother surface roughness.

3. Increase in the number of flutes in the hob gives a smoother surface finish.

4. Feed, hob speed and hob D.P. have a highly significant influence on surface roughness.

5. The spheroidized structure, En 8 (183 HB) steel gave by far the best performance, but microstructure studies is needed.

CHAPTER VI

VIBRATION DURING HOBBING

6.1 Introduction

The machine tool will deflect if a force is applied between the workpiece and the cutting tool. Typically the static stiffness of the hobbing machine was found to be of the order of 600×10^4 Kg/m[10]. Since the machine has distributed mass, it will have a number of resonant frequencies. These may be excited in obvious manners by hobbing cutters with cut intermittently at high frequencies.

For purposes both of analytical and experimental investigation the machine tool and the cutting process may be regarded as two distinct elements which from a closed loop typical of those found in control systems. The output from one is the input to the other. If each part of this loop, shown in Fig. 47 can be described, then the behaviour of the machine as a production unit can be described, and its liability to chatter assessed.

Here, a very brief description of the behaviour of the machine is presented. The theoretical analysis of the structure behaviour and the influence on chatter is not attempted where vibration measurements were taken in the same time as torques and power were measured. The objective of this section is to observe the effect of cutting parameters on vibration.

6.1.1 Cutting forces

Despite very large variations of the instantaneous values of cutting forces, mean values can be measured accurately.

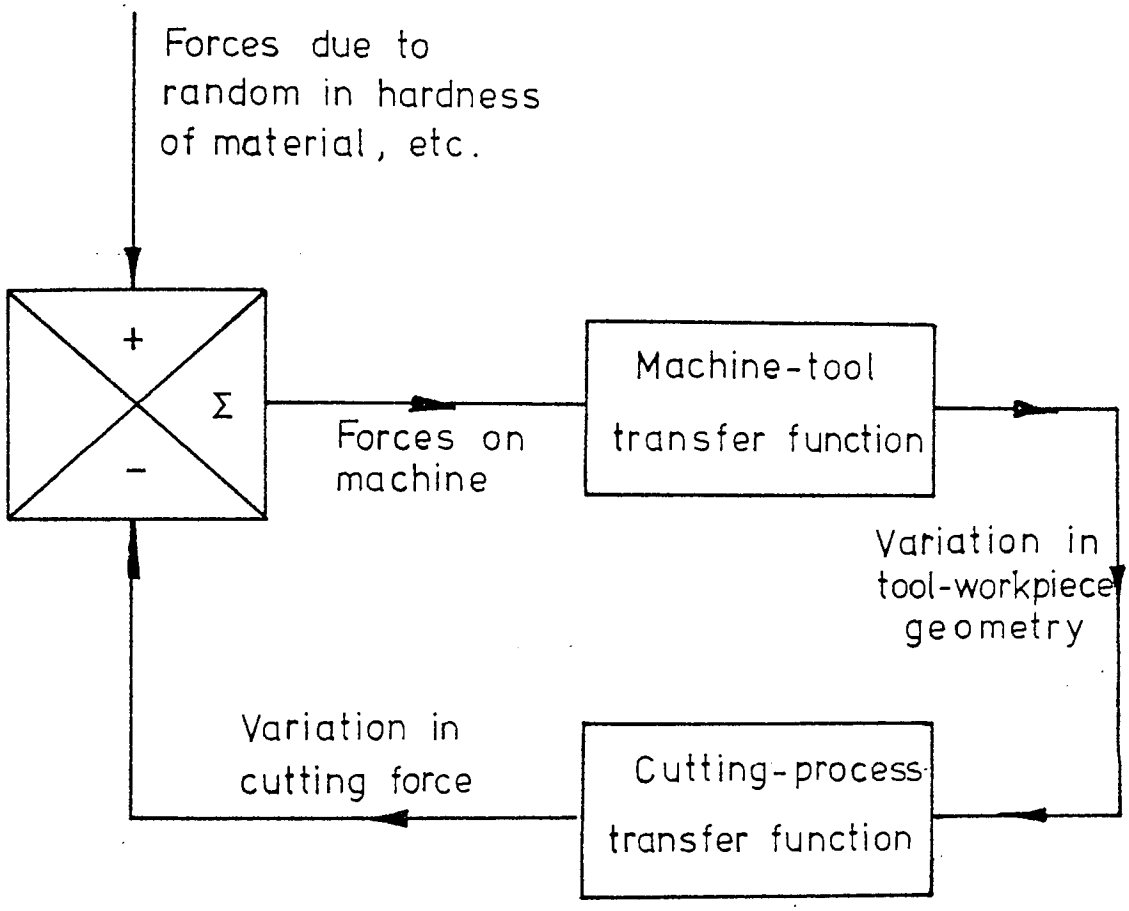

Fig. 47 CLOSED LOOP FOR MACHINE TOOL

Forces during hobbing were discussed in Chapter 4 of this study, where the mean and peak values obtained when cutting steadily may be very consistent; the detailed moment to moment variation of cutting forces may be very complex indeed, as shown in the recordings, Fig. 16.

6.1.2 Dynamic Cutting Forces

When a machine tool is chattering steadily, the surface generated is roughly sinusoidal in nature. Much study has therefore been put into the forces which occur, and measurements show that :

a. the force traces obtained may be very far from sinusoidal, and/or very noisy.

b. A very heavy second harmonic component of force may be present.

c. the force components are not necessarily in phase with the sinusoidal variation of surface or of tool.

d. the phase shift may sometimes be leading and sometimes lagging.

The tracings of hobbing show curves for which the force during the individual cut is very far from sinusoidal, and for which the content of higher harmonics is high. This process therefore introduces complex forcing terms on the workpiece and machine, which can excite resonance.

6.1.3 Chatter

A great deal of effort has been developed during recent years to the investigation of chatter occurring during machining gears on hobbing machines. In hobbing machines chatter may often be encountered which strongly limits the rate of production.

Chatter in hobbing has some special features distinguishing it from chatter on other kinds of machine tools. Direct application of the as yet published methods of chatter analysis, as in references [25,26 and 27] on hobbing is difficult, due to problems of chatter which are additional for hobbing. Slavicek [9] dealt with some general problems of chatter in hobbing distinguishing it from that on other kinds of machine tools. The essential differences were discovered then in the more complicated form of chips being cut. A theoretical analysis of the behaviour of the structure and of the influence of its dynamic constants on chatter was discussed.

6.2 Effect of Cutting Parameters on Vibration

Generally, it is assumed that relative vibration between the tool and workpiece causes variation of cutting force. Mostly it is further assumed that the cutting force varies because of the variation of chip thickness. In hobbing chips are cut from the bottom as well as from both flanks of the tooth profile. Consequently, vibrations of any direction in the plane perpendicular to the cutting speed will influence the cutting force.

The cutting process itself differs considerably from other kinds of machining. In orthogonal cutting, the width and thickness of cut are clearly defined; in hobbing, however, both quantities vary in a wide range during the revolution of the hob and depend further on the parameters of the cutting process, e.g. axial feed, blank diameter, blank material, D.P., hob speed, etc.

The analysis of chatter in hobbing [9] revealed that the influence of the properties of the machine structure is

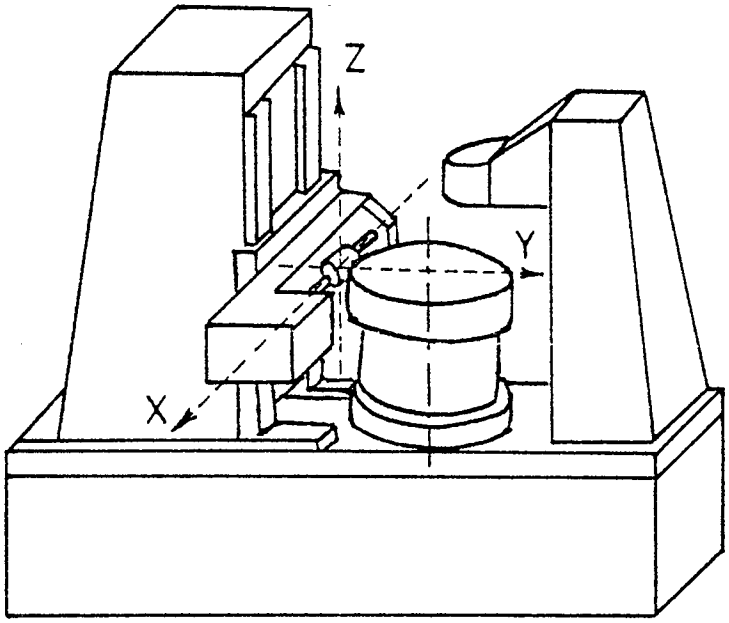

Fig. 48 DIRECTION OF RECEPTANCES OF THE HOBBING MACHINE STRUCTURE

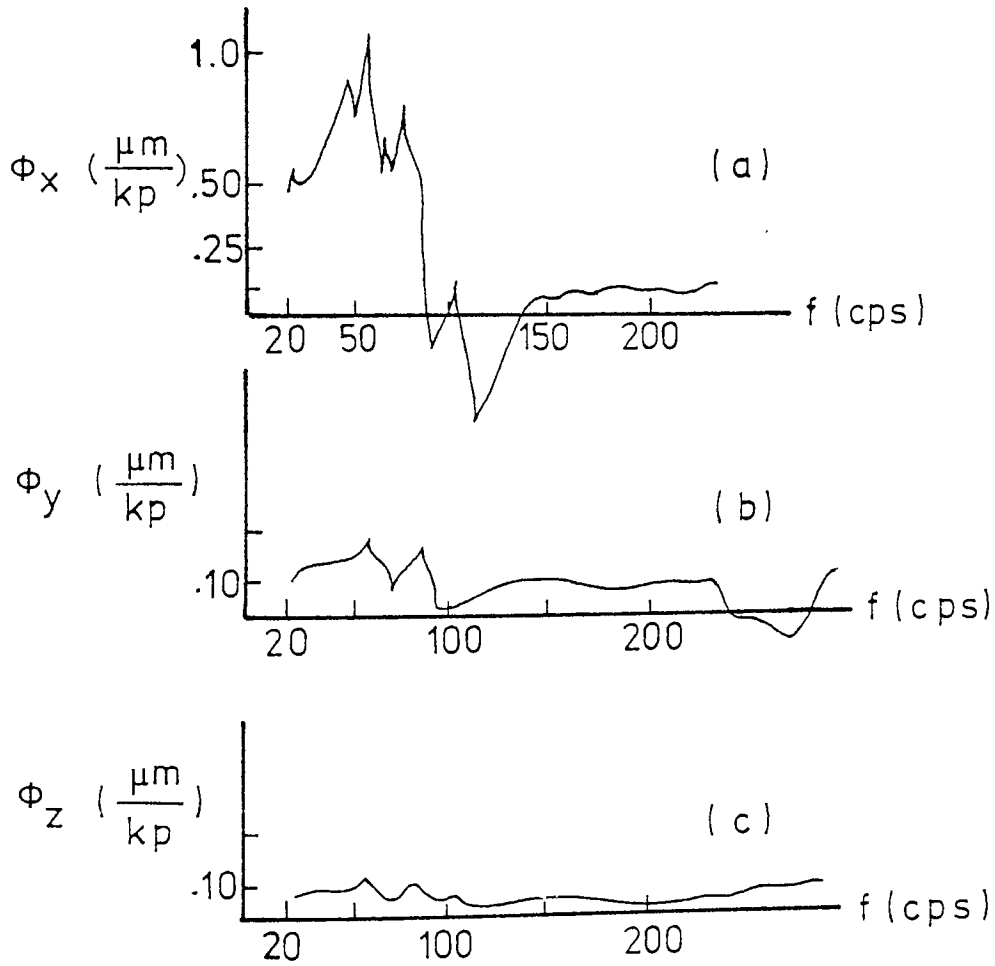

Fig. 49 RECORDING OF THE BASIC RECEPTANCES [10]

expressed by the two receptances Φ_x and Φ_y (see Fig. 48) and tests carried out proved a great significance of the receptance Φ_x has been found.

Direct receptances in x,y,z directions of a middle size hobbing machine (Table dia. 500 mm) have been measured[10]. In the measurement forces and vibration, signals were processed in a semi-automatic transfer-function analyser and recorded. The results were given from even rough analysis that the static and also dynamic compliance of the structure in the x-direction is two to three times greater than in y and z as shown in Fig.49. Thus the ϕ_x receptance will be decisive for the value of the stability limit and for the chatter frequency.

6.3 Vibration Measurement

The important variable in machine-tool structure under given load conditions is the relative displacement between cutting tool and workpiece since this controls machine accuracy and metal cutting capacity. The primary measurement in cutting processes is the dynamic response between tool and workpiece. This is usually determined under test conditions using a vibrator to cover the frequency range of interest to produce a machine resonance curve. When the frequencies of the resonances have been established, the deflected shape of the machine is required to allow the contributions of the separate parts of the machine to the total deflection to be assessed.

6.4 Experimental Set-up and Procedure

It was decided to measure the maximum amplitude of vibration in the x-direction as shown in Fig. 48 in order to observe the effect of cutting parameters (axial feed, blank

material, hob speed and hob D.P.) on the vibration of the hob spindle. The definition and measurement of displacement "D_{peak}" is covered by VDl/lSO standards.

6.4.1 Measurement Procedure

A portable vibration analyser, EE model 2100 was suggested for this measurement. The vibration transducer was connected and placed in contact with the hob spindle bearing surface as shown in Fig. 51 by means of a magnet after ensuring that it is firmly in contact with no tendency to slide or rock about the surface; the vibration analyser was connected to an oscilloscope to record the output signals. The instrument was tuned for a maximum signal on the meter after considering the required frequency band, the effective frequency range for the measurements being 22 Hz(1320 CPM) - 3000 Hz.

6.4.2 Design of Experiment

Vibration was measured at the same time as torque and power for spur gears were measured. A 4x4x3x3 non-factorial design of experiment was used in order to investigate the variation of vibration with cutting variables when hobbing spur gears at full depth of cut as follows:

Axial feeds; 0.609, 0.914, 1.270 and 1.987 mm/rev.

Hob speeds; 74, 115 and 178 r.p.m.

Blank materials; En 1A, En 34, En 8 and En 16T.

Hobs; 8, 10 and 12 D.P.

Cutting fluid; active type EP cutting oil containing sulphur, chlorine and fat.

(a) HOB : 10.D.P. ; BLANK : En 8
FEED 0.914 mm/rev , SPEED 178 r.p.m
1 - NO LOAD , 2 - FULL-LOAD
N_h=74 r.p.m.: 3 - no load 4 - full load

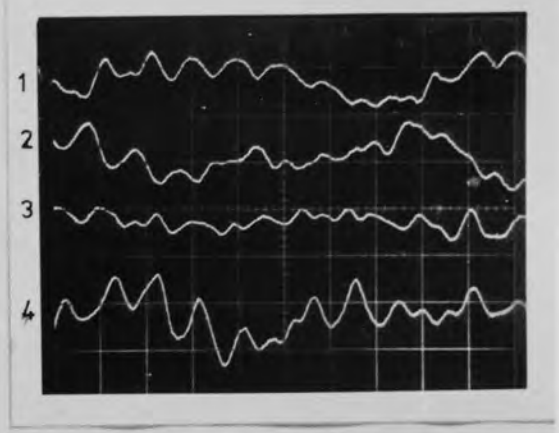

(b) HOB : 12 D.P. , BLANK : En 8
SPEED : 178 r.p.m.
f= 1.270 mm/rev 1-no load 2-full load
f= 0.609 mm/rev 3-no load 4-full load

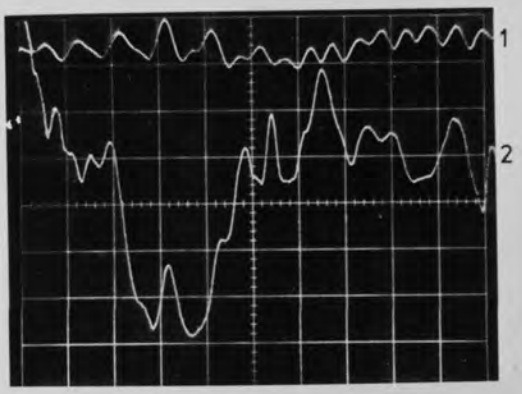

(c) HOB 8 D.P. BLANK En 34
f = 1.987 mm/rev N_h=178 rpm
1 - NO LOAD 2 - FULL LOAD

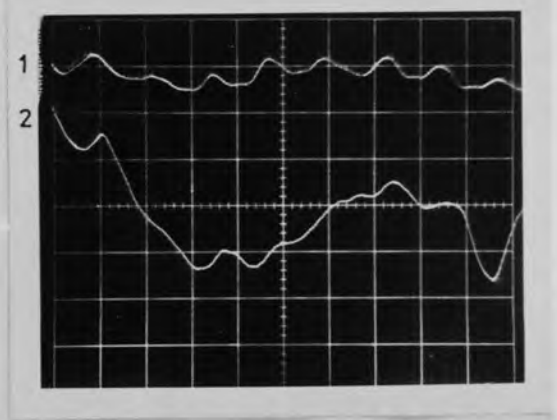

(d) HOB 8 D.P. BLANK En 34
f =1.270 mm/rev N_h= 74 rpm
1 - NO LOAD 2 - FULL LOAD

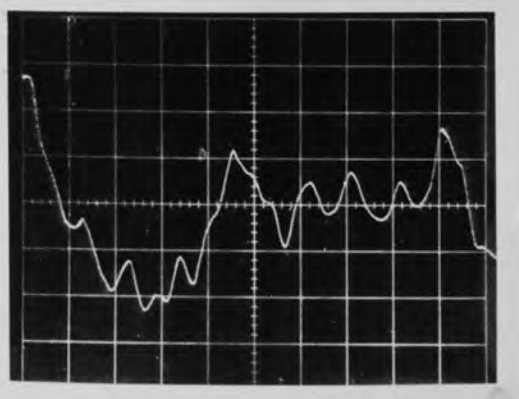

(e) HOB 8 D.P. BLANK En 16 T
f = 1.270 mm/rev N_h= 178 rpm

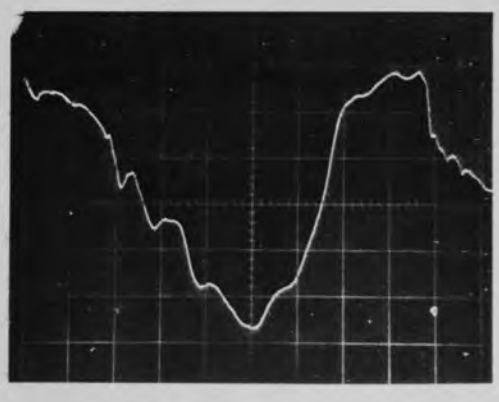

(f) HOB 8 D.P. BLANK En 16 T
f=1.987 mm/rev N_h = 115 rpm

Fig. 50. VIBRATION RECORDINGS FROM OSCILLOSCOPE

SCALE : VERTICAL 0.01 V/ DIV
HORIZONTAL 5 m s/ DIV

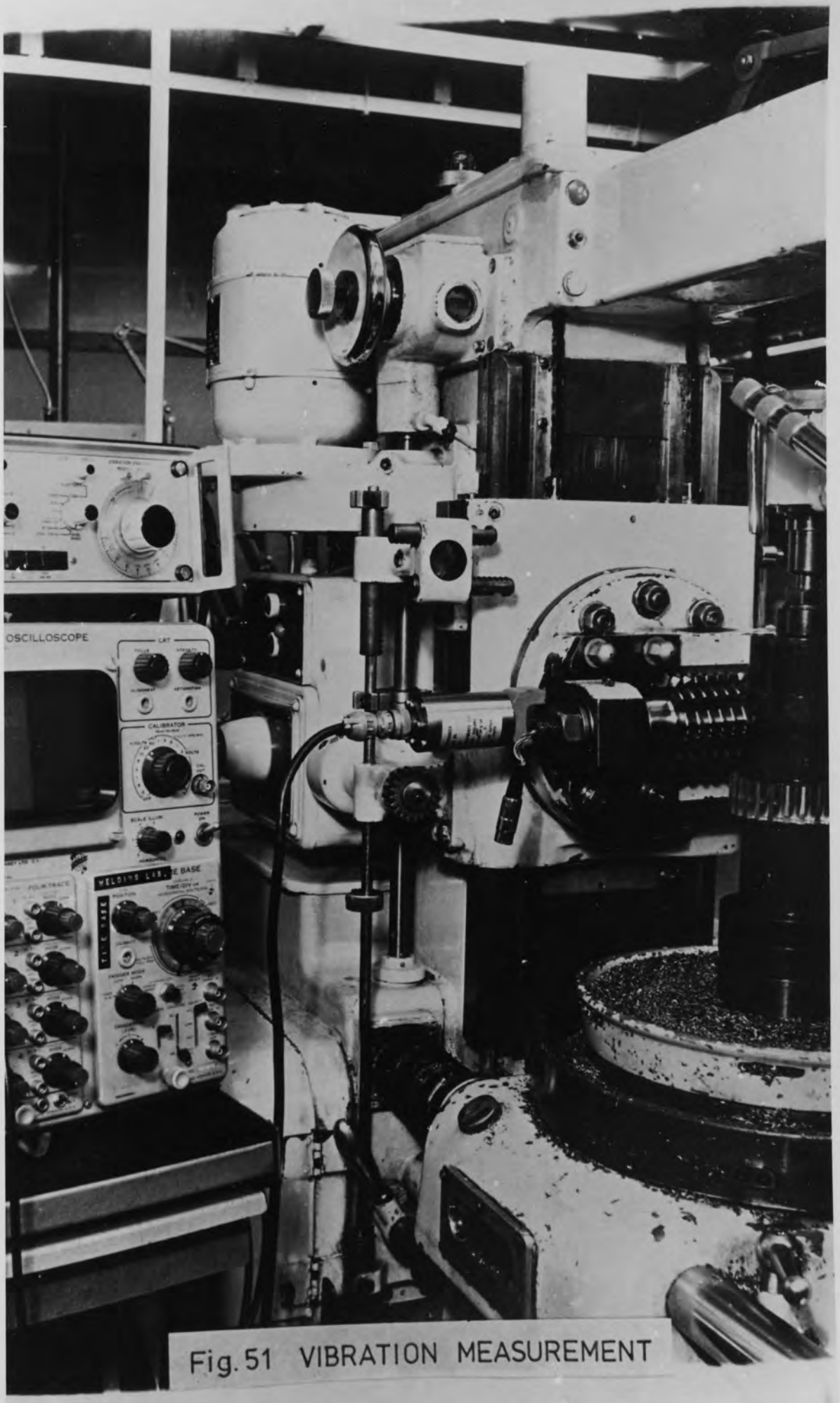

Fig. 51 VIBRATION MEASUREMENT

6.5 Test Results and Discussion

6.5.1 Recording from Oscilloscope

Figs. 50a, b, c, d, e and f, represent some of the recordings of the observations measured by the vibration analyser for En 8 steel. These graphical traces thus obtained express the electrical analogue of amplitude of vibration from peak to peak under no load conditions, before full depth of cut is achieved and at full depth of cut at different feeds, speeds and hob D.P.

Horizontal scale 5ms/Div and vertical 0.01 Volt/Div.

6.5.2 Graphical representation of tabulated Results

The results of amplitude of vibration D_{peak} were obtained for different combinations of feed, hob speed, material hardness and hob D.P. These results are presented in Table 19 and some of the results are represented in graphical form as shown in Figs. 52 to 55.

6.5.3 Vibration versus Axial Feed

Figs. 52 and 53 show in graphical form that vibration amplitude D_{peak} have been plotted against axial feed for spur gears 8 D.P. hob for four types of steel blanks at three hob speed levels.

From each of these figures, it is observed that vibration generally increases with the increase of axial feed. In the cases of En 1A and En 16T steel, a slight drop in vibration was observed between feed values of 0.609 mm/rev and 0.914 mm/rev. It is also observed that vibration increases with the increase of hob speed in the particular figures shown.

TABLE 19

VIBRATION RESULTS; D_{peak} , μm

Axial feed f, mm/rev	MTRL (HB)	Hob D.P.	HOB SPEED; N_h , rpm		
			74rpm	115rpm	178rpm
0.609	En1A (115)	8	4.2	4.3	5.8
		10	3.0	2.5	5.0
		12	2.8	4.2	3.4
	En34 (164)	8	2.4	3.8	4.3
		10	3.2	2.6	4.2
		12	3.3	4.5	4.0
	En 8 (183)	8	3.0	3.5	4.2
		10	2.8	2.4	5.0
		12	2.3	3.7	2.8
	En16T (269)	8	4.6	4.8	7.0
		10	4.2	2.6	4.8
		12	2.4	4.3	3.0
0.914	En1A	8	3.6	5.0	5.5
		10	4.2	3.0	6.7
		12	2.6	4.0	3.2
	En34	8	3.9	4.6	6.2
		10	4.8	3.4	6.6
		12	2.8	4.2	3.6
	En 8	8	3.5	4.0	4.8
		10	4.7	3.0	7.3
		12	2.2	3.4	2.6
	En16T	8	4.0	5.2	6.4
		10	6.6	3.3	7.2
		12	3.7	5.2	4.4
1.270	En1A	8	5.4	6.8	7.2
		10	6.0	3.7	9.3
		12	3.2	5.0	4.0
	En34	8	6.0	8.6	9.4
		10	6.4	4.0	9.0
		12	3.2	5.2	3.8
	En 8	8	5.6	8.0	8.8
		10	6.4	3.4	8.2
		12	2.8	4.4	3.3
	En16T	8	6.0	8.3	9.0
		10	7.0	3.7	9.0
		12	5.2	6.8	5.9
1.987	En1A	8	7.7	8.6	9.0
		10	7.0	4.3	10.9
		12	4.7	6.6	5.2
	En34	8	6.4	9.3	10.4
		10	8.9	4.5	11.6
		12	4.0	7.0	5.3
	En 8	8	8.5	9.2	11.7
		10	7.0	4.0	8.8
		12	3.2	5.8	4.0
	En16T	8	11.7	13.0	14.5
		10	11.0	4.2	12.0
		12	5.3	8.0	6.8

TABLE 20

ANALYSIS OF VARIANCE FOR VIBRATION

Source of Variation	Degrees of Freedom	Sum of Squares	Variance	Variance ratio, F
f	3	0.2228E3	74.274	22.126 ††
HB	3	0.2190E2	7.301	2.975 †
D.P.	2	0.8924E2	44.619	13.292 ††
N_h	2	0.9895E2	49.473	14.738 ††
f.HB	9	0.6238E1	0.693	0.359
HB.(D.P.)	6	0.1098E2	1.830	0.948
f.(D.P.)	6	0.2814E2	4.689	2.429 †
f.N_h	6	0.3887E2	6.478	3.355 ††
HB.N_h	6	0.1251E2	2.085	1.080
(D.P.).N_h	4	0.1643E3	41.095	21.285 ††
f.HB.(D.P.)	18	0.3599E2	1.999	1.635
HB.(D.P.).N_h	12	0.1919E2	1.599	1.306
f.HB.N_h	18	0.4801E2	2.434	1.988
f.(D.P.).N_h	12	0.4226E2	3.522	2.876 †
RESIDUAL	36	0.4407E2	1.224	
TOTALS	143	0.8794E3	6.149	

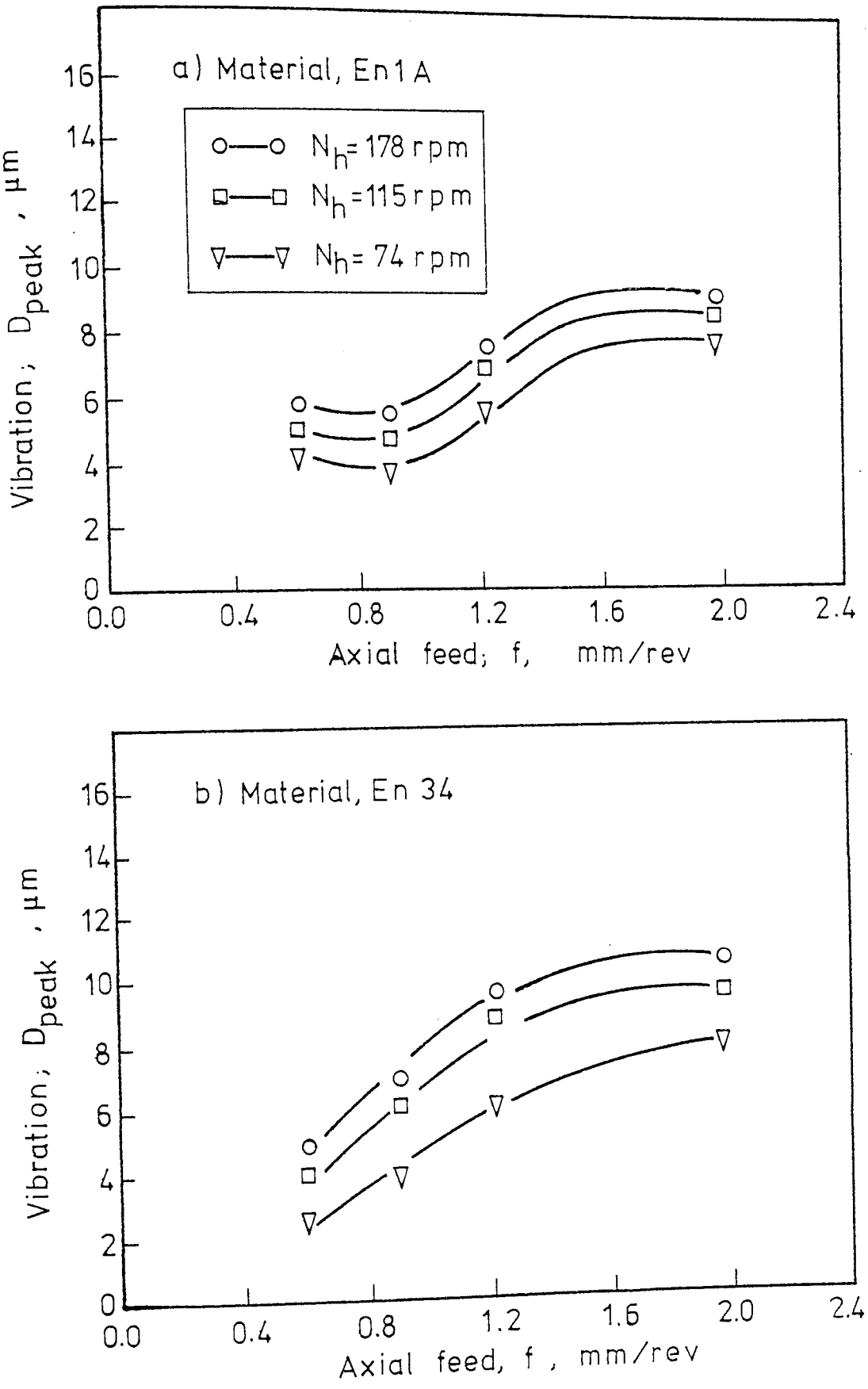

Machining Data:

hob; 8 D.P., 12 gashes, 74.8 mm O.D.

Fig.52 EFFECT OF FEED AND SPEED ON VIBRATION

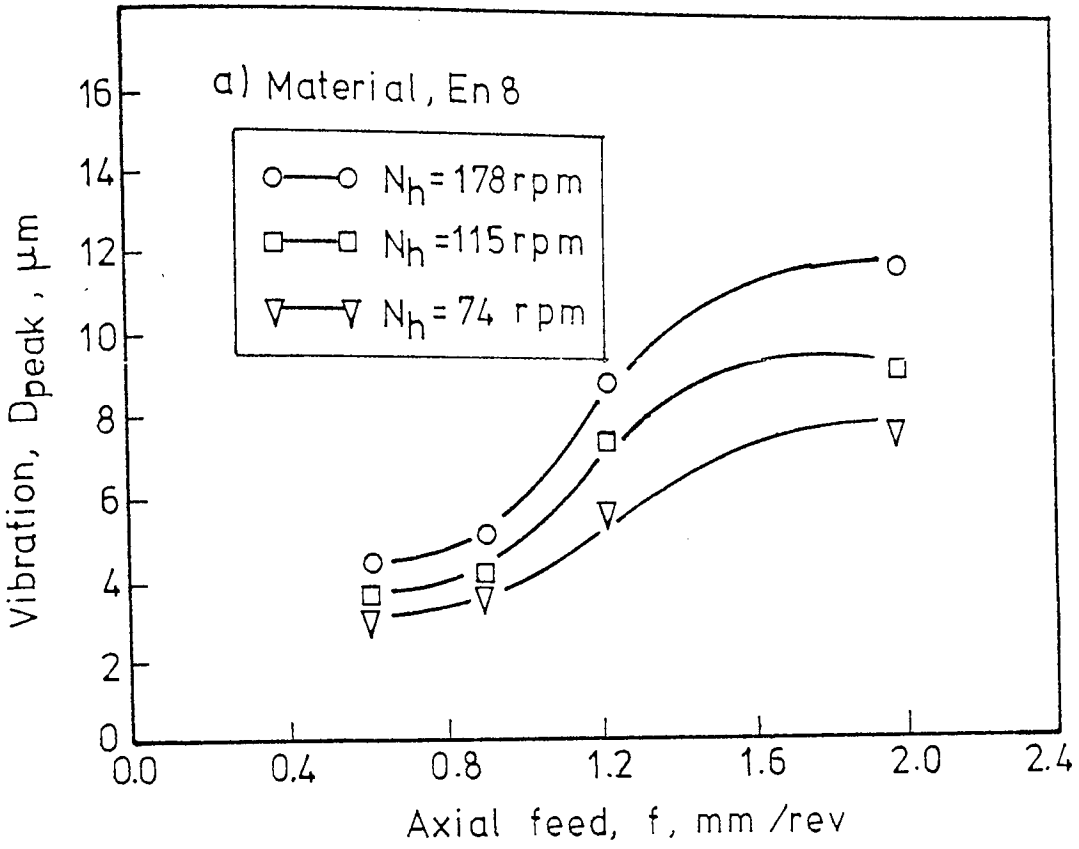

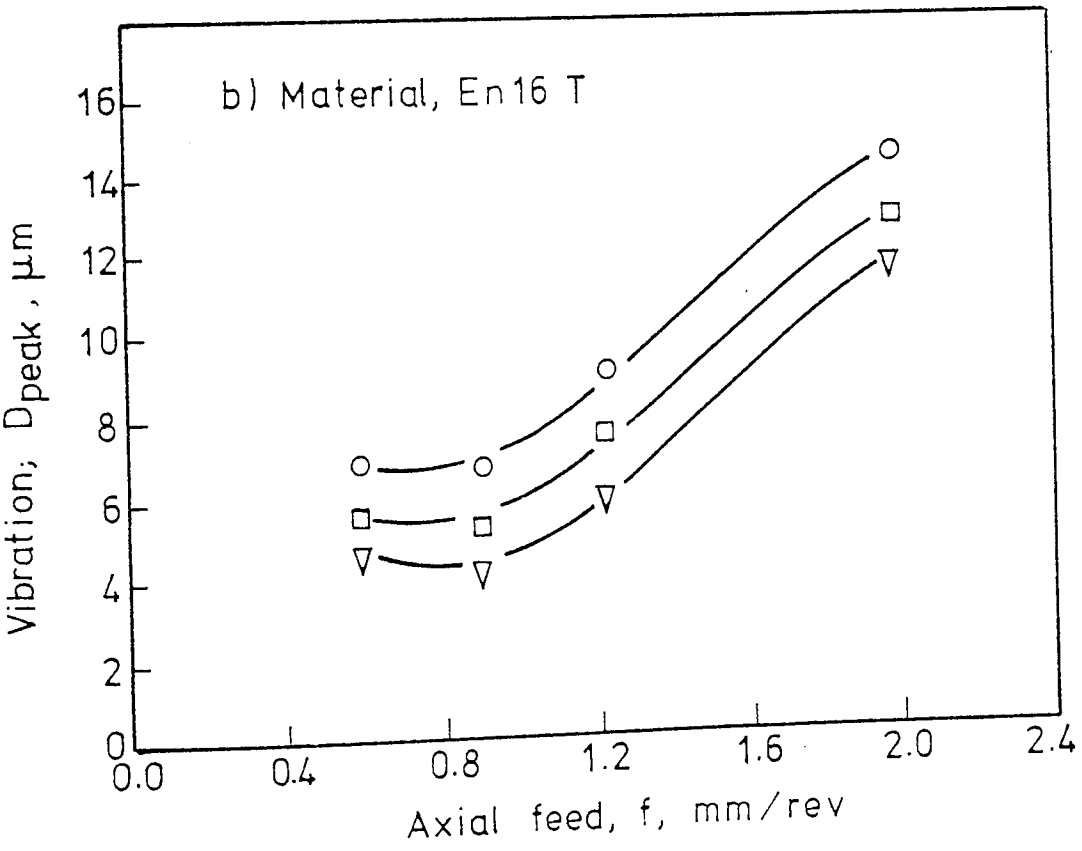

Machining Data :

hob; 8 D P, 12 gashes, 74.8 mm O.D.

Fig. 53 EFFECT OF FEED AND SPEED ON VIBRATION

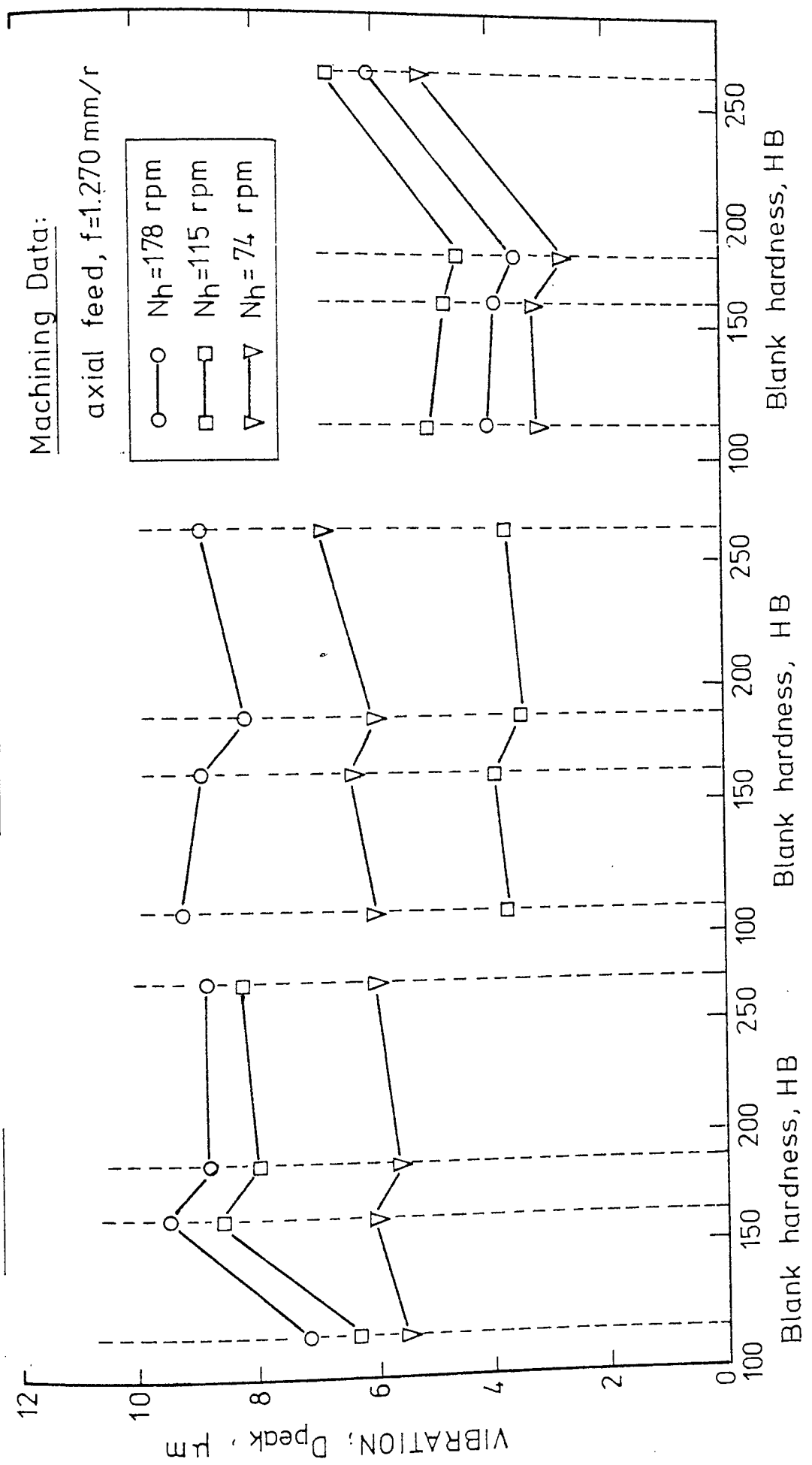

Fig. 54 EFFECT OF HARDNESS AND SPEED ON VIBRATION

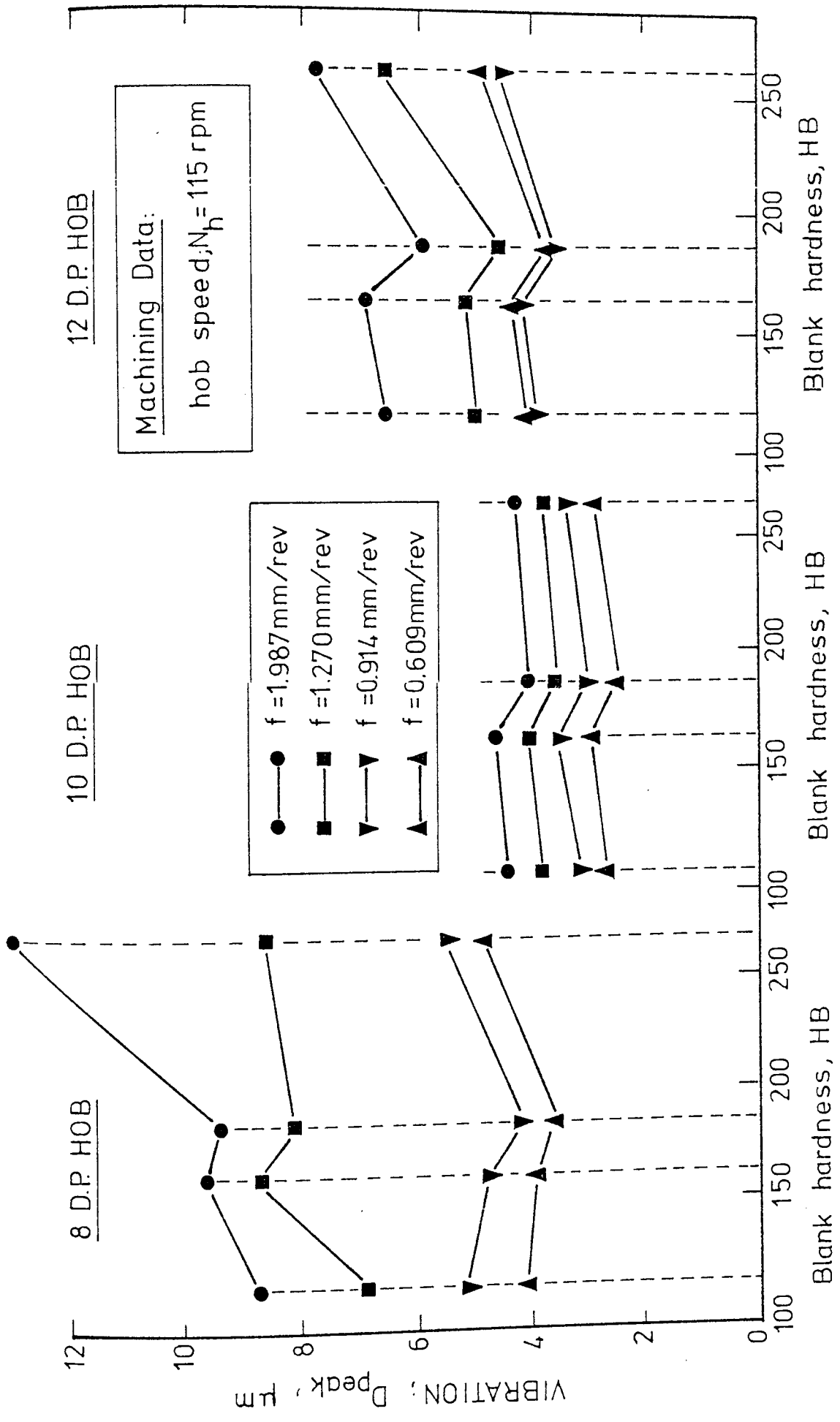

Fig.55 EFFECT OF HARDNESS AND FEED ON VIBRATION

6.5.4 Vibration versus Material Hardness

Figs. 54 and 55 show in graphical form the variation of vibration against material hardness at constant feed and constant speed respectively.

In Fig. 54 the curves show that at a constant feed of 1.270 mm/rev, vibration increases between En 1A and En 34 steels then drops between En 34 and En 8, and increases again. It is also observed that the values of vibration at three speed levels for 12 D.P. hob is less than that of 8 and 10 D.P. hobs at the same hob speed levels.

In Fig. 55 the curves show that at a constant hob speed of 115 r.p.m. vibration generally increases with the increase of material hardness with a slight drop in value between En 34 and En 8 steels. It can also be seen that 10 D.P. hob produces a more uniform pattern of vibrations at the four levels of feed with values less than the corresponding values of vibration for 8 and 12 D.P. hobs.

6.5.5 Analysis of Variance

A set of 144 tests was provided by combinational arrangement of feed, speed, hardness and D.P. to observe the significance of cutting parameters on vibration. Table 20 gives the analysis of variance and it follows that axial feed, hob speed and hob diametral pitch have a high significant effect on vibration as well as interaction between feed and hob speed, and D.P. and speed, while material hardness is less significant.

It is clear that feed has the most significant effect followed by speed and D.P.

6.5.6 Generalised Vibration Equation

A general relationship between vibration D_{peak} and the cutting parameters was needed in order to estimate the limit of stability for different machining conditions over a wide range of cutting, the results in Table 19 were considered, and the proposed relationship was of the form:

$$D_{peak} = C_d \; f^{\theta_1} \; (D.P.)^{\theta_2} \; (HB)^{\theta_3} \; V^{\theta_4} \qquad (37)$$

where, D_{peak} is displacement in μm peak

C_d is constant

$\theta_1, \theta_2, \theta_3$ and θ_4 are parameters

By applying multiple regression analysis, the following relationship was obtained when hobbing spur gears,

$$D_{peak} = \frac{5.6812 \; f^{0.592} \; HB^{0.223} \; V^{0.277}}{(D.P.)^{0.946}} \quad \mu m \qquad (38)$$

with error sum of squares = 0.11128 E2,

Residual error = 0.2860

and Multiple Correlation = 0.785

6.5.7 Discussion of Results

It is clear from analysis of variance that axial feed, hob speed and hob D.P. have high significant influence on cutting vibrations. From Figs. 52 and 53 it can be seen that vibration increases with the increase of axial feed because of the increase of the chip thickness on the side hob edges. With the increase of the feed rate also the total width of cut on peripheral edges increases. Vibration increases with the increase of cutting speed, but this increase is less than that with feed.

The effect of hob D.P. on vibration is not clear from Figs. 54 and 55 although highly significant, but a general trend shows that vibration decreases with the increase of hob D.P. (decrease in gear module) with evidence that with the increase in the number of gashes of the hob, vibration will decrease and follow a more uniform pattern at constant hob speed as can be seen in Fig. 55.

A drop in the values of vibration in the zone between En 34 and En 8 steel was expected since torques, power and surface roughness have dropped in the same zone for the same cutting conditions. Material hardness appeared to be less significant although high levels of vibration were recorded when hobbing En 16T (HB 269) using 8 and 12 D.P. hobs at constant speed.

The hobbing machine performance showed satisfactory stability results under the cutting range covered when compared with vibration standards. The VDI/ISO standards are provided in (Appendix II).

6.6 Conclusions

The following conclusions can be made from all previous facts:

1. Stability of hobbing depends strongly on the parameters of the cutting process, namely on axial feed, hob speed and hob D.P.

2. Material hardness has less significant effect on vibration and no monotic function exists between vibration and hardness.

3. With the increase of module, the width of uncut chip increases and therefore stability decreases.

4. The number of gashes in the hob has a slight improving influence on stability.

These conclusions are in good agreement with the results of experimental investigations of the influence of cutting parameters on stability.

CHAPTER VII

ANALYSIS OF THE MECHANICS OF UNCUT-CHIPS IN HOBBING

7.1 Introduction

In hobbing, the influence of cutting conditions is more complex than in orthogonal cutting, where the width and thickness of cut are clearly defined. Many teeth of the hob are cutting simultaneously with very different width and thickness of chip, these varying also during the rotation of the hob, both quantities vary in a wide range, and depend further on the parameters of the cutting process, e.g. the blank diameter, D.P., axial feed, rate, etc. A sample of some chips are shown in Fig. 56.

It is difficult to determine the total width of chip on the bottom and the flank, which have an essential influence on stability, variation of cutting forces and power and hob wear.

Principally, however, the analysis of the influence of the parameters of the cutting process on chip width and chip thickness enables one to determine their influence in order to explain certain experimentally obtained results.

Here, a practical method is presented to calculate the volume of metal removed during hobbing, a theoretical analysis of the uncut-chip thickness and width is attempted as well as an attempt to evaluate tool wear theoretically.

Fig. 56 SAMPLE OF CHIPS COLLECTED WHEN USING 10 DP HOB

7.2 Volume of metal removed during Hobbing

Calculating the volume of metal removed per unit time for gear hobbing is a simple matter once the basic mechanics of the operation is understood.

Area of cut for one tooth space, A_c assuming full depth of cut, as shown in Fig. 57 is obtained as follows,

$$A_c = \{t_0 + 2 \tan \alpha \ (add - ded)\} \ (add + ded)/2 \qquad (39)$$

where, A_c is area of cut, cm^2

t_0 is circular arc thickness = πm

m is gear module, mm.

α is pressure angle

Thus $A_c = 3.51 \ m^2$, for add = 1.16m

$A_c = 3.72 \ m^2$, for add = 1.25m (40)

Total volume of metal removed is obtained in a general expression as shown in equation (41), where gear helix angle, β is considered as well as the normal module, m and helical module, m_s. The helical module is given by,

$$m_s = m/\cos \beta$$

and

$$V_T = \frac{A_c . b . Z_g}{\cos^2 \beta}$$

$$= 0.0035 \ m^2 . b . Z_g / \cos^2 \beta \qquad (41)$$

where, V_T is total volume of metal removed, cm^3

b is width of the gear blank, mm

Z_g is number of teeth in the gear.

The feed rate is usually given in terms of mm per revolution of the gear blank, the helical feed is obtained as follows,

$$f_s = f/\cos\beta \qquad (42)$$

where, f_s is helical feed, mm/rev.

f is axial feed, mm/rev.

The volume of metal removed per revolution of the blank is given by equation (43) as follows,

$$V_s = 0.0035\ m^2.f.Z_g/\cos^3\beta \quad Cm^3/rev. \qquad (43)$$

Cutting time in the hobbing process is given by,

$$t = \frac{Z_g}{S_h.N_h} \qquad (44)$$

where, t is cutting time, min.

S_h is number of starts in the hob

N_h is hob speed, r.p.m.

A general expression for the total volume of metal removed per unit time is now obtained as follows,

$$V_s' = \frac{V_s}{t} = 0.0035\ m^2.f.S_h.N_h/\cos^3\beta \quad cm^3/min. \qquad (45)$$

A quick and simple method of obtaining the volume of metal removed per unit time when the most simple hobbing process is assumed: the hobbing of spur gears with a single start hob,

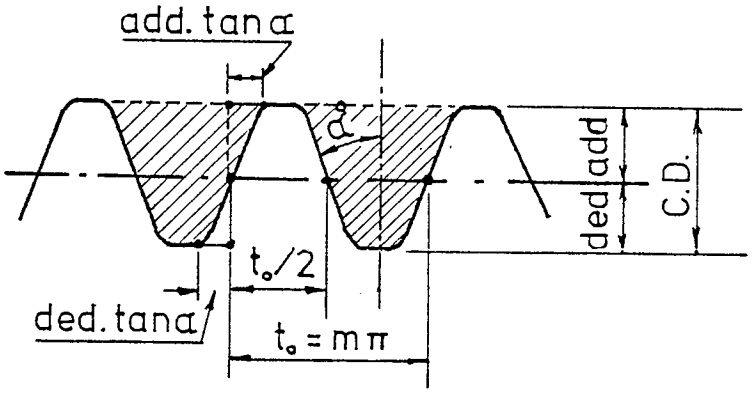

Fig. 57 BASIC PROFILE OF GEAR

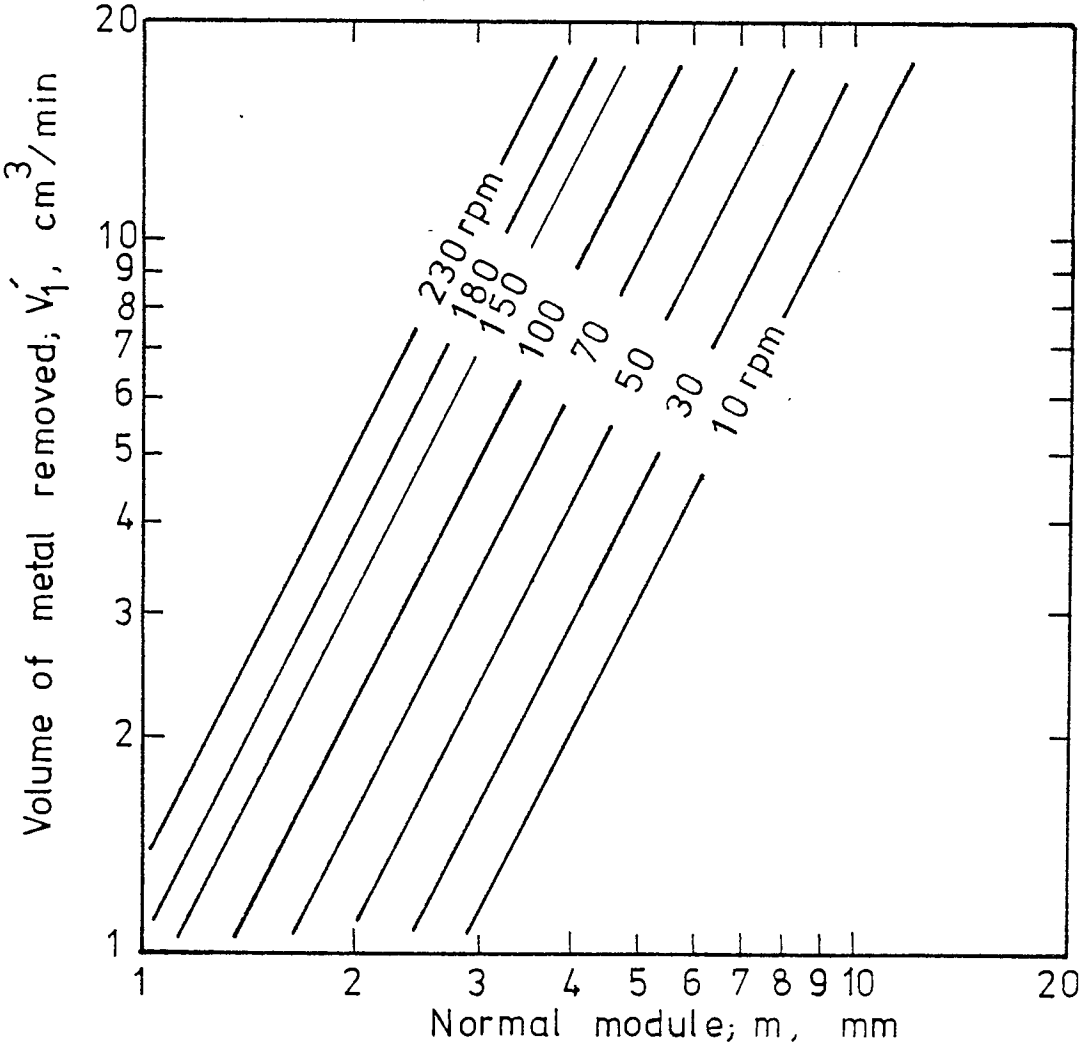

Fig. 58 THE RELATIONSHIP BETWEEN VOLUME OF METAL REMOVED AND MODULE AT DIFFERENT HOB SPEEDS

unit axial feed is applied. Fig. 58 shows the volume of metal removed V_1' at a given normal module and hob speed for unit axial feed. The actual volume of metal removed per minute V_s' is obtained from the following relation,

$$V_s' = V_1' \cdot f \cdot S_h / \cos^3 \beta \qquad (46)$$

Example:

10 D.P. hob, m = 2.540, Z_g = 29, f = 1.270 mm/rev. helix angle $\beta = 30^\circ$, N_h = 100 rpm, single start hob.

From Fig. 58, V_1' = 3.6 $cm^3/min.$

and the actual volume of metal removed becomes,

$$V_s' = \frac{3.6 \times 1.270}{\cos^3 15} = 5.252 \quad cm^3/min.$$

7.3 Theory of Action of Top Cutting Edges of the Hob

Fundamental distinction can be found between the work of the peripheral cutting edges of the hob and the work of the side cutting edges, where peripheral edges cut off a major part of the gear blank material and side edges merely shape the gear teeth flanks. The ratio of the work of both kinds of edges is shown in Fig. 59 .

7.3.1 Traces of top edges during cutting

During conventional hobbing, the peripheral cutting edges of the hot advance axially to cut the gear blank on the common perpendicular line of both the hob and gear axes. The generated pitch point is located on this line and the common perpendicular is on the centre of generation. The generating

portions of hob K_o lie on both sides of this point and is given as follows:

$$K_o = \frac{\text{add. } \cos \nu}{\tan \alpha_s . \cos \beta} \quad \text{mm} \qquad (47)$$

where, add. is hob addendum

α_s is transverse pressure angle, $\tan \alpha_s = \tan\alpha/\cos\beta$

β is gear helix angle

ν is hob lead angle

The roughing portion of the hob is located outside the generating portion, the gear teeth are roughed by the roughing portion which cuts away the greater part of the gear blank material, and wear in this part restricts the hob life.

Fig. 60 demonstrates the state of right hand hobbing where a right hand gear is being cut by a right hand hob, the profile generating portion and the roughing portion are shown in the figure. The intersecting point of the common perpendicular and the hob axis is taken as the origin O.

Reproduced from reference [28] an investigation was carried out into the trace of point P, which is located at distance K from point O, in the direction of the hob axis.

The co-ordinates of point P are represented by axes x, y and z as shown in Fig. 61, where y is taken to the direction of arrow from the gear axis for convenience. The co-ordinates of P in its rotation around point A, on the hob axis is given by the following equations:

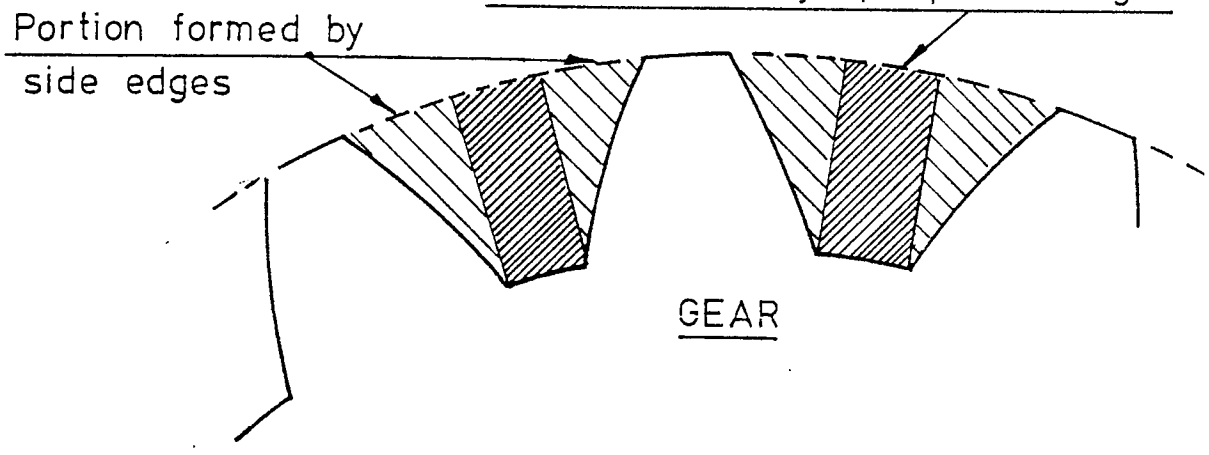

Fig. 59 VOLUME OF METAL CUT OFF BY INDIVIDUAL HOB EDGES

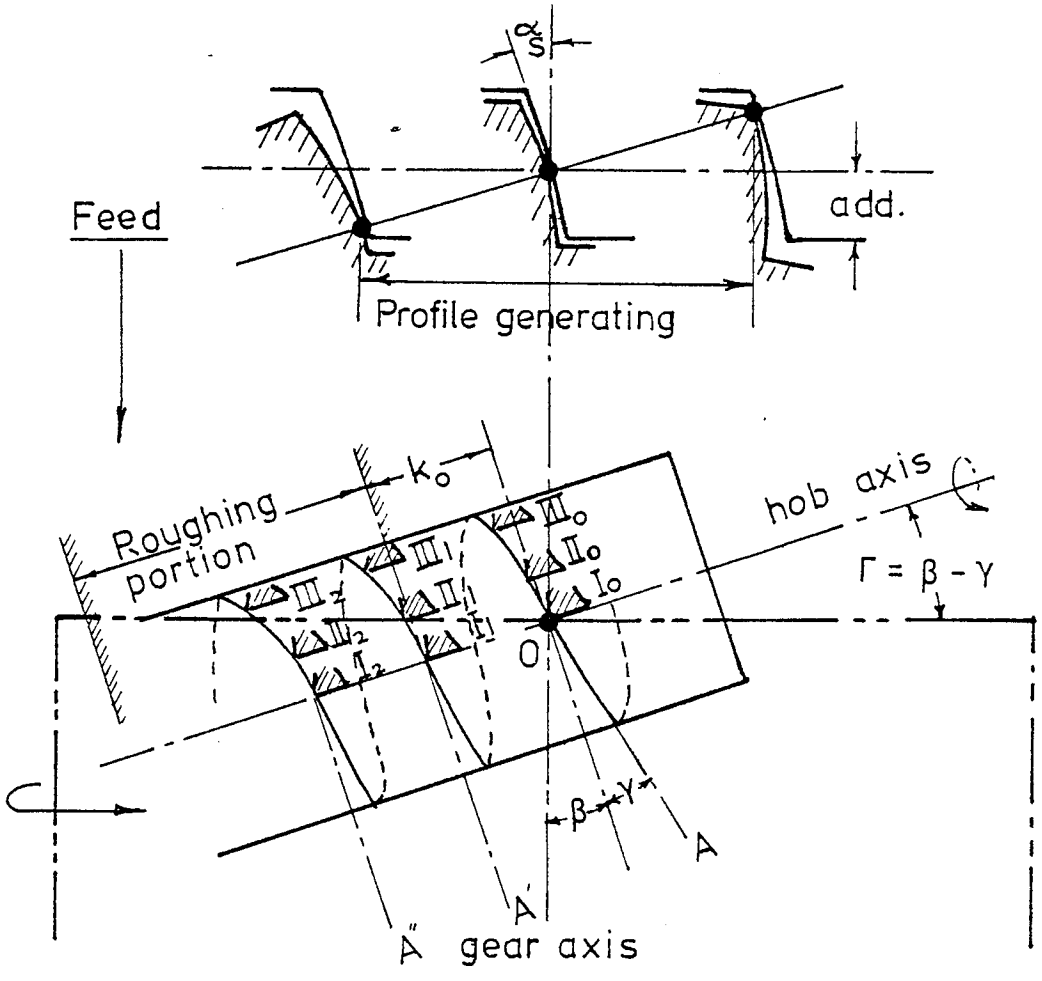

Fig. 60 THE STATE OF RIGHT HAND HOBBING

$$x = K\cos\Gamma - r\sin\theta\sin\Gamma = R\sin\psi \quad (48)$$

$$y = C - r\cos\theta = R\cos\psi \quad (49)$$

$$z = K\sin\Gamma + r\sin\theta\cos\Gamma \quad (50)$$

$$R^2 = x^2 + y^2 \quad (51)$$

where, Γ is the hob setting angle

r is the hob outside radius

R is radius of point P from the gear axis

C is the centre distance

ψ is the rotating angle of point P from yz-plane

In the axial section of gear, the position of P is represented by Z and R.

The traces of hob peripheral edges are shown in Fig. 62 as they are drawn by the change of from O as shown in Fig. 61. It is noted here that traces of these cutting edges are not in the same cross-section with the gear blank, the figure shows the traces superimposed by rotating around the gear axis.

The envelope of these traces constitutes the root line of the gear tooth.

The relation between the contact point of each trace and the profile of root surface is expressed as follows:

$$\tan\psi = \tan\theta\sin\Gamma \quad (52)$$

$$\tan\theta = (K/C)\cot\Gamma \quad (53)$$

The root line of the tooth is, therefore obtained by solving Eqs. (48), (49) and (52).

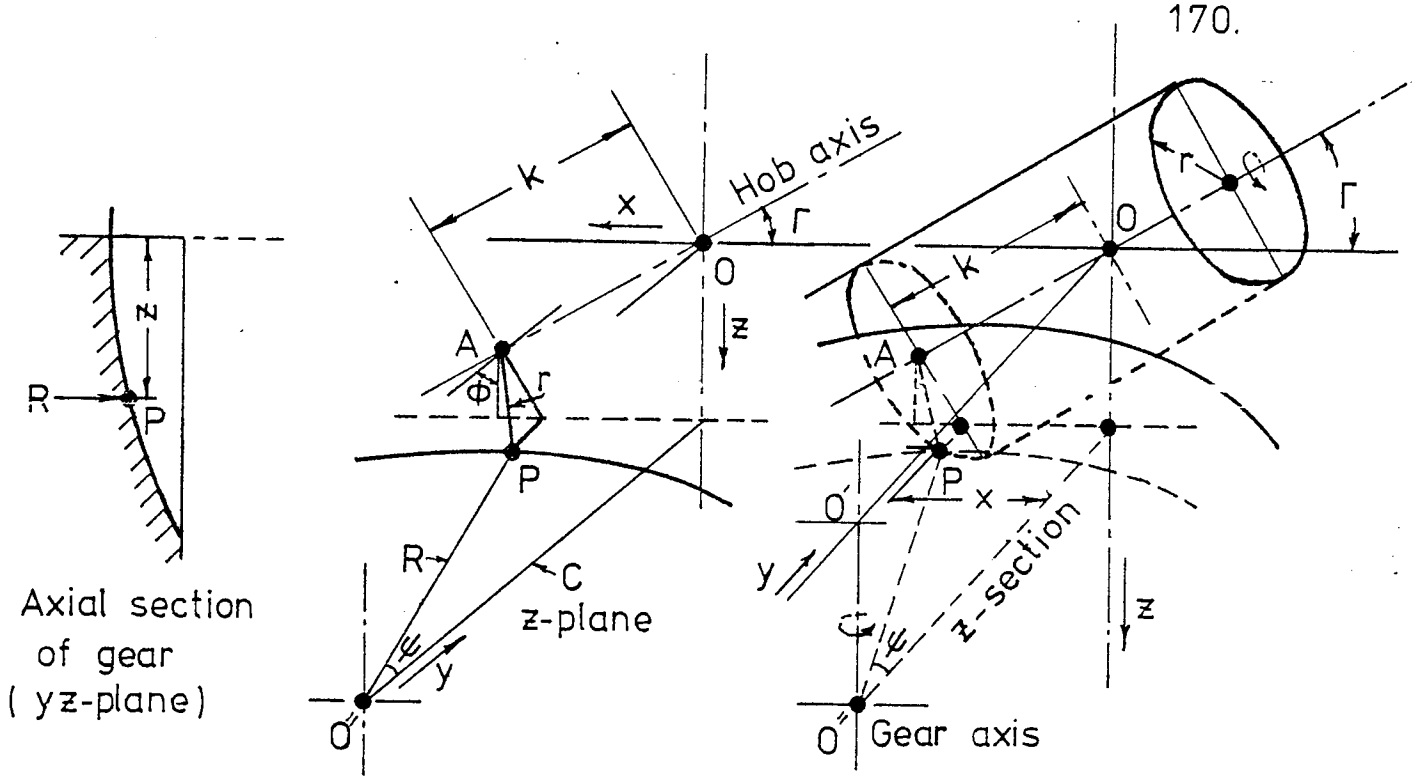

Fig. 61 LOCATION OF CONTACT POINT "P"

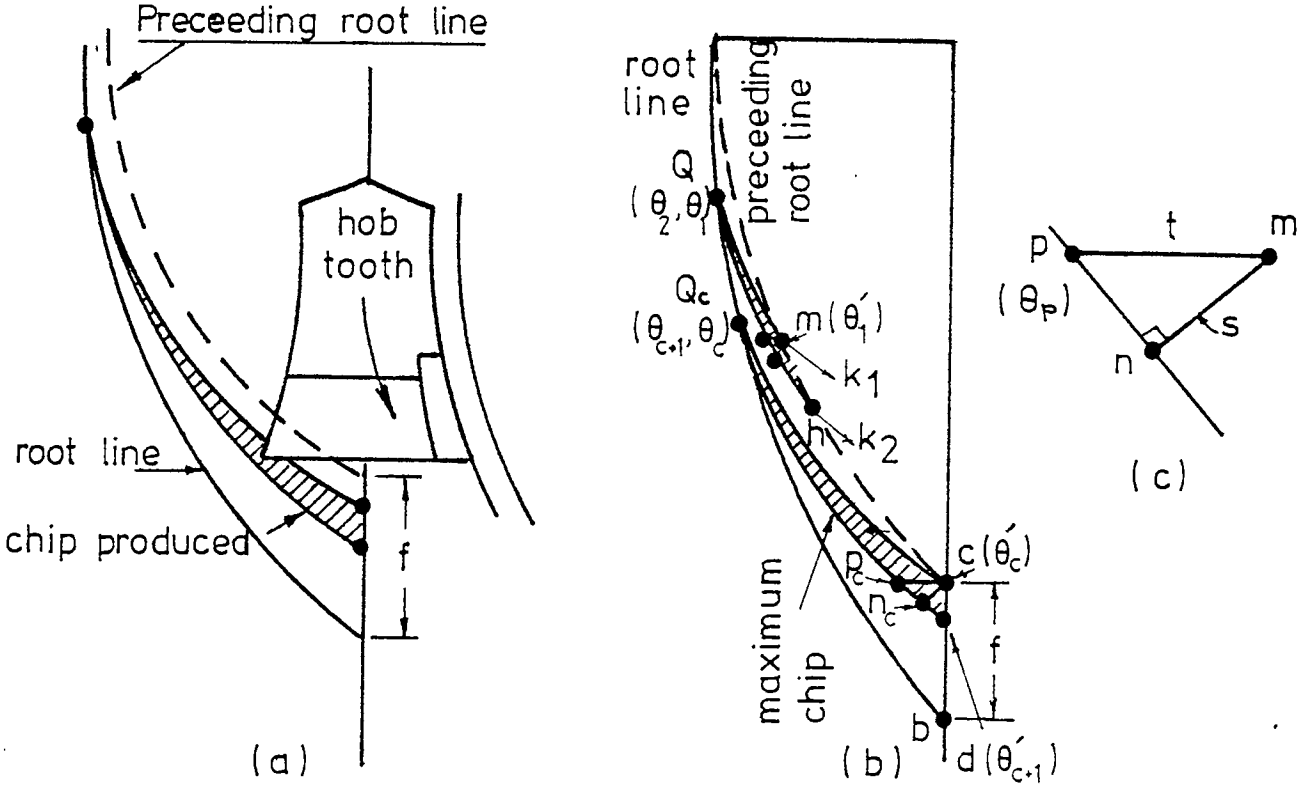

Fig.62 DIMENSIONS OF CHIP CUT OFF BY PERIPHERAL CUTTING EDGES

The root line of the tooth and the preceding root line are separated by feed (f).

7.3.2 Chip thickness, S and chip length, L

The mechanic of uncut-chip during hobbing is explained as the cutting edge K_2 starts to cut in from point Q as shown in Fig. 62 (b), that is the cross point of the curves traced by the preceding cutting edge K_1, the cut finishes when K_2 intersects with the former root line (dotted line) at point h.

Maximum chip is produced at point Q_c, and ends at the cross point of the trace with the circumference line (feed line) of the gear.

There are two methods of obtaining length (L) and thickness (S) of the chips:

(i) Measurement by magnifying the drawings in Fig. 62 (b) and (c).

(ii) Calculation can be carried out by solving Eqs. (48) to (52), and the following formula,

$$L_2 = r(\theta_2' - \theta_2) \text{ or } L_c = r(\theta_c' - \theta_c)$$
$$S = \overline{mn} \text{ or } \overline{Cn}_c \qquad (54)$$

The severity of the cutting works may be evaluated by the product L x S, where it has been noticed that the hob wears most at the parts where the values of L x S are high.

In order to evaluate chip length L, and thickness S, cut off by each hob edges, hob and gear specifications being shown in Table 21, the following calculations are carried out,

TABLE 2 1

HOBBING DATA FOR SPUR GEAR

GEAR		HOB DETAILS	
D.P.	10	D.P.	10
Pressure angle	20^{o}	Pressure angle	20^{o}
Helix angle	0^{o}	Outside Dia.	76.35 mm
Z_g	36	Length of working part	70 mm
Outside Dia.	96.52 mm		
Width	25.4 mm	No. of starts	1
Material	En 8	Lead angle	$2^{o}\ 6'$
Hardness,HB	183	Cutting gashes	straight,14
CUTTING CONDITIONS		Top rake angle	8^{o}
Cutting speed	24.28m/min	SYKES No.	HP 368-20/v2
Axial feed	1.727mm/rev	Addendum	3.175 mm
Cutting depth	5.715 mm	Dedendum	2.54 mm

$$x = 0.999\ K - 1.397 \sin\theta = R \sin\psi \quad (55)$$

$$y = 80.720 - 38.175 \cos\theta = R \cos\psi \quad (56)$$

$$z = 0.0784\ K + 38.056 \sin\theta \quad (57)$$

$$\tan\psi = 0.078 \tan\theta \quad (58)$$

The contact point of each trace and the profile of root surface are obtained by solving Eqs. (55) to (58). Chips length, L and thickness, S were measured and the cutting load (i.e. L and S) was plotted against the hob cutting edges as shown in Fig. 63.

It is seen from the figure that at feed rate 1.727 mm/rev, the cutting edge which gives maximum value of S, are close to one another, for the example considered.

The cutting product (L x S) for the same gear and hob was plotted against the hob cutting edges as shown in Fig. 64. It is clear from the graph that the loads on the hob edges are not equal, and edge number 27 from the centre of generation seems to give maximum cutting load. It was also observed when measuring the hob wear, that deterioration of the hob edges becomes maximum at the working portion of the hob where the product L x S is largest.

If the working portion of the hob is changed by shifting the hob axially, the hob wear will scatter among other parts which supports the view.

Therefore, hob wear can be evaluated by calculation of the cutting product (L x S).

7.3.3 Effect of feed on chip thickness

Investigation into the effect of axial feed and gear blank diameter on chip thickness was carried out. Mean chip

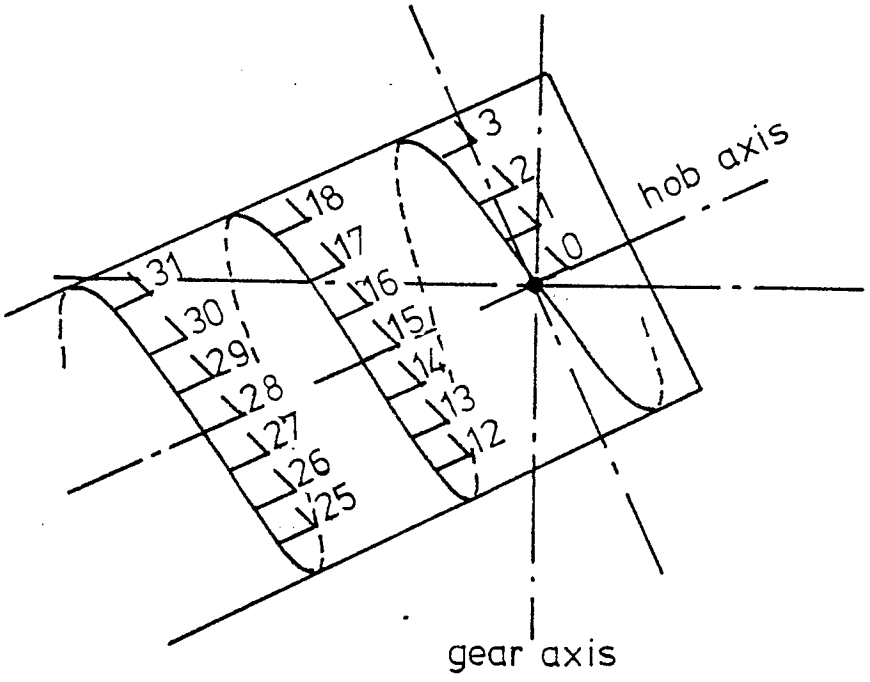

a) Numbers given to hob teeth

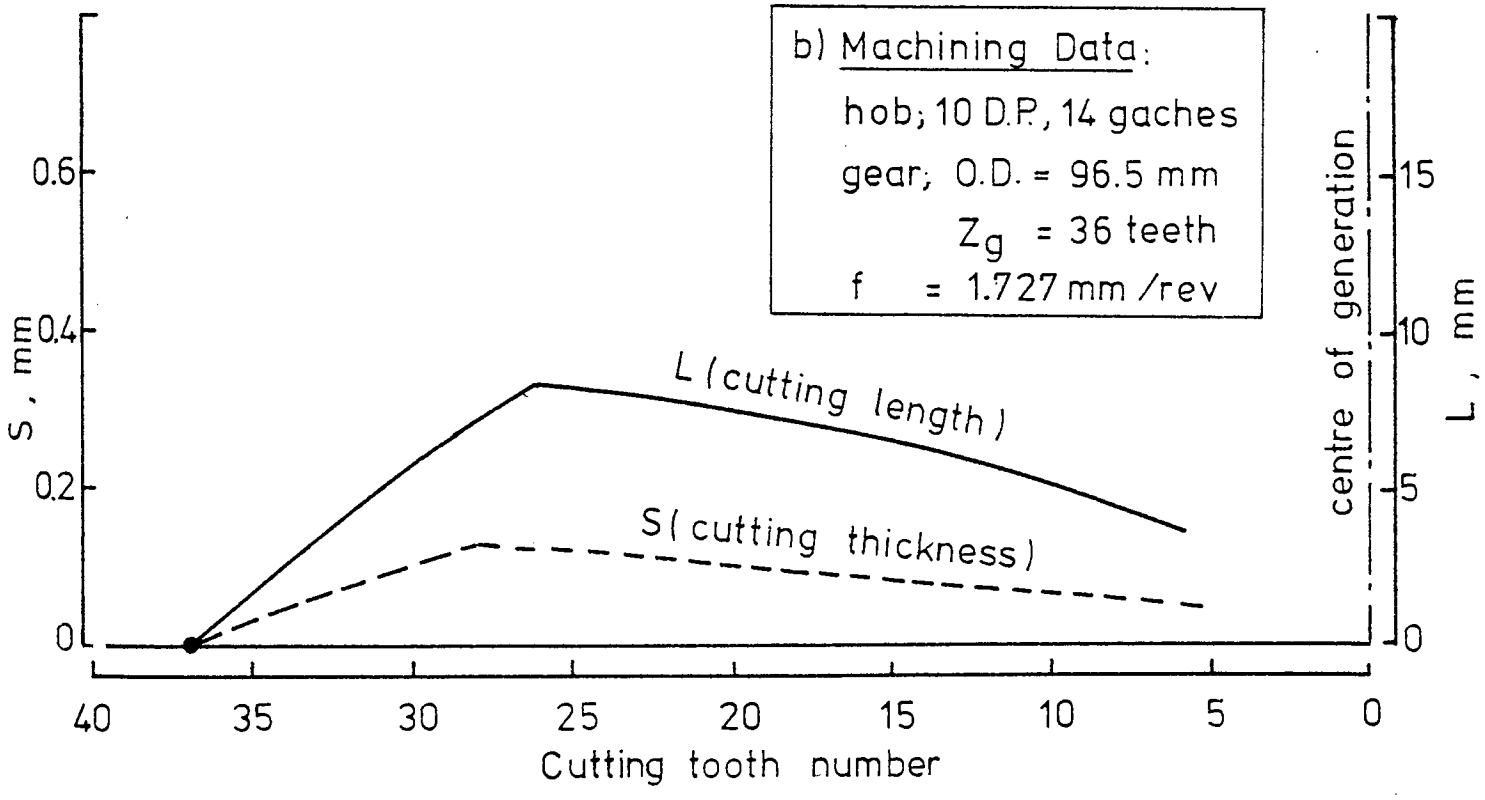

Fig. 63 CHIP LENGTH AND THICKNESS OF TOP HOB EDGES

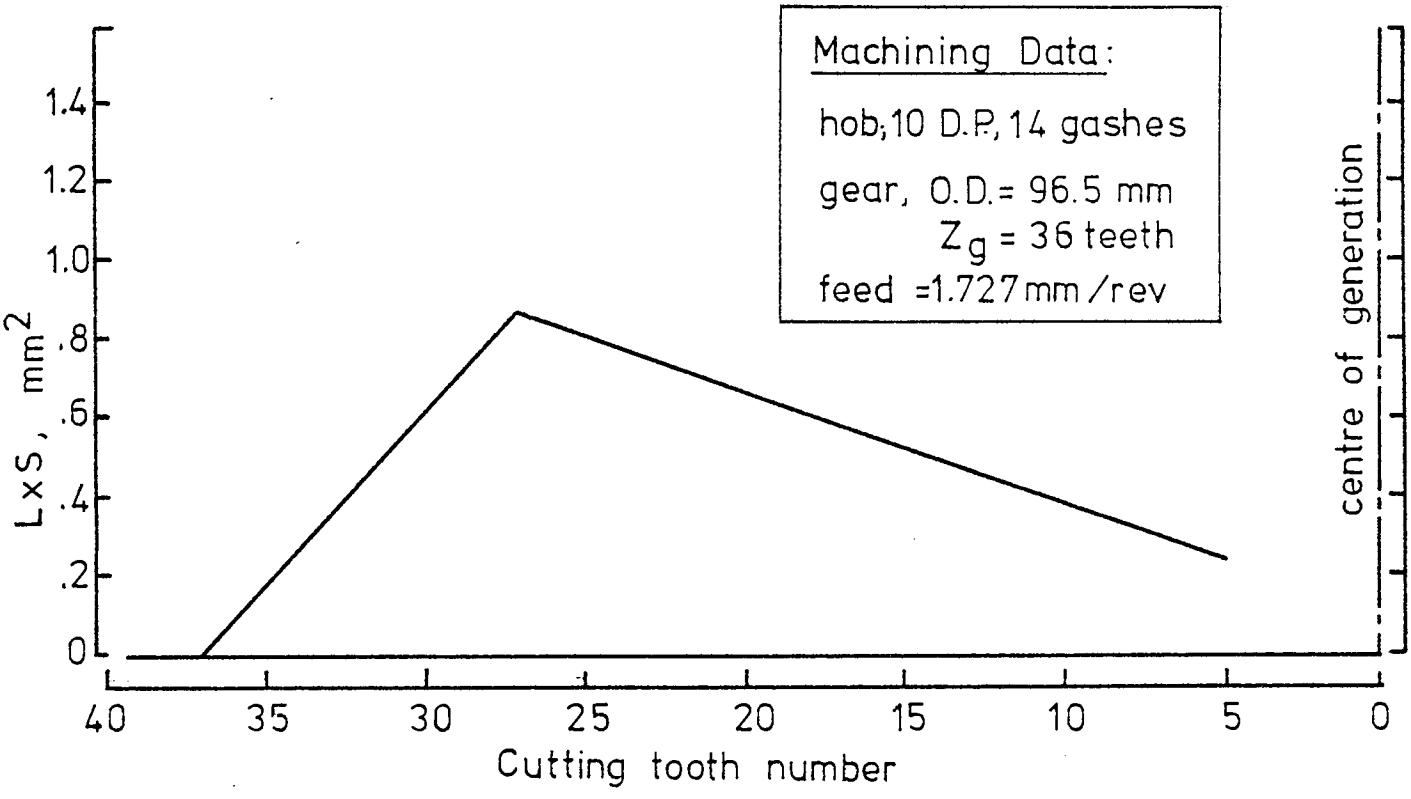

Fig. 64 THE PRODUCT (L x S) OF EACH TOP EDGE

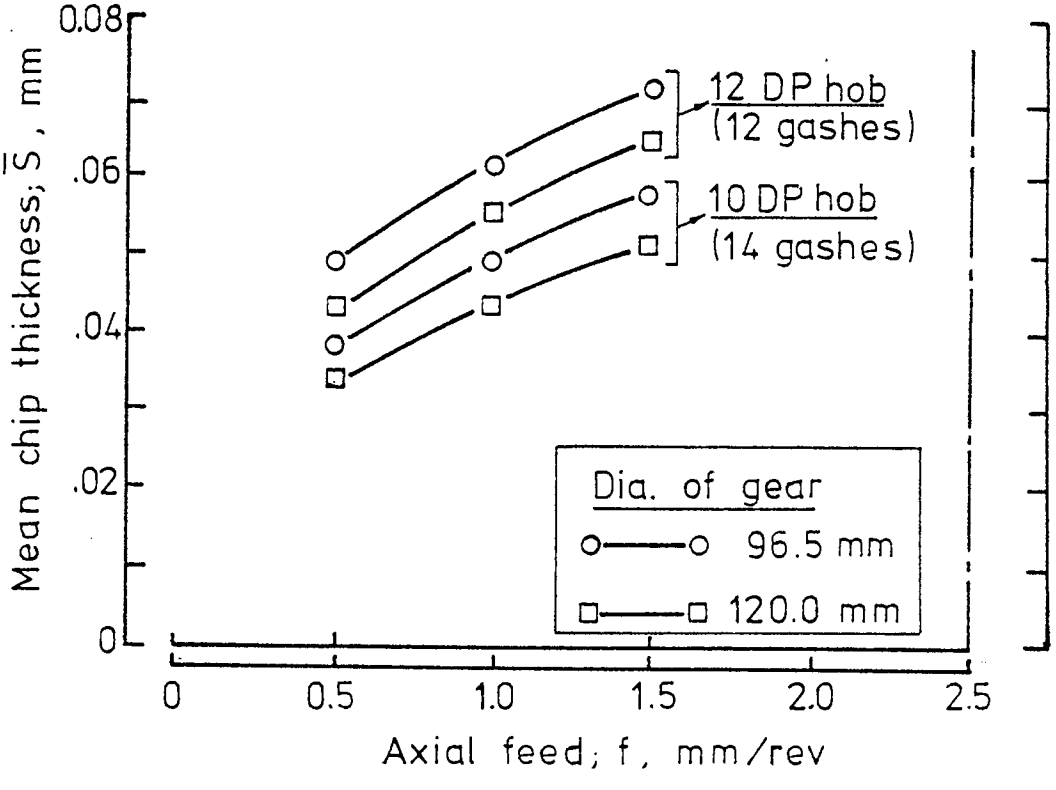

Fig. 65 EFFECT OF FEED ON MEAN CHIP THICKNESS

thickness ($\bar{S}$) ,was calculated as average values of all edges in the working portion for two types of hob; 10 D.P. and 12 D.P. and two different gear diameters; 96.52 mm and 120.00 mm.

Fig. 65 shows the variation of mean chip thickness $\bar{S}$ against hob axial feed. From the graphs it is clear that increasing axial feed from 0.5 mm/rev to 1.5 mm/rev, resulted in an increase in mean chip thickness cut off by peripheral edges, and increasing the blank diameter will decrease mean chip thickness. The number of gashes in the hob influences chip thickness; with increasing it, thickness decreases.

7.3.4 Effect of chip thickness on stability

The influence of chip thickness cut off by top edges on stability is not significant. As Slavicek[9] reported that stability strongly decreases for thickness values of $S < .035$ mm , and on the other hand, with the increase of S, stability increases to some extent for $S > .035$ mm. From Fig. 63 it is clear that chip thickness cut off by top edges has the values 0.030 - 0.070 mm.

7.3.5 The Cutting zone and Cutting period of top cutting edges

The developed plan of the hob outside cylinder is shown in Fig. 66, $r\theta$ being the distance of starting point of cutting. The cutting zone may be determined by laying $r\theta$ and $r\theta'$ in the direction perpendicular to the hob axis.

The cutting zone and working periods of the hob and gear specifications given in Table 21 are shown in Fig. 67. In this example, tooth I_o starts cutting just at a moment when the cutting edges along the preceding gash has finished

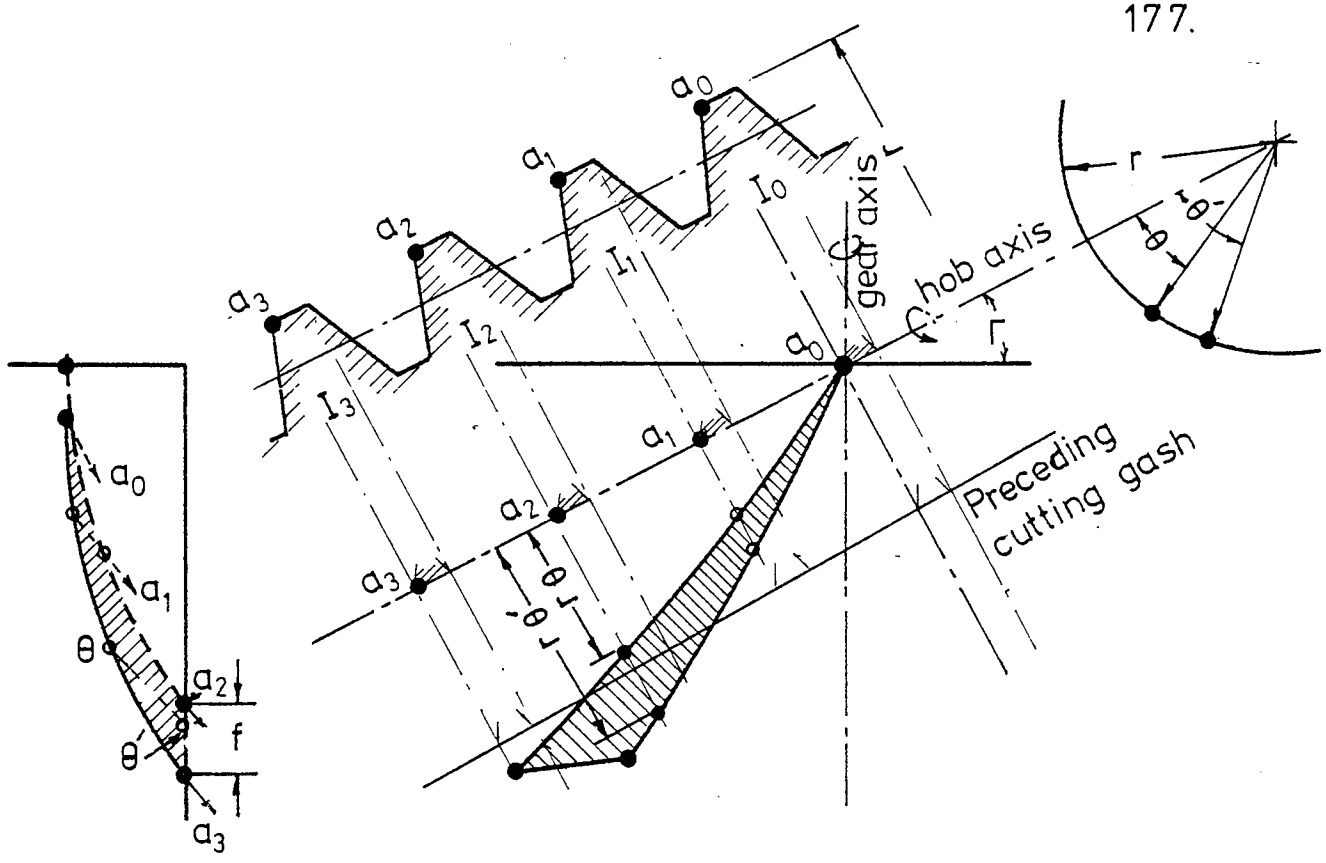

Fig.66 THE MECHANIC OF CHIP IN HOBBING

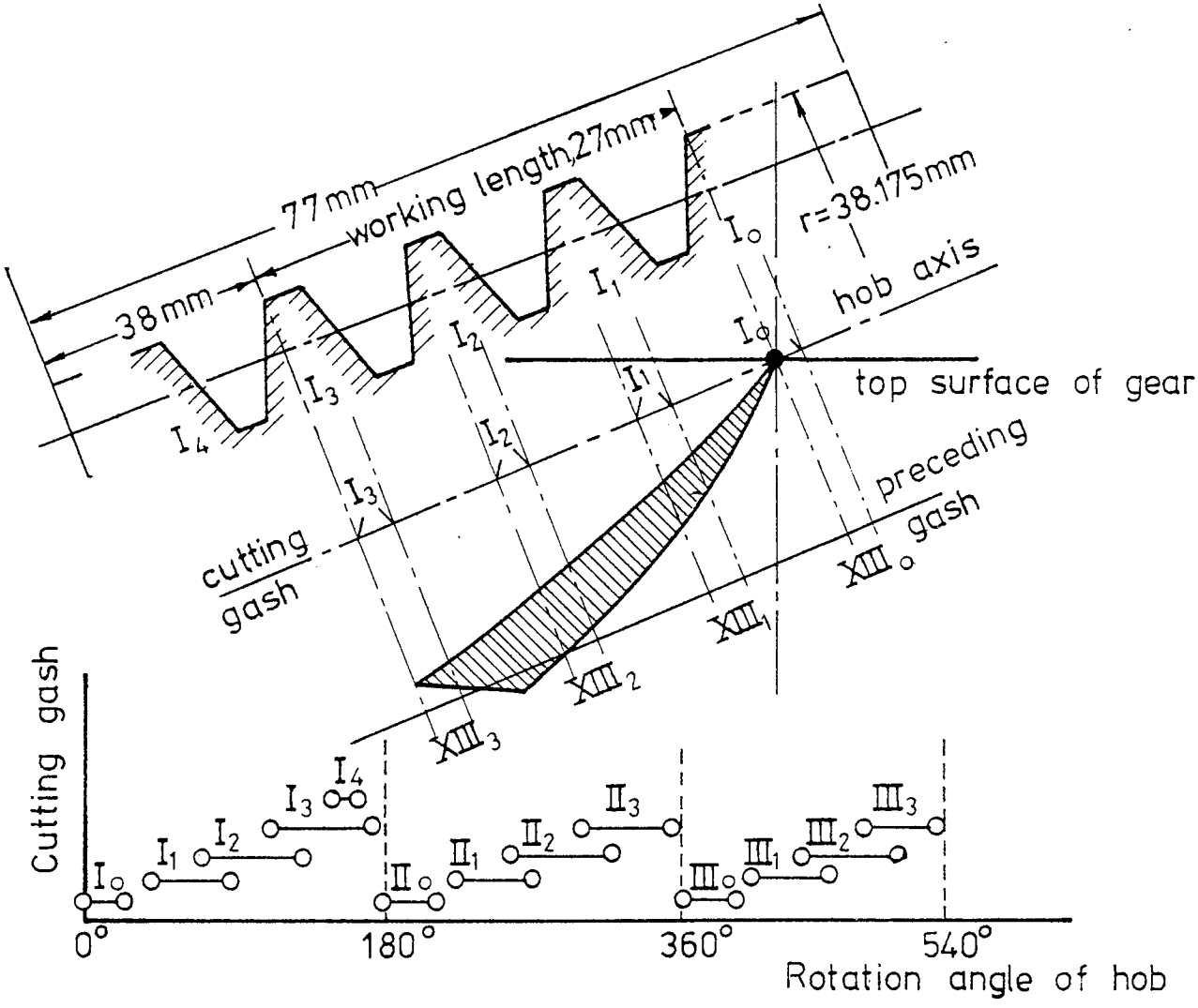

Fig.67 CUTTING ZONE AND WORKING PERIODS FOR THE HOB AND GEAR SHOWN IN TABLE.21

cutting, the cutting periods of the hob gashes at full depth of cut, are shown at the bottom of Fig. 67, the illustration shows clearly that the edge I_4 cuts only in the first hob rotation at the beginning of full cutting depth, while edges I_1, I_2 and I_3 have longer cutting periods.

The illustration of cutting periods shows that the problem of designing hob gashes is important, where it reduces fluctuation of the cutting forces. This problem appears particularly in hobbing large gears where high cutting forces are involved.

7.4 Theory of action of side cutting edges

It is very difficult to find any data about the shape of chips cut off by side edges. This matter is not of interest from the production and tool wear point of view, because the main part of the chip volume is cut off by peripheral edges. It is clear, however, that chip width and thickness cut off by the side edges have the same influence on surface roughness, force and stability as those cut off by peripheral edges. These values must therefore be investigated.

7.4.1 The traces of side cutting edges in action

The traces of peripheral cutting edges described previously is taken here as a basis for the theory of action of side cutting edges of the hob.

Fig. 68 shows the proportion of the hob depth of cut, and depth of cut for the side cutting edges.

In order to calculate thickness S , and length L, of chips cut off by side cutting edges of the hob teeth, it

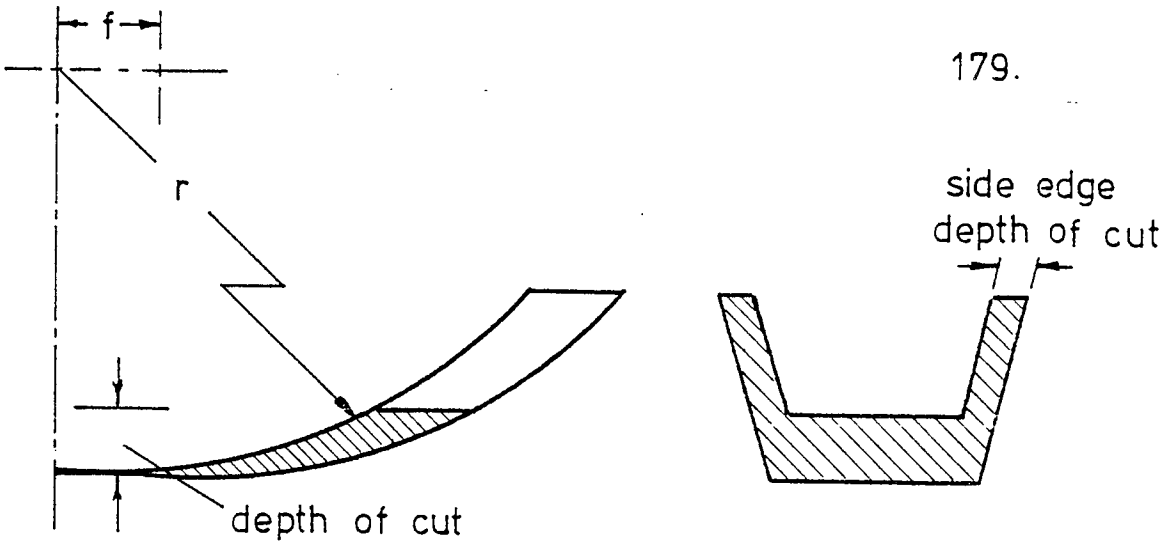

Fig. 68 DEPTH OF CUT FOR SIDE CUTTING EDGE

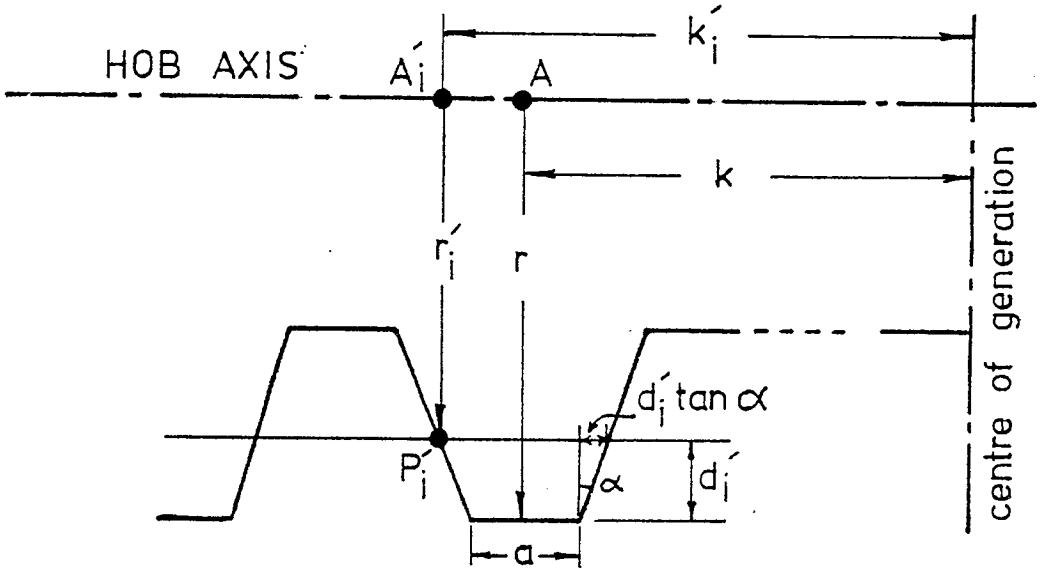

Fig. 69 CONTACT POINT ON SIDE EDGES

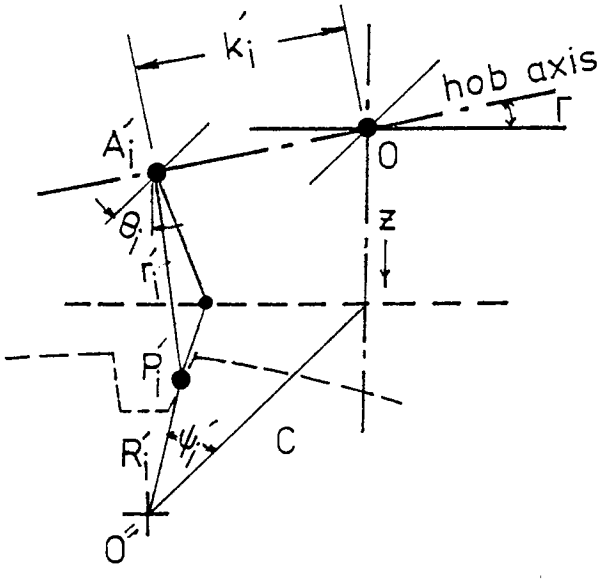

Fig. 70 LOCATION OF SIDE EDGE CONTACT POINT

is essential to trace the point of contact P_i', which is located on the side cutting edge. Fig. 69 shows the location of P_i' with respect to the hob axis, and the centre of generation, while Fig. 70 shows the location of P_i with respect to the gear blank-hob intersecting axis. Axes x, y and z are taken as given in Fig. 61.

The hob radius at point P_i' and locating distance from the centre of generation are represented as follows:

$$r_i' = r - d_i' \tag{59}$$

$$k_i' = k \pm \left(\frac{a}{2} + d_i' \tan\alpha\right) \tag{60}$$

where, r_i' is the hob radius at point P_i, mm.

d_i' is the distance between P_i and hob periphery, mm.

k_i' is the distance between P_i and centre of generation, mm.

a is the width of peripheral edge, mm.

α is normal pressure angle.

By substituting the values of r_i' and k_i' in Eqs. 48 to 52 according to change in hob radius r_i, the root line of side cutting edges of the tooth is therefore obtained by solving Eqs. (48), (49), (50), (51), (52), (59) and (60).

In order to observe the proportion between tool wear and chip width, an example is shown in Fig. 71 for hob and gear given in Table 21.

The following steps are carried out in order to calculate chip thickness cut off by peripheral and side cutting edges of the hob teeth:

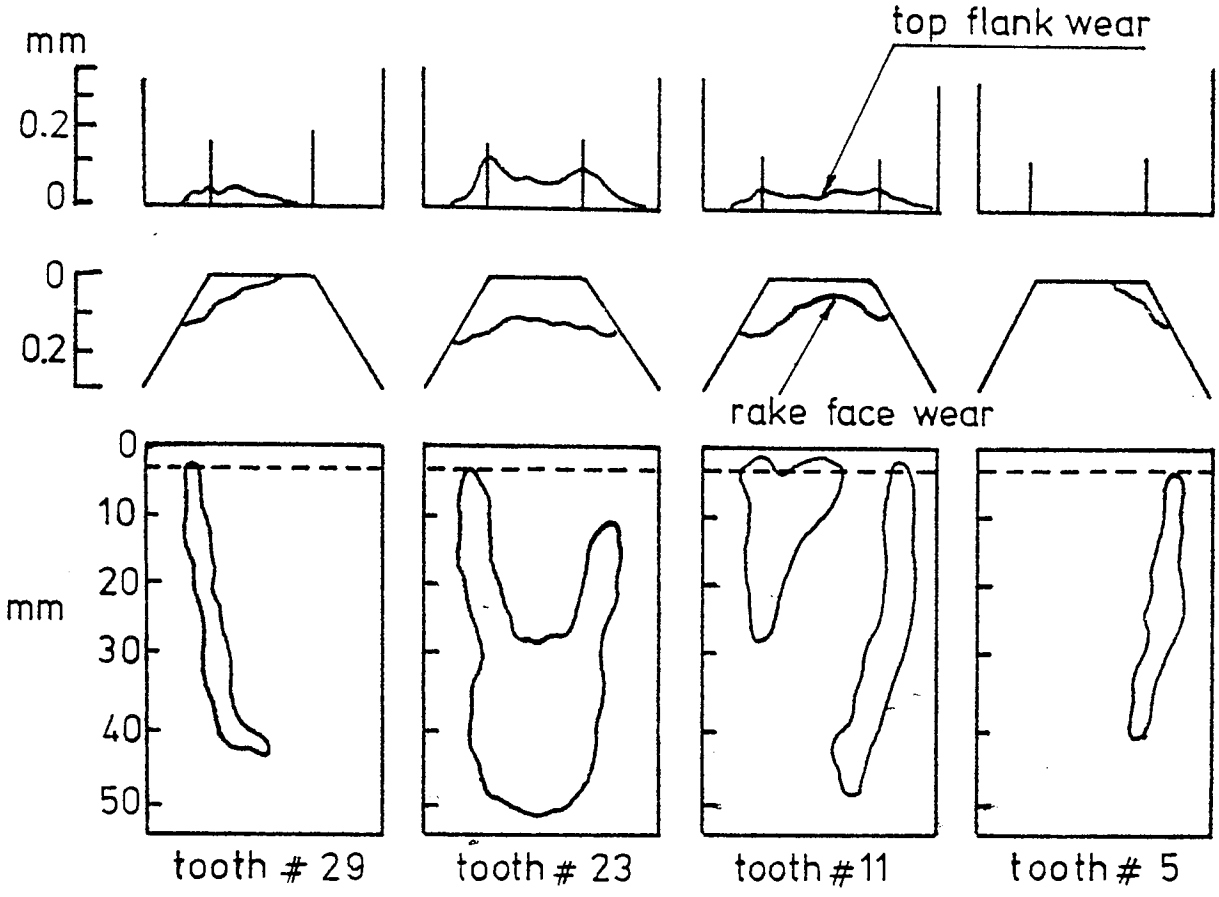

Fig. 71 THE RELATIONSHIP BETWEEN AREA OF UNCUT CHIP AND TOOL WEAR FOR 10 D.P. HOB

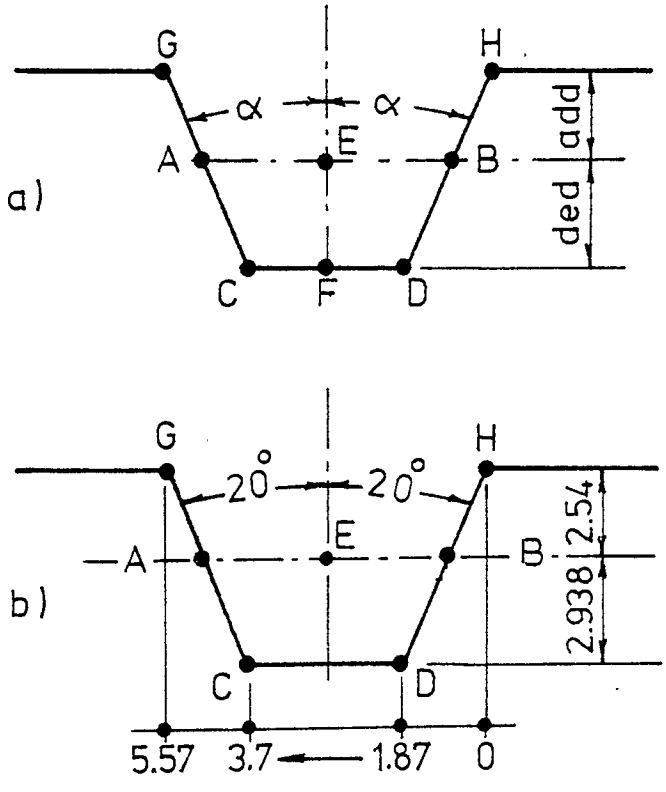

Fig. 72 10 D.P. HOB TOOTH DIMENSIONS

a) The hob tooth dimensions must be accurately calculated as shown in Fig. 72(a) where,

$$\begin{aligned} &\text{circ. arc thickness, } AB = \pi m/2 \\ &AE=EB=AB/2= \pi m/4 \\ &CF=FD=AE-EF \tan\alpha \\ &\qquad = \pi m/4 - \text{ded.} \tan\alpha \\ &HD=GC=(\text{add}+\text{ded}) \cos\alpha \\ &GH=2(\text{add}+\text{ded}) \sin\alpha + 2CF \end{aligned} \tag{61}$$

b) Define the hob centre of generation

c) Estimate the location of contact point P, on the peripheral and side cutting edges with respect to the hob centre line and centre of generation.

d) For each given value of z, as shown in Fig. 70 substitute the corresponding values of r_i' and k_i' in Eqs. (48), (49) and (50).

e) By solving Eqs. (48) to (53), the values of chip thickness at each point on the cutting edge can be obtained.

To demonstrate the method using hob gear and cutting conditions given in Table 21, hob dimensions are given as follows:

$m = 2.540$ mm, $\alpha = 20^{\circ}$, ded = 2.938 mm,

add = 2.540 mm and circ. arc thickness = 3.989 mm.

Therefore

$$CF = \frac{\pi}{4} \times 2.540 - 2.938 \times 0.364 = 0.92557 \text{ mm}$$

$$CD = 1.852 \text{ mm.}$$

$$GH = 10.956 \sin\alpha + CD$$

$$= 5.5982 \text{ mm.}$$

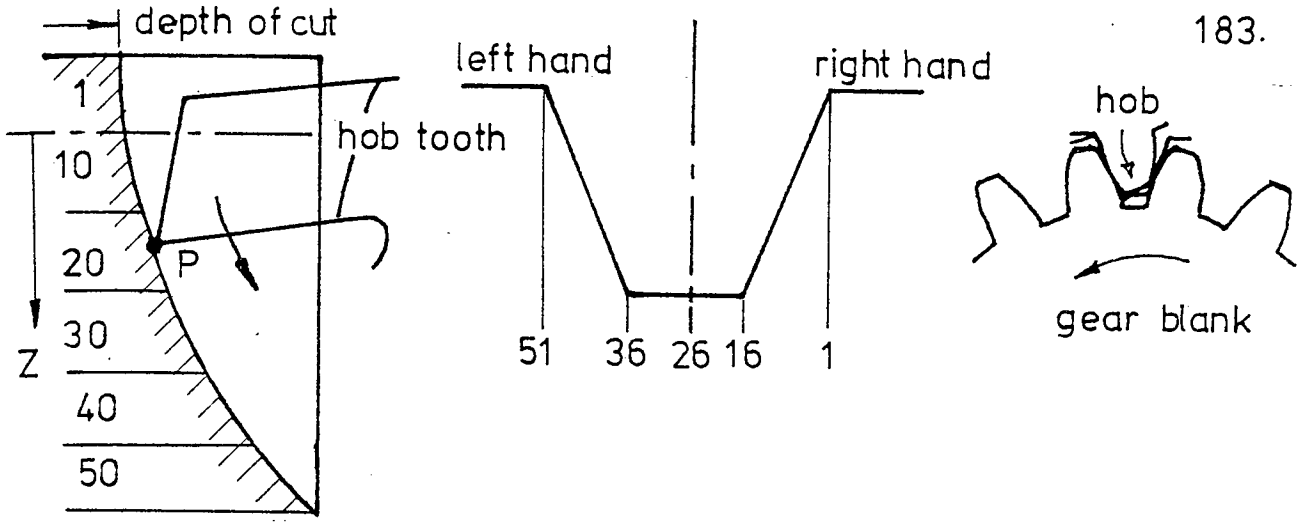

a) Dimensions of hob tooth and axial section of gear

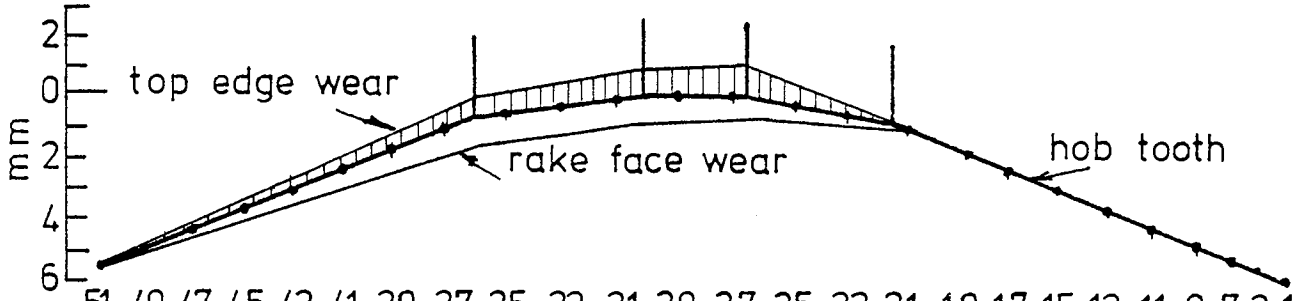

Z \	51	49	47	45	43	41	39	37	35	33	31	29	27	25	23	21	19	17	15	13	11	9	7	3	1
1	0	0	0	0	0	0	0	0	0	0	0	0	0	0	0	0	0	0	0	0	0	0	0	0	0
3	0	0	0	0	0	0	0	0	0	0	0	0	0	0	0	0	0	0	0	0	0	0	0	0	0
5	0	3	6	1	0	0	0	0	0	0	0	0	0	0	0	0	0	0							
7	0	6	17	0	0	0	0	0	0	0	0	0	0	0	0	0	0	0							
9	0	5	16	0	0	0	0	0	0	0	0	0	0	0	0	0	0	0							
11	0	4	15	20	0	0	0	0	0	0	0	0	0	0	0	0	0	0							
13	0	3	13	20	0	0	0	0	0	0	0	0	0	0	0	0	0	0							
15	0	2	11	21	15	0	0	0	0	0	0	0	0	0	0	0	0	0							
17	0	1	9	19	19	0	0	0	0	0	0	0	0	0	0	0	0	0							
19	0	0	6	16	24	9	0	0	0	0	0	0	0	0	0	0	0	0							
21	0	0	2	13	24	18	0	0	0	0	0	0	0	0	0	0	0	0							
23	0	0	1	9	21	24	5	0	0	0	0	0	0	0	0	7	9	2							
25	0	0	0	7	18	28	17	0	0	0	0	0	0	0	0	8	14	5							
27	0	0	0	2	11	21	19	0	0	0	0	0	0	0	0	2	7	2							
29	0	0	0	1	7	18	30	17	0	0	0	0	0	0	0	0	1	0							
31	0	0	0	0	4	12	25	21	0	0	0	0	0	0	0	0	0	0							
33	0	0	0	0	1	10	21	32	22	0	0	0	0	0	0	0	0	0							
35	0	0	0	0	0	6	16	28	45	70	59	47	23	0	0	0	0	0							
37	0	0	0	0	0	1	12	23	38	77	94	102	82	55	24	5	0	0	0	0	0	0	0	0	0
39	0	0	0	0	0	0	6	18	37	75	96	101	106	109	82	37	5	0	0	0	0	0	0	0	0
41	0	0	0	0	0	0	0	12	35	69	91	110	105	104	99	70	11	3	0	0	0	0	0	0	0
43	0	0	0	0	0	0	0	6	27	62	86	99	104	108	107	92	13	0	0	0	0	0	0	0	0
45	0	0	0	0	0	0	0	0	15	56	83	97	103	106	108	91	37	0	0	0	0	0	0	0	0
47	0	0	0	0	0	0	0	0	12	54	79	95	101	105	107	101	62	0	0	0	0	0	0	0	0
49	0	0	0	0	0	0	0	0	0	42	74	90	99	103	103	70	0	0	0	0	0	0	0	0	0
51	0	0	0	0	0	0	0	0	0	0	0	0	0	0	0	0	0	0	0	0	0	0	0	0	0
53	0	0	0	0	0	0	0	0	0	0	0	0	0	0	0	0	0	0	0	0	0	0	0	0	0

HOB	
D.P.	10
α	20°
gashes	14
O.D.	67.2
GEAR	
D.P.	10
Z_g	36
O.D.	96.5
f, mm/r	1.727
CD	5.715

b) Distribution of chip thickness over the top and side edges of tooth no. 25 in 10 D.P hob

Fig.73 EVALUATION OF CHIP THICKNESS CUT OFF BY TOP AND SIDE CUTTING EDGES OF A HOB TOOTH

Fig. 73-a shows the hob tooth dimensions and the distribution of locating points on the hob cutting tooth and along z direction, where the uncut chip thickness is to be calculated.

The relationship between uncut-chip thickness S and hob wear can be observed as shown in Fig. 73(b) where hob wear at top flank and rake face for tooth no. 25 from the centre of generation of 10 D.P. hob wear was measured, chip thickness was calculated at each of the locating points on hob tooth and along axial section of the gear z. Thus chip thickness and chip width can be evaluated methematically and related to tooth wear.

7.5 Analysis of Uncut-chip area created by top and side Cutting Edges

Based upon the method explained in ref.[3] evaluation of uncut-chip cross-section area cut off by peripheral and side edges of the hob is attempted, when axial hob feed is applied.

Fig. 74 illustrates the cutting action between a hob tooth and the gear blank at full depth of cut. A_L and A_R being chip cross section area formed by left and right hand sides of hob tooth respectively, A_T being chip cross section formed by peripheral edge. Generation of chips start from points T, P and Q at a constant generating angle, ϕ_o.

Chip generating angle, ϕ_o depends on the following parameters,

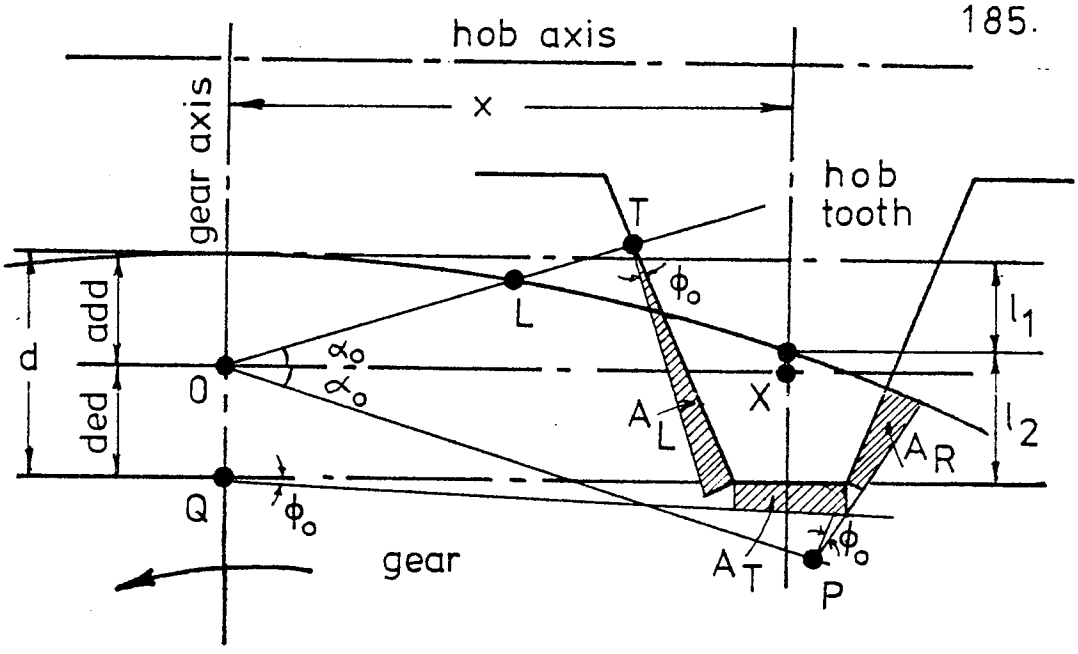

Fig.74 CROSSECTIONAL CHIP AREA CUT OFF BY TOP AND SIDE EDGES OF A HOB TOOTH

Fig.75 APPROXIMATION USED FOR CALCULATIONS

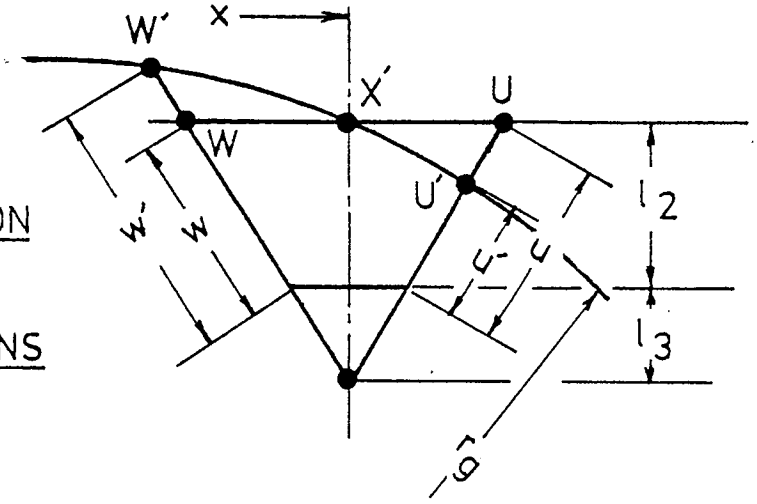

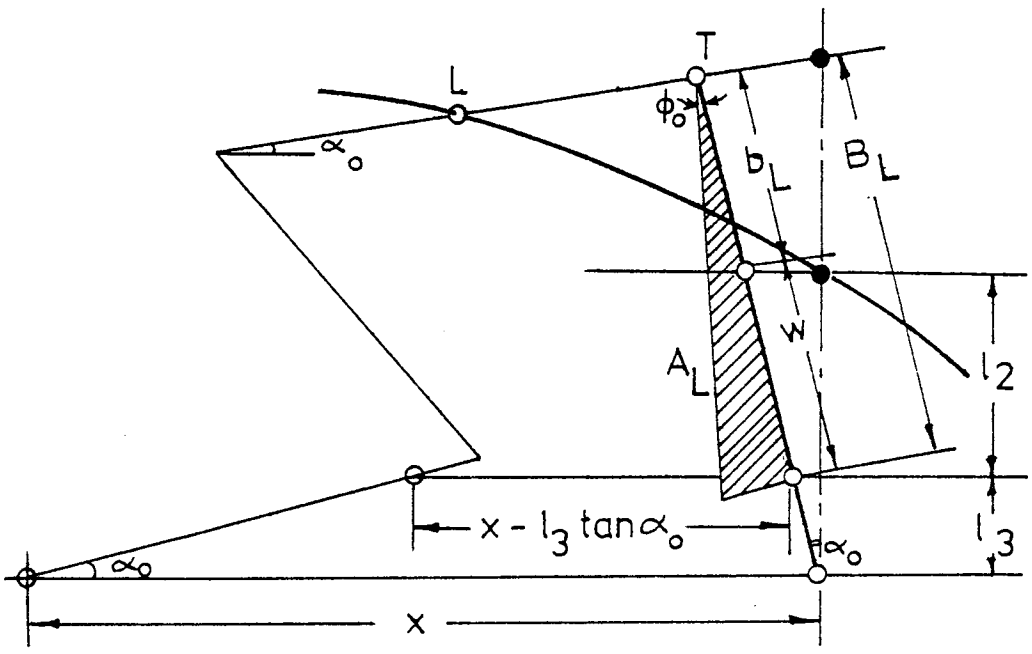

Fig.76 CHIP PRODUCED BY LEFT SIDE CUTTING EDGE

- number of teeth in the gear blank; z_g
- number of starts in the hob ; S_h
- gear module ; m
- axial feed rate; f

Honda[3] described generating angle, ϕ_o as follows:

$$\phi_o = \frac{2\pi S_h}{z_g . i} \qquad (62)$$

where, $i = \frac{m\pi}{f}$

In order to evaluate chip areas A_L, A_R and A_T cut off by left, right sides and peripheral cutting edges of the hob tooth respectively, the following approximation is considered, as seen in Fig. 75 where the hob tooth axis is located at distance (x) from gear blank centre line. As the tooth centre approaches the gear centre line, the chip area cut off by the side cutting edges tend to be equal,

Therefore,

$$U' = U = W' = W \qquad (63)$$

Under that assumption, the chip area cut off by the left hand side of the cutting edge, A_L is estimated as shown in Fig. 76 and as follows:

$$W = \ell_2 \cos\alpha \qquad (64)$$

$$d = \ell_1 + \ell_2 \qquad (65)$$

$$\ell_1 = r_g - \sqrt{r_g^2 - x^2} \qquad (66)$$

where, d is cutting depth, mm.

r_g is gear blank radius, mm.

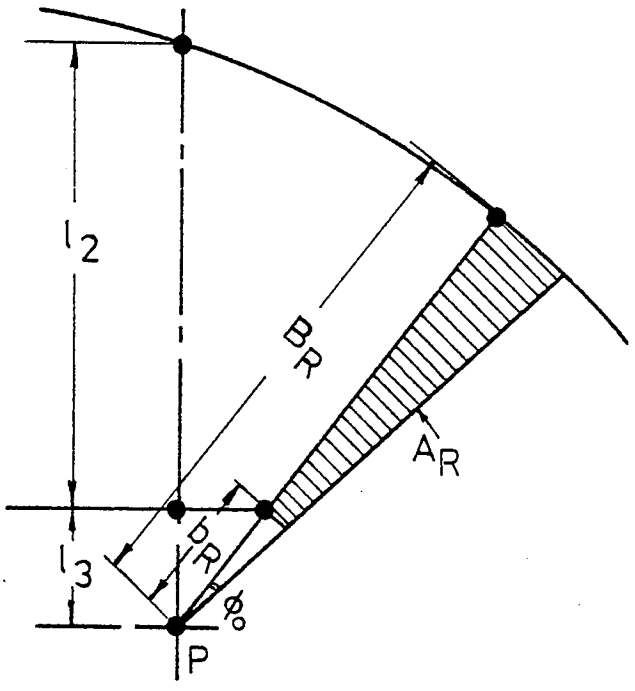

Fig.77 CHIP PRODUCED BY RIGHT SIDE EDGE

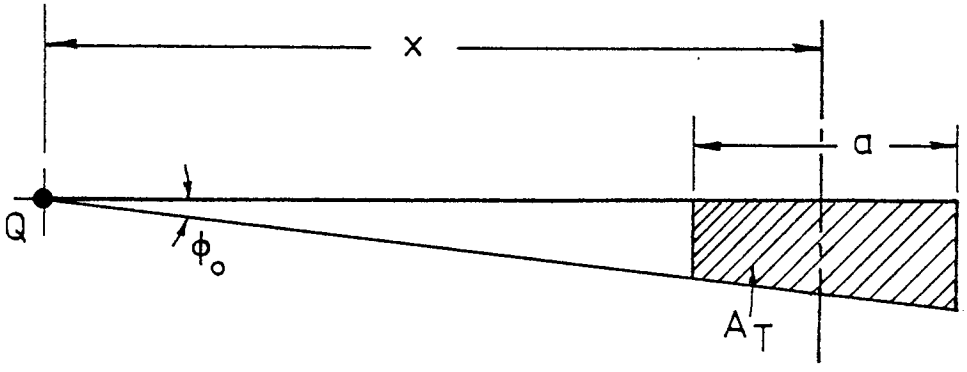

Fig.78 CHIP PRODUCED BY TOP CUTTING EDGE

x is centre distance between the cutting tooth axis and gear blank C.L.

Chip cross section A_L is then obtained as follows:

$$\left.\begin{aligned} A_L &= \tfrac{1}{2} B_L^2 \phi_o \quad , b_L \leqslant 0 \\ A_L &= \tfrac{1}{2} (B_L^2 - b_L^2) \phi_o \quad , b_L > 0 \end{aligned}\right\} \qquad (67)$$

where,

$$B_L = \text{ded.}/\cos\alpha + (x - \tfrac{a}{2}) \sin\alpha$$

$$b_L = B_L - W = (x - \tfrac{a}{2}) \sin\alpha + \text{ded.}/\cos\alpha - \\ - \iota_2/\cos\alpha .$$

a is width of peripheral cutting edge, mm.

b_L, B_L, ι_1 , ι_2 , ι_3 , and W are lengths shown in Fig. 76.

Chip area cut off by the right hand side of the hob cutting edge, A_R is obtained in a similar manner as shown in Fig. 77 and as follows:

$$\left.\begin{aligned} A_R &= \tfrac{1}{2} B_R^2 \phi_o \quad , b_R \leqslant 0 \\ A_R &= \tfrac{1}{2} (B_R^2 - b_R^2) \phi_o \quad , b_R > 0 \end{aligned}\right\} \qquad (68)$$

where,

$$b_R = (x + \tfrac{a}{2}) \sin\alpha - \text{ded}/\cos\alpha$$

$$B_R = b_R + W$$

$$= (x + \tfrac{a}{2}) \sin\alpha - \text{ded}/\cos\alpha + \iota_2/\cos\alpha.$$

Chip area cut off by peripheral cutting edge A_T is obtained as shown in Fig. 78 and as follows:

a) chip cross-section area cut off by 10 DP hob.

(A), mm^2

x, mm	1	3	5	7	9	11	13	15	17	19	21	23	25
A_L	0.18	0.22	0.27	0.31	0.37	0.45	0.52	0.59	0.66	0.69	0.63	0.53	0.24
A_R	0.32	0.40	0.42	0.49	0.55	0.60	0.62	0.61	0.55	0.49	0.37	0.25	0.11
A_T	0.07	0.21	0.34	0.48	0.62	0.76	0.89	1.03	1.17	1.31	1.45	1.42	0.50
ΣA^t	0.57	0.83	1.04	1.28	1.55	1.81	2.03	2.23	2.38	2.49	2.46	2.20	0.85

† $\Sigma A = A_L + A_R + A_T$

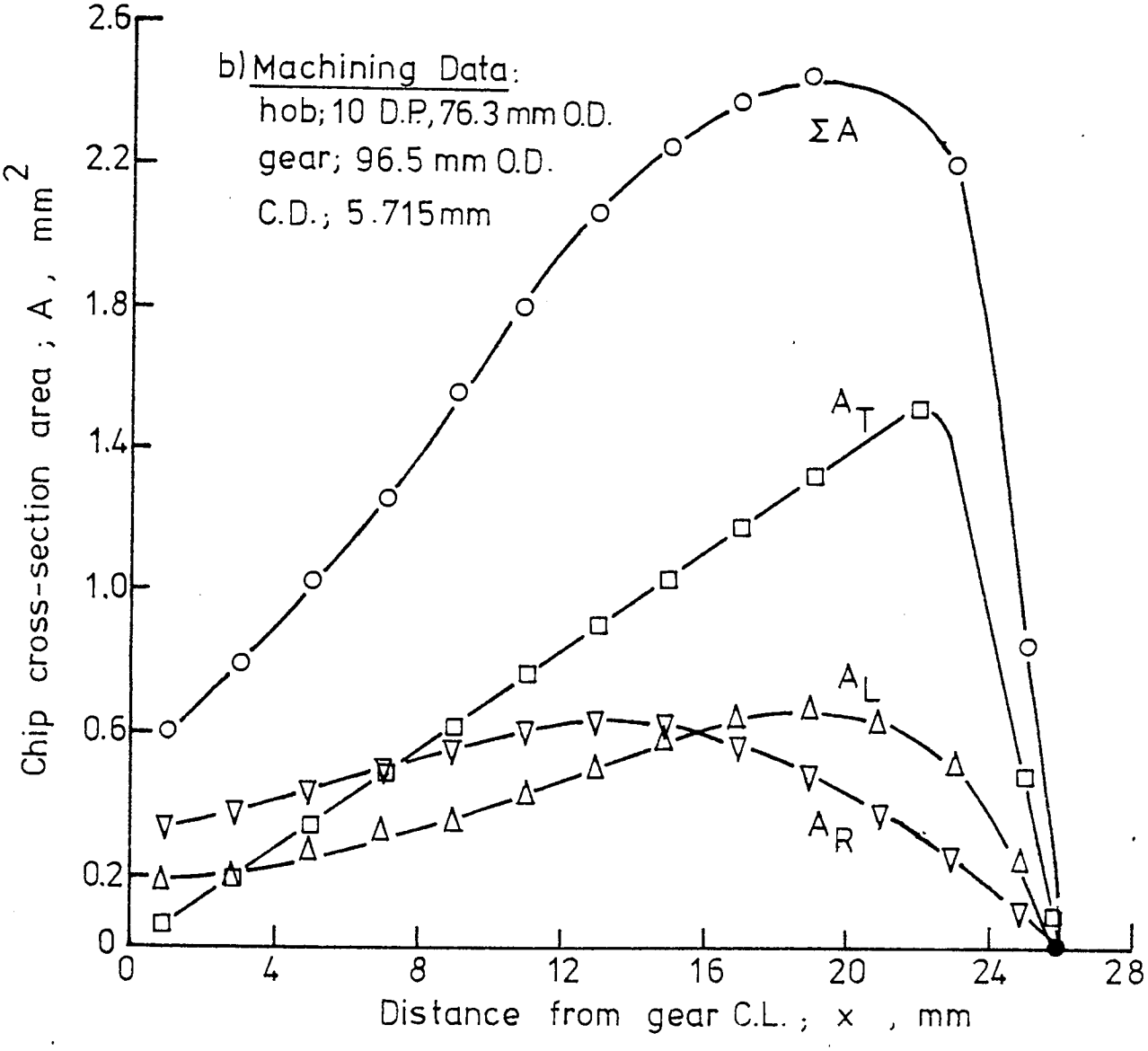

Fig. 79 DISTRIBUTION OF CROSSECTION AREA OF CUT OVER THE DISTANCE FROM GEAR C.L.

$$A_T = \frac{(x + \frac{a}{2})^2}{2} \phi_o - \frac{(x-\frac{a}{2})^2}{2} \phi_o \qquad (69)$$

ϕ_o being very small, therefore,

$$A_T \simeq a \cdot x \cdot \phi_o \qquad (70)$$

It is possible to calculate chip cross section area cut off by both sides and peripheral cutting edges of the hob, by solving Eqs. (67), (68) and (70).

Taking for example the hob-gear dimensions together with cutting conditions represented in Table 21, chip areas A_L, A_R and A_T were calculated at a variable distance (x) from the centre of the blank, and presented in Fig. 79(a).

Fig. 79(b) shows the distribution of chip cross-section area cut off by sides and peripheral edges over the central distance x.

From Fig. 79 it is observed that ship area cut off by both sides of the hob edges are equal, and chip area cut off by the peripheral edge is larger than that cut off by either side edge, over the distance covered.

7.5.1 Ratio of work on side edges

The mean chip thickness cut off by side edges can be approximately determined using the following consideration; if one side edge removes, according to Fig. 59, only 20 per cent of the chip volume and the peripheral edge removes 60 percent of that, and the number of cuts are equal for both, then the chip thickness on the side edge is approximately three times smaller than that on the peripheral edge and has consequantly the value about 0.01-0.02 mm.

7.5.2 Variation of chip width and thickness during hob rotation

Chip thickness and width take different values during hob rotation, in order to estimate the variation of chip area cut off by both sides and peripheral hob edges at any angle θ, during hob rotation, the basic fundamentals of chip formation in cylindrical milling is taken as a basis for comparison and analysis.

Fig. 80(a) shows the transformation in chip cross-section area during rotation of the milling cutter, chip area A_r was taken when the cutter rotated angle θ. The maximum chip cross section area is produced when the cutter rotates at an angle equal to θ_{max} as shown in Fig. 80(b), and is estimated as follows:

$$A_a = a.d$$

$$A_r = h.a \simeq f.\theta \ . \ a$$

$$A_{r\ max} = h_{max}.a \simeq f.\ \theta_{max}.\ a$$

$$= a.f.\ \sqrt{\frac{2a}{r_c}} \qquad (71)$$

where, a is width of the cutter

d is depth of cut

h is chip thickness at angle θ

θ is cutter angle of rotation

r_c is cutter outside radius

f is feed rate

$A_{r\ max}$ is chip area produced at angle θ_{max}.

The variation in chip area during the hob rotation is similar to the variation in cylindrical milling, and therefore, the

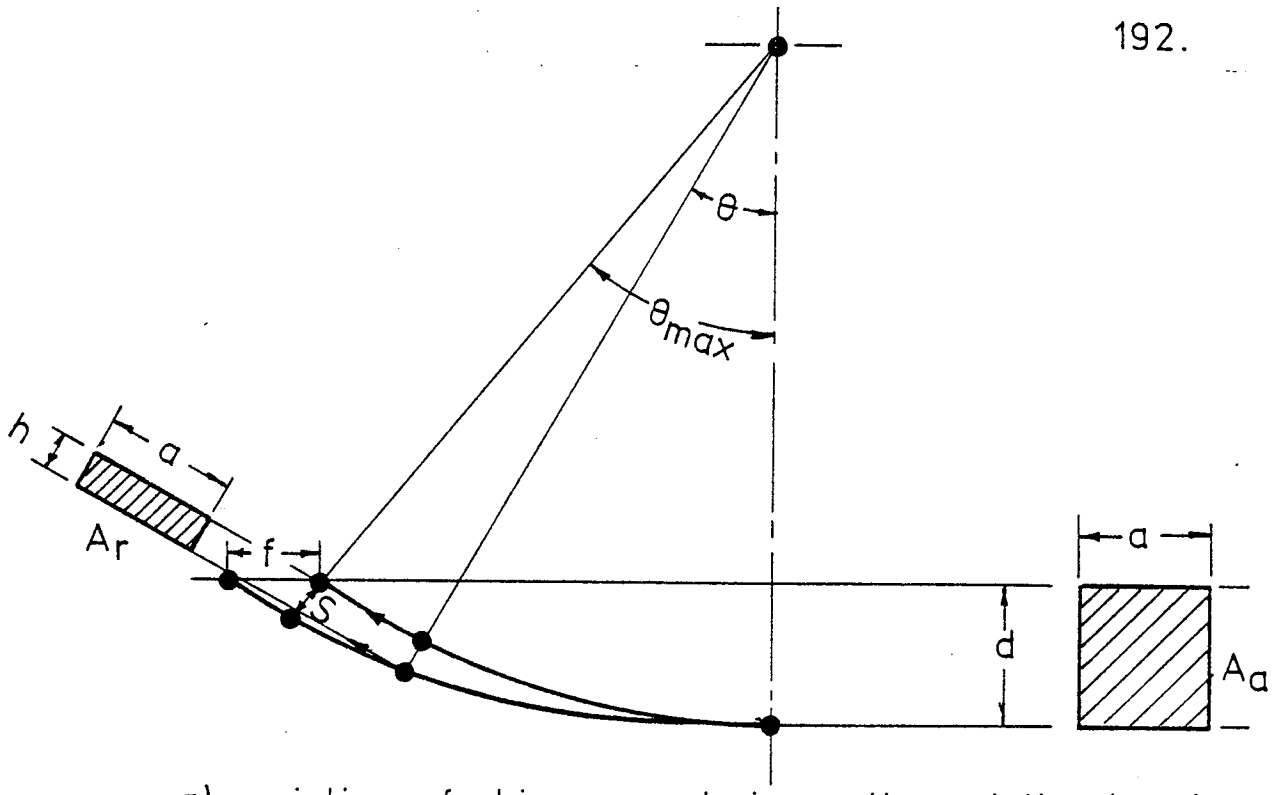

a) variation of chip area during cutter rotation in milling

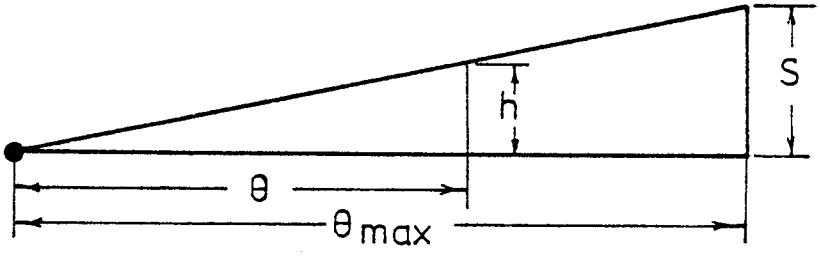

b) variation of chip thickness with angle of rotation

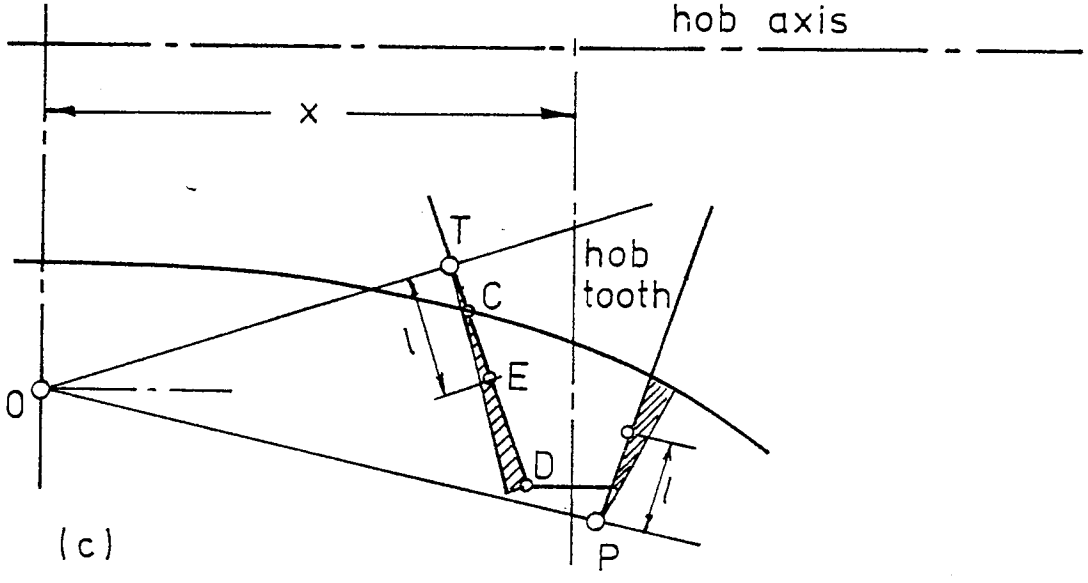

Fig.80 CHIP FORMATION IN CYLINDRICAL MILLING AND HOBBING

analysis will take a similar approach.

Fig. 80(c) shows a hob tooth engaged at full depth of cut with a gear blank. E is a selected point on the hob side edge at distance ι from chip generating point T, where:

$$\overline{TE} \cdot \phi_o = \iota \cdot \phi_o \tag{72}$$

Maximum chip thickness at point E is derived as follows:

$$S_\iota = f \cdot \Theta$$

$$\Theta_\iota = \sqrt{\frac{2\iota\phi_o/\sin\alpha}{r_\iota}}$$

$$= \sqrt{\frac{2\iota\phi_o}{r_\iota \cdot \sin\alpha}} \tag{73}$$

Therefore,

$$S_{\iota\ max} = f \cdot \sqrt{\frac{2\iota\phi_o}{r_\iota \cdot \sin\alpha}} \tag{74}$$

where, Θ_ι is hob angle of rotation at point E

r_ι is hob radius at point E

S_ι is chip thickness produced at point E

Maximum chip thickness at point C is obtained as follows:

$$S_{bL} = f \cdot \Theta$$

$$\Theta_{bL\ max} = \sqrt{\frac{2\,b_L \cdot \phi_o}{r_c \cdot \sin\alpha}}$$

$$S_{bL\ max} = f \cdot \sqrt{\frac{2\,bL\ \phi o}{r_c \cdot \sin\alpha}} \tag{75}$$

where, S_{bL} is chip thickness cut off at point C.

Similarly, maximum chip thickness at point D is obtained as follows:

$$S_{BL} = f.\theta$$

$$\theta_{BL\ max} = \sqrt{\frac{2\ BL.\ \phi\ o}{r_D.\ \sin\ \alpha}}$$

$$S_{BL\ max} = f\sqrt{\frac{2\ BL.\ \phi_o}{r_D.\ \sin\alpha}} \qquad (76)$$

where, r_C and r_D are hob radii at points C and D respectively

b_L and B_L are distances from point T as shown in Fig.76

Maximum angle of rotation, θ_{max} increases along the cutting line under the following condition:

$$\theta_{bL\ max} < \theta_{l\ max} < \theta_{BL\ max} \qquad (77)$$

It is possible now under condition (77) to estimate the values of A_L, A_R and A_T, the chip areas cut off by left and right hand sides and peripheral edges of the hob tooth respectively at any angle θ , as follows:

When $\theta \leqslant \theta_{bL\ max}$.

$$A_L = \int_{b_L}^{BL} S_l \ .\ dl\ .\ \sin\alpha$$

$$= (B_L - b_L)\ \sin\alpha\ .\ f.\ \theta \qquad (78)$$

and when $\theta > \theta_{bL\ max}$

$$A_L = \int_{l}^{BL} S_l \ .\ dl\ \sin\alpha$$

$$= (B_L - l)\ \sin\alpha\ .\ f.\ \theta \qquad (79)$$

By substituting the value of Θ in Eq. (73), therefore

$$\Theta = \sqrt{\frac{2\, l\, \phi_o}{r_l \,.\, \sin\alpha}} \quad ,$$

$$l = \frac{r_l \sin\alpha}{2\phi_o} \,.\, \Theta^2$$

and

$$A_L = (B_L - \frac{r_l \,.\, \sin\alpha}{2\,\phi_o} \,.\, \Theta^2)\,.\, f.\,\Theta \sin\alpha \qquad (80)$$

Thus a general expression of chip area A_L is obtained in terms of angle of hob rotation Θ.

Similarly, chip area cut off by right hand side of hob cutting edge, A_R is obtained as follows:

when $\Theta \leqslant \Theta_{bR}$

$$A_R = (B_R - b_R) \sin\alpha \,.\, f. \,\Theta \qquad (81)$$

and when $\Theta > \Theta_{bR}$

$$A_R = (B_R - \frac{r_l \sin\alpha}{2\,\phi_o} \,.\, \Theta^2)\,.\, f.\,\Theta \sin\alpha \qquad (82)$$

where, b_R and B_R are distances from point P as shown in Fig. 77.

The general expression for variation of chip area cut off by peripheral edge, A_T with angle of hob rotation is obtained as follows:

$$\Theta_{D\ max} = \sqrt{\frac{2x\ \phi_o}{r_h}}$$

and

$$S_{D\ max} = f.\sqrt{\frac{2x\ \phi_o}{r_h}}$$

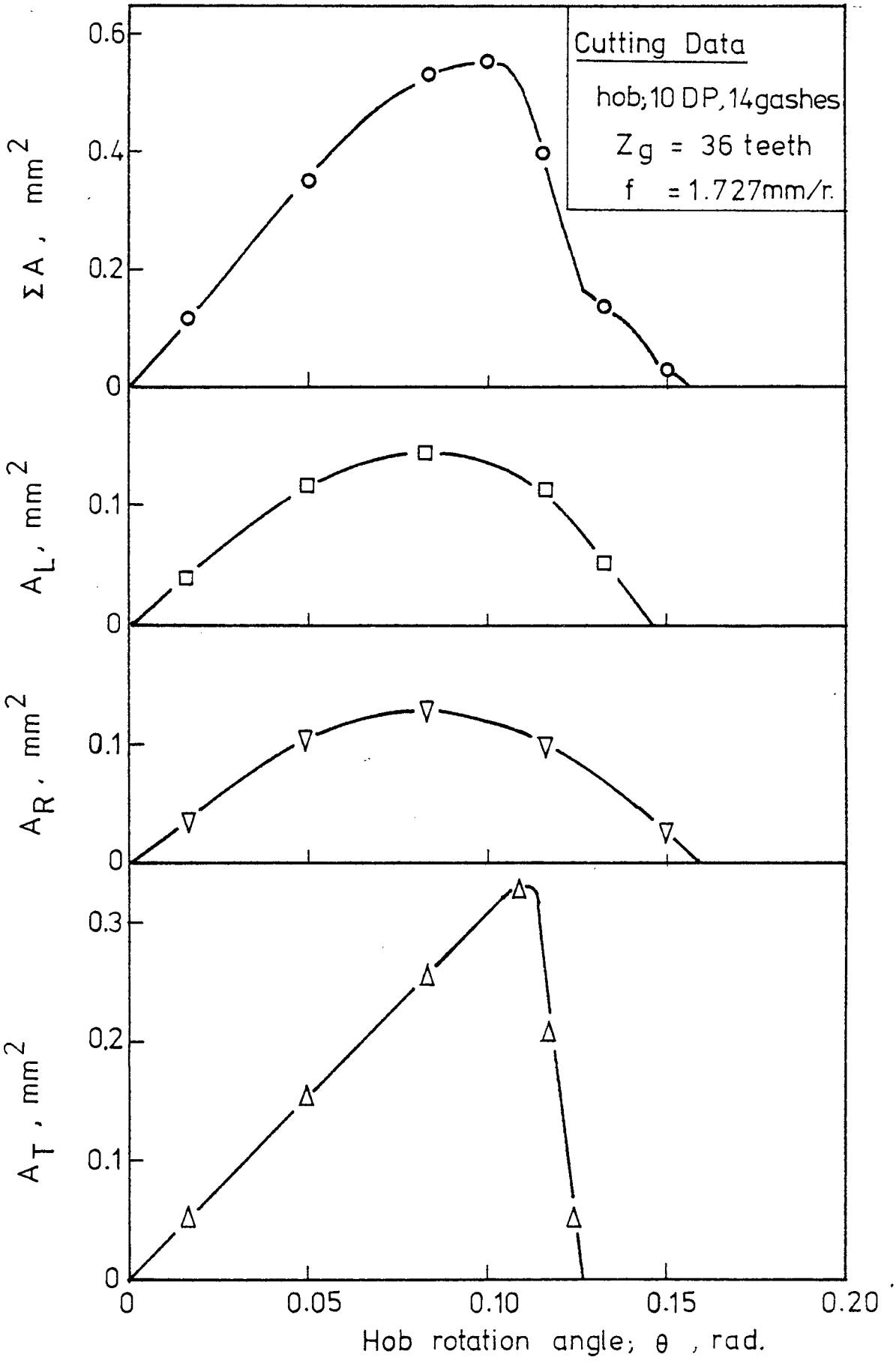

Fig. 81 VARIATION OF CHIP CROSSECTIONAL AREA WITH HOB ROTATION ANGLE

Therefore, $A_T = S_D.a = a.f.\theta$ (83)

where, x is distance between hob tooth axis and gear blank C.L.

a is hob tooth peripheral width

r_h is hob outside radius

An example for the variation of chip cross sectional area cut off by sides and peripheral edges of the hob tooth is shown in Fig. 81. Machining conditions and gear blank-hob specifications are obtained from Table 21. It is clear from the figure that chip area cut off by peripheral edges increases linearly with the increase of angle of hob rotation, it is also observed that chip areas cut off by side edges are approximately equal during the hob rotation. The peak value of chip area cut off by peripheral hob edges is much greater than those cut off by side edges.

7.5.3 Experimental method to evaluate chip surface area

In this experiment, it was decided to measure the surface area of chips cut off by sides and peripheral hob edges. In order to make accurate and efficient measurements, a wax blank was machined on the hobbing machine under the following machining conditions,

Axial feed rate ; 1.987 mm/rev.

Hob details; 8D.P.; S.S.R.H.; 12 gashes

Wax blank ; spur, 29 teeth; 984 mm. O.D.

7.112 mm. C.D.

Chips have been collected, then unfolded, the surface area of chips cut off by sides and peripheral hob teeth were measured

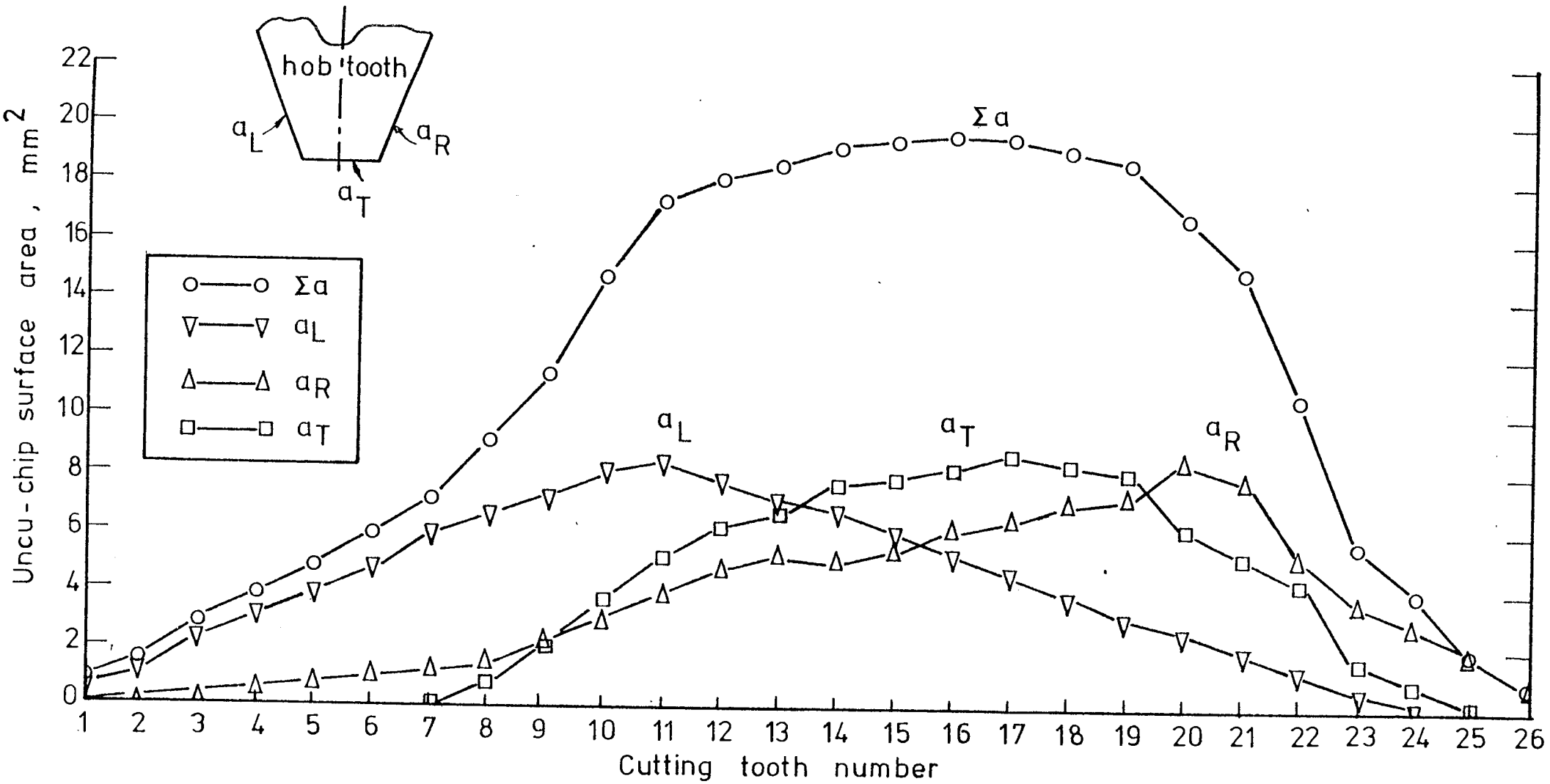

Machining Data:

hob; 8 D.P., 12 gashes
blank; wax, 29 teeth
f = 1.987 mm/rev

Fig. 82 DISTRIBUTION OF CHIP SURFACE AREA CUT OFF BY SIDES AND PERIPHERAL HOB EDGES

and plotted against each cutting tooth. Fig. 82 shows the distribution of chip surface area over the hob cutting teeth in action; tooth number starts from centre of generation. It is clear from the figure that mean chip surface area cut off by both side edges is equal, also the mean chip surface area cut off by peripheral edges is approximately equal to that cut off by each side edge.
These observations are in good agreement with the results obtained by previous researches.

7.6 Summary and Conclusions

Fundamental distinction was found between the work of peripheral cutting edges of the hob and work of edges cutting the flanks of the gear blank teeth.

Peripheral edges cut off a major part of the gear blank material and side edges merely shape the flanks. The severity of cutting works may be evaluated by the product (L x S) It has been noticed that hob wears most at the working portion where the product LxS is largest.

From the previous analysis, the following conclusions can be drawn:

1. Increasing axial feed resulted in an increase in mean chip thickness, and an increase in blank diameter resulted in a decrease in mean chip thickness.
2. The influence of chip thickness cut off by hob peripheral edges on stability is not significant, and stability decreases with the increase in feed rate because chip thickness on side edges will increase.
3. The problem of hob gashes design is important, where it reduces fluctuation of the cutting forces.

4. Chip cross section-area cut off by both sides of the hob edges are equal, and chip area cut off by the peripheral edge is larger than that cut off by either side edge.

5. Mean chip surface area cut off by both side edges are equal, also mean chip surface area cut off by peripheral edges is approximately equal to that cut off by each side edge.

CHAPTER VIII

TOOL WEAR AND TOOL LIFE IN GEAR HOBBING

8.1 Introduction

Tool-life is an important parameter in assessing manufacturing costs in metal cutting operations. It has a direct influence on the physical operation of the plant as well as on the economics and profitability of cutting.

In recent years, the number of people involved with the development and evaluation of improved cutting tool materials has grown considerably. But very little work was done in the field of gear hobbing, and mainly in Japan and the U.S.S.R.

The purpose of this section is to discuss wear mechanism in hobbing, to study the effect of cutting parameters on hob life and to establish a generalised mathematical model to describe tool life in terms of six independent cutting parameters covering a wide range of cutting conditions.

8.1.1 Description of tool-wear

The practical consequences of tool-wear, vary from both cutting conditions and the quality specifications of the material being machined. As a result, "Tool-life" will have different meanings in different contexts, and "wear-rate" will have different meanings for different people.

8.1.2 Tool-wear in hobbing

Fig. 83 shows schematically the wear on a typical hob, it is noted that all of the wear zones do not always appear,

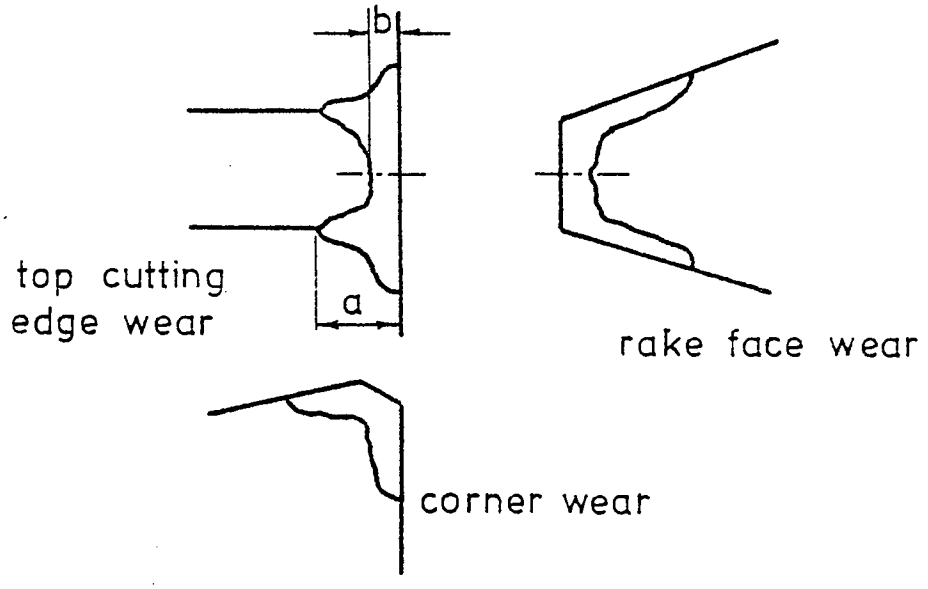

Fig.83 GEOMETRY OF HOB WEAR

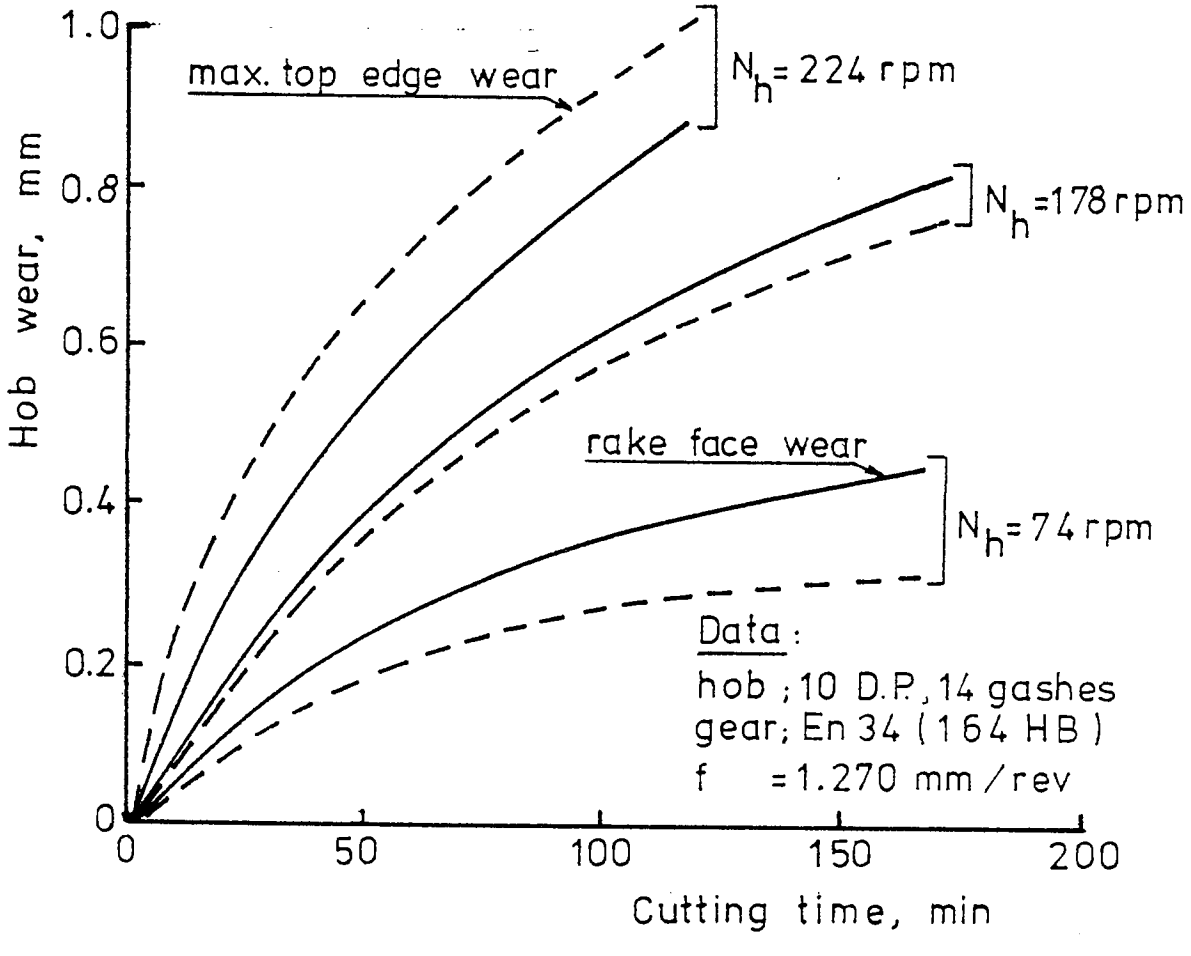

Fig.84 HOB WEAR AS A FUNCTION OF SPEED

and frequently one will predominate. The three general wear zones are as follows:

1. Top cutting edge wear; appears at the top edges of hob teeth and is more or less uniform wear zone. Under high speed conditions, the top edge wear predominates. Measurement of wear in this zone can take two values, maximum width (a) or the value of wear width (b) at the centre.

2. Rake face wear; appears at the top and sides of the tooth face, which forms where one would normally expect most wear due to the high contact stresses and high interface temperature. Under low cutting speed conditions, rake face wear predominates as seen in Fig. 84, and can be easily measured optically in terms of maximum width at the centre.

3. Corner wear; forms on corner edge of the hob teeth. The wear here is partially a continuation of the top edge wear around the corners.

Wear on top cutting edge and rake face are usually observed, but sudden wear may occur on the corner edges of the the tooth as described in reference [31].

8.2 Tool-life Criteria

Unlike turning, gears are cut in hobbing by means of form tools. The types of wear that can develop was discussed. Now the question is, what are the consequences of this wear? From a functional point of view, a tool can be kept in service so long as it continues to produce "satisfactory" parts. However, it may be removed earlier due to system economic conditions.

In order to discuss the principle tool life criteria and the manner in which they depend upon the various wear zones,

Fig. 84 shows a set of typical wear at the top cutting edges and rake face of a hob versus time curves for 10 D.P. hob cutting En 34 steel blanks, it is clear that at lower hob speeds, the top edge wear becomes negligible relative to the rake face wear, while at higher hob speeds both the top edge and rake face wear rates will increase. However, the top edge wear rate would grow faster, and become predominant.

In order to determine a suitable tool-life criteria for gear hobbing, it is essential to consider the following:

a) Tool Failure

A tool is considered "failed" when it either will not cut, or cuts in a manner much different from a sharp tool. Normally, total failure is considered a tool life criterion when surface finish and tolerance are not important, but in the case of gear cutting, tolerance as well as gear tooth profile are of great importance. Therefore tool failure must have a different criterion in gear cutting.

b) Amount of chip removed

In the previous chapter, a fundamental distinction was found between the work of the peripheral cutting edges and the side edges of the hob. Peripheral edges cut off a major part of the blank material which was estimated at 60% while the side edges merely shape the flanks.

c) Gear dimensional tolerance

It is essential that the hob must be removed from service, while it is cutting perfectly well, because the gears produced are out of tolerance and the hob cannot be adjusted.

This obviously can occur long before the hob "fails". The degree of tolerance degradation clearly is associated with the wear on the sides and peripheral edges.

d) Surface finish

Modern gear production has been developed to a remarkably high degree of accuracy and yet difficulty is still experienced in obtaining the quality required by present standards. It is still necessary therefore for further finishing operations to be carried out to refine the errors. On finishing cuts, the determination of surface finish and gear tooth profile can determine the useful tool-life; poor surface finish may be associated with the wear zones.

e) Economic considerations

It is advisable for economic considerations that the hob should be removed from service before any of the wear zones appear, and that depends on an estimate of the average cost per cutting edge over the life of the tool[30]. If a tool is removed from service early, the number of reground times will increase, especially when top edge wear occurs in large amounts.

f) The nature of hob wear

The shape and dimensions of tooth wear vary from tooth to tooth on the hob and depends strongly on the cutting parameters. The tooth tip having the largest L x S product undergoes the greatest failure.

In an experiment to observe wear zones on the hob teeth, En 16T alloy steel blanks were cut under the following cutting conditions:

axial feed rate, f; 1.270 and 1.987 mm/rev

hob speed, N_h; 74 and 224 r.p.m.

depth of cut, d; 7.00 mm

blank specifications; 269 HB, width 35.4 mm, 29 teeth.

hob specifications; 8 D.P., 12 gashes, 748 mm O.D.

The width of wear land at the centre and corners of the flank of the top cutting edge as well as the centre of the rake face, were measured using a micrometer microscope.

Figs. 85 and 86 show the rake face wear and top edge wear on 8 D.P. hob.

Fig. 87 shows the shape and dimensions of wear at the centre and corners of the top cutting edges and the centre of the rake face of the hob cutting teeth at the cutting speed of 74 r.p.m. The distribution of the three types of wear over hob cutting teeth is observed in Fig. 88. It is clear from the figures that rake face wear predominates at the low speed of 74 r.p.m., maximum rake face wear and maximum wear at centre and corners of the top cutting edge occurred at the same cutting tooth.

Fig. 89 shows the shape and dimensions of hob wear zones at the relatively high speed of 224 r.p.m., from which the variation of wear along the hob teeth is shown in Fig. 90. It follows that the values of maximum wear at the corners of the top cutting edge is much greater than the maximum value of rake face wear and wear at the centre of the top cutting edge. Although it may be too early to draw a conclusion from the results of this experiment alone, the wear at the corner edges varied with even the slightest difference in rounding

Fig. 85 RAKE FACE WEAR OF 10 DP HOB EDGES

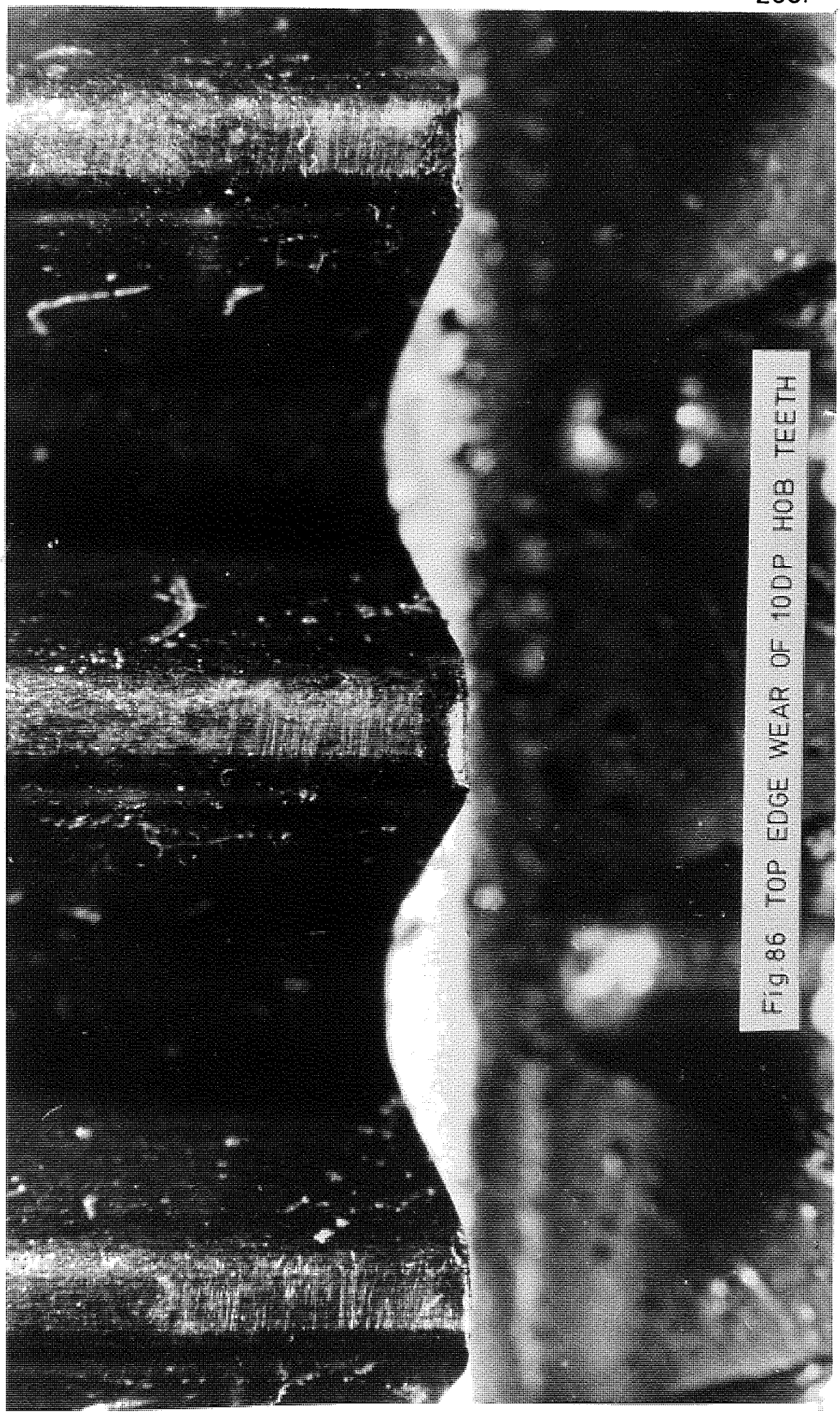

Fig 86 TOP EDGE WEAR OF 10DP HOB TEETH

and it is difficult to obtain steady values, while rake face wear appeared to be more uniform and consistant for the range of cutting conditions covered.

For the previous considerations and for the following experiments where due to the machine limitations, low to medium range of cutting speeds are employed. Therefore rake face wear at the centre of the top cutting edge was mainly used for estimating tool-life. Tool-life criteria was taken as the maximum width of wear of 1.00 mm.

8.3 Calculation of gear cutting time

The following relation gives the cutting time for hobbing spur gears at full depth of cut

$$\text{Time taken "T"} = \left(\frac{b'}{f}\right) \cdot \left(\frac{Z_g}{S_h}\right) \cdot \left(\frac{1}{N_h}\right) \quad \text{min} \qquad (84)$$

where, b' is total distance travelled by the hob and is given as follows:

b' = face width of the gear + overtravel and approach

f is axial feed rate, mm/rev.

Z_g is number of teeth in the gear

S_h is number of starts in the hob

N_h is hob speed, r.p.m.

The approach distance obviously varies with the depth of cut and hob diameter.

8.4 Preliminary Cutting Tests

After consideration of the general problem and examination of some specific machining line, a preliminary

investigation was undertaken to find out and test the significance of the effect of cutting parameters on tool-life.

A HV-14 "SYKES" Universal hobbing machine has been employed in carrying out these tests for cutting spur gears under conventional hobbing practice.

8.4.1 Experimental Design

It was decided to investigate the variation in tool-life under a wide range of machining conditions.

Upon this decision and to keep the experiment as simple as possible, preliminary tests were carried out with 10 D.P. hob. In the experiment, a combinational arrangement of five cutting parameters were selected as follows:

axial feed rate, f ; 0.609 and 2.286 mm/rev.

cutting speed, N_h ; 74, 115 and 178 r.p.m.

or V ; 15.6, 24.3 and 37.6 m/min

depth of cut, d ; 5.45 and 4.762 mm

blank material ; En 34 (164 HB), En 8 (183 HB) and En 16T (269 HB)

number of teeth in the blank, Z_g; 36 and 29 teeth

8.4.2 Results and Discussion

The obtained tool-life results for the analysis of variance are represented in Table 22 according to a 3x2x2x2x3 non-factorial design of experiment where tool-life, T is measured in minutes.

Figs. 91 and 93 represent some of the tabulated results when cutting spur gears of three different types of

TABLE 22

TOOL LIFE DATA FOR ANALYSIS OF VARIANCE

Machining Data: hob, 10D.P.,S.S.R.H.,14 gashes

Cutting speed V, m/min	Axial feed f, mm/rev	No. of teeth, Zg	Depth of cut, d=5.45 mm			Depth of cut, d=4.76 mm		
			En 34	En 8	En16T	En 34	En 8	En16T
V_1=15.6	f_1=0.609	Z_1=36	485	254	28	510	275	31
		Z_2=29	458	240	27	484	261	30
	f_2=2.286	Z_1=36	372	200	20	400	219	24
		Z_2=29	355	192	19	382	208	23
V_2=24.3	f_1=0.609	Z_1=36	259	79	9	265	86	10
		Z_2=29	245	73	8	252	82	10
	f_2=2.286	Z_1=36	118	65	6	126	70	7
		Z_2=29	112	62	6	120	67	7
V_3=37.6	f_1=0.609	Z_1=36	49	26	3	51	28	3
		Z_2=29	45	24	3	48	26	2
	f_2=2.286	Z_1=36	40	19	2	41	21	2
		Z_2=29	38	18	2	38	20	2

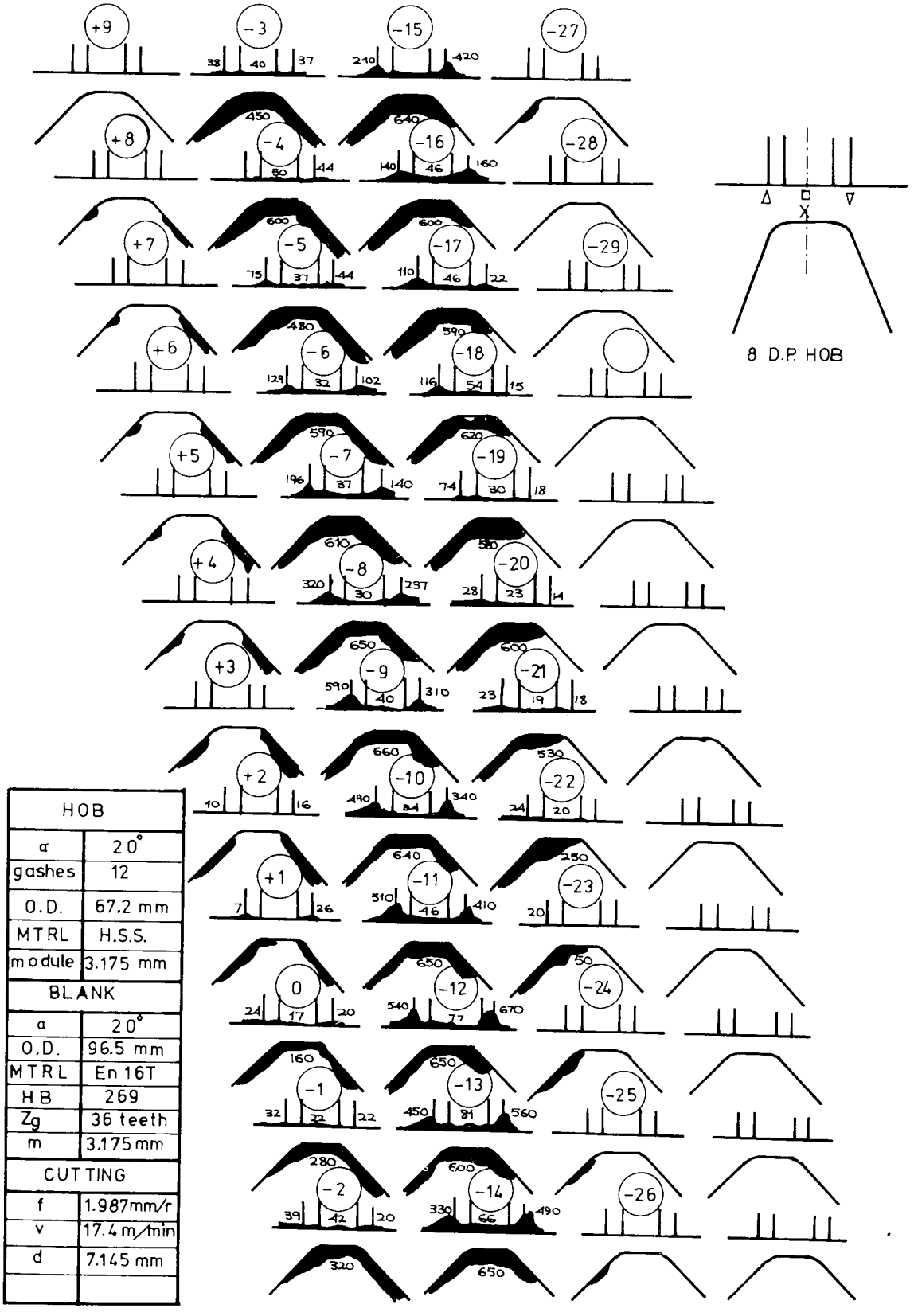

HOB	
α	20°
gashes	12
O.D.	67.2 mm
MTRL	H.S.S.
module	3.175 mm
BLANK	
α	20°
O.D.	96.5 mm
MTRL	En 16T
HB	269
Z_g	36 teeth
m	3.175 mm
CUTTING	
f	1.987 mm/r
v	17.4 m/min
d	7.145 mm

Fig. 87 HOB WEAR AT LOW SPEED

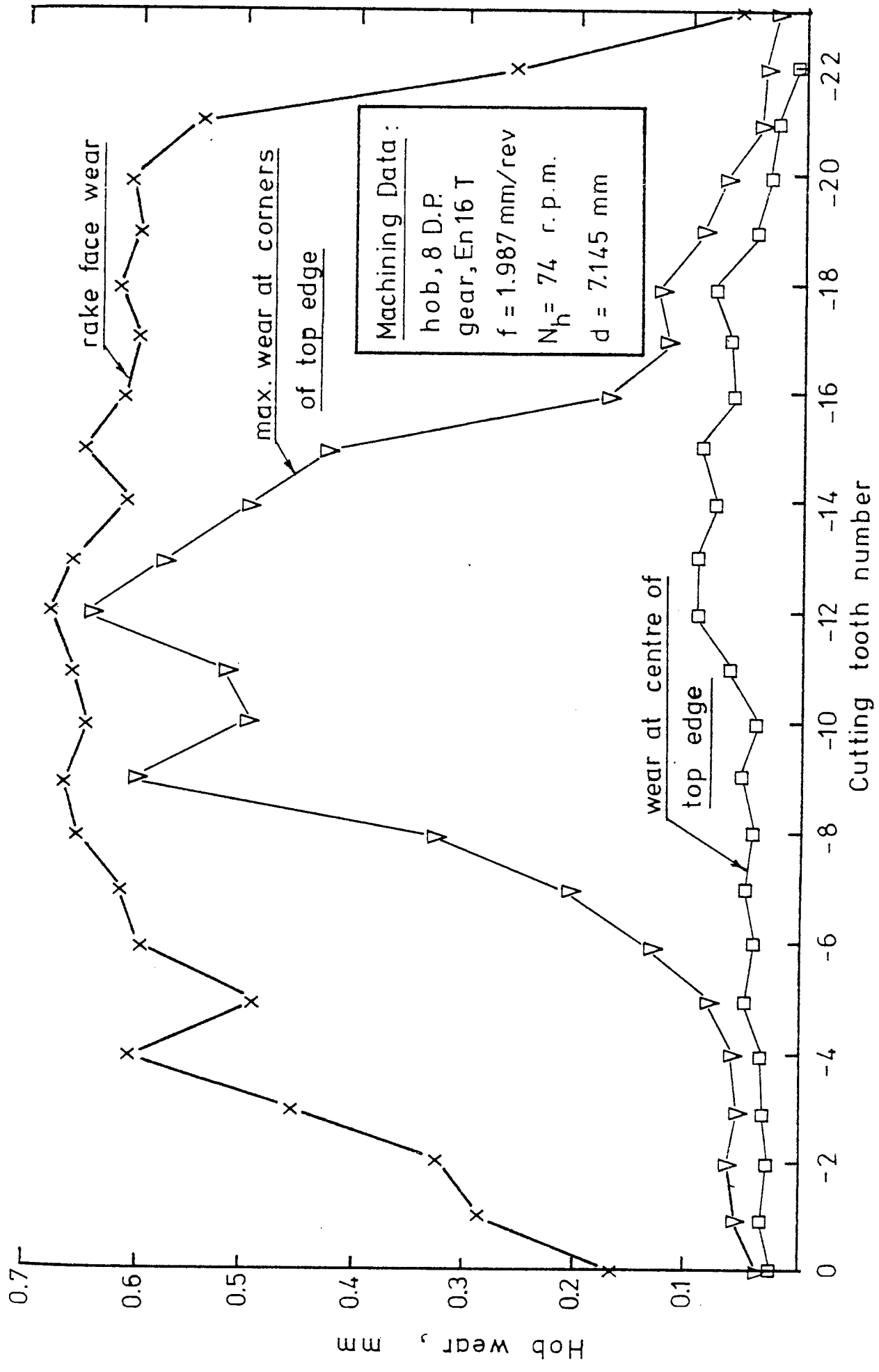

Fig. 88 DISTRIBUTION OF HOB WEAR AT LOW SPEED

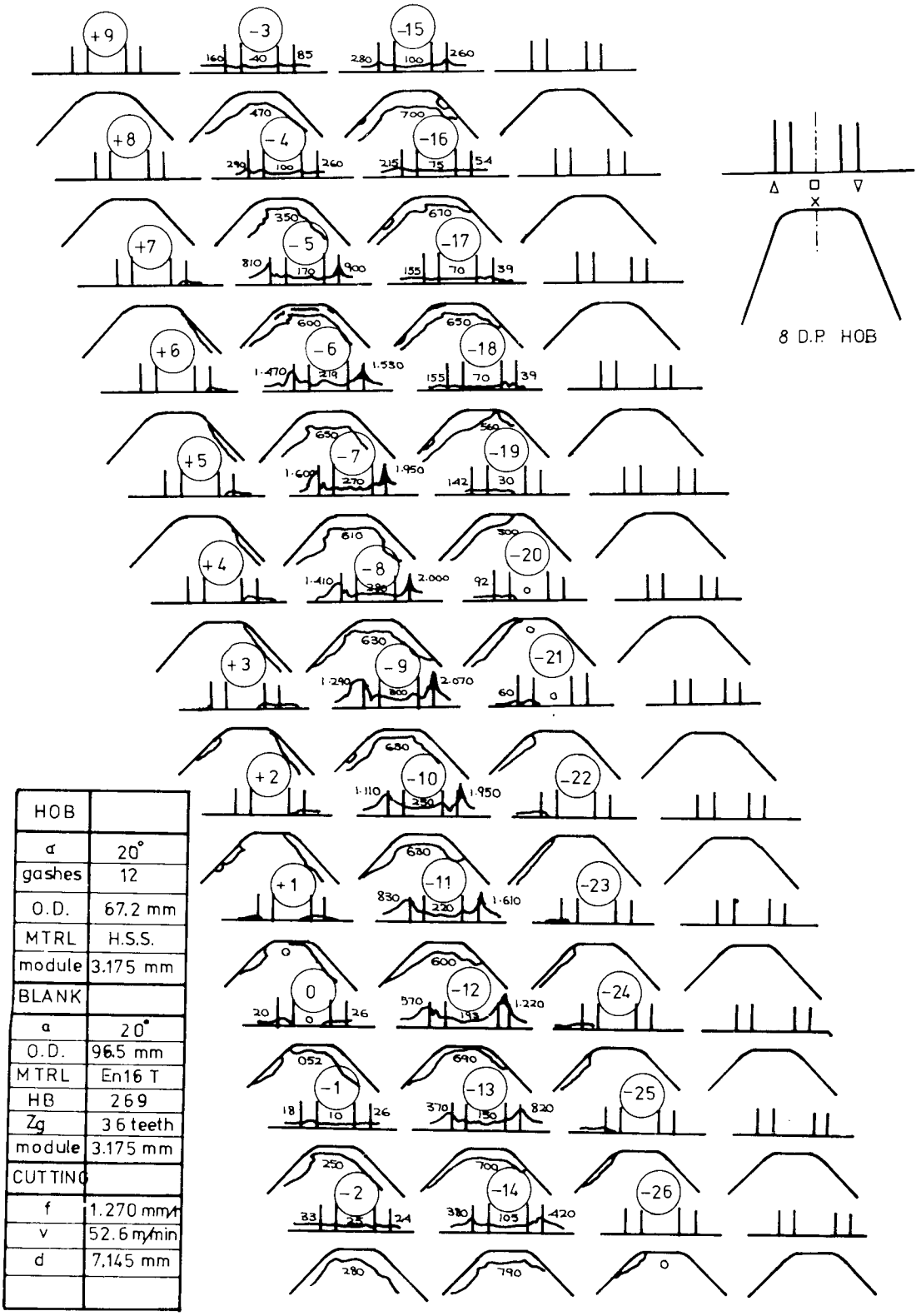

HOB	
α	20°
gashes	12
O.D.	67.2 mm
MTRL	H.S.S.
module	3.175 mm
BLANK	
α	20°
O.D.	96.5 mm
MTRL	En16 T
HB	269
Zg	36 teeth
module	3.175 mm
CUTTING	
f	1.270 mm/r
v	52.6 m/min
d	7.145 mm

Fig. 89 HOB WEAR AT HIGH SPEED

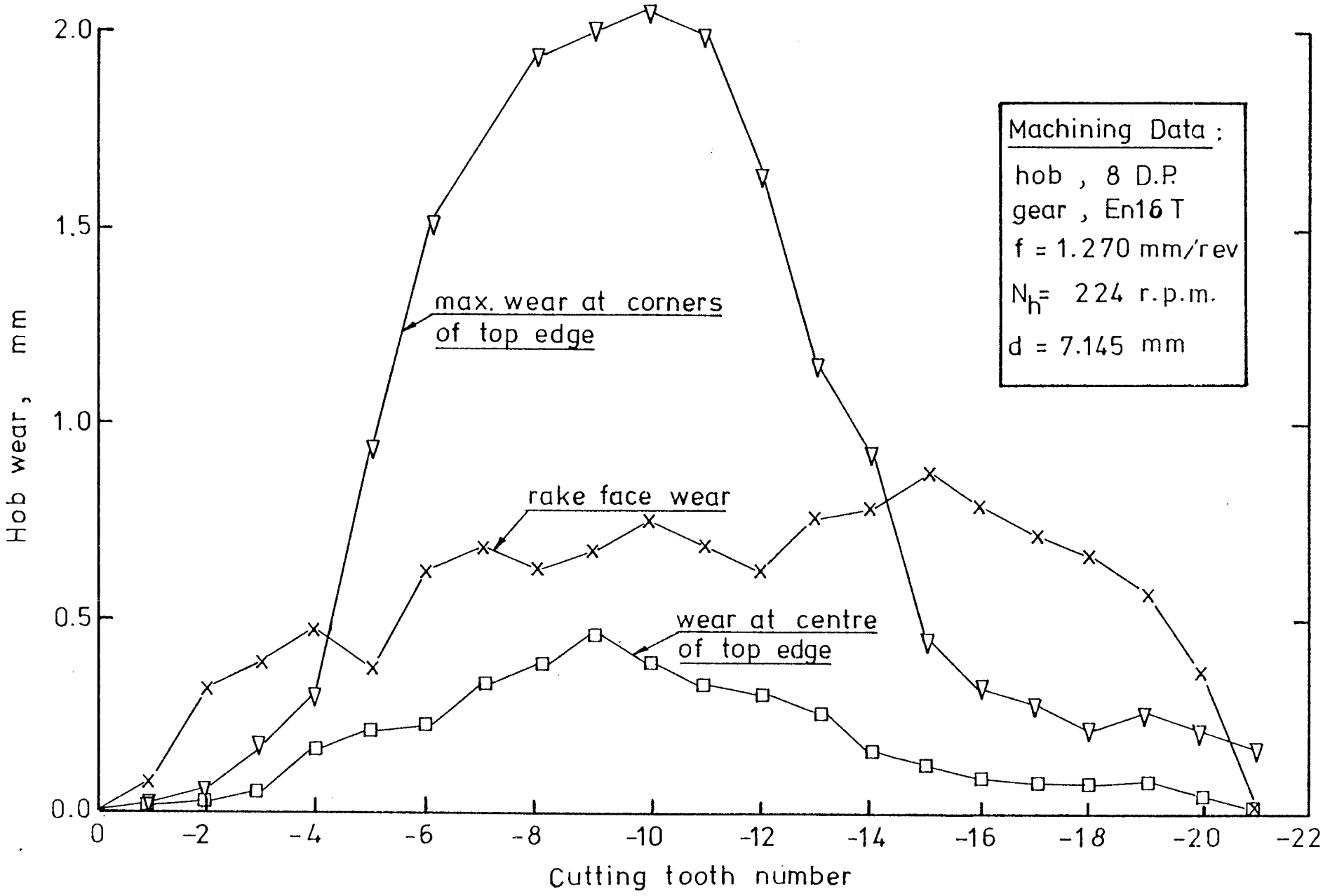

Fig. 90 DISTRIBUTION OF HOB WEAR AT HIGH SPEED

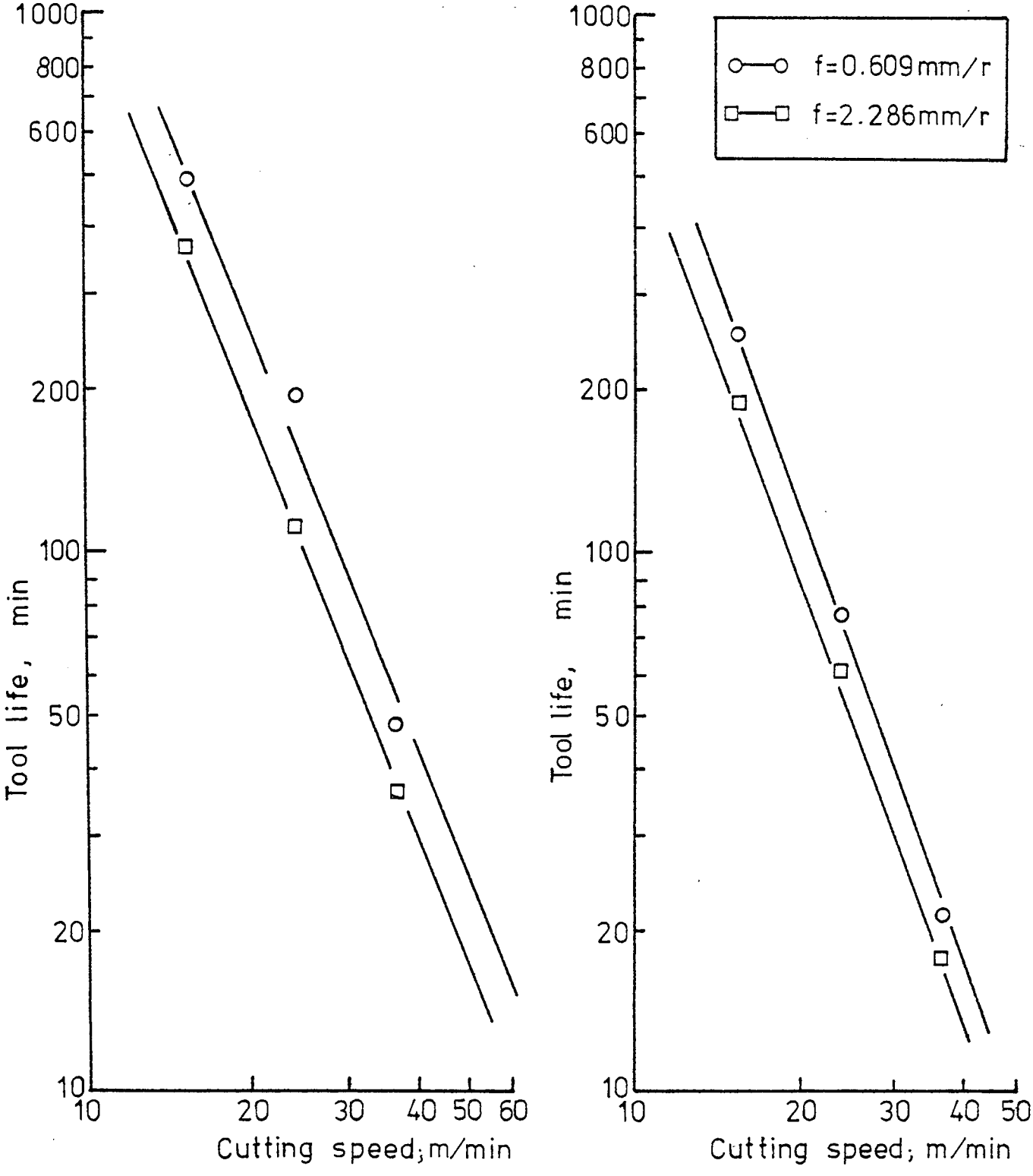

a) Machinig Data:

hob; 10 D.P., 14 gashes

gear; En 34 (164 HB),

Z_g = 36

d = 5.45 mm

b) Machining Data:

hob; 10 D.P., 14 gashes

gear; En 8 (183 HB),

Z_g = 36

d = 5.45 mm

Fig. 91 VARIATION OF TOOL LIFE WITH HOB SPEED

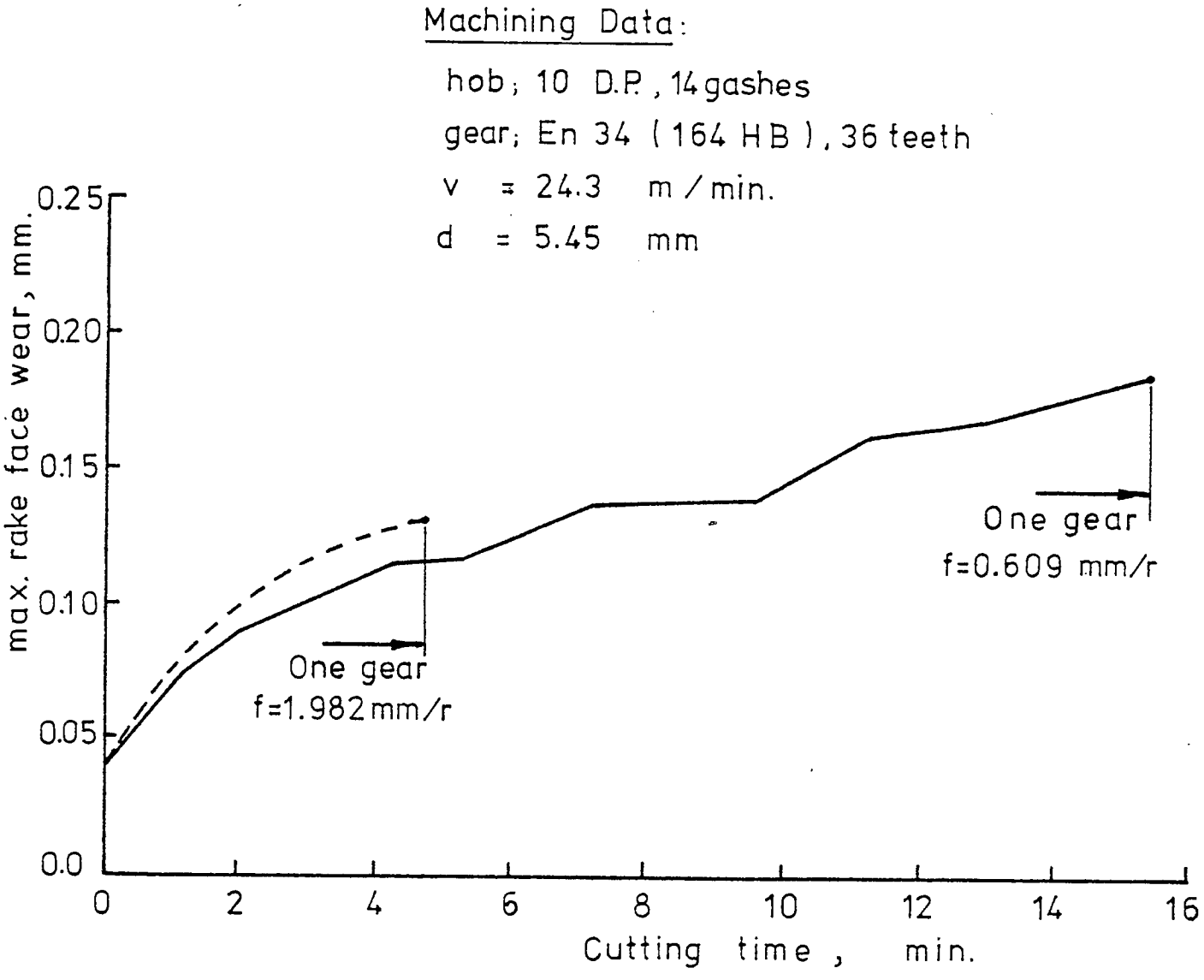

Fig. 92 EFFECT OF FEED ON HOB WEAR

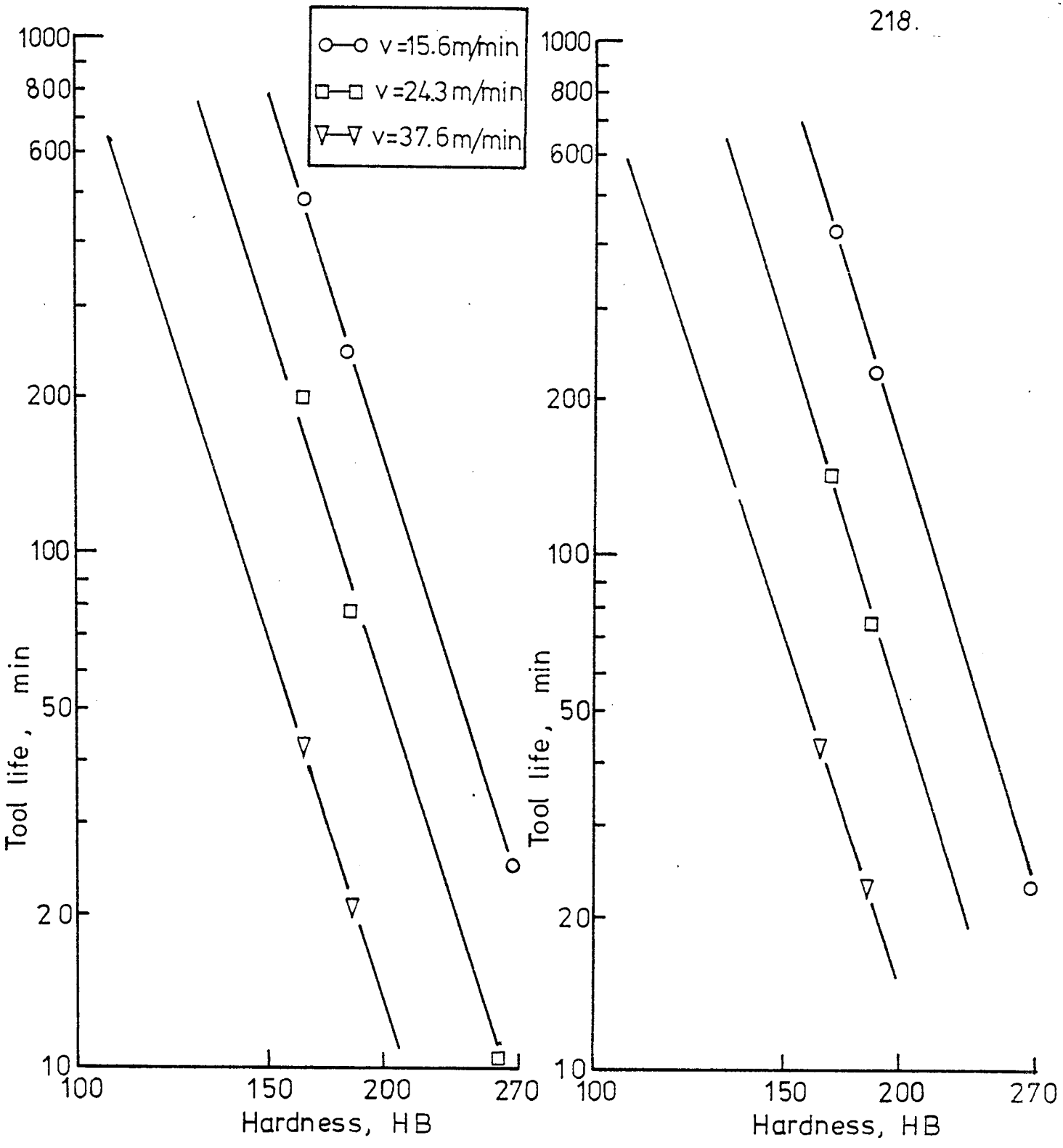

a) Machining Data:

hob; 10 D.P., 14 gashes

gear; 36 teeth

f = 0.609 mm/rev

d = 5.45 mm

b) Machining Data:

hob; 10 D.P., 14 gashes

gear; 36 teeth

f = 0.609 mm/rev

d = 4.762 mm

Fig. 93 VARIATION OF TOOL LIFE WITH HARDNESS

steel blank by 10 D.P. hob.

8.4.3 Effect of Cutting Conditions on Tool-life

8.4.3.1 Effect of Cutting Speed. To study the effects due to variation in cutting speed, tests were carried out at constant feeds of 0.609 and 2.286 mm/rev, and cutting speeds of 15.6, 24.28 and 37.6 m/min when cutting En 34, En 8 and En 16T steel blanks. Fig. 91 shows the variation of tool-life with hob speed for En 34 and En 8 steels. It is clear from the figure that tool-life decreases sharply when the speed was increased from 15.6 m/min. to 24.28 m/min.

8.4.3.2 Effect of axial feed. It was observed that when cutting at different feeds while all other cutting parameters were kept constant that hob wear was very small after completion of cutting corresponding to one En 34 gear blank at constant hob speed of 24.3 m/min and varying axial feed to 0.609 and 1.987 mm/rev. Fig. 92 shows the width of the rake face wear, and it is seen that the wear is somewhat greater at the lowest feed of 0.609 mm/rev.

The numbers of cutting cycles required to cut a gear using the feeds, 0.609 and 1.987 mm/rev are of the ratio 1/.609 : 1/1.987. Wear per cutting cycle does not increase so much with axial feed. Moreover, the cutting length and cutting thickness increase approximately in the same proportion as feed increases. It is thought that the wear of cutting edges of H.S.S. hobs is hardly affected by the cutting length or the rubbing at penetration into work material. Thus it seems more advantageous to use a larger axial feed without

affecting the hob life.

8.4.3.3 Effect of material hardness. Tests were carried out in order to cut spur gears of three different types of steel, En 34 (164 HB), En 8 (183 HB) and En 16T (269 HB) under constant cutting conditions. Fig. 93 shows clearly that tool-life decreases sharply with the increase of blank material hardness. A small amount of chipping was observed when hobbing En 16T steel at the speed of 37.6 m/min.

8.4.3.4 Effect of the number of teeth and depth of cut. The number of teeth in the blank, Z_g and depth of cut, d were selected at two levels each, and rough observations of tool-life showed that tool life increases with the decrease of depth of cut and decreases with the increase of the number of teeth in the gear blank.

To test the significance of cutting parameters, further analysis is provided through the analysis of variance.

8.4.3.5 Analysis of Variance. A set of 72 tool-life tests was provided by combinational arrangement of feed, speed, material hardness, depth of cut and number of teeth in the gear blank in order to test the significance on tool-life. Table 23 gives the analysis of variance and it follows that cutting speed, material hardness and depth of cut are highly significant as well as the following interactions:
hob speed and depth of cut; speed and hardness, depth of cut and hardness; speed, feed and hardness; speed, depth of cut and hardness and feed, depth of cut and hardness.

Axial feed and the number of teeth in the blank show no significant effect on tool life, and speed appeared to have the most significant influence on hob life.

TABLE 23

ANALYSIS OF VARIANCE FOR TOOL LIFE

Sourse of Variation	Degrees of Freedom	Sum of Squares	Variance	Variance ratio; F
N_h	2	255243	127622	24.097 ††
f	1	10464	20513	1.976
Zg	1	4900	4632	0.925
d	1	50668	49315	9.567 ††
HB	2	181443	90721	17.130 ††
N_h.f	2	3641	1821	0.891
N_h.Z	2	1756	878	0.430
N_h.d	2	39954	19977	9.777 ††
N_h.HB	4	92030	23007	11.261 ††
f.Z	1	249	249	0.122
f.d	1	1200	651	0.588
f.HB	2	5187	2593	1.270
Z.d	1	1840	1733	0.901
Z.HB	2	2658	1329	0.651
d.HB	2	98491	49245	24.102 ††
N_h.f.Z	2	138	69	0.467
N_h.f.d	2	589	294	1.987
N_h.f.HB	4	2756	689	4.646 ††
N_h.Z.d	2	992	496	3.346
N_h.Z.HB	4	993	248	1.675
N_h.d.HB	4	791	19786	133.376 ††
f.Z.d	1	138	138	0.936
f.Z.HB	2	235	117	0.795
Z.d.HB	2	1171	586	3.948 †
f.d.HB	2	2811	1405	9.474 ††
N_h.f.Z.d	2	112	56	0.919
N_h.f.Z.HB	4	445	111	1.825
N_h.f.d.HB	4	1435	358	5.878 ††
N_h.Z.d.HB	4	570	142	2.335
f.Z.d.HB	2	160	80	1.311
N_h.f.Z.d.HB	4	244	61	0.823
RESIDUALS	0	0.002		
TOTALS	71	841672	11854.53	

8.5 Hobbing Tool-life Tests

After the preliminary investigation and analysis of variance tests, a clear view about tool-life behaviour is established. Then it was decided to carry out comprehensive tests in order to observe the effect of hob diametral pitch and axial feed on tool-life more carefully and to establish a general mathematical model to describe tool-life in terms of six cutting parameters.

Based upon analysis of variance, Table 23, the experimental conditions were designed to cover a wide range of cutting conditions. The cutting parameters and selected levels are as follows:

axial feed rates; f : 0.609, 1.727 and 2.286 mm/rev
cutting speeds; N_h: 74, 115, 143, 178 and 224 r.p.m.
blank materials: En 34 (164 HB), En 8 (183 HB) and En 16T (269 HB)
hob specifications: 8 D.P. (12 gashes), 10 D.P. (14 gashes) and 12 D.P. (12 gashes)
depth of cut, d: 4.7 mm, 5.7 mm and 7.14 mm.
number of teeth in the gear, Z_g: 29, 36 and 44 teeth
cutting fluid; active type EP cutting oil containing sulphur chlorine and fat.

8.6 Results

Tool-life results consist of 258 observations of tool-life are represented in Table 24 to Table 26.

From the results, the effect of hob diametral pitch on tool life can be observed as in Fig. 94 where tool life increases with the increase of hob D.P. at a constant hob

TABLE 24

TOOL LIFE RESULTS

Machining Data: hob; 8 D.P.,S.S.R.H., 12gashes

Material (HB)	Hob speed N_h, rpm	Axial feed f, mm/rev	Tool-life, min. d=7.145 mm Zg=29	d=7.145 mm Zg=36	d=5.715 mm Zg=29	d=5.715 mm Zg=36
En 34 (164)	74	0.609	474	515	480	535
		1.727	386			
		2.286	358	397	400	445
	115	0.609	273			
		1.727	216			
		2.286	202			
	143	0.609	151	168	157	173
		1.727	122			
		2.286	111	120	126	140
	178	0.609	86			
		1.727	69			
		2.286	62			
	224	0.609	47	52	49	55
		1.727	39			
		2.286	35	39	40	44
En 8 (183)	74	0.609	252			
		1.727	206	230	222	248
		2.286	187			
	115	0.609	146			
		1.727	116	128	129	143
		2.286	108			
	143	0.609	78			
		1.727	64	70	72	80
		2.286	58			
	178	0.609	44			
		1.727	38	42	41	45
		2.286	33			
	224	0.609	26			
		1.727	21	24	23	26
		2.286	19			
En 16T (269)	74	0.609	28	31	29	32
		1.727	22			
		2.286	4	5	4	5
	115	0.609	17			
		1.727	13			
		2.286	2			
	143	0.609	9	10	10	10
		1.727	7			
		2.286	1	2	2	2
	178	0.609	6			
		1.727	4			
		2.286	0.8			
	224	0.609	4	5	4	6
		1.727	3			
		2.286	0.5	1	1	2

TABLE 25

TOOL LIFE RESULTS

Machining Data: hob; 10 D.P., S.S.R.H., 14gashes

Material (HB)	Hob speed N_h, rpm	Axial feed f, mm/rev	Tool-life, min.			
			d=5.715 mm		d=4.762 mm	
			Zg=36	Zg=29	Zg=36	Zg=29
En 34 (164)	74	0.609	485	458	510	420
		1.727	390			
		2.286	372	358	400	325
	115	0.609	282			
		1.727	221			
		2.286	214			
	143	0.609	259	245	265	160
		1.727	126			
		2.286	118	112	126	100
	178	0.609	89			
		1.727	74			
		2.286	74			
	224	0.609	49	45	51	42
		1.727	42			
		2.286	40	38	41	32
En 8 (183)	74	0.609	254	240	275	215
		1.727	207			
		2.286	200	192	219	174
	115	0.609	148			
		1.727	117			
		2.286	115			
	143	0.609	79	73	86	70
		1.727	66			
		2.286	65	62	70	54
	178	0.609	45			
		1.727	38			
		2.286	38			
	224	0.609	26	24	28	21
		1.727	22			
		2.286	19	18	21	18
En 16T (269)	74	0.609	28	27	31	29
		1.727	23			
		2.286	20	19	22	20
	115	0.609	16			
		1.727	13			
		2.286	11			
	143	0.609	9	8	10	9
		1.727	7			
		2.286	6	6	7	7
	178	0.609	6			
		1.727	4			
		2.286	4			
	224	0.609	3	3	3	2
		1.727	2			
		2.286	2	2	2	2

TABLE 26

TOOL LIFE RESULTS

Machining Data: hob; 12 D.P.,S.S.R.H.,12 gashes

Material (HB)	Hob speed Nh , rpm	Axial feed f, mm/rev	Tool-life, min Depth, d=4.76 mm Zg=44	Zg=29
En 34 (164)	74	0.609	1420	1270
		1.727	1100	
		2.286	1050	940
	115	0.609	755	
		1.727	620	
		2.286	600	
	143	0.609	452	403
		1.727	355	
		2.286	340	306
	178	0.609	254	
		1.727	208	
		2.286	190	
	224	0.609	148	132
		1.727	114	
		2.286	109	98
En 8 (183)	74	0.609	724	650
		1.727	615	
		2.286	588	525
	115	0.609	430	
		1.727	355	
		2.286	325	
	143	0.609	240	215
		1.727	191	
		2.286	157	141
	178	0.609	138	
		1.727	114	
		2.286	102	
	224	0.609	75	69
		1.727	60	
		2.286	55	50
En 16T (269)	74	0.609	84	75
		1.727	65	
		2.286	62	55
	115	0.609	46	
		1.727	37	
		2.286	34	
	143	0.609	27	24
		1.727	21	
		2.286	18	16
	178	0.609	15	
		1.727	12	
		2.286	10	
	224	0.609	8	7
		1.727	7	
		2.286	7	6

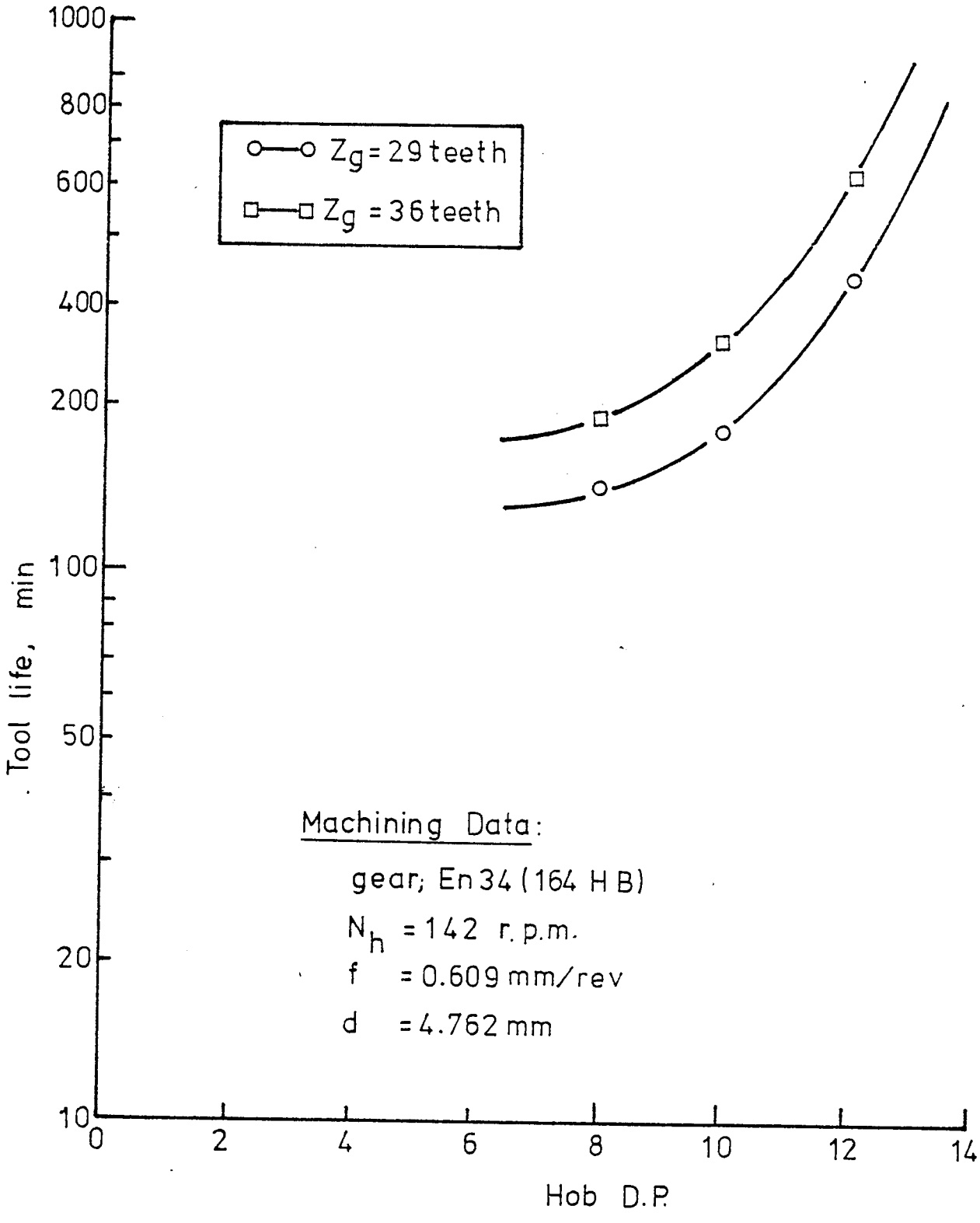

Fig. 94 VARIATION OF TOOL LIFE WITH HOB D.P.

speed of 115 r.p.m. This may be different when measuring tool life at constant cutting speed (V) for different hob D.P., where it is expected that tool life will decrease with the increase of hob D.P. as the hob outside diameter is not the same for each D.P. and cutting speed will decrease with the increase of hob D.P. for the same hob speed (N_h).

Although cutting feed and the number of teeth in the blank are not significant as individual parameters, they are to be included in the generalised tool-life equation, since interactions between feed, depth of cut and material hardness, and between the number of teeth, depth of cut and hardness proved to have a significant effect on tool-life.

8.7 The Tool-life Equation and the Estimated Error Variance

It has been assumed in previous investigations that for a given set of operating conditions the parameters in tool-life equation are constants. In reality, the parameters are subject to uncertainty because of experimental error on the determination of tool life, as seen in Fig. 91 to Fig. 94 it is convenient to work with the logarithmic form of tool life equation.

$$\hat{y} = \ln T = b_o + b_1 \ln V + b_2 \ln f + b_3 \ln D.P. + b_4 \ln d + b_5 \ln HB + b_6 \ln Z \qquad (85)$$

where, y is the predicted value of tool life on a logarithmic scale,

$b_0, b_1, \ldots, b_6$ are the least-squares estimates of the parameters $\beta_0, \ldots, \beta_6$ from the postulated model (85)

$$E(y) = E(\ln T) = \beta_0 x_0 + \beta_1 x_1 + \beta_2 x_2 + \beta_3 x_3 + \beta_4 x_4 + \beta_5 x_5 + \beta_6 x_6 \qquad (86)$$

where, E(y) is the expected value of the average tool life on a logarithmic scale,

x_0 is unity at all levels,

x_1, x_2, x_3, x_4, x_5 and x_6 are cutting speed, feed rate, hob D.P., depth of cut, hardness and number of teeth in the blank respectively, all on a log. scale.

To determine the confidence intervals an estimate of the experimental error is needed. The magnitude of the experimental error is estimated by the error variance as follows:

$$S^2 = \frac{\sum_{i=1}^{N} (y_i - \hat{y}_i)^2}{N - q} \qquad (87)$$

where, y_i is the ith observation of tool life on a log. scale

N is the number of observations

q is the number of parameters to be estimated.

In the case of tool-life equation in gear hobbing, the postulated model to fit the data is given by eq. (86).

The least-squares estimates are found from

$$b = (x' x)^{-1} x' y \qquad (88)$$

where, x is the matrix of independent variables

y is the column vector of obersations

The data consists of 258 observations of tool-life, with a logarithmic transformation of the experimental cutting conditions the $(x' x)$ matrix is:

$$(x'x) = \begin{bmatrix} a_{00} & a_{01} & a_{02} & \cdots & a_{06} \\ a_{10} & a_{11} & & & \\ a_{20} & a_{21} & & & \\ a_{30} & a_{31} & & & \\ a_{40} & a_{41} & & & \\ a_{50} & a_{51} & & & \\ a_{60} & a_{61} & \cdots & & a_{66} \end{bmatrix}$$

$$= \begin{bmatrix} 258.00 & 760.09 & 49.33 & 1220.25 & 520.25 & 807.19 & 396.89 \\ 760.09 & 2547.12 & 164.60 & 4049.62 & 1726.92 & 2679.30 & 1317.11 \\ 49.33 & 164.60 & 93.83 & 260,99 & 11.14 & 175.77 & 87.18 \\ 1220.25 & 4049.62 & 260.99 & 6517.13 & 2771.91 & 4301.71 & 2115.27 \\ 520.25 & 1726.92 & 111.14 & 2771.91 & 1187.71 & 1837.43 & 896.51 \\ 807.19 & 2679.30 & 175.77 & 4301.71 & 1837.42 & 2851.14 & 1396.22 \\ 396.89 & 1317.11 & 87.18 & 2115.27 & 896.51 & 1396.22 & 694.6 \end{bmatrix}$$

and $(x'x)^{-1} = \begin{bmatrix} a^{00} & a^{01} & a^{02} & a^{03} & a^{04} & a^{05} & a^{06} \\ a^{10} & a^{11} & & & & & \\ a^{20} & a^{21} & & & & & \\ a^{30} & a^{31} & & & & & \\ a^{40} & a^{41} & & & & & \\ a^{50} & a^{51} & & & & & \\ a^{60} & a^{61} & \cdots & & & & a^{66} \end{bmatrix}$

From Eq. (88)

$$\begin{bmatrix} b_0 \\ b_1 \\ b_2 \\ b_3 \\ b_4 \\ b_5 \\ b_6 \end{bmatrix} = \begin{bmatrix} 32.408 \\ -2.63 \\ -0.21 \\ -0.66 \\ -0.46 \\ -5.79 \\ 0.26 \end{bmatrix} = (x'x)^{-1} \begin{bmatrix} 897.53 \\ 2920.62 \\ 177.68 \\ 4708.96 \\ 2051.90 \\ 3174.00 \\ 1543.81 \end{bmatrix} \tag{89}$$

The fitted equation is

$$y = \ln T = 32.408 - 2.63 \ln V - 0.21 \ln f - 0.66 \ln D.P. - 0.46 \ln d - 5.79 \ln HB + 0.26 \ln Z_g$$

And the generalized tool-life equation becomes

$$T = \frac{(200)^{2.62} \; Z_g^{0.26}}{V^{2.63} \; f^{0.21} \; (D.P.)^{0.66} \; d^{0.46} \; \left(\frac{HB}{200}\right)^{+5.79}} \tag{90}$$

The uncertainty of the least-squares estimates $b_0, b_1, \ldots, b_6$ is indicated by the 95 percent confidence intervals for $\beta_0, \beta_1, \ldots\ldots, \beta_6$.

The confidence interval (C.I.) for a given parameter β_i, under the assumption of spherical normality is

$$\text{C.I.}\ (\beta_i) = b_i \pm t_{\nu,\gamma/2} \; (S^2 a^{ii})^{\frac{1}{2}} \tag{91}$$

where, $t_{\nu,\gamma/2}$ is student's t-statistic with ν degrees of freedom and level of significance γ,

a^{ii} is the element of the ith row and ith column of $(x'x)^{-1}$.

The estimate of error variance was found as follows:

$$S^2 = \frac{0.386325}{258-6} = 0.0017093$$

At $\gamma = 0.05$ and $\nu = 258$, $t = 1.645$, and the 95 percent confidence interval for β_0 is:

$$CI(\beta_0) = 32.408 \pm 1.645 \{(0.00171)(1314.73)\}^{\frac{1}{2}}$$

$$= \begin{cases} 34.8745 \\ 29.9415 \end{cases}$$

and for β_1 is

$$CI(\beta_1) = -2.63 \pm 1.645 \{(0.00171)(0.8563)\}^{\frac{1}{2}}$$

$$= \begin{cases} -2.562 \\ -2.693 \end{cases}$$

and for β_2 is

$$CI(\beta_2) = -0.21 \pm 1.645 \{(0.00171)(1.3572)\}^{\frac{1}{2}}$$

$$= \begin{cases} -0.1309 \\ -0.2892 \end{cases}$$

and for β_3 is

$$CI(\beta_3) = -0.66 \pm 1.645 \{(0.00171)(1.2574)\}^{\frac{1}{2}}$$

and for β_4 is

$$CI(\beta_4) = -0.46 \pm 1.645 \{(0.00171)(-0.433)\}^{\frac{1}{2}}$$

$$= \begin{cases} -0.4153 \\ -0.5046 \end{cases}$$

and for β_5 is

$$CI(\beta_5) = -5.79 \pm 1.65 \{(0.00171)(4.0873)\}^{\frac{1}{2}}$$

$$= \begin{cases} -5.6528 \\ -5.9271 \end{cases}$$

and for β_6 is

$$CI\ (\beta_6) = 0.26 \pm 1.645\ \{(0.00171)(0.3201)\}^{\frac{1}{2}}$$

$$= \begin{cases} 0.2984 \\ 0.2216 \end{cases}$$

The resulting confidence limits are expressed under the assumption that the coefficients are uncorrelated is generally accepted. However, the estimates $b_0, b_1, \ldots, b_6$ are, as in the six-parameter case, correlated with each other. Therefore the individual confidence limits are inadequate for interpreting the joint uncertainty in the estimation of $b_0, b_1, \ldots\ldots, b_6$.

To interpret this joint uncertainty, an analytical method, applying orthogonal transformations, and a chance-constrained programming concept are discussed and illustrated in Chapter 9 of this research.

8.8 Summary

In the cutting tests conducted on the hobbing machine when cutting spur gear conventionally, a difference in the hob wear rate was observed at the top, corners and rake face of the cutting edges. Rake face wear was selected as tool-life criteria for the cutting range covered. Preliminary cutting test and analysis of variance proved that hob speed, material hardness and depth of cut have high significant influence on tool life. Axial feed and number of teeth in the blank showed little effect on tool life but not significant.

Comprehensive tool-life tests were carried out in order to establish a general mathematical model to describe tool life in terms of six cutting parameters and the estimated error variance was calculated.

8.9 Conclusions

In this section the author has tried to describe briefly the more important features of tool life and wear from one person's point of view.

The discussion was limited to wear under normal cutting speed conditions, as the speed is increased and temperature becomes too high, where diffusion is very significant, other wear mechanisms will prevail. In those cases, tool strength and hardness will be important parameters. However, the following conclusions can be drawn from this study:

1. "Rake face" wear is a suitable tool-life criterian in gear hobbing when cutting materials less than (270 HB) hardness and under normal cutting conditions.

2. Cutting speed has the highest significant influence on tool-life followed by material hardness and depth of cut, for the cutting range covered.

3. It seems more advantageous to use higher axial feeds without affecting the hob life and thus decrease the cutting time.

CHAPTER IX

ECONOMICS OF GEAR HOBBING

This is a general viewpoint of the economic problem in gear hobbing in terms of the reduction in machining cost. The problem involves, however, a great number of variables and it must be conceded as axiomatic that the number of variables which can be conveniently handled mathematically is such that a great deal of generality is lost.

Here is an attempt to achieve the initial goal of including at least the fundamental variables in the analysis by using the concept of statistical inference, and to apply an analytical method in a chance-constrained programming concept to determine the optimum cutting conditions considering the probabilistic nature of the objective function and constraints.

9.1 Introduction

The determination of the optimum machining conditions in metal cutting is an important aspect in an economic manufacturing process, and although the problem of economic machining has been acknowledged for many years (as early as 1929 by Forsberg [32]), no one has solved this problem satisfactorily, the reason being that the generalized tool-life equation obtained is too uncertain to enable one to state a certain optimum of cutting data with certainty.

It has been shown in previous studies of machining economics that the determination of the optimum cutting

conditions depend on the cost and time parameters and the parameters in tool life equation [33,34 and 35]. These investigators have assumed that for a given set of operating conditions, the parameters in tool-life equation are constants, and subject to uncertainty because of the experimental error in tool-life testing.

The amount of tool-wear varies from tool to tool due to inherent variations in the tool wear mechanism along with experimental variation. Therefore, tool-life estimated from tool wear observations should be treated as a random instead of a deterministic variable. The coefficients in experimentally determined constraints such as surface roughness, power temperature, ... etc. should be treated as random variables subject to a degree of uncertainty instead of a deterministic variable.

The probalistic nature of the coefficients was considered by Wu[35] and Ermer [36] in their studies of the most economic cutting speed for the turning operation. However, their considerations were limited to the uncertainty of the coefficients in Taylor's tool-life equation when no constraints existed. Economics of cylindrical milling was studied by Draghici [37], when the optimisation function, represented by the cost price of cutting, and the expression of the system of the kinematic cutting process parameters, have been simulated by a convex mathematical model.

An analytical method, applying a chance-constrained programming concept [38] is used to analyse the results obtained previously in this study to determine the optimum cutting conditions in the case of gear hobbing, considering the

probabilistic nature of the objective function and the constraints.

9.2 The General Cost Expression

The basic model, which describes the total cost/piece (C_p) by means of a simple, rough hobbing operation is the sum of four costs:

1. Machining Cost = $C_o t$

where, C_o is the cost of operating time, £/min.

t is the time to machine a gear blank, min/piece

cutting time in hobbing was estimated as follows:

$$t = \frac{b'}{f} \cdot \frac{z_g}{S_h} \cdot \frac{1}{N_h} \cdot \frac{d_c}{d} \quad \text{min.} \qquad (92)$$

where, b' is total distance travelled by the hob, mm.

f is axial feed, mm/rev.

d_c is depth of cut, mm.

d is full depth of cut, mm.

2. Tool cost = $C_t \quad \frac{t}{T}$

where, C_t is the tool cost, £/cutting edge,

T is tool-life, min.

t/T is the number of tool edges required per work piece.

3. Tool changing cost = $C_o t_c \cdot t/T$

where, t_c is tool changing time, min

Tool changing cost = (cost/tool change)

(number of tool changes/piece)

4. Handling cost = $C_o\ t_h$

where, t_h is the handling time, min/piece.

Hence, the total cost per piece (C_p) can be expressed as follows:

$$C_p = C_o t + \frac{t}{T}\ (C_o t_c + C_t) + C_o t_h$$

$$= t\left[C_o + \left(\frac{C_o t_c + C_t}{T}\right)\right] + C_o t_h \qquad (93)$$

9.3 Tool-life Equation

Normally the tool is withdrawn from service when the cutting time reaches tool-life time; it is convenient in the case of gear hobbing to work with the Time-Taylor's tool life equation of the form,

$$V = \frac{C_v\ d^{\alpha_3}\ Z_g^{\alpha_4}.D_h^{\alpha_5}}{T^{\alpha_1}\ f^{\alpha_2}\ (D.P.)^{\alpha_6}\ (HB)^{\alpha_7}} \quad m/min \qquad (94)$$

where, C_v is constant

D_h is hob diameter, mm.

$\alpha_1, \ldots, \alpha_7$ are coefficients

The cutting speed, V is also equal to:

$$V = \frac{\pi.\ D_h.N_h}{1000} \quad m/min \qquad (95)$$

Therefore, the general tool life expression is obtained as follows:

$$T = \left(\frac{1000\ C_v}{\pi}\right)^{1/\alpha_1} \frac{d^{\alpha_3/\alpha_1}\ Z_g^{\alpha_4/\alpha_1}\ D_h^{\alpha_5-1/\alpha_1}}{f^{\alpha_2/\alpha_1}\ (D.P.)^{\alpha_6/\alpha_1}\ (HB)^{\alpha_7/\alpha_1} N_h^{1/\alpha_1}} \qquad (96)$$

By substituting the relationships (92) and (96) in the price cost eq. (93), then

$$C_p = \frac{b'.Z_g.d_c}{f.S_h.N_h.d}\left[C_o + (C_o t_c + C_t)\left(\frac{1000\,C_v}{\pi}\right)^{-1/\alpha_1}\cdot\right.$$

$$\left.\cdot\frac{f^{\alpha_2/\alpha_1}\,(D.P.)^{\alpha_6/\alpha_1}}{d^{\alpha_3/\alpha_1}\,Z_g^{\alpha_4/\alpha_1}}\cdot\frac{HB^{\alpha_7/\alpha_1}\,N_h^{1/\alpha_1}}{D_h^{\alpha_5-1/\alpha_1}}\right]+C_o t_h \qquad (97)$$

The desired optimisation function becomes:

$$C_p = \text{function of } \{f,\ (D.P.),\ HB,\ N_h,\ d,\ Z_g,\ D_h\} \qquad (98)$$

In order to solve this mathematical model which contains seven parameters, the problem can be simplified when the most simple hobbing process is assumed in all the following analysis: the rough hobbing of spur gears with a single thread hob. Full depth of cut corresponding to the particular module and conventional hobbing are concerned.

For a given gear-hob specification, the desired optimisation function can be reduced to only two parameters as follows

$$C_p = C(V, f) \qquad (99)$$

The generalized tool-life equation was obtained in the following logarithmic form:

$$\ln T = 29.9415 - 2.693 \ln V - 0.289 \ln f - 0.684 \ln(D.P.) - 5.927 \ln HB + 0.222 \ln Z_g \qquad (100)$$

where tool-life (T) was estimated on a deterministic basis, i.e. at 50% probability level.

9.4 Determination of the restrictive functions

There are several factors which constrain the selection of cutting conditions. An attempt was made in this study to cover a wide range of restrictions as follows:

1. The restrictions of the kinematics of the machine tool;

   a) The available maximum cutting speed $V \leqslant V_{max}$ (101)

   b) The available minimum cutting speed $V \geqslant V_{min}$ (102)

   c) The available maximum feed $f \leqslant f_{max}$ (103)

   d) The available minimum feed $f \geqslant f_{min}$ (104)

2. The restrictions of the machine-tool dynamics;

   a) The tangential component of cutting force P_T in gear hobbing has the following form

$$P_T = \frac{C_F \, f^{x_f} \cdot N_h^{y_F} \cdot d^{z_F} \, (D.P.)^{U_F}}{D_h^{w_F}} \qquad (105)$$

   where; x_F, y_F, z_F, u_F and w_F are coefficients to be estimated.

   The allowable maximum cutting force must satisfy the following conditions

$$P_T \leqslant P_{T_{max}} \qquad (106)$$

The allowable tangential cutting force affects the dimensional component errors and the tool-work deflections.

The tangential force P_T depends on the cutting conditions and the amount of tool wear and must satisfy the relationship (106) through the time of the effective tool life.

b) The power consumed during cutting (W_p) must also satisfy the relationship (107) as follows

$$W_p \leqslant W_{p\ max} \tag{107}$$

for the time of the effective tool life, and for a specific smount of rake face wear, W_p is given by

$$W_p = \frac{P_T \cdot V}{6120\ \eta} \tag{108}$$

where η is mechanical efficiency

c) The stable cutting region;

Chatter in hobbing may often be encountered which strongly limits the rate of production. The amplitude of vibration "D_{peak}" was measured in the X-direction on the hobbing machine as described in Chapter III of this research. The stable cutting region is determined by the occurrance of chatter vibration, and is given by

$$D_{peak} \leqslant D_{peak.C} \tag{109}$$

where, $D_{peak.C}$ is the amplitude of chatter vibration.

Maximum amplitude of vibration D_{peak} was taken as a criteria for measurement and was obtained as follows

$$D_{peak} = \frac{C_p\ f^{x_p} \cdot V^{y_p}\ HB^{z_p}}{(D.P.)^{u_p}}\ \mu m\ peak \tag{110}$$

where, C_p, x_p, y_p, z_p and u_p are parameters to be estimated.

3. The restrictions of the machine-tool structure

a) the restrictions of bending and twisting resistance of the hob arbor,

Assuming for simplicity that the maximum load acts at the centre of the hob. The design formula for shafts under bending and twisting is given as follows:

$$\sigma_{max} = \frac{0.5\ S_{yp}}{F.S} = \frac{16}{\pi d_s^3}\sqrt{(C_m M)^2 + (C_n T)^2} \qquad (111)$$

where, σ_{max} is maximum shear stress

S_{yp} is yield stress N/m^2

F.S. is factor of safety N/m^2

M is bending moment N/m

T is the acting torque N.m

d_s is the shaft diam. m

C_m and C_n are constants

If the two stresses are composed according to the second hypothesis[37], then

$$0.35M + 0.65\sqrt{M^2 + T^2} \leqslant \sigma_a . J \qquad (112)$$

where, σ_a is the allowable shear stress, N/m^2

where, σ_a is the allowable shear stress, N/m^2.

$$J = \frac{\pi d_s^3}{32} \quad , \quad M_{max} = \frac{P_T \cdot l}{8} \quad \text{and} \quad T_{max} = \frac{P_T \cdot D_h}{2}$$

where, l is arbor length between the supports, m.

Substituting the value of P_T in Eq. (112) then,

$$\frac{K.C_F.f^{x_F}.N_h^{y_F}.d^{z_F}.(D.P.)^{u_F}}{D_h^{w_F}} \leq \frac{\pi.d_s^3.\sigma_a}{32} \qquad (113)$$

where, k is stiffness of the hob arbor, and is determined from the following relationship:

$$k = \frac{0.38}{8} + 0.65 \sqrt{(\frac{l}{8})^2 + (\frac{D_h}{2})^2}$$

b) The restriction of the maximum loading of the feeding mechanism

It is essential that maximum loading of the feeding mechanism of the hob during cutting must be greater than the cutting force P_T, that is

$$P_T = \frac{C_F f^{x_F}. N_h^{y_F}.d^{z_F} (D.P.)^{u_F}}{D_h^{w_F}} \leq F_a \qquad (114)$$

where, F_a is maximum loading of the feeding mechanism, Newton.

4) The restriction of the maximum surface roughness.

The allowable surface roughness restricts the operability region when it is specified due to a requirement in a following finishing operation, the dimensional accuracy of a gear blank

has a significant effect on the finished product. Blanks, therefore are usually made to a tolerance depending upon the grade or class and type of gear being produced. When surface roughness is restricted, upper and lower limits are specified for economic considerations. But in the case of gear production the upper limit of surface roughness is only considered. The relationship between geometrical surface roughness along the gear teeth and cutting parameters is given by the following:

$$S_R = C_r \, f^{x_r} . \, N_h^{y_r} . \, d^{z_r} (D.P.)^{u_r} . (HB)^{v_r} . Z_g^{w_r} . D_h^{T_r} \qquad (115)$$

where, S_R is surface roughness measured in CLA(μm).

C_r is constant

$x_r, y_r, z_r, u_r, v_r, w_r$ and T_r are coefficients

and the restrictive function becomes

$$S_R \leqslant S_{R\,Lim} \qquad (116)$$

where, $S_{R\,Lim}$ is the limit for surface roughness.

9.5 Chance-Constrained Programming

The optimisation problem with linear constraints can be presented as follows:

$$H = \phi(x_1, x_2, x_3, ---, x_n)$$

Subject to the constraints:

$$\sum_{j=1}^{n} a_{ij} . \, x_j \geqslant b_i \qquad i = 1,2,3,---,m.$$

where, a_{ij}'s are the technological coefficients,

b_i's are the constraint coefficients,

$\phi(x_1, x_2, ---, x_n)$ may be a linear or non-linear function of the x_j's

Now the problem is to determine the x_j's $(j=1,2,---,n)$ to satisfy the above conditions. The optimization problem is considered when some or all of the a_{ij} and b_j are random variables, while H is a deterministic function of the x_j's. This problem can be formulated by the chance constrained programming concept [38], as follows:

Under the chance-constraints

$$\text{Prob} \left(\sum_{j=1}^{n} a_{ij} x_j \geq b_i \right) \geq p_i \qquad (117)$$

where, $i = 1,2, ---, m.$ and $j=1,2,---,n.$

p_i's are the predetermined probability levels at which the corresponding constraints must be satisfied.

When the technological and constraint coefficients are assumed to be normally distributed, the chance-constraints in equation (117) are equivalent to the following deterministic constraints;

$$\sum_{j=1}^{n} \bar{a}_{ij} x_i + \psi(p_i) \left[\sum_{j,k=1}^{n} r(a_{ij} a_{ik}) \sigma_{a_{ij}} x_j x_k - 2 \sum_{j,k=1}^{n} r(a_{ij} b_i) \sigma_{bi} x_j + \sigma_{bi}^2 \right] \geq \bar{b}_i \qquad (118)$$

where, $p_i = \frac{1}{2\pi} \int_{\psi(p_i)}^{\infty} e^{-t^2/2} \, dt,$

$\bar{a}_{ij}$ and $\bar{b}_i$ are the mean values of a_{ij} and b_i respectively,

$r(a_{ij}a_{ik})$ and $r(a_{ij}b_i)$ are the correlation coefficients between a_{ij} and a_{ik} and between a_{ij} and b_i respectively.

Thus, the chance-constrained programming problem is reduced to the equivalent non linear programming problem of minimizing the objective function, H under the deterministic non-linear constraints in Eq. (118).

It is noticed that the objective function is treated as a deterministic function in the above formulation. Although the objective function is often probabilistic, where tool-life coefficients are estimated from practical experiments and are probabilistic values, one possible method of optimizing such an objective function is to choose the values of the coefficients to represent either the upper or lower confidence limit at the predetermined probability level. In this study, the lower confidence limit was taken at 90%, probability level.

9.6 Drawing up the Mathematical Models

The optimization function and the restrictive functions being known, it is then possible to draw the mathematical models of the problems of determining the optimum cutting regime for the cases examined.

The mathematical models for the rough hobbing of spur gears are as follows:

Minimize the objective function of the cost price

$$C_p = \frac{b' z_g}{f.N_h}\left[C_o + (C_o t_c + C_t)\left(\frac{1000\, C_v}{\pi}\right)^{-1/\alpha_1} . f^{\alpha_2/\alpha_1} . (D.P.)^{\alpha_6/\alpha_1} . HB^{\alpha_7/\alpha_1} . N_h^{1/\alpha_1} . d^{-\alpha_3/\alpha_1} . Z_g^{-\alpha_4/\alpha_1} . D_h^{-(\alpha_5 - 1/\alpha_1)}\right] \quad (119)$$

When the constraints are:

$$\left.\begin{array}{l} V \leqslant V_{max} \\ V \geqslant V_{min} \\ f \leqslant f_{max} \\ f \geqslant f_{min} \end{array}\right\} \qquad (120)$$

$$\left.\begin{array}{l} \dfrac{C_F f^{x_F} . N_h^{y_F} . d^{z_F} . (D.P.)^{u_F}}{D_h^{w_F}} \leqslant P_{T\ max} \\ \dfrac{1000 . C_F . f^{x_F} . N_h^{y_{F+1}} . d^{z_F} . (D.P.)^{u_F}}{6120\eta . D_n^{w_{F-1}}} \leqslant W_{p\ max} \\ \dfrac{C_p . f^{x_p} . V^{y_p}_{(HB)}{}^{z_p}}{(D.P.)^{u_p}} \leqslant D_{peak.C} \\ \dfrac{k . C_F . f^{x_F} . N_h^{y_F} . d^{z_F} . (D.P.)^{u_F}}{D_h^{w_F}} \leqslant \dfrac{\pi . d_s^3 . \sigma_a}{32} \\ \dfrac{C_F f^{x_F} . N_h^{y_F} . d^{z_F} . (D.P.)^{u_F}}{D_h^{w_F}} \leqslant F_a \\ C_r . f^{w_r} . N^{y_r} . d^{z_r} . (D.P.)^{u_r} (HB)^{v_r} . Z_g^{w_r} . D_h^{T_r} \leqslant S_R . Lim \end{array}\right\} \qquad (121)$$

9.7 Conversion of the Chance-Constraints into Deterministic Forms

In this study, constraints (120) are considered as deterministic, where the factors are predetermined on the

basis of the machine-tool characteristics and gear-hob specifications. Constraints (121) contain probabilistic coefficients, where these constraints may be linearized by logarithmic transformations. The normality assumptions for these logarithmic transformed responses are generally accepted in regression analysis[36], implying that the parameters estimates are also normally distributed. Therefore, these constraints under consideration can be converted into deterministic forms by applying the relationship given in Eq. (118).

The resulting constraints are expressed under the assumption that the coefficients in the equations are uncorrelated, after appropriate transformations and conversions as follows:

$$g_1 = \log V_{max} - x_1 \geq 0 \qquad (120\text{-}1)$$

$$g_2 = x_1 - \log V_{min} \geq 0 \qquad (120\text{-}2)$$

$$g_3 = \log f_{max} - x_2 \geq 0 \qquad (120\text{-}3)$$

$$g_4 = x_2 - \log f_{min} \geq 0 \qquad (120\text{-}4)$$

An example to demonstrate the conversion from a chance constraint into deterministic is given as follows:

If a general case of a chance constraint takes the form

$$10^{\alpha_1} . f^{\alpha_2} . V^{\alpha_3} . d^{\alpha_4} \leq F \qquad (122)$$

Then the conversion into deterministic is,

$$g = \log F - \bar{\alpha}_1 - \bar{\alpha}_2 \log f - \bar{\alpha}_3 \log V - \bar{\alpha}_4 \log d + \psi (p) (g')^{\frac{1}{2}} \geq 0 \qquad (123)$$

where, $g' = \sigma^2_{\alpha_2} (\log f)^2 + \sigma^2_{\alpha_3} (\log V)^2 + \sigma^2_{\alpha_4} (\log d)^2 + \sigma^2_{\alpha_1}$,

σ_α is standard deviation of α,

$\psi(p)$ is predetermined probability level,

$\bar{\alpha}_1, \bar{\alpha}_2, ---$ are mean values of $\alpha_1, \alpha_2, ---$

In the case of gear hobbing, results taken from previous experiments carried out in the course of this research are to be used in order to establish the appropriate mathematical models to describe cutting force, power consumed during cutting, vibration, surface roughness and tool-life in terms of the cutting parameters. The mathematical models are then solved under the optimum cutting conditions formed by the optimization function, Eq. (119) after the data have been introduced.

9.8 Machinability Data

The following example will illustrate the effects of variations in the coefficients on the determination of optimum cutting conditions for the case of gear hobbing. Machinability data relating to tool-life as well as other dependent variables were put in a form which is readily applicable for cost determination.

The chosen gear blank specifications are as follows:

Outside dia: 96.52 mm

width : 25.4 mm

Pitch dia : 91.44 mm

number of teeth, Z_g; 36

material : En 34 steel (164 HB)

The selected hob specifications are as follows:

Outside dia; 67.2 mm

rake ; 0

helix angle; 2^{o} 6'

add ; 2.54 mm

ded ; 3.175 mm

Pressure angle; 20^{o}

D.P. ; 10

module, m ; 2.540 mm

bore ; 31.75 mm

Sykes No.; HP 368-20/V2E S.S.R.H. Conform to B.S. 2062/1963 (Grade B)

The gear blank was cut in one stroke, full depth of cut, d being 5.715 mm.

"SYKES" HV-14 Hobbing Machine Specifications:

Main drive motor; 2 HP ,1450 rpm

table diam. ; Maximum with steady column, 355 mm.

feeds ; Variation by means of pick-off gears,
minimum 0.024 in/rev (0.6096) mm/rev)
maximum 0.160 in/rev (4.064 mm/rev)

Speeds; 6 speeds by means of pick-off gears.
74, 92, 115, 143, 178 and 224 rpm.

number of teeth, Z_g; minimum 6. maximum 600

maximum loading of the feeding mechanism; 2500 kg.

The estimation of the optimum cutting conditions, namely cutting speed V, and axial feed f, at a constant depth of cut which minimizes the cost function, C_p under constraints (120) and (121) was carried out when tool-life was evaluated at 1.00 mm rake face wear.

The numerical values of the coefficients were estimated from experimental data obtained and listed in Appendix III. As for the Constraints (121), which have probability levels, all are assumed to be satisfied at the same probability levels, and 0.50 and 0.90 are selected, where the probability level of 0.50 is equivalent to treating the constraints as deterministic.

9.9 Illustration of the Proposed Method

The effect of variations in the coefficients on the determination of optimum cutting conditions are illustrated in Fig. 95 when a 10 D.P. hob was used to cut En 34 steel spur gears.

The operability region restricted by constraints (120) and (121) is shown graphically in the figure, where power, tangential force and surface roughness constraints are at 0.50 and 0.90 probability level, while vibration and feeding mechanism constraints are only at 0.50 probability level, as they, together with resistance of hob arbor restriction, are outside the operability region at all probability levels for the conditions considered.

The operability region shrinks as shown in Fig. 95 as the specified probability region increases. The cutting force constraint is little affected by the change in cutting speed. The power consumption constraint shifts toward both lower speed and feed as the probability level increases. At the probability level of 0.90, the operability region is restricted only by the power consumption, cutting force and surface roughness constraints.

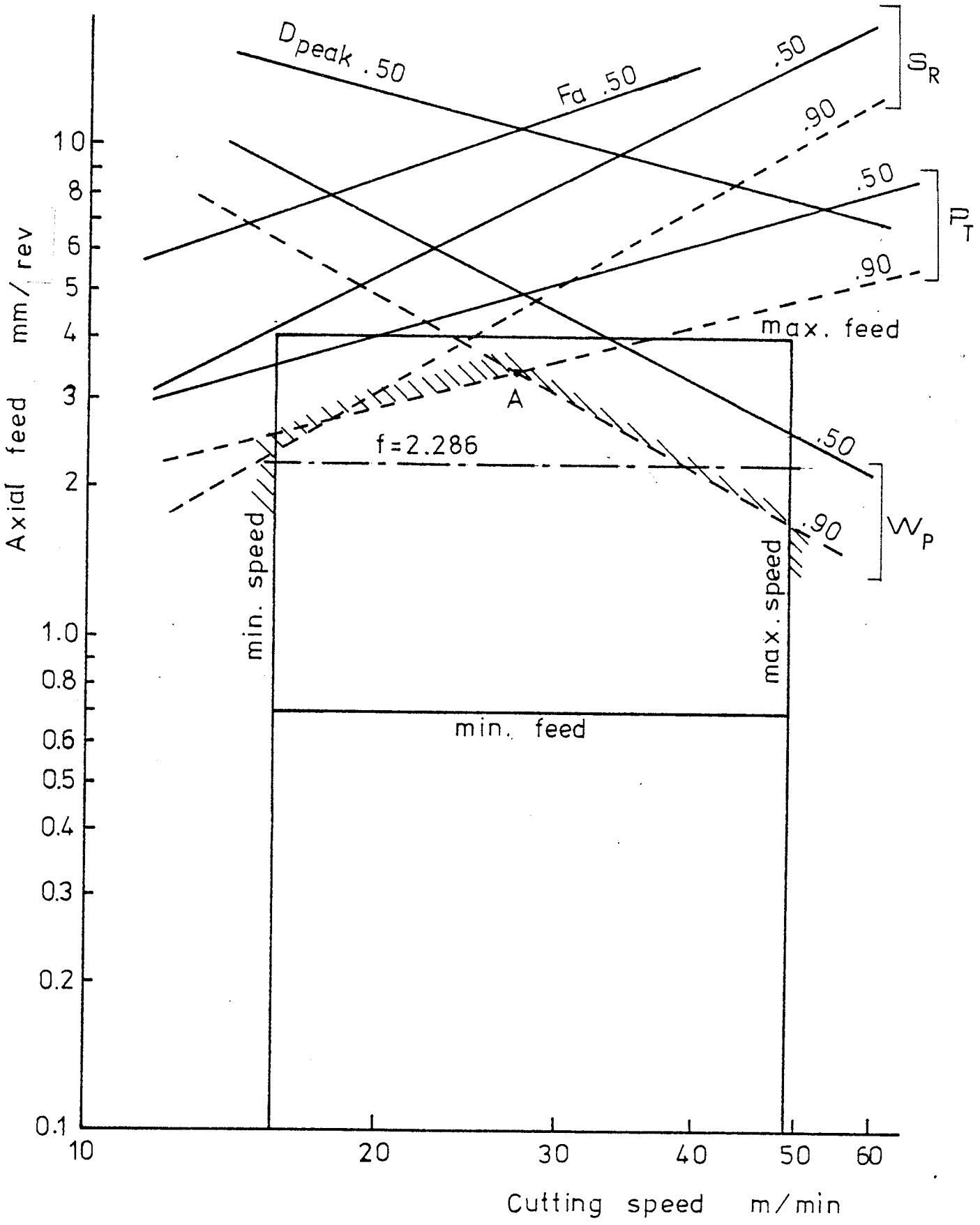

Fig. 95 The Operability Region and Optimum Cutting Conditions

10 D.P hob ; En 34 blank (HB 163)

9.10 Minimization of Production Cost

A non-linear objective function (119) based on the production cost per component is minimized under power, cutting force and surface roughness constraints. Fig. 96 shows the effect of the selected 0.90 probability level on the cost contour lines.

The values of cost and time parameters were assumed to be as follows

C_o = £0.20/min, C_t = £1.00/regrind and

t_h = 1 min.

The resulting objective function is obtained as follows:

$$C_p = \frac{b' Z_g}{f.N_h} \left(0.20 + \frac{0.20}{T_{.90}}\right) + 0.20$$

$$= \frac{228}{f.N_h} + \frac{273.6}{f.N_h.T_{.90}} + 0.20 \qquad (124)$$

where, $T_{.90}$ is 0.90 probability level of tool-life

By substituting the values of speed and tool-life, Eq. (124) becomes:

$$C_p = \frac{45.6}{f.V} + 0.0008 \left(\frac{V^{1.23}}{f^{0.82}}\right) + 0.20 \qquad (125)$$

Production cost per component is calculated from equation (125) as a function of cutting speed and axial feed. Table 27 shows the variation of cost when changing feed and speed, it follows that minimum production cost of £0.709/pc was found at the following cutting conditions:

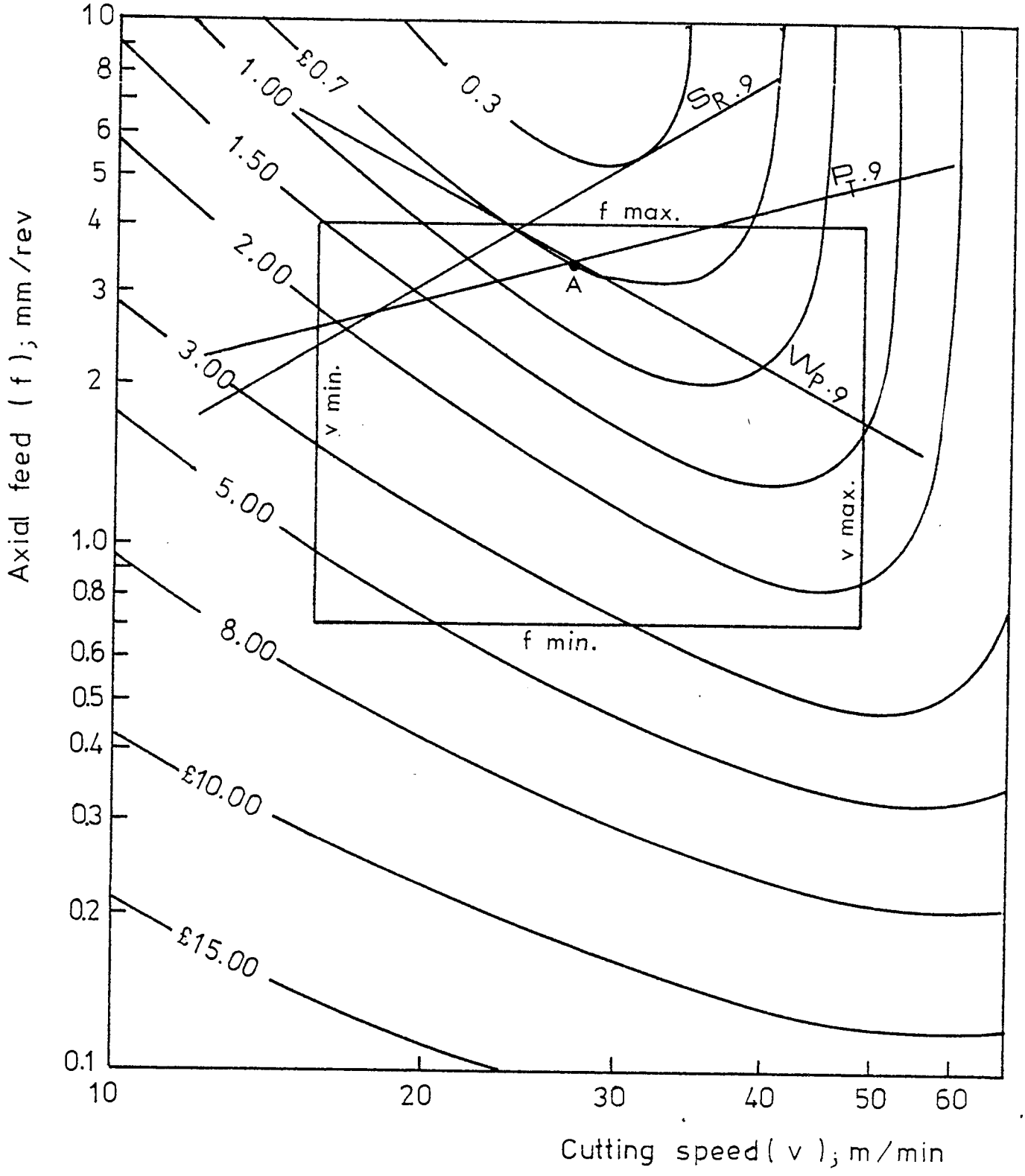

Fig. 96 The Operability Region and Production Cost Contours.

Machining Data: hob, 10 D.P.; 14 gashes
blank, En 34 (HB 163); 36 teeth

TABLE 27

OPTIMUM CUTTING CONDITIONS & PRODUCTION COST

Cutting speed V, m/min	Axial feed f, mm/rev	Volume of metal removed, cm^3/min.	Production cost, £/pc
15.62	0.609	0.183	5.028
	1.981	0.594	1.686
	2.286	0.686	1.489
	2.400	0.720	1.427
19.42	0.609	0.395	4.101
	1.981	1.287	1.402
	2.286	1.486	1.242
	2.500	1.625	1.153
	2.700	1.755	1.083
24.28	0.609	0.669	3.344
	1.981	2.179	1.171
	2.286	2.515	1.042
	3.000	3.300	0.842
	3.200	3.520	0.802
30.19	0.609	1.047	2.704
	1.981	3.407	0.971
	2.286	3.932	0.869
	2.500	4.300	0.811
	2.700	4.644	0.766
	3.000	5.160	0.709*
37.58	0.609	2.314	2.296
	1.981	7.528	0.852
	2.100	7.980	0.815
	2.286	8.686	0.766
47.29	0.609	4.263	1.921
	1.016	7.112	1.239
	1.270	8.890	1.034
	1.473	10.311	0.921
	1.680	11.760	0.834

* Minimum Production Cost

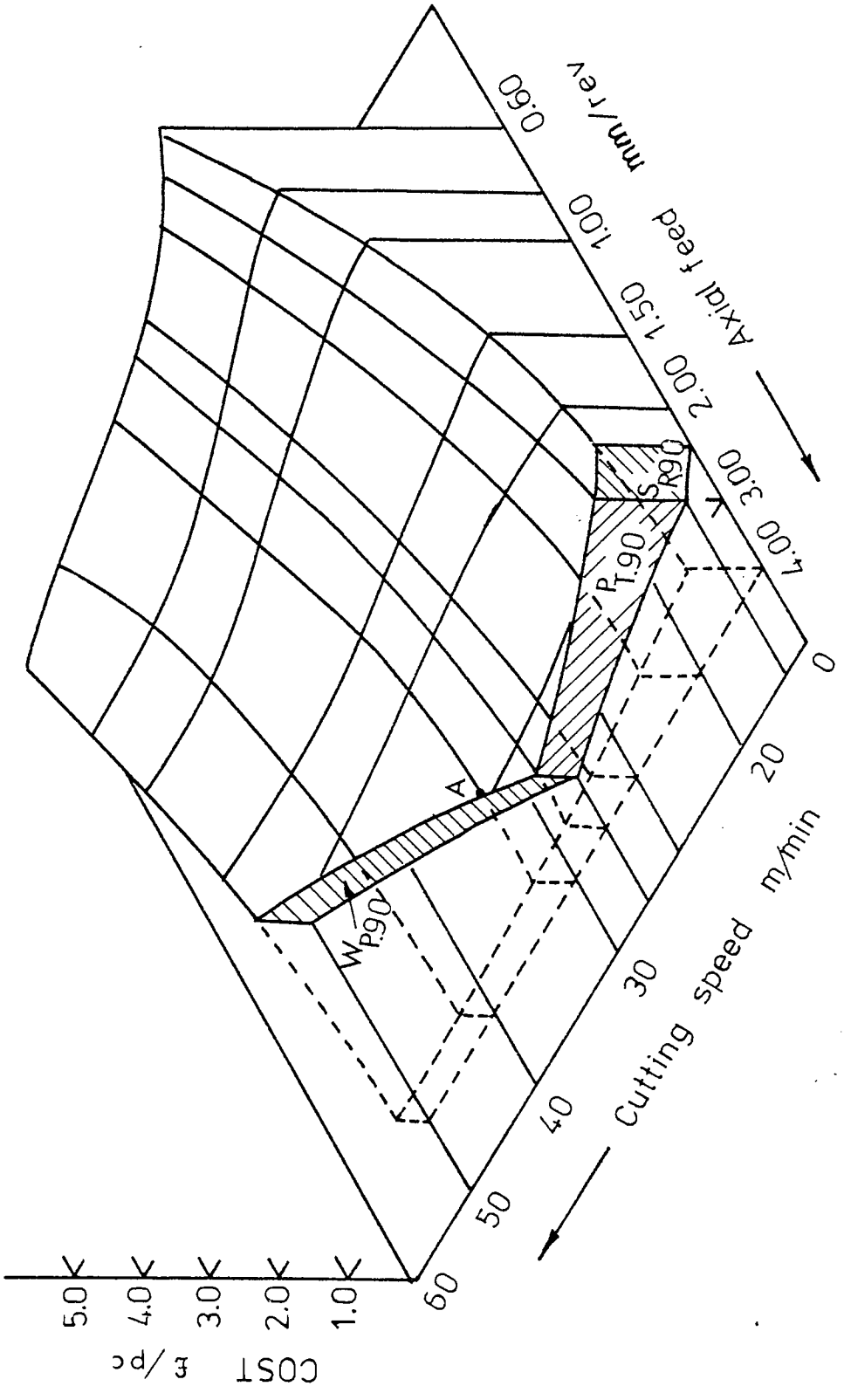

Fig. 97. PRODUCTION COST SURFACE AND CONSTRAINTS

C_o = £ 0.20/min , C_t = £1.00/regrind ; t_h = 1 min

axial feed = 3.00 mm/rev

cutting speed = 30.19 m/min.

The overall minimum cost in the operability region is attained at point "A" in Fig. 96.

Fig. 97 shows the production cost surface cut by the three constraints. It is clear from the figure that minimum production cost "point A" lies on the power constraint.

9.11 Conclusions

1. Power, Surface roughness and tangential cutting force were the constraints restricting the operability region for the given machining conditions. Other constraints moved outside the operability region at all probability levels.

2. An analytical method based on the chance-constrained programming concept was proposed as an effective optimization technique in gear hobbing.

3. The overall minimum cost in the operability region was observed to be along the power consumed constraint, when this constraint is an effective constituent of the operability region.

CHAPTER X

FUTURE WORK

This investigation was limited to rough hobbing with a single start hob, full depth of cut corresponding to the particular module and conventional hobbing concerned. The obvious extension of the present work is to consider climb hobbing and multi-start hobs.

The next stage for advancement of the investigation would be to expand the present work by chaning the cutter geometry, i.e. hob diameter, number of flutes, lead angle, clearance angle, rake angle and cutter material as well as cutting fluids along with the other independent variables.

10.1 Cutting torques and power consumed

The instrumentation has been proved for hobbing procedures involving standard hob with various parameters. Further investigation can be conducted to study the effect of cutting torques and power consumed on worms and worm wheels.

It is probable that the same instrumentation and design of experiment could be used for more detailed investigation of the hobbing process:

a) The formation of individual peaks on the traces resulting from all the teeth on the hob coming into engagement is not very clear. If a special hob was made having only one helical pitch circle, results obtained from this configuration could yield data showing how the amount of work done is related to the cutter and work-piece position. It then requires only synchronisation

to relate a particular tooth to one peak on the trace.

b) With the test results it would be plausible to correlate the surface roughness along the flank of the generated tooth to the peaks on the traces. In this way it could be possible to establish the relation of cutting torque influenced by hob tooth to the surface finish obtained on blank tooth. By the suggested single tooth hob, this correlation can be investigated more closely.

10.2 The Nature and Surface Topography of the Gear Teeth

The process of manufacture of the gear along with the tool geometry, feeds and speeds, will determine the surface roughness. The geometric accuracy of the machine tool carrying out the process will determine the degree of waviness or errors of the surface. The overall roughness and waviness of a surface contributes to the surface topography which in itself is a three-dimensional term. It is, therefore,necessary in future work to be able to measure and display the characteristics in three dimensions. To carry out three-dimensional measurements of a small surface is relatively difficult if a large number of points are to be considered. However, methods do exist which give the average surface topology or spot to spot readings such as map contours and Rochdale Flatness Testers. A method suitable for gear tooth surfaces is the Autoregressive-Moving Average Models[24]. This analysis is developed through the criteria of ergodicity, sensitivity and describability.

10.3 Analysis of the Chatter Problem in Hobbing

The present investigation has shown how various

parameters affect the machine structure vibration. Due to time and the complexity of the problem little analytical evidence has been put forward. Recent work carried out by Slavicek[9] and [10] has helpted to throw light on the problem of determining the effect of cutting variables on chatter in hobbing, and it is hoped that further investigation, after modifying the measuring sircuits, will enable the dynamic stiffness to be calculated.

10.4 Tool Wear and Tool-Life

In this investigation the author has tried to describe briefly the more important features of tool life and wear in hobbing, from one person's point of view. The discussion was limited to wear under normal cutting speed range, as the speed is increased and temperature becomes too high, where diffusion is very significant, other wear mechanisms will prevail.

In those cases, tool strength and hardness will be important parameters. Further work should be done with different cutting fluids in order to compare the life of hobs with the cooling of the cutting zone by flooding and mist cooling with various compositions of the cutting fluid and in various delivery conditions (air pressure, fluid delivery rate and shape of jet). Greater speeds should also be employed with different stiffness of the workpiece-tool-machine system..

The possibilities for improving tool-life in hobbing that follow from this work, such as cooling the hob or its parts (for example, inserts), and cooling the hob in combination with cooling the workpiece, or in combination with heating the

workpiece (hot machining) should be also considered in future work.

10.5 Temperature Relationships in Hobbing

The same design of experiment in this work can be used in order to determine the effect of cutting parameters on temperature and to relate force to temperature.

The cutting temperature can be measured by means of a thermocouple formed by the hob and gear being hobbed. For this purpose, the hob should be insulated from the machine by means of laminated plastics bushes on which a current collector ring and a tooth number marker are mounted.

10.6 Economics of Gear Hobbing

The analytical method based on the chance-constrained programming concept was proposed as an effective optimization problem was reduced to only two cutting parameters, namely axial feed and cutting speed, and the investigation was limited to one gear blank material and one hob.

Further work is required to investigate further the effect of more cutting parameters on the reduction of machining cost, such as variable blank and hob specifications, in order to generalize the economic problem.

CHAPTER XI

CONCLUSIONS

The conclusions that can be drawn from the investigation of this research are as follows:

1. Cutting speed has a significant effect on cutting torques on the hob shaft and average power consumed during hobbing spur and helical gears in a conventional manner.

2. It is advisable to vary the axial feed rate by applying a greater rate at the start of cutting and reducing it towards the full depth of cut in order to make the process more efficient and that may involve a design of variable feed mechanism.

3. The magnitude of maximum torque increased considerably with the increase of gear module from 12 D.P. to 8 D.P. An increase of 100% in axial feed produced an equivalent increase of 87% in maximum torque at constant speed.

4. The gear helix angle has little or no effect on cutting torques and power consumed when hobbing En 34 steel blanks.

5. It is useful to check the hardness as well as the microstructure when inspecting a work material, where it is explicit that no monotic function exists for cutting torques and power as a function of harness.

6. Axial feed, hob speed and hob D.P. have high significant influence on gear teeth surface roughness.

7. Increase in axial feed rate within normal hobbing machine cutting range promotes a rougher surface finish on spur gear teeth.

8. Increase in hob speed results in a smoother surface roughness.

9. The spheroidized structure, En 8 steel (HB=183) gave the best performance as far as torque, power, surface roughness and vibration are concerned, but microstructure studies are needed.

10. Stability of hobbing depends strongly on the parameters of the cutting process, namely, upon axial feed, hob speed and hob D.P.

11. Material hardness has less significant effect upon vibration, and no monotic function exists between hardness and vibration.

12. With the increase of module, the width of uncut-chip increases and therefore stability decreases.

13. Increasing the number of gashes in the hob have a slight improving influence on stability.

14. Increasing axial feed resulted in an increase in mean chip thickness, and an increase in blank diameter resulted in a decrease in mean chip thickness.

15. The influence of chip thickness cut off by hob peripheral edges on stability is not significant.

16. The problem of hob gashes design is important, where it reduces fluctuation of the cutting forces.

17. Chip cross-section area cut off by both sides of the hob edge are equal, and chip area cut off by the peripheral edge is larger than that cut off by either side edge.

18. "Rake face" wear is a suitable tool-life criterion in hobbing, when gear blank hardness is less than (270 HB) and under normal cutting conditions.

19. Cutting speed has the highest significant influence on the hob-life followed by material hardness and depth of cut for the cutting range covered.

20. It seems more advantageous to use higher axial feeds without affecting the hob life, and thus decrease the cutting time.

21. Power, surface roughness and tangential cutting force were the constraints restricting the operability region when hobbing En 34 spur gears with 10 D.P. hob. Other constraints moved outside the operability region at all probability levels.

22. The overall minimum cost in the operability region was observed to be along the power constraint, when this constraint is an effective constraint of the operability region.

23. An analytical method based on the chance-constrained programming concept was proposed as an effective optimization technique in gear hobbing.

REFERENCES

1. Woodburn, R.S. "History of the Gear Cutting Machine" The Technology Press, M.I.T. 1958

2. Bhattacharyya, A. and Deb, S.R. "Mechanics of Gear Hobbing". Trans. ASME, Vol. 92, Feb. 1970, pp. 103-108

3. Honda, F. - Japanese Government Mechanical Laboratory, "Study on the Hobbing Process". Report 42, 1961.

4. Padham, S.S. "Experimental Investigation of Cutting Torque and Power in the Hobbing Process". M.Sc. Thesis, The University of Aston in Birmingham, 1972.

5. Fel'dshtein, E. "Mist Cooling of Gear Cutting Tools". Machines and Tooling, Vol. 34, No. 2, 1963, pp. 36-41.

6. Cooke, D.A. and Welbourn, D.B. "Forces in Gear Hobbing - 1 Spur Gears". Machinery and Production Engineer, Feb. 7th 1968, pp. 475-477.

7. Cooke, D.A. and Welbourn, D.B. "Forces in Gear Hobbing - 2 Helical Gears". Machinery and Production Engineer, Feb. 7th 1968, pp. 258-261

8. Khardin, Y.P., et al. "Cutting Forces in Hobbing Worm Wheels". Machines & Tooling, Vol. 38, No. 2, 1967. pp. 35-38.

9. Slavicek, J. "Stability of Hobbing Machines". Advances of M.T.D.R. Conference, 1966, pp. 177-190, Birmingham.

10. Slavicek, J. "A New Exciter for Hobbing Machines". Advances of M.T.D.R. Conference, 1967, pp. 605-614, Manchester.

11. Inozemtsev, G.G. "Hobs with Changed Cutting Edge Geometry". Machines & Tooling ,Vol. 32, No. 4, 1961, pp. 22-25.

12. Severilov, V.S. "Power Relationships in Gear Hobbing". Machines & Tooling, Vol. 40, No.7, 1969, pp. 40-43.

13. Fujkawa, A., et al. "Hobbing with Sintered Carbide Hobs". Int. J. Mach. Tool Des. Res., Vol. 7, 1967. pp. 289-302.

14. Sheryshev ,V.I. "Force and Temperature Relationships in Hobbing Creep Resisting and Titanium Alloy Steel Gears". Machines & Tooling, Vol. 34, No. 2, 1963, pp. 38-41.

15. Rapp, J.W. "High-Speed Hobbing ----- proved Practical". The Tool Engineer, June 1954, pp. 77-80.

16. Severilov ,V.S. "Optimum Design of a Roughing Taper on Hobs for Helical Gears". Machines & Tooling, Vol. XXXV, No. 12, 1964, pp. 32-33.

17. Proskiryakov ,Yu.G., et al. "Sintered Carbide Hob Tools". Stanki i Inst., Vol. 31, No. 4, 1960, pp. 23-25.

18. Bhattacharyya, E., Singh, G.D., et al., "Analysis of Milling Forces". J. of Inst. of Engineers, India, Vol. XIIV, No. 11, Part ME6, July 1964.

19. Shaw, M., Cook, N.H., and Lowen, E.A., "Machine Tool Dynamometers - A Current Appraisal". American Mechanist, May 1oth 1954, pp. 71-72.

20. Milner, D.A. and Raafat, H; ,"An Experimental Investigation of the Variation of Peak Torque and Power in Gear Hobbing". Int. J. Prod. Res., 1976, Vol. 14, No. 5, pp. 568-581.

21. Rozenberg, A. and Adam, J., "Gear Production". Mashgiz, Moscow, 1961, pp. 236-241.

22. Nekrasov ,S.S. and Saifullin, V.N., "Hobbing with Large Diameter Multi-Start Hobs". Russian Engineering Journal, No. 6, 1966.

23. Peklenik, J., "Investigation of the Surface Typology". Annals of the C.I.R.P., Vol. XV, 1967, pp. 381-385.

24. Devor, R. and Wu ,S.M., "Surface Profile Characterization by ARMA Models". Trans. ASME , J. of Eng. for Ind., Aug. 1972, pp. 825-832.

25. Tlusty, J., "A Method of Analysis of Machine Tool Stability", Int. J. of MTDR Conference, 1965, pp. 5-14, Manchester.

26. Tobias, S.A., "The Vibration of Vertical Milling Machines under Test and Working Conditions". Proc. Inst. Mech. Eng. Vol. 173, 1959, pp.

27. Slavicek, J. "The Effect of Irregular Tooth Pitch on Stability of Milling" ,Int. J. of MTDR, 6th Conference, 1965, pp. 15-22, Manchester.

28. Wakuri, A., Ueno, T. and Ainoura, M. "A Study of Gear Hobbing", Bulletin of JSME, Vol. 9, No. 34, 1966, pp. 409-416.

29. Colwell, L.V., and Mazur, J.C. "International Co-op Research Program on Tool-wear", Air Force Technical Report AFML-TR-66-387, 1966.

30. Cook, N.H. "Tool Wear and Tool Life". Trans. ASME, J. of Eng. for Ind., Nov. 1973, pp. 931-937.

31. Wakuri, A., Ueno, T. and Ainoura, M. "Fundamental Research on Hobbing Hard Gears using Fly-Tools". Bulletin of the JSME, Vol. 15, No. 87, 1972, pp. 1130-1142.

32. Forsberg, E.A. "Investigation as to Cutting Speeds for Swedish Materials". Inegniors Vetenskaps Akademien, Handlingar, No. 95, Stockholm, Sweden, 1929, pp. 108.

33. Brewer, R.C., "On the Economics of Basic Turning Operation". Trans. ASME, J. of Eng. for Ind., Vol. 80, 1958, pp. 1470-1489.

34. Gilbert, W., "Economics of Machining - Theory and Practice", Am. Society for Metals, 1950, pp. 465-485.

35. Wu, S.M. and Ermer, D.S., "Maximum Profit as the Criterion in the Determination of the Optimum Cutting Conditions". Trans. ASME, series B, Vol. 88, 1966, pp. 435-442.

36. Ermer, D.S., and Morris, M.S., "A Treatment of Errors of Estimation in Determining Optimum Machining Conditions". Int. J. Mach. Tool Des. & Res., Vol. 9, 1969, pp. 357-362, Manchester.

37. Draghici, G. and Paltinea, C., "Calculation by Convex Mathematical Programming of Optimum Cutting Conditions when Cylindrical Milling". Int. J. MTDR, Vol. 14, 1974, pp. 143-160, Birmingham.

38. Iwata, K., Murotsu, Y. and Fujii, S., "A Probabilistic Approach to the Determination of the Optimum Cutting Conditions". Trans. ASME, J. of Eng. for Ind., Series B, 1972, pp. 1099-1107.

39. Sidorenko, A.K. "Advances in Gear Hobbing", Mashgiz, 1961, Moscow.

40. Perry, C.C. and Lissner, H.R., "The Strain Gauge Primer". McGraw-Hill, 1965.

41. Potma, T. "Strain Gauges - Theory and Application". Phillips Paperbacks, 1964.

42. Broersma, I.R. G., "Manufacture and Testing of Gears". Technical Publications H. Stam, The Netherlands, 1969.

43. Crockett, J.C. "Gear Cutting Practice, Machines and Tools". The Machinery Publication Co., 1971.

44. Welbourn, D.B. and Smith, J.D. "Machine-Tool Dynamics - An Introduction", Cambridge University Press, 1970.

45. Brocken, J. and McCormick, G.P., "Selected Applications of Non-Linear Programming", John-Wiley, N.Y. 1968.

46. Phelan, R.M., "Fundamentals of Mechanical Design", Third Edition, McGraw-Hill, N.Y., 1970.

47. Watson, H.J., "Modern Gear Production", Pergamon Press, 1970.

APPENDIX I

STRAIN GAUGE DESIGN CALCULATIONS

First of all, the diameter on which the strain gauges are bonded was calculated.

Assuming for simplicity that the shaft is simply supported at P and Q as shown in Fig. 98 and considering section A-A of the shaft.

Using the design formula for shafts under bending and torsion [46].

$$S_{max} = \frac{0.5\ S_{yp}}{F.S.} = \frac{16}{\pi d^3} \sqrt{(C_m M)^2 + (C_t T)^2} \qquad (I\text{-}1)$$

where, S_{max} = Maximum Shear Stress (N/m^2)

S_{yp} = Yield stress (N/m^2)

F.S. = Factor of Safety

d = diameter of shaft (m)

M = bending moment (Nm)

T = torque (Nm)

C_m and C_t are constants

From Fig. 99, assuming that maximum load of 3000 N. acts at the centre of hob, the bending moment is obtained for simplified force system. At Section A-A, M = 30 Nm

Assuming, T = 113 Nm

$S_{yp} = 468.84 \times 10^6 \quad N/m^2$

F.S.= 2

$C_m = C_t = 2 = C$

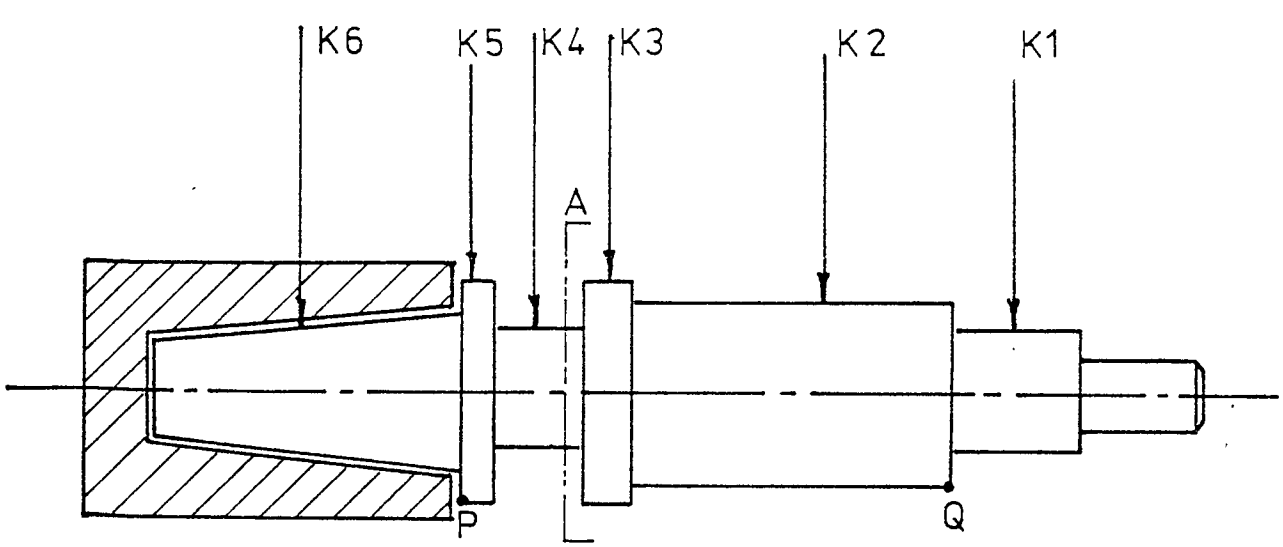

Fig.98 SKETCH OF TORQUE DYNAMOMETER

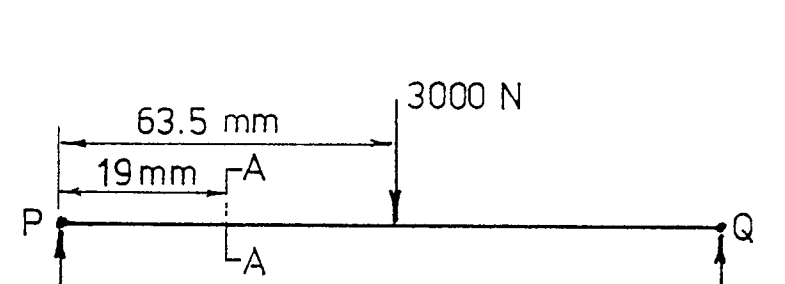

a) SIMPLE FORCE EQUILIBRIUM DIAGRAM

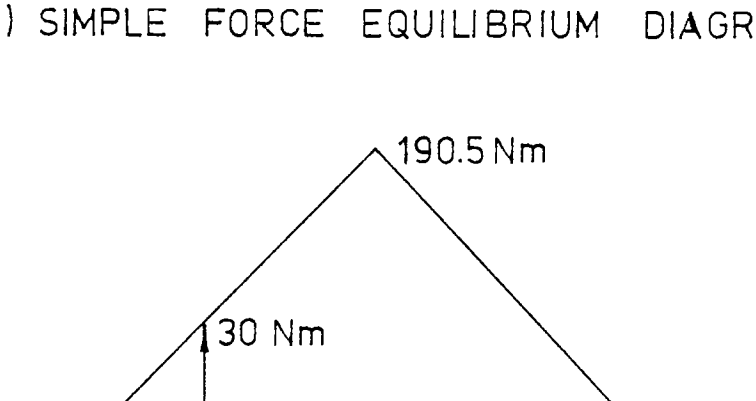

b) BENDING MOMENT DIAGRAM

Fig.99 FORCE AND MOMENT DIAGRAMS

Substituting these values in equation

$$0.5 \times 468.84 \times 10^6 = \frac{2 \times 16 \times \sqrt{(30)^2 + (113)^2}}{\pi \times d^3}$$

$\therefore \quad d = 21.844$ mm

For design consideration shaft diameter was selected as follows:

$d = 22.225$ mm ($\frac{7}{8}$ in.dia.)

From Fig. 98, using the appropriate notations for stiffness, the shaft stiffness and the "gauge area" stiffness was determined as follows by using the following formula

$$\frac{T}{J} = \frac{S_s}{r} = \frac{G\theta}{L} \qquad \text{(I-2)}$$

where, T = torque in shaft (Nm)

J = polar moment of intertia ($Kg.m^2/sec$)

S_s = shear stress (N/m^2)

r = radius of shaft (m)

G = modulus of rigidity (N/m^2)

θ = angular twist of shaft (radians)

L = length of shaft (m)

K = stiffness of shaft (Kg/m)

From equation (I-2), stiffness is obtained as follows:

$$K = \frac{T}{\theta} = \frac{\pi d^4 G}{32} \qquad \text{(I-3)}$$

Using equation (I-3), the different stiffnesses for sections of shaft are obtained as follows:

letting $\frac{\pi.G}{32} = \frac{\pi \times 73.08 \times 10^9}{32} = 7.175 \times 10^9 \ N/m^2 = C'$

$$K_1 = \frac{C' \times (d_1)^4}{\ell_1} = \frac{7.175 \times (0.022)^4 \times 10^9}{0.05397} = 51.09 \times 10^5 \text{ Kg/m}$$

$$K_2 = \frac{C' \times (d_2)^4}{\ell_2} = \frac{7.175 \times (0.031)^4 \times 10^9}{0.1016} = 113.397 \times 10^5 \text{ Kg/m}$$

$$K_3 = \frac{C' \times (d_3)^4}{\ell_3} = \frac{7.175 \times (0.0377)^4 \times 10^9}{0.006} = 328.58 \times 10^6 \text{ Kg/m}$$

$$K_4 = \frac{C' \times (d_4)^4}{\ell_4} = \frac{7.175 \times (0.022)^4 \times 10^9}{0.0143} = 192.86 \times 10^5 \text{ Kg/m}$$

$$K_5 = \frac{C' \times (d_5)^4}{\ell_5} = \frac{7.175 \times (0.0377)^4 \times 10^9}{0.0063} = 437.5 \times 10^6 \text{ Kg/m}$$

K_5 is much reduced because of the machined collar, therefore it was assumed that

$$K_{5'} = K_{5/2} = 2187.5 \times 10^5 \text{ Kg/m}$$

Taking into account the housing (female section) into which the tapered end of the shaft fits,

$$K_{6'} = \frac{C' \times (d_{6'})^4}{\ell_6} = \frac{7.175 \times (0.044)^4 \times 10^9}{0.127} = 344.6 \times 10^5 \text{ Kg/m}$$

Total hob arbor stiffness, K_H is obtained as follows:

$$K_H = \frac{1}{1/K_1 + 1/K_2 + 1/K_3 + 1/K_4 + 1/K_{5'} + 1/K_{6'}}$$

$$K_H = \frac{10^5}{9.360218} = 0.1068 \times 10^5 \text{ Kg/m}$$

Stiffness of the shaft diameter over which gauges are bonded is :

$$K_4 = 192.86 \times 10^5 \text{ Kg/m}$$

The natural frequency of the shaft (hob arbor) was evaluated as follows:

The natural frequency, f_n, is given by the formula,

$$f_n = \frac{\sqrt{K/J}}{2\pi} = \frac{\sqrt{G/L}}{2\pi} \qquad \text{(I-4)}$$

$$f_n = \frac{\sqrt{73.08 \times 10^9}}{2\pi \times \sqrt{0.01428}}$$

$$f_n = 695 \text{ c.p.s.}$$

APPENDIX II.

VIBRATION STANDARDS

Aston University

Content has been removed for copyright reasons

APPENDIX III

Numerical Values of Constraints and Variances

1) $P_T = 10^{\alpha_1} f^{\alpha_2} (HB)^{\alpha_3} (D.P.)^{\alpha_4}$ (III-1)

$\alpha_1 = 4.751$	$\sigma_{\alpha_1} = 0.1038$
$\alpha_2 = 0.624$	$\sigma_{\alpha_2} = 0.046$
$\alpha_3 = 0.1138$	$\sigma_{\alpha_3} = 0.032$
$\alpha_4 = -0.372$	$\sigma_{\alpha_4} = 0.012$
$\alpha_5 = -0.372$	$\sigma_{\alpha_5} = 0.012$

2) $W_p = 10^{\alpha_6} f^{\alpha_7} (HB)^{\alpha_8} V^{\alpha_9} (D.P.)^{\alpha_{10}}$ (III-2)

$\alpha_6 = 1.02$	$\sigma_{\alpha_6} = 0.212$
$\alpha_7 = 0.624$	$\sigma_{\alpha_7} = 0.046$
$\alpha_8 = 0.114$	$\sigma_{\alpha_8} = 0.032$
$\alpha_9 = 0.628$	$\sigma_{\alpha_9} = 0.23$
$\alpha_{10} = -1.662$	$\sigma_{\alpha_{10}} = 0.66$

3) $S_R = 10^{\alpha_{11}} f^{\alpha_{12}} (HB)^{\alpha_{13}} (D.P.)^{\alpha_{14}} V^{\alpha_{15}}$ (III-3)

$\alpha_{11} = 0.007$	$\sigma_{\alpha_{11}} = 0.0001$
$\alpha_{12} = 0.398$	$\sigma_{\alpha_{12}} = 0.0126$
$\alpha_{13} = 0.188$	$\sigma_{\alpha_{13}} = 0.021$
$\alpha_{14} = -0.147$	$\sigma_{\alpha_{14}} = 0.018$
$\alpha_{15} = -0.460$	$\sigma_{\alpha_{15}} = 0.036$

4) $D_{peak} = 10^{\alpha_{16}} f^{\alpha_{17}} (HB)^{\alpha_{18}} V^{\alpha_{19}} (D.P.)^{\alpha_{20}}$ (III-4)

α_{16}	= 0.756	$\sigma_{\alpha_{16}}$	= 0.124
α_{17}	= 0.592	$\sigma_{\alpha_{17}}$	= 0.044
α_{18}	= 0.223	$\sigma_{\alpha_{18}}$	= 0.012
α_{19}	= 0.277	$\sigma_{\alpha_{19}}$	= 0.016
α_{20}	=-0.946	$\sigma_{\alpha_{20}}$	= 0.068

5) $T = 10^{\alpha_{21}} Z_g^{\alpha_{22}} V^{\alpha_{23}} f^{\alpha_{24}} (D.P.)^{\alpha_{25}} d^{\alpha_{26}} \left(\frac{HB}{200}\right)^{\alpha_{27}}$ (III-5)

α_{21}	= 6.08	$\sigma_{\alpha_{21}}$	= 0.680
α_{22}	= 0.26	$\sigma_{\alpha_{22}}$	= 0.051
α_{23}	=-2.63	$\sigma_{\alpha_{23}}$	= 0.302
α_{24}	=-0.21	$\sigma_{\alpha_{24}}$	= 0.032
α_{25}	=-0.66	$\sigma_{\alpha_{25}}$	= 0.128
α_{26}	=-0.46	$\sigma_{\alpha_{26}}$	= 0.088
α_{27}	=-5.79	$\sigma_{\alpha_{27}}$	= 0.48

Where these values are at the amount of rake face wear, 1.00 mm.

6) P_{Tmax} = 1667 (N.)

W_{pmax} = 2 HP.

S_{Rmax} = 9 μm (CLA)

$D_{peak\ max}$ = 24.4 μm (peak to peak)

K = 33.928 x 10^5 Kg/m, d_s = 22 mm.

σ_a = 4685 x 10^6 (N/m^2)

F_a = 2450 (N.)

APPENDIX VI

Conversion Tables for Units

Length

1 ft = 0.3048 m

1 in = 25.4 mm

0.001 in = 25.4 μm

Mass

1 ton= 1016.05 Kg

1 lb = 0.4536 Kg

Area

1 sq.in = 6.4516×10^{-4} sq.m

1 sq.ft = 9.2903×10^{-2} sq.m

Volume

1 cu.in = 1.000×10^{-3} cu.m

= 16.387 cu.cm

Force

1 lb f = 4.448 N = 0.453 Kp

(Mnemonic : 1 apple weighs roughly 1 Newton)

Torque

1 lbf.in = 0.11298 Nm

Stress

1 lbf/in^2 = 6894.76 N/m^2 = 0.0703 Kp/cm^3

Work

1 hph = 2.684 MJ

1 kWh = 3.6 MJ

1 ft lbf = 1.3558 J

Stiffness

1 lbf/in = 175.127 N/m = 17.858 Kp/m